TECHNISCHE UNIVERSITÄT WIEN

institute of telecommunications

DISSERTATION

MULTIUSER COMMUNICATION WITH QUANTIZED FEEDBACK

ausgeführt zum Zwecke der Erlangung des akademischen Grades eines Doktors der technischen Wissenschaften

unter der Leitung von
Ao. Univ.-Prof. Dipl.-Ing. Dr.techn. Gerald Matz
Institute of Telecommunications

eingereicht an der Technischen Universität Wien
Fakultät für Elektrotechnik und Informationstechnik

von
Ing. Dipl.-Ing. Stefan Farthofer, BSc
Arndtstrae 53/11
1120 Wien

Wien, im Februar 2019 _____

Die Begutachtung dieser Arbeit erfolgte durch:

1. Univ.-Prof. Dipl.-Ing. Dr.-Ing. Norbert Görtz
   Institute of Telecommunications
   Technische Universtiät Wien

2. Prof. Dr. Michèle Wigger
   Télécom ParisTech
   Université Paris-Saclay

Abstract

This thesis considers communication over various types of Gaussian channels with quantized channel output feedback. Here, the received signals are quantized and then directly fed back to one or multiple transmitters. We study point-to-point and multiuser communication scenarios. In the case of multiple users we consider the multiple access channel, i.e., two users communicating data to one single receiver, and the broadcast channel where one transmitter sends data to two receivers.

A key performance indicator in such communication scenarios is the channel capacity, which characterizes the maximum rates achievable with infinite blocklengths. It is known that even perfect feedback does not increase the channel capacity for point-to-point communication. By contrast, feedback can actually increase the channel capacity for multiuser communication. Since a perfect feedback link is a rather unrealistic assumption we consider the more realistic scenario of quantized feedback. This is justified by the fact that in modern digital communication systems each signal has to be quantized with some fidelity.

We use the Gaussian information bottleneck method to model the channel output compression of Gaussian vector channels and to characterize the optimal tradeoff between quantization rate and preserved transmit information. Traditionally, when designing quantization the source is considered to be fixed. We restrict to Gaussian source distributions and include the variable transmit power allocation as an additional parameter. We characterize the tradeoff between preserved transmit information, quantization rate allocation, and transmit power allocation. The optimal tradeoff amounts to a difference of convex functions program. We solve this optimization problem and demonstrate that this approach generally yields superior results.

For the actual feedback communication scheme, we propose a superposition coding method that superimposes a conventional coding component (which ignores the feedback link) and a feedback-based coding scheme in the spirit of Schalkwijk-Kailath and Ozarow. Optimizing the performance of the proposed scheme amounts to a resource allocation problem which again results in a difference of convex functions program. We solve this problem, discuss its performance, and show that this scheme achieves

higher rates than communication without feedback at a wide range of parameters. We show that the penalty due to limited feedback accuracy is outweighed by the increased feedback-capacity.

In addition to the rate constraint on the feedback link, practical scenarios impose constraints on the blocklength. Therefore, we adapt and study the proposed superposition coding scheme in the finite-blocklength regime. We here have to jointly optimize the transmit power and blocklength allocation. We propose a procedure that approximately solves this resource allocation problem. Numerical results show that due to the faster error probability decay of the feedback-based code component the proposed coding scheme demonstrates its strengths especially in the finite-blocklength region.

Kurzfassung

Diese Dissertation untersucht verschiedene Typen von Gauß'schen Kanälen mit quantisiertem Feedback des Kanalausgangs. Das heißt, die Empfangssignale werden quantisiert und dann direkt zu einem oder mehreren Sendern zurückgeführt. Wir beschäftigen uns mit Punkt-zu-Punkt-Kommunikation und Mehrbenutzerkommunikation. Im Fall von mehreren Benutzern untersuchen wir den Mehrfachzugriffskanal über welchen zwei Benutzer Daten zu einem Empfänger übertragen und den Broadcastkanal über welchen ein Sender Daten an zwei Empfänger sendet.

Eine Leistungskennzahl solcher Kommunikationssysteme ist die Kanalkapazität, welche die maximal erzielbare Datenrate für unendliche Blocklängen angibt. Es ist bekannt, dass sogar perfektes Feedback die Kanalkapazität von Punkt-zu-Punkt-Verbindungen nicht erhöhen kann; die Kanalkapazität von Mehrbenutzerkommunikation kann durch Feedback hingegen tatsächlich erhöht werden. Da eine perfekte Feedback-Verbindung eine sehr idealisierte Annahme darstellt, untersuchen wir das realistischere Szenario mit quantisiertem Feedback. Gerechtfertigt ist diese Verallgemeinerung aufgrund des Umstandes, dass in modernen digitalen Kommunikationssystemen jedes Signal mit einer gewissen Genauigkeit quantisiert werden muss.

Wir verwenden die Gauß'sche Information-Bottleneck-Methode um die Kanalausgangskompression von Gauß'schen Vektorkanälen zu beschreiben und um den optimalen Tradeoff zwischen Quantisierungsrate und erhaltener Transinformation zu charakterisieren. Bei dem Design von Quantisierern wird die Quelle üblicherweise als gegeben angenommen. Wir hingegen beschränken uns zwar auf Gauß'sche Quellverteilungen, inkludieren die variable Sendeleistungszuteilung aber als weiteren Parameter. Dementsprechend untersuchen wir den Tradeoff zwischen erhaltener Transinformation, Quantisierungsratenzuteilung und Sendeleistungszuteilung. Wir zeigen, dass der optimale Tradeoff die Lösung eines Optimierungsproblems mit Differenzen konvexer Funktionen erfordert. Wir lösen dieses Problem und demonstrieren, dass dieser Ansatz im Allgemeinen bessere Ergebnisse liefert.

Für das eigentliche Feedback-Kommunikationssystem entwickeln wir eine Superpositions-Kodierungsmethode, welche eine konventionelle Kodierungskomponente (die

die Feedbackverbindung ignoriert) mit einem feedback-basierten System nach Schalkwijk-Kailath und Ozarow überlagert. Die Optimierung dieses Kommunikationssystems ist ein Ressourcenzuteilungsproblem, welches wiederum in einem Optimierungsproblem mit Differenzen konvexer Funktionen resultiert. Wir lösen dieses Optimierungsproblem, diskutieren seine Leistungsfähigkeit und zeigen, dass dieses Kommunikationssystem höhere Raten als Kommunikation ohne Feedback über eine großen Bereich an Parametern erreicht. Wir zeigen, dass die Einbußen aufgrund limitierter Feedbackgenauigkeit durch eine erhöhte Feedbackkapazität kompensiert werden.

Zusätzlich zur Ratenbeschränkung der Feedbackverbindung ergeben sich in praktischen Szenarien auch Beschränkungen der Blocklänge. Wir adaptieren daher das entwickelte Superpositions-Kodierungssystem und untersuchen seine Leistungsfähigkeit bei endlichen Blocklängen. Dies erfordert die gemeinsame Optimierung der Sendeleistungs- und Blocklängenzuteilung. Wir schlagen eine Methode zur näherungsweisen Lösung dieses Ressourcenzuteilungsproblems vor. Numerische Ergebnisse belegen, dass das entwickelte Kodierungssystem aufgrund des schnelleren Abklingens der Fehlerwahrscheinlichkeit der feedback-basierten Kodierungskomponente seine Stärken vor allem im Bereich endlicher Blocklängen zeigt.

Acknowledgements

First and foremost, I want to thank my advisor Gerald Matz for his continuous support during the years of this project. Thank you, Gerald for your great guidance while still granting the freedom to develop my own ideas. I am grateful for offering me a master thesis that eventually led to this dissertation project and being a part of this exciting research group.

Especially, I want to thank my co-advisor of my master thesis and later Ph.D. colleague Andreas for introducing me into this challenging topic and enabling such a great start at the Institute of Telecommunications. I want to thank all people at the Institute who made this time so enjoyable, in particular my former group colleagues Georg and Michael.

Meinen Eltern, Veronika und Manfred, bin ich zutiefst dankbar, dass sie bei allem immer an mich geglaubt, mich ermutigt, mich unterstützt und mir gleichzeitig aber Freiheit gelassen haben.

Zuletzt möchte ich mich ganz besonders bei meiner Verlobten Christine bedanken. Danke für deine liebevollen Aufmunterungen, wenn es mal zu mühsam war, danke für unsere gemeinsamen Unternehmungen und Erlebnisse um meinen Kopf frei zu bekommen. Besonders während der letzten Monate hast du dafür gesorgt, meinen Stress auch mal zu vergessen und mit deiner Unterstützung alle anderen Sorgen von mir ferngehalten.

Contents

1 Introduction 1

1.1 Motivation and Scope of Work 1
1.2 Outline and Contributions 4
1.3 Notation 7
1.4 Acronyms 8

2 Preliminaries 9

2.1 Additive White Gaussian Noise Channel 9
2.1.1 Capacity 10
2.1.2 Finite Blocklength Performance 10
2.2 Additive White Gaussian Noise Channel with Feedback 11
2.2.1 Capacity 11
2.2.2 Error Probability Decay 12
2.3 Gaussian Multiple Access Channel 13
2.3.1 Capacity 13
2.3.2 Finite Blocklength Performance 14
2.4 Gaussian Multiple Access Channel with Feedback 16
2.4.1 Capacity 16
2.4.2 Error Probability Decay 18
2.5 Gaussian Broadcast Channel 19
2.5.1 Capacity 19
2.5.2 Finite Blocklength Performance 21
2.6 Gaussian Broadcast Channel with Feedback 22
2.6.1 Capacity – Duality 23
2.6.2 Error Probability Decay 24
2.7 Convex Optimization 24
2.8 Difference of Convex Functions Programming 26

2.8.1 Convex-Concave Procedure 26

3 MIMO Gaussian Information Bottleneck with Optimal Power Allocation 29

3.1 Introduction 30
3.2 Gaussian Information Bottleneck 30
3.2.1 Derivation of the GIB Information-Rate Function for Gaussian Channels 31
3.3 Scalar Gaussian Information Bottleneck 32
3.3.1 Equivalent Gaussian Channel 34
3.4 MIMO Gaussian Information Bottleneck 35
3.4.1 System Model 35
3.4.2 Generalization of the System 36
3.4.3 Information Bottleneck 37
3.4.4 Equivalent Gaussian Channel 44
3.4.5 MISO Gaussian Information Bottleneck 45
3.5 Gaussian Information Bottleneck with Optimal Power Allocation 46
3.5.1 Introduction 46
3.5.2 Properties of the Information-Rate-Power Function $I(R, P)$ 52
3.5.3 Discussion 54

4 Feedback Model 59

4.1 Introduction 59
4.2 Source Signal Model 60
4.3 Feedback Coding 62
4.3.1 AWGN Channel Transceiver Scheme 62
4.3.2 MAC Transceiver Scheme 63
4.3.3 Sum Capacity 66
4.4 Transition from Matrix to Superposition Coding 66
4.5 Superposition Feedback Coding 67
4.5.1 AWGN Channel Model 67
4.5.2 MAC Model 68
4.5.3 BC Model 70
4.5.4 Proposed Coding Scheme 72
4.5.5 Feedback Quantization 73

5 Asymptotic Superposition Coding 75

5.1 Introduction 75
5.2 Asymptotic Superpostion Performance - Gaussian Channel 75

5.2.1 Power Constraints . . . 76
5.2.2 Achievable Sum Rate . . . 77
5.2.3 Concave and Convex Component . . . 78
5.2.4 Difference of Convex Functions Programming Solution . . . 78
5.3 Asymptotic Superposition Performance - Symmetric Multiple Access Channel 82
5.3.1 Power Constraints . . . 82
5.3.2 Achievable Sum Rate . . . 83
5.3.3 Concave and Convex Component . . . 85
5.3.4 Difference of Convex Functions Programming Solution . . . 86
5.4 Asymptotic Superposition Performance - Asymmetric Multiple Access Channel 90
5.4.1 Power Constraints . . . 90
5.4.2 Achievable Sum Rate . . . 91
5.4.3 Concave and Convex Component . . . 92
5.4.4 Difference of Convex Functions Programming Solution . . . 93
5.4.5 Numerical Solution . . . 94
5.5 Asymptotic Superposition Performance - Symmetric Broadcast Channel . . 98
5.5.1 Power Constraints . . . 98
5.5.2 Achievable Sum Rate . . . 98
5.5.3 Difference of Convex Functions Programming . . . 100
5.5.4 Numerical Solution . . . 101
5.6 Asymptotic Superposition Performance - Asymmetric Broadcast Channel . 105
5.6.1 Power Constraints . . . 105
5.6.2 Achievable Sum Rate . . . 106
5.6.3 Partly Symmetrized Solution . . . 108
5.6.4 Concave and Convex Component . . . 109
5.6.5 Difference of Convex Functions Programming Solution . . . 110
5.6.6 Numerical Solution . . . 111

6 Finite Blocklength Superposition Coding 115

6.1 Introduction . . . 116
6.2 Finite Blocklength Superposition Performance – Gaussian Channel . . . 116
6.2.1 Error Probabilities . . . 116
6.2.2 Achievable Rates versus Blocklength and Error Probability . . . 118
6.2.3 Optimization Problem . . . 119
6.2.4 Impact of Blocklength Allocation . . . 120
6.2.5 Impact of Blocklength . . . 121
6.3 Finite Blocklength Superposition Performance – Gaussian MAC . . . 125
6.3.1 Error Probabilities . . . 125
6.3.2 Achievable Rates versus Blocklength and Error Probability . . . 127
6.3.3 Optimization Problem . . . 127

6.3.4 Impact of Blocklength Allocation 129
6.3.5 Impact of Blocklength 129
6.4 Finite Blocklength Superposition Performance – Gaussian BC 134
6.4.1 Error Probabilities 134
6.4.2 Achievable Rates versus Blocklength and Error Probability 136
6.4.3 Optimization Problem 137
6.4.4 Impact of Blocklength Allocation 138
6.4.5 Impact of Blocklength 139
6.5 Discussion 143

7 Conclusion and Outlook 145
7.1 Outlook 147

Bibliography 151

List of Figures

2.1 AWGN channel. 10
2.2 AWGN channel with feedback. 12
2.3 Gaussian MAC. 13
2.4 Gaussian MAC with feedback. 17
2.5 Gaussian BC. 19
2.6 Gaussian BC with feedback. 23

3.1 Basic communication system with quantizer. 30
3.2 GIB equivalent scalar system. 33
3.3 Vector system model. 35
3.4 GIB equivalent vector system. 37
3.5 Information-rate functions. 42
3.6 Waterfilling power allocation. 46
3.7 Reverse waterfilling rate allocation. 47
3.8 Information-rate-power function over power 56
3.9 Information-rate-power function over rate 57

4.1 Gaussian distribution and discrete approximation 61
4.2 AWGN channel with feedback link. 62
4.3 Two-user Gaussian MAC with common feedback link. 64
4.4 AWGN channel with feedback link and superposition coding. 68
4.5 Two-user Gaussian MAC with common feedback link and superposition coding. 69
4.6 Two-user Gaussian BC with feedback link and superposition coding. 71

5.1 AWGN channel achievable rate region 80
5.2 AWGN channel achievable rate region 81
5.3 Sum rate for quantized feedback versus quantization rate 84
5.4 Sum capacity versus power allocation 88

5.5 Symmetric MAC achievable rate region 89
5.6 Symmetric MAC achievable rate region 89
5.7 Performance of superposition coding for the asymmetric MAC with quantized feedback 96
5.8 Performance of superposition coding for the asymmetric MAC with quantized feedback 97
5.9 Sum rate versus quantization rate 100
5.10 Performance of superposition coding for the symmetric BC with quantized feedback 103
5.11 BC achievable rate region 104
5.12 BC achievable rate region 104
5.13 Performance of superposition coding for the asymmetric BC with quantized feedback 113
5.14 Performance of superposition coding for the asymmetric BC with quantized feedback 114

6.1 Finite-Blocklength performance of superposition coding for the symmetric AWGN channel with quantized feedback 122
6.2 Finite-Blocklength performance of superposition coding for the symmetric AWGN channel with quantized feedback 123
6.3 Finite-Blocklength performance of superposition coding for the symmetric AWGN channel with quantized feedback 124
6.4 Finite-Blocklength performance of superposition coding for the symmetric MAC with quantized feedback 131
6.5 Finite-Blocklength performance of superposition coding for the symmetric MAC with quantized feedback 132
6.6 Finite-Blocklength performance of superposition coding for the symmetric MAC with quantized feedback 133
6.7 Finite-Blocklength performance of superposition coding for the symmetric BC with quantized feedback 140
6.8 Finite-Blocklength performance of superposition coding for the symmetric BC with quantized feedback 141
6.9 Finite-Blocklength performance of superposition coding for the symmetric BC with quantized feedback 142

1

Introduction

1.1 Motivation and Scope of Work

In our more and more connected world the amount of communicated data constantly increases each year and there is no end in sight. On the one hand there is an ever increasing demand of internet bandwidth especially from private users. One driving factor here is the popularity of high-definition video streaming services. On the other hand professional services that demand high reliability and low latency are currently developed and are now the main selling point for future mobile networks, such as the soon to be rolled out fifth generation mobile network 5G.

The main limiting factors for the performance of wireless communication systems are the available bandwidth, the available or legally allowed transmit power, and the number of users that simultaneously use the shared medium. In the last three decades there was tremendous effort in research and development to efficiently use these resources. High signal processing power in combination with modern coding such as low-density parity-check (LDPC) coding or polar coding allows operation very close to the theoretical channel capacity if the blocklength is sufficiently large.

In multiuser scenarios, where either more transmitters communicate with one single receiver or one single transmitter communicates with more receivers, today's communication standards rely on establishing largely non-interfering logical communication links. The user separation is either in the frequency domain (frequency division multiple access), time domain (time division multiple access) or logical code domain (code division multiple access). In contrast to this separation approach it is known since the 1970s that user collision can increase the channel capacity of multiple access scenarios [31]. To allow user coordination the transmitters need additional information through a feedback link. Practical communication standards already use a low rate

feedback link, e.g., to inform the transmitters about the channel state, transmit and receive power control, and other control signals. By contrast, a lot of research considered an unrealistic perfect feedback link since this assumption simplified the analysis of such systems. In the last years research shifted to noisy feedback links or rate-limited feedback links to incorporate more realistic models.

Since the beginning of communication theory it was of great interest how well communication systems could possibly perform under low latency requirements [74, 78, 79], or in other words, in the finite blocklength regime. However, due to the great success of asymptotic performance analysis research early shifted to studying such ultimate limits. Especially in the early days of wireless communication the contrast between practice and theoretical research could not have been larger: practical analog communication or later relatively short blocklengths in the first digital communication devices on the one hand, and asymptotic channel capacity research results on the other hand. Over the years industry pretty much closed this gap using modern coding such as the already mentioned low-density parity-check (LDPC) codes with extremely large blocklengths. These excellent achievable rates very close to channel capacity are favoured for applications where high latency is no problem, e.g., digital video broadcasting (DVB).

In real-time applications high latencies due to coding delays cannot be tolerated and one has to use substantially shorter blocklengths. In this regime there is significant capacity backoff. Recent breakthroughs in finite blocklength analysis [65–67] characterized and quantified this backoff. Intuitive expressions analogous to the channel capacity in the asymptotic regime were derived. This resulted in an increasing focus on this research area. Instead of only having the capacity as the only value that characterizes the ultimate performance limit, in the finite-blocklength regime there are the error probability and blocklength as additional parameters. Generally, tolerating higher error probabilities (for a specific blocklength) or increasing the blocklength (for a specific error probability) reduces the backoff from channel capacity. For code designers it is of central importance to be able to quantify and distinguish the portion of the gap between channel capacity due to the code itself and due to the fundamental finite-blocklength limits.

In the finite-blocklength regime the potential gain due to channel output feedback is twofold: In multiuser communication scenarios the channel capacity can be increased [31] and thus the ultimate finite-blocklength limit with zero backoff is also increased. Furthermore, feedback coding schemes (such as [60, 61, 69, 70]) can drastically simplify the coding and decoding complexity. And most importantly, the error decay behaviour as a function of the blocklength is much faster (at least doubly exponential versus exponentially without feedback). This is well known for perfect feedback, that is, if the transmitter(s) are provided with the exact channel output signal. For imperfect feedback many of the benefits still hold and were widely studied [1, 3–5, 10, 11, 13–15, 33–35, 42, 43, 46, 47, 51, 54, 55, 63, 75, 76, 89, 90].

Although direct channel output feedback is still mainly of theoretical interest (with some exceptions, such as [44]), commercial communication standards already rely on low-rate feedback links.

- 3G cellular networks (3GPP Release - 99) use feedback for exchanging control information. It implements fast power control feedback on uplink and downlink. In addition it was the first standard with codebook based beamforming that required codebook based feedback [50].

- Long-Term Evolution (LTE) cellular networks support broad feedback such as feedback of channel quality, choice of frequency bands, or channel spatial information via a codebook; however LTE is still designed to yield a feedback overhead of one percent or less [36].

- Feedback will be a key ingredient for future 5G cellular networks with coordinated multipoint transmission [21].

- In WLAN (IEEE 802.11n) feedback is used to establish reciprocity in the transmit directions; two users exchange training data and afterwards each user sends its quantized channel estimate to the other user [50].

Motivated by these practically available low-rate feedback links we investigate whether coordinated communication with low-rate quantized channel output feedback can still be beneficial depending on the amount of quantization rate. We are interested in quantized feedback because this is the most general reasonably realistic assumption since due to digital signal processing the feedback is at least quantized. On the other end there are scenarios with almost perfect feedback such as the communication of a satellite with a ground station. The satellite is highly limited in transmit power whereas the ground station has almost unbounded available transmit power for feedback. Here the ground station could drastically help the satellite to efficiently use the available transmit power.

Although recent communication standards rely on side-information for the transmitter(s) to establish coordination between them, none of the above exemplarily mentioned standards uses feedback at a rate near that of the forward channel. The feedback is still considered "necessary evil" and limited to the absolute minimum due to the large overhead.

However, new requirements for future cellular networks, most importantly high reliability and low latency, that is, low blocklength, might eventually enforce providing a relatively high-rate feedback link to comply with those contradictory requirements. At this stage, state-of-the-art coding schemes already narrow the space for future improvements to a gap where half the backoff from capacity is already due to the fundamental finite-blocklength limit [66].

Motivated by these disillusioning results we study if quantized feedback could possibly be a last resort to overcome these problems in the regime of ever decreasing latency requirements and hence decreasing blocklengths.

1.2 Outline and Contributions

We next briefly summarize our contributions and outline each remaining chapter of this thesis.

Chapter 2: Preliminaries

In this chapter we introduce the relevant concepts and summarize previous research that serve as a basis throughout this thesis. We review the channel models for the Gaussian channel without and with feedback, Gaussian multiple access channel without and with feedback, and Gaussian broadcast channel without and with feedback, including channel capacity and finite-blocklength achievability results. Then, we briefly discuss convex optimization and difference of convex programming together with the efficient concave-convex procedure algorithm.

Chapter 3: MIMO Gaussian Information Bottleneck with Optimal Power Allocation

The focus of this thesis is on quantized feedback. In Chapter 3 we use the information bottleneck method to abstractly model the channel output compression as a Gaussian information bottleneck. We derive the information-rate function for the Gaussian MIMO channel that characterizes the maximum mutual information between source and compressed signal under a rate constraint. This rate constraint represents the quantization rate. We then give an equivalent representation of the channel output compression where in addition to the channel noise we have additive quantization noise. We thus show how to represent the overall system as an equivalent Gaussian channel.

Furthermore, we broaden the scenario of interest to the case where the transmit power allocation is variable as well. Hence, we introduce the information-rate-power function that jointly characterizes the maximum mutual information between source and compressed signal under a quantization rate and transmit power constraint. We then show that solving the information-rate-power function means solving a difference of convex functions program. Eventually, we discuss the properties of the information-rate-power function.

This chapter builds on the following publications: Parts of this chapter, especially the formulation of the Gaussian information bottleneck for the Gaussian vector channel, have been originally published in [24] and [86].

Chapter 4: Feedback Model

Throughout this thesis we study communication over Gaussian channels in conjunction with GIB-modelled channel output compression. This analysis strictly holds only for Gaussian source distributions. In Chapter 4 we thus start by defining a discrete source model that asymptotically converges to a Gaussian distribution.

We next formulate the algebraic feedback coding structure for the AWGN channel, the Gaussian multiple access channel, and the Gaussian broadcast channel. Following this algebraic coding structure we propose a superposition coding scheme that superimposes a feedback-based coding component with a conventional coding component that completely ignores the feedback. We further describe how the receiver is aware of the quantization noise and how this side-information positively affects the performance of the proposed superposition scheme.
Specifically, we propose a block-structure for the superposition that allows to decode the conventional component first and second the feedback coding component without any interference due to the superposition.

This chapter builds on the following publications: The source signal model has been originally published in [24] and the idea of the superposition coding scheme has been previously published in [25].

Chapter 5: Asymptotic Superposition Coding

In Chapter 5 we extensively study the proposed superposition coding scheme for various Gaussian channel scenarios in the asymptotic regime. We start with superposition coding for the AWGN channel and confirm that a superposition is not beneficial in this scenario, since feedback cannot increase the channel capacity for the AWGN channel.

The AWGN channel setting is then extended to the symmetric Gaussian multiple access channel and the symmetric Gaussian broadcast channel. We formulate the achievable sum rates and work out how to maximize the achievable sum rates. To this end, we show how to split the maximization problems into concave and convex components such that the resulting problem can be solved using difference of convex functions programming. We give adapted convex-concave procedure algorithms that solve each optimization problem. Then, we numerically discuss the performance of these solutions.

Next, we extend the previous symmetric discussions to asymmetric settings and propose a necessary symmetrization procedure for the Gaussian broadcast channel to be able to optimize its performance using the same tool set. We again show how to split the problem into concave and convex components and give adapted convex-concave procedure algorithms that solve each optimization problem. Subsequently, we numerically discuss the performance of these asymmetric solutions and especially concentrate on

the influence of the channel asymmetry.

This chapter builds on the following publications: Superposition coding for the symmetric MAC has been previously published in [25], the asymmetric MAC has been published in [26] and the symmetric BC has been published in [27].

Chapter 6: Finite Blocklength Superposition Coding

In Chapter 6 we use recent findings of achievable rates for non-vanishing error probabilities in the finite-blocklength regime to specialize our proposed suerposition coding scheme to this regime. We thus derive error probability expressions for each component of the superposition coding scheme for the AWGN channel, the Gaussian MAC, and the Gaussian BC. Next, we show that due to imperfect decoding the error probabilities are coupled and we propose regions where the approximation of decoupled error probabilities is sufficiently accurate.

We then formulate a partly combinatorial optimization problem that jointly finds the optimal power allocation (as in the asymptotic regime) and blocklength allocation. We propose an approximate solving procedure that successively finds the asymptotic power allocation and blocklength allocation. Eventually, we numerically assess the performance of this successive optimization procedure.

This chapter builds on the following publications: A first analysis of the error probability for the AWGN channel with quantized feedback has been previously published in [29]. Superposition coding for the symmetric MAC has been previously published in [28].

Chapter 7: Conclusion and Outlook

Lastly, we conclude this thesis with a summary and we give an outlook where we discuss open problems for potential future research.

1.3 Notation

$\mathbb{N}$	Natural numbers
$\mathbb{R}$	Real numbers
$\mathcal{M}$	Cardinality of a set (calligraphic letters)
x	Deterministic scalar (lowercase italic serif letters)
$\boldsymbol{x}$	Deterministic column vector (lowercase bold italic serif letters)
$\boldsymbol{x}^\intercal$	Deterministic row vector (lowercase bold italic serif letters)
$\boldsymbol{X}$	Deterministic matrix (capital bold italic serif letters)
x	Random scalar (lowercase sans-serif letters)
$\mathbf{x}$	Random column vector (lowercase bold sans-serif letters)
$\mathbf{x}^\intercal$	Random row vector (lowercase bold sans-serif letters)
$\mathbf{X}$	Random matrix (capital bold sans-serif letters)
$f_{\mathbf{x}}(\boldsymbol{x})$	Probability density function; alternatively with a slight abuse of notation just $f(\boldsymbol{x})$
$F_{\mathbf{x}}(\boldsymbol{x})$	Cumulative distribution function; alternatively with a slight abuse of notation just $F(\boldsymbol{x})$
$p_{\mathbf{x}}(\boldsymbol{x})$	Probability mass function; alternatively with a slight abuse of notation just $p(\boldsymbol{x})$
$\mathrm{P}\{\cdot\}$	Probability
$\mathrm{E}\{\cdot\}$	Expectation
$h(\cdot)$	Differential entropy
$H(\cdot)$	Entropy
$I(\cdot;\cdot)$	Mutual information
$\boldsymbol{X}^\intercal$	Transpose of matrix $\boldsymbol{X}$
$\lvert\boldsymbol{X}\rvert$	Determinant of matrix $\boldsymbol{X}$
$[\boldsymbol{X}]_{i,j}$	Element in row i and column j of matrix $\boldsymbol{X}$
$\mathbf{1}$	All-one vector
$\boldsymbol{I}$	Identity matrix
$\mathrm{diag}\{x_n\}_{n=1}^N$	$N \times N$ Diagonal matrix with diagonal entries x_n
$\log$	Natural logarithm or any other base that is clear in the used context
$\log_2$	Binary logarithm
$\log_c$	Logarithm to base c

1.4 Acronyms

AWGN	Additive white Gaussian noise
BC	Broadcast channel
CCP, CCCP	Concave-convex procedure or convex-concave procedure
cdf	Cumulative distribution function
DC	Difference of convex
GIB	Gaussian information bottleneck
IB	Information bottleneck
IBM	Information bottleneck method
i.i.d.	Independent and identically distributed
LDPC	Low density parity check
LTE	Long-Term Evolution
MAC	Multiple access channel
MMSE	Minimum mean square error
MIMO	Multiple-input and multiple-output
MSE	Mean squared error
pdf	Probability density function
pmf	Probability mass function
RD	Rate-distortion
SK	Schalkwijk-Kailath (coding scheme)
SNR	Signal-to-noise ratio
w.l.o.g.	Without loss of generality
WLAN	Wireless local area network
3G	Third generation cellular network
4G	Fourth generation cellular network
5G	Fifth generation cellular network

2

Preliminaries

In this chapter we introduce the relevant concepts and summarize previous research that serve as a basis throughout this thesis. We review the channel models for the Gaussian channel without feedback in Section 2.1 and with feedback in Section 2.2, the Gaussian multiple access channel without feedback in Section 2.3 and with feedback in Section 2.4, and Gaussian broadcast channel without feedback in Section 2.5 and with feedback in Section 2.6, including channel capacity and finite-blocklength achievability results. Then, we briefly introduce the technique of convex optimization in Section 2.7 and difference of convex programming in Section 2.8 together with the efficient concave-convex procedure algorithm.

2.1 Additive White Gaussian Noise Channel

We consider the classical additive white Gaussian noise scenario where one transmitter wants to send information to one single receiver (see Figure 2.1). The transmitter sends the signal $\mathsf{x}[k]$ with transmit power P. The transmitter should be able to communicate messages at rate R over the channel $\mathsf{y}[k] = h\mathsf{x}[k] + \mathsf{z}[k]$. The receiver faces the Gaussian channel noise $\mathsf{z}[k] \sim \mathcal{N}(0, \sigma^2)$. The channel gain h is assumed fixed.

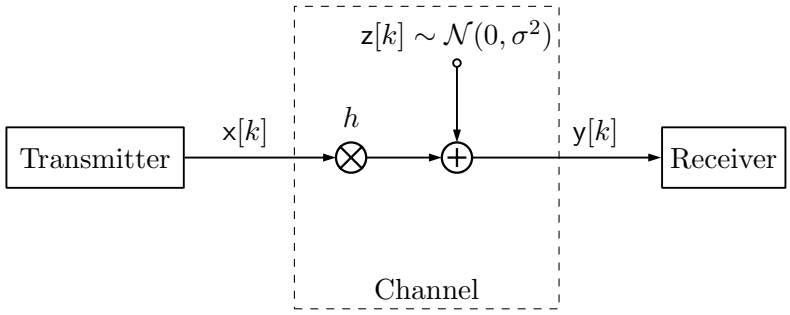

Figure 2.1: AWGN channel.

2.1.1 Capacity

The famous Shannon capacity is named after Claude Shannon, who first proved it in 1948 in his original paper [72, 73]. Capacity is the largest rate that permits reliable decoding.

Theorem 2.1 ([72]). *The channel capacity for the additive white Gaussian noise channel with total available transmit power P, channel noise variance σ^2, and fixed channel gain h is given as*

$$R \leq \frac{1}{2} \log \left(1 + \frac{h^2 P}{\sigma^2} \right). \tag{2.1}$$

For what follows it is often convenient to use the shorthand notation

$$C(\gamma) \triangleq \frac{1}{2} \log(1 + \gamma). \tag{2.2}$$

The achievable rate region R is then bounded as

$$R \leq C(h^2 P/\sigma^2). \tag{2.3}$$

Here, with a slight abuse of notation, the number of arguments indicates that $C(\cdot)$ is the AWGN capacity. The meaning is made clear in the used context or explicitly with indexing, if needed.

2.1.2 Finite Blocklength Performance

In the finite-blocklength regime there is a substantial backoff from the asymptotic channel capacity. The signal-to-noise ratio (SNR) is compactly denoted by $\gamma = h^2 P/\sigma^2$. Polyanskiy et al. found following theorem [66, Thm. 54].

Theorem 2.2 ([66]). *For the AWGN channel with SNR γ and error probability $0 <$*

$\epsilon < 1$, the maximum number of messages $M^*(n,\epsilon)$ is given by[1]

$$\log M^*(n,\epsilon) = nC - Q^{-1}(\epsilon)\sqrt{nV} + O(\log n) \tag{2.4}$$

where C is the classical AWGN channel capacity (2.3) *and V is the channel dispersion given by*

$$V = \frac{\gamma}{2}\frac{\gamma+2}{(\gamma+1)^2}\log^2 e. \tag{2.5}$$

The channel dispersion, which basically characterizes the variability of the channel for finite blocklength, now strictly bounds away the performance from the channel capacity. Formally defined, $M^*(n,\epsilon)$ is the maximum number of messages that we could possibly transmit with blocklength n and error probability ϵ using a (n, M, ϵ)-code, that is,

$$M^*(n,\epsilon) = \max\{M : \exists(n, M, \epsilon)\text{-code}\}. \tag{2.6}$$

Thus, $\frac{1}{n}\log M^*$ can be interpreted as a communication rate. For blocklengths $n \to \infty$ and error probabilities $\epsilon \to 0$, Theorem 2.2 becomes equivalent to Theorem 2.1.

2.2 Additive White Gaussian Noise Channel with Feedback

Like for the AWGN channel without feedback (see Section 2.1) a single transmitter sends the signal $\mathsf{x}[k]$ with transmit power P to communicate information with rate R to one single receiver that receives the signal $\mathsf{y}[k] = h\mathsf{x}[k] + \mathsf{z}[k]$ (see Figure 2.2). The receiver faces the Gaussian channel noise $\mathsf{z}[k] \sim \mathcal{N}(0, \sigma^2)$. The channel gain h is assumed fixed. Now, the receiver feeds back the signal $\mathsf{w}[k]$ to the transmitter. Classically, the feedback was assumed to be exact [69, 70], that is, $\mathsf{w}[k] = \mathsf{y}[k]$, also termed perfect channel output feedback. The transmitter then uses this additional side information to communicate more efficiently. Later research studied more realistic scenarios such as the presence of a noisy feedback link [11,13,84], rate-limited feedback [54,55] and quantized feedback [11,13,51].

2.2.1 Capacity

One might be tempted to think that a perfect feedback link from receiver to transmitter could increase the channel capacity. Surprisingly, this is not the case and was already shown by Shannon in 1956 [71]; Schalkwijk and Kailath proposed a remarkably simple iterative scheme that achieves the AWGN feedback capacity [69, 70] which equals the Shannon AWGN capacity [71, Thm. 6].

[1] with the Q-function $Q(x) = \frac{1}{2\pi}\int_x^\infty \exp(-u^2/2)du$.

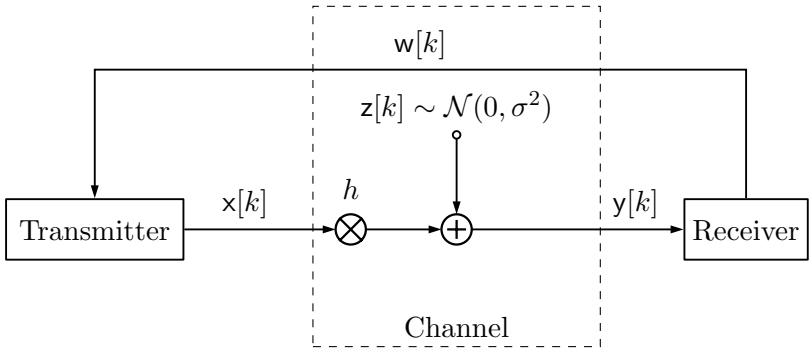

Figure 2.2: AWGN channel with feedback.

Theorem 2.3 ([71]). *The channel capacity for the additive white Gaussian noise channel with perfect feedback with total available transmit power P, channel noise variance σ^2, and fixed channel gain h is given as*

$$R \leq \frac{1}{2} \log \left(1 + \frac{h^2 P}{\sigma^2} \right). \tag{2.7}$$

2.2.2 Error Probability Decay

The celebrated Schalkwijk-Kailath (SK) scheme uses the initial time slot to send the pure message with rate nR to the receiver. The receiver calculates the minimum mean squared error (MMSE) estimate of the message or equivalently of the channel noise. Since the transmitter has the same information due to its causal access via the perfect feedback link it can calculate the MMSE estimates as well and then transmit a correction term in the following time slot. The receiver then incorporates the received (perturbated) correction term to calculate a better estimate. Repeating this procedure for the remaining iterations yields a doubly exponentially decreasing error probability. The original idea of such iterative coding even dates back on Elias in 1956 [23].

Theorem 2.4 ([32]). *The error probability of the SK linear feedback scheme decreases doubly exponentially as*

$$P_e \leq 2Q \left(2^{n(C(\gamma)-R)} \right) \tag{2.8}$$

if $R < C(\gamma)$.

The message transmitted in the initial timeslot comes from an alphabet of size $\mathcal{M} = 2^{nR}$, where R is the transmission rate and n the number of iterations. For $n \to \infty$ this procedure yields to a performance formulated in Theorem 2.3.

More advanced schemes that even show super-exponentially decreasing error probabilities were developed. As a drawback these schemes are non-linear such as the partial

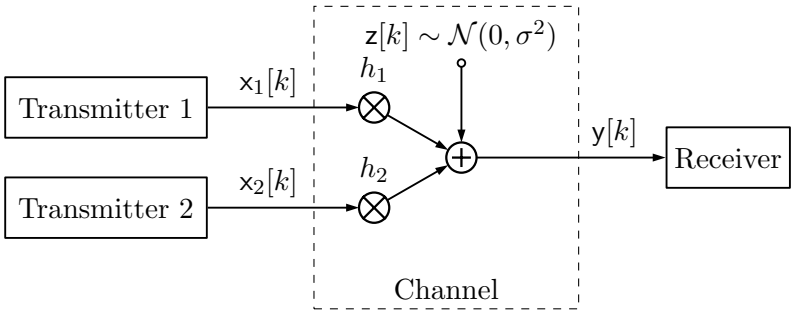

Figure 2.3: Gaussian MAC.

sequential feedback scheme in [1]. Other schemes even show error probabilities that decrease in any exponential order [22,45,64]. In [32,55] the error probability is even of the form $P_e = \exp(-\exp(\ldots \exp(O(1)) \ldots))$[2] with n repetitions of $\exp(\cdot)$.

2.3 Gaussian Multiple Access Channel

Here, we consider the classical multiple access scenario where two transmitters want to send information to a single receiver (see Figure 2.3). The transmitters send the signals $\mathsf{x}_1[k]$ and $\mathsf{x}_2[k]$ and have available transmit powers P_1 and P_2, respectively. Each transmitter should be able to communicate the independent messages with rates R_1 and R_2 over the channel $\mathsf{y}[k] = h_1\mathsf{x}_1[k] + h_2\mathsf{x}_2[k] + \mathsf{z}[k]$. The receiver faces the Gaussian channel noise $\mathsf{z}[k] \sim \mathcal{N}(0, \sigma^2)$. The channel gains h_1 and h_2 are assumed fixed, where without loss of generality $h_2 \leq h_1$.

2.3.1 Capacity

Intuitively, each transmitter cannot convey more information as in the point-to-point scenario where only this transmitter and the receiver are present. Thus, both achievable rates are definitely limited by $R_1 \leq C(h_1^2 P_1/\sigma^2)$ and $R_2 \leq C(h_2^2 P_2/\sigma^2)$. On the other hand, if one transmitter sends with maximum power, e.g., let us assume that transmitter 1 sends with power P_1. This signal interferes at the receiver and results in an effective point-to-point channel with reduced SNR for transmitter 2. As a consequence, the achievable rate is reduced in this scenario and is then given by $R_2 \leq C\left(\frac{h_2^2 P_2}{\sigma^2 + h_1^2 P_1}\right)$. First decoding the message from transmitter 2 and subtracting out this component enables the remaining component from transmitter 1 to be decoded without any interference. This approach is usually termed *onion-peeling*. The rates of transmitter 2 and transmitter 1 can be interchanged in this reasoning. In combination with time-sharing the whole achievable rate region can be found and yields to following statement in the

[2] $f(n) = O(n)$ implies that $\limsup_{n\to\infty} \frac{|f(n)|}{n} < \infty$.

form as in [20] that was formally proved by Ahlswede in 1973 [2]. Instead of time-sharing a rate-splitting approach yields the same achievable rate region that requires only single-user coding without any synchronization among users [68].

Theorem 2.5 ([19]). *The capacity region of the Gaussian multiple-access channel with available transmit powers P_1 and P_2, channel noise variance σ^2, and fixed channel gains h_1 and h_2 is given as*

$$R_1 \leq C\left(\frac{h_1^2 P_1}{\sigma^2}\right), \tag{2.9}$$

$$R_2 \leq C\left(\frac{h_2^2 P_2}{\sigma^2}\right), \tag{2.10}$$

$$R_1 + R_2 \leq C\left(\frac{h_1^2 P_1 + h_2^2 P_2}{\sigma^2}\right). \tag{2.11}$$

For what follows it is often convenient to give a parameterized notation of the achievable sum rate region $R_1 + R_2$ as

$$\begin{aligned} R_1 + R_2 &\leq \min\left(C\left(\frac{h_1^2 P_1}{\sigma^2}\right) + C\left(\frac{h_2^2 P_2}{\sigma^2}\right), C\left(\frac{h_1^2 P_1 + h_2^2 P_2}{\sigma^2}\right)\right) \\ &= C\left(\frac{h_1^2 P_1 + h_2^2 P_2}{\sigma^2}\right) \\ &\triangleq C(h_1^2 P_1, h_2^2 P_2, \sigma^2), \end{aligned} \tag{2.12}$$

since it always holds that (2.9) + (2.10) > (2.11).

Here, with a slight abuse of notation, the number of arguments indicates that $C(\cdot,\cdot,\cdot)$ is the MAC capacity and $C(\cdot)$ is the AWGN capacity. The meaning is clear from in the context or stated, if necessary.

Especially in the symmetric case it might desired that both receivers can achieve the same rates $R_1 = R_2$, that is,

$$R_1 = R_2 \leq \min\left(\frac{1}{2}C\left(\frac{h_1^2 P_1 + h_2^2 P_2}{\sigma^2}\right), C\left(\frac{h_1^2 P_1}{\sigma^2}\right), C\left(\frac{h_2^2 P_2}{\sigma^2}\right)\right). \tag{2.13}$$

2.3.2 Finite Blocklength Performance

In the asymptotic case all messages can be decoded error free if the rates fulfil Theorem 2.5 and especially the onion peeling approach does not cause any error concatenation. In the finite blocklength regime we cannot be certain about correct decoding at any point and therefore we have to account for possible decoding errors and resulting error propagation. This makes the analysis inherently difficult. MolavianJazi and Laneman proved following inner bound for the achievable rates using independent codebooks in 2015 [57, Thm. 1].

Theorem 2.6 ([57]). *For the Gaussian MAC with with available transmit powers P_1 and P_2, channel noise variance σ^2, and fixed channel gains h_1 and h_2, and error probability $0 < \epsilon < 1$,*[3]

$$\log M_1^*(n,\epsilon) = nC_1 - \sqrt{n}[Q^{-1}(\epsilon, \boldsymbol{V}(\gamma_1,\gamma_2))]_1 + O(n^{1/4}), \tag{2.14}$$

$$\log M_2^*(n,\epsilon) = nC_2 - \sqrt{n}[Q^{-1}(\epsilon, \boldsymbol{V}(\gamma_1,\gamma_2))]_2 + O(n^{1/4}), \tag{2.15}$$

$$\log M_1^*(n,\epsilon) + \log M_2^*(n,\epsilon) = nC_{1,2} - \sqrt{n}[Q^{-1}(\epsilon, \boldsymbol{V}(\gamma_1,\gamma_2))]_3 + O(n^{1/4}), \tag{2.16}$$

where $C_1 = C(\gamma_1)$, $C_2 = C(\gamma_2)$, and $C_{1,2} = C(\gamma_1+\gamma_2)$ are the classical AWGN channel capacities (2.3) *with partial SNRs $\gamma_1 = h_1^2P_1/\sigma^2$ and $\gamma_2 = h_2^2P_2/\sigma^2$ and $\boldsymbol{V}(\gamma_1,\gamma_2)$ is the channel dispersion matrix*

$$\boldsymbol{V}(\gamma_1,\gamma_2) = \begin{pmatrix} V(\gamma_1) & V_{1,2}(\gamma_1,\gamma_2) & V_{1,3}(\gamma_1,\gamma_2) \\ V_{1,2}(\gamma_1,\gamma_2) & V(\gamma_2) & V_{2,3}(\gamma_1,\gamma_2) \\ V_{1,3}(\gamma_1,\gamma_2) & V_{2,3}(\gamma_1,\gamma_2) & V(\gamma_1+\gamma_2) + V_3(\gamma_1,\gamma_2) \end{pmatrix}, \tag{2.17}$$

with the point-to-point AWGN channel dispersion V as in (2.5) *and*

$$V_{1,2}(\gamma_1,\gamma_2) = \frac{\gamma_1}{2}\frac{\gamma_2}{(\gamma_1+1)(\gamma_2+1)}\log^2 e, \tag{2.18}$$

$$V_{i,3}(\gamma_1,\gamma_2) = \frac{\gamma_i}{2}\frac{\gamma_1+\gamma_2+2}{(\gamma_1+1)(\gamma_1+\gamma_2+1)}\log^2 e, \quad i \in \{1,2\}, \tag{2.19}$$

$$V_3(\gamma_1,\gamma_2) = \frac{\gamma_1\gamma_2}{(\gamma_1+\gamma_2+1)^2}\log^2 e. \tag{2.20}$$

If we relax the problem to the generally highly suboptimal assumption that leads to a tractable analysis is that we do not study the onion peeling approach that possibly yields to error propagation. Instead, for decoding each transmitted signal we consider the signals from the other transmitter as noise, that is, the effective SNR for decoding the signal from transmitter 1 now is $h_1^2P_1/(\sigma^2+h_2^2P_2)$ and for the signal from transmitter 2 it is $h_2^2P_2/(\sigma^2+h_1^2P_1)$. This then reduces to two separate Gaussian point-to-point channels and adapting Theorem 2.2 yields following Corollary.

Corollary 2.7. *For the Gaussian multiple-access channel with available transmit powers P_1 and P_2, fixed channel gains h_1 and h_2, channel noise variance σ^2, and error probabilities $0 < \epsilon_1 < 1$ and $0 < \epsilon_2 < 1$,*

$$\log M_1^*(n,\epsilon_1) = nC_1 - Q^{-1}(\epsilon_1)\sqrt{nV_1} + O(\log n), \tag{2.21}$$

$$\log M_2^*(n,\epsilon_2) = nC_2 - Q^{-1}(\epsilon_2)\sqrt{nV_2} + O(\log n), \tag{2.22}$$

where $C_1 = C(\gamma_1)$ and $C_2 = C(\gamma_2)$ are the classical AWGN channel capacities (2.3) *with effective SNRs $\gamma_1 = h_1^2P_1/(\sigma^2+h_2^2P_2)$ and $\gamma_2 = h_2^2P_2/(\sigma^2+h_1^2P_1)$ and V_1 and V_2*

[3] with the multi-dimensional Q-function $Q(\boldsymbol{x},\Sigma) = P\{\mathbf{x} \geq \boldsymbol{x}\}$, where $\mathbf{x} \sim \mathcal{N}(\mathbf{0},\Sigma)$.

are the channel dispersions given by

$$V_1 = \frac{\gamma_1}{2}\frac{\gamma_1+2}{(\gamma_1+1)^2}\log^2 e, \tag{2.23}$$

$$V_2 = \frac{\gamma_2}{2}\frac{\gamma_2+2}{(\gamma_2+1)^2}\log^2 e. \tag{2.24}$$

For the interesting scenario where we want to maximize the achievable sum rate in the all symmetric case with the same channel gains $h_1 = h_2 = h$ and symmetric power constraints $P_1 = P_2 = P$ Theorem 2.6 drastically simplifies. In the point of maximum sum rate the sum (2.14)+(2.15) is strictly larger than (2.16). Thus, Theorem 2.6 reduces to the following Corollary [56, eqn. (53)].

Corollary 2.8. *For the symmetric Gaussian multiple-access channel with available transmit powers $P_1 = P_2 = P$, fixed channel gains $h_1 = h_2 = h$, channel noise variance σ^2, and error probability $0 < \epsilon < 1$ the achievable sum rate is*

$$2\log M^*(n,\epsilon) < nC(2\gamma) - Q^{-1}(\epsilon)\sqrt{nV(2\gamma)} + O(n) \tag{2.25}$$

with effective SNRs $\gamma = h^2P/\sigma^2$ and $V(\gamma)$ are the channel dispersions given by

$$V(\gamma) = \frac{\gamma}{2}\frac{\gamma+2}{(\gamma+1)^2}\log^2 e. \tag{2.26}$$

2.4 Gaussian Multiple Access Channel with Feedback

Like for the MAC without feedback (see Section 2.3), two transmitters send the signals $\mathsf{x}_1[k]$ and $\mathsf{x}_2[k]$ with transmit powers P_1 and P_2 to communicate information with rates R_1 and R_2, respectively, to one single receiver that receives the signal $\mathsf{y}[k] = h_1\mathsf{x}_1[k] + h_2\mathsf{x}_2[k] + \mathsf{z}[k]$ (see Figure 2.4). The receiver faces the Gaussian channel noise $\mathsf{z}[k] \sim \mathcal{N}(0,\sigma^2)$. The channel gains h_1 and h_2 are assumed fixed, where without loss of generality $h_2 \leq h_1$. Classically, the feedback was assumed to be perfect, that is, $\mathsf{w}[k] = \mathsf{y}[k]$, where the same feedback is provided for both transmitters [60]. The transmitters then use this additional side information to communicate more efficiently and can thus especially for the MAC establish some user coordination. Later research studied more realistic scenarios such as the presence of a noisy feedback link [33, 34, 46, 47] or rate-limited feedback [75, 76].

2.4.1 Capacity

Based on the Schalkwijk-Kailath coding scheme (see Section 2.2) Ozarow proposed a similar scheme for the two-user Gaussian MAC with perfect feedback [60]. The key concept of this scheme still is the iterative refinement of the message estimate. In the

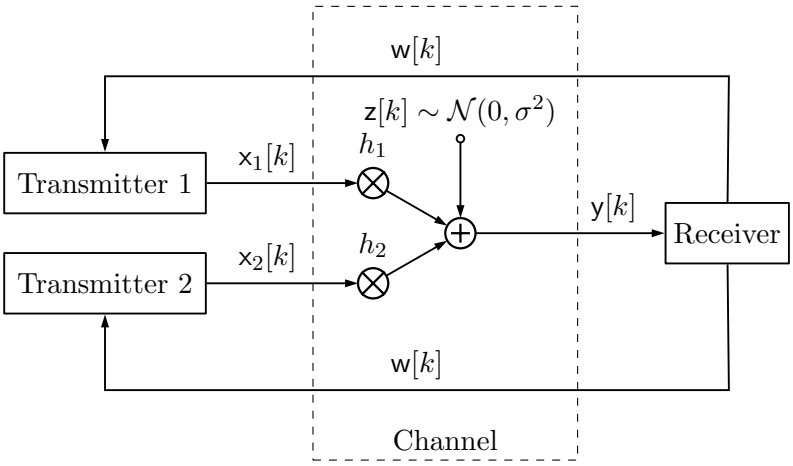

Figure 2.4: Gaussian MAC with feedback.

first two time slots, both transmitters alternately send their raw messages. The remaining time slots are used to transmit updates of the message estimates at the receiver. For infinite blocklength, this simple linear scheme is capacity-achieving. Surprisingly, and in sharp contrast to the point-to-point case, in this multiple user scenario the presence of a perfect feedback link actually increases the channel capacity. Ozarow showed that the full capacity region of the Gaussian MAC with perfect feedback is given by following theorem [60, eqn. (3)].

Theorem 2.9 ([60]). *The capacity region of the two-user Gaussian MAC with perfect channel output feedback with available transmit powers P_1 and P_2, channel noise variance σ^2, and fixed channel gains h_1 and h_2 is the union over $0 \leq \rho \leq 1$ of the rate pairs (R_1, R_2) satisfying*

$$R_1 \leq C\left(\frac{h_1^2 P_1}{\sigma^2}(1-\rho^2)\right), \tag{2.27}$$

$$R_2 \leq C\left(\frac{h_2^2 P_2}{\sigma^2}(1-\rho^2)\right), \tag{2.28}$$

$$R_1 + R_2 \leq C\left(\frac{h_1^2 P_1 + h_2^2 P_2 + 2\sqrt{h_1^2 P_1 h_2^2 P_2}\rho}{\sigma^2}\right). \tag{2.29}$$

If we compare (2.27)–(2.29) with (2.9)–(2.11) we see that the achievable rate region with feedback is strictly larger than without feedback; only for $\rho = 0$ the two regions coincide. Here, ρ can be interpreted as a correlation coefficient that defines the amount of coordination of the two transmitters. The coordination of the transmitters is not explicit via a direct link where they can exchange information but rather implicit as they share some common information due to the same perfect feedback to each transmitter.

In what follows, it is often convenient to give a parameterized notation of the

achievable sum rate region $R_1 + R_2$ as

$$R_1 + R_2 \leq \max_{0\leq\rho\leq 1} \min\left(C\left(\frac{h_1^2 P_1}{\sigma^2}(1-\rho^2)\right) + C\left(\frac{h_2^2 P_2}{\sigma^2}(1-\rho^2)\right), C\left(\frac{h_1^2 P_1 + h_2^2 P_2 + 2\sqrt{h_1^2 P_1 h_1^2 P_2}\rho}{\sigma^2}\right)\right) \triangleq C^{\mathrm{FB}}(h_1^2 P_1, h_2^2 P_2, \sigma^2). \tag{2.30}$$

Here, with a slight abuse of notation, the number of arguments indicates that $C^{\mathrm{FB}}(\cdot,\cdot,\cdot)$ is the MAC capacity with perfect feedback and $C^{\mathrm{FB}}(\cdot) = C(\cdot)$ is the AWGN capacity with perfect feedback.

Since (2.27) and (2.28) are decreasing in ρ so is the first argument in the $\min(\cdot,\cdot)$ in (2.30), whereas the second argument (2.29) in the $\min(\cdot,\cdot)$ in (2.30) is strictly increasing. Consequently, there is one single value ρ^* where both arguments are equal and thus maximizes the achievable sum rate (2.30). Thus, ρ^* is the solution of the quartic equation

$$\left(\sigma^2 + h_1^2 P_1(1-\rho^2)\right)\left(\sigma^2 + h_2^2 P_2(1-\rho^2)\right) = \sigma^2\left(\sigma^2 + h_1^2 P_1 + h_2^2 P_2 + 2\sqrt{h_1^2 P_1 h_1^2 P_2}\rho\right). \tag{2.31}$$

2.4.2 Error Probability Decay

As in the original SK scheme the receiver calculates the MMSE estimate for each message. Via the feedback link both transmitters share the same information about the current estimate of the receiver about its messages. Now, the transmitters cannot only send correction terms for a better estimate at the receiver in the following time slots, but can coordinate and send a correlated common signal. The receiver then again incorporates the received (perturbed) correction terms to calculate better estimates. Repeating this procedure for the remaining iterations yields a doubly exponentially decreasing error probability for each message estimate [60, eqn. (13)].

Theorem 2.10 ([60]). *The error probabilities of the Ozarow linear feedback scheme decrease doubly exponentially as*

$$P_{e_1} \leq 2Q\left(\frac{\sigma^2}{2\sqrt{\sigma^2/12 h_1^2 P_1}(\sigma^2 + h_1^2 P_1(1-\rho^{*2}))} e^{n\left(C\left(\frac{h_1^2 P_1}{\sigma^2}(1-\rho^{*2})\right) - R_1\right)}\right), \tag{2.32}$$

$$P_{e_2} \leq 2Q\left(\frac{\sigma^2}{2\sqrt{\sigma^2/12 h_2^2 P_2}(\sigma^2 + h_2^2 P_2(1-\rho^{*2}))} e^{n\left(C\left(\frac{h_2^2 P_2}{\sigma^2}(1-\rho^{*2})\right) - R_2\right)}\right), \tag{2.33}$$

if

$$R_1 < C\left(\frac{h_1^2 P_1}{\sigma^2}(1-\rho^{*2})\right), \tag{2.34}$$

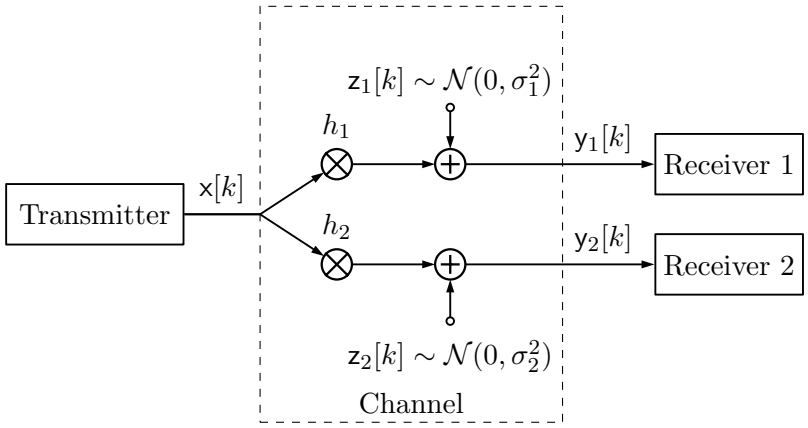

Figure 2.5: Gaussian BC.

$$R_2 < C\left(\frac{h_2^2 P_2}{\sigma^2}(1-\rho^{*2})\right). \tag{2.35}$$

The messages transmitted in the initial times lots have an alphabet size $\mathcal{M}_1 = 2^{nR_1}$ and $\mathcal{M}_2 = 2^{nR_2}$, where R_1 and R_2 are the transmission rates of each transmitter and n the number of iterations. For $n \to \infty$ this procedure yields the performance formulated in Theorem 2.9.

2.5 Gaussian Broadcast Channel

Here, we consider the classical broadcast scenario where a single transmitter wants to send information to two receivers (see Figure 2.5). The transmitter sends the signal $\mathsf{x}[k]$ and has a total available transmit power P. Each receiver should be supplied with independent messages with rates R_1 and R_2 over the channel $\mathsf{y}_1[k] = h_1\mathsf{x}[k] + \mathsf{z}_1[k]$ and $\mathsf{y}_2[k] = h_2\mathsf{x}[k] + \mathsf{z}_2[k]$, respectively. The receivers face the Gaussian channel noises $\mathsf{z}_1[k] \sim \mathcal{N}(0, \sigma_1^2)$ and $\mathsf{z}_2[k] \sim \mathcal{N}(0, \sigma_2^2)$. The channel gains h_1 and h_2 are assumed fixed, where without loss of generality $h_2^2/\sigma_2^2 \leq h_1^2/\sigma_1^2$.

2.5.1 Capacity

The transmitter uses two separate codebooks for conveying information to receiver 1 and receiver 2. Thus, communication to receiver 1 with rate R_1 uses a fraction αP ($0 \leq \alpha \leq 1$) of the transmit power and communication to receiver 2 with rate R_2 with the remaining transmit power $(1-\alpha)P$. Since we assumed $h_2^2/\sigma_2^2 \leq h_1^2/\sigma_1^2$, the weaker receiver 2 is additionally interfered by the signal for the stronger receiver 1. Therefore, receiver 2 has an even worse effective SNR of $h_2^2(1-\alpha)P/(\sigma_2^2 + h_2^2\alpha P)$. On the contrary, the stronger receiver 1 can first decode the interference caused by the

signal for the weaker receiver 2 in the same way as receiver 2 itself, that is, it first considers its designated information as interference noise and decodes the message for the other receiver. Then, the stronger receiver 1 can subtract the decoded codeword for receiver 2 and thus sees the non-interfered SNR $h_1^2\alpha P/\sigma_1^2$.

The capacity region for this classical setup was proven by Thomas Cover in 1972 [19] and is given by following theorem.

Theorem 2.11 ([19]). *The capacity region of the Gaussian broadcast channel with total available transmit power P, channel noise variances σ_1^2 and σ_2^2, and fixed channel gains h_1 and h_2 is given by the union over $0 \leq \alpha \leq 1$ of*

$$R_1 \leq C\left(\frac{h_1^2\alpha P}{\sigma_1^2}\right), \tag{2.36}$$

$$R_2 \leq C\left(\frac{h_2^2(1-\alpha)P}{\sigma_2^2 + h_2^2\alpha P}\right), . \tag{2.37}$$

For what follows it is often convenient to give a parameterized notation of the achievable sum rate region $R_1 + R_2$ as

$$R_1 + R_2 \leq C\left(\frac{h_1^2\alpha P}{\sigma_1^2}\right) + C\left(\frac{h_2^2(1-\alpha)P}{\sigma_2^2 + h_2^2\alpha P}\right) \triangleq C(h_1^2\alpha P, h_2^2(1-\alpha)P, \sigma_1^2, \sigma_2^2). \tag{2.38}$$

Here, with a slight abuse of notation, the number of arguments indicates that $C(\cdot,\cdot,\cdot,\cdot)$ is the BC capacity and $C(\cdot)$ is the AWGN capacity.

Note that in the symmetric case, where $h_1^2/\sigma_1^2 = h_2^2/\sigma_2^2 = h^2/\sigma^2$ the achievable sum rate (2.38) reduces to

$$R_1 + R_2 \leq C\left(\frac{h_1^2\alpha P}{\sigma_1^2}\right) + C\left(\frac{h_2^2(1-\alpha)P}{\sigma_2^2 + h_2^2\alpha P}\right) = C(h^2P/\sigma^2), \tag{2.39}$$

that does not depend on the actual value α. Especially in the symmetric case it might be desired that both receivers can achieve the same rates $R_1 = R_2$, that is,

$$C\left(\frac{h_1^2\alpha P}{\sigma_1^2}\right) = C\left(\frac{h_2^2(1-\alpha)P}{\sigma_2^2 + h_2^2\alpha P}\right), \tag{2.40}$$

which is equivalent to

$$\frac{h_1^2\alpha P}{\sigma_1^2} = \frac{h_2^2(1-\alpha)P}{\sigma_2^2 + h_2^2\alpha P}. \tag{2.41}$$

This condition is fulfilled if α satisfies the following equation,

$$\alpha^2 + \alpha\frac{\sigma_1^2/h_1^2 + \sigma_2^2/h_2^2}{P} - \frac{\sigma_1^2/h_1^2}{P} = 0, \tag{2.42}$$

which is solved by

$$\alpha = -\frac{\sigma_1^2/h_1^2 + \sigma_2^2/h_2^2}{2P} + \sqrt{\left(\frac{\sigma_1^2/h_1^2 + \sigma_2^2/h_2^2}{2P}\right)^2 + \frac{\sigma_1^2/h_1^2}{P}}. \tag{2.43}$$

While in the symmetric case the achievable sum rate does not change for such power choices it clearly does in the asymmetric case.

2.5.2 Finite Blocklength Performance

In the asymptotic case the receiver with higher SNR was able to decode both its designated message as well as the message for the weaker receiver. This only applies for infinite blocklengths where no decoding errors occur. For finite blocklength, even the receiver with higher SNR might decode the message for the weaker receiver erroneous and thus introduces additional degradation before decoding its designated message. This very fact complicates the finite blocklength treatment of the broadcast channel.

There is some effort to overcome this problem, e.g., via a specialization of superposition coding [58], but the general problem of finding an expression analogous to the AWGN channel (2.4) remains open.

A simplification occurs if the transmitter does not need to communicate independent messages to each transmitter, but only broadcasts one common message to all transmitters. As a consequence, error propagation cannot happen and the performance is equal to point-to-point AWGN channels as in Theorem 2.2. The SNRs are $\gamma_1 = h_1^2 P/\sigma_1^2$ and $\gamma_2 = h_2^2 P/\sigma_2^2$. Even though the transmit power is not split as αP and $(1-\alpha)P$ as in Theorem 2.11 both receivers still have different SNRs and therefore also different performance.

Corollary 2.12. *For the common message Gaussian broadcast channel with SNRs $\gamma_1 = h_1^2 P/\sigma_1^2$ and $\gamma_2 = h_2^2 P/\sigma_2^2$, and error probabilities $0 < \epsilon_1 < 1$ and $0 < \epsilon_2 < 1$,*

$$\log M_1^*(n, \epsilon_1) = nC_1 - Q^{-1}(\epsilon_1)\sqrt{nV_1} + O(\log n), \tag{2.44}$$

$$\log M_2^*(n, \epsilon_2) = nC_2 - Q^{-1}(\epsilon_2)\sqrt{nV_2} + O(\log n) \tag{2.45}$$

where C_1 and C_2 are the classical AWGN channel capacities (2.3) *and V_1 and V_2 are the channel dispersions given by*

$$V_1 = \frac{\gamma_1}{2}\frac{\gamma_1 + 2}{(\gamma_1 + 1)^2}\log^2 e, \tag{2.46}$$

$$V_2 = \frac{\gamma_2}{2}\frac{\gamma_2 + 2}{(\gamma_2 + 1)^2}\log^2 e. \tag{2.47}$$

As we communicate one common message, $M_1^*(n, \epsilon_1) = M_2^*(n, \epsilon_2)$ since both alphabets are the same. However, the different point-to-point capacities result in different decoding error probabilities. Due to $h_2^2/\sigma_2^2 \leq h_1^2/\sigma_1^2$ it follows that $\epsilon_2 \geq \epsilon_1$.

If both receivers should be supplied with independent messages an exact classification would have to account for the possible error propagation. A generally highly suboptimal assumption that leads to a tractable analysis is that for both receivers we consider the signals from the other receiver as noise, that is, instead of the achievable rate of the stronger receiver being of the form (2.36) both achievable rates now have the form (2.37). Note that in contrast to Theorem 2.12 where all the power is used to transmit the common message we now still split the power as αP and $(1-\alpha)P$ as in Theorem 2.11. Adapting Corollary 2.12 then yields the following related Corollary.

Corollary 2.13. *For the Gaussian broadcast channel with total available transmit power P, fixed channel gains h_1 and h_2, channel noise variances σ_1^2 and σ_2^2, and error probabilities $0 < \epsilon_1 < 1$ and $0 < \epsilon_2 < 1$,*

$$\log M_1^*(n, \epsilon_1) = nC_1 - Q^{-1}(\epsilon_1)\sqrt{nV_1} + O(\log n), \tag{2.48}$$

$$\log M_2^*(n, \epsilon_2) = nC_2 - Q^{-1}(\epsilon_2)\sqrt{nV_2} + O(\log n) \tag{2.49}$$

where $C_1 = C(\gamma_1)$ and $C_2 = C(\gamma_2)$ are the classical AWGN channel capacities (2.3) *and V_1 and V_2 are the channel dispersions given by*

$$V_1 = \frac{\gamma_1}{2}\frac{\gamma_1 + 2}{(\gamma_1 + 1)^2}\log^2 e, \tag{2.50}$$

$$V_2 = \frac{\gamma_2}{2}\frac{\gamma_2 + 2}{(\gamma_2 + 1)^2}\log^2 e, \tag{2.51}$$

where the tradeoff parameter α is in $[0, 1]$ that defines the effective SNRs

$$\gamma_1 = \frac{\alpha h_1^2 P}{\sigma_1^2 + (1-\alpha)h_1^2 P}, \tag{2.52}$$

$$\gamma_2 = \frac{(1-\alpha)h_2^2 P}{\sigma_1^2 + \alpha h_2^2 P}. \tag{2.53}$$

2.6 Gaussian Broadcast Channel with Feedback

As for the BC without feedback (see Section 2.5), a single transmitter sends the signal $\mathsf{x}[k]$ with transmit power P to communicate information with rates R_1 and R_2 to two receivers that receive the signals $\mathsf{y}_1[k] = h_1\mathsf{x}[k] + \mathsf{z}_1[k]$ and $\mathsf{y}_2[k] = h_2\mathsf{x}[k] + \mathsf{z}_2[k]$, respectively (see Figure 2.6). The receivers face the Gaussian channel noises $\mathsf{z}_1[k] \sim \mathcal{N}(0, \sigma_1^2)$ and $\mathsf{z}_2[k] \sim \mathcal{N}(0, \sigma_2^2)$. The channel gains h_1 and h_2 are assumed fixed, where without loss of generality $h_2^2/\sigma_2^2 \leq h_1^2/\sigma_1^2$. Classically, the feedback was assumed to be perfect [61], that is, $\mathsf{w}_1[k] = \mathsf{y}_1[k]$ and $\mathsf{w}_2[k] = \mathsf{y}_2[k]$. The transmitter then uses this additional side information to communicate more efficiently. Later research studied more realistic scenarios such as the presence of a noisy feedback link [63] or rate-limited feedback [89, 90].

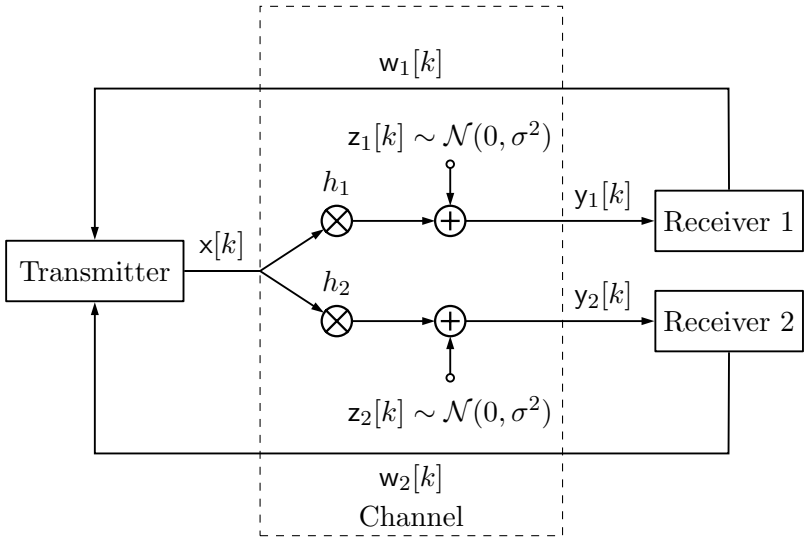

Figure 2.6: Gaussian BC with feedback.

2.6.1 Capacity – Duality

The capacity of the Gaussian broadcast channel with perfect feedback is still unknown [5]. Similar as for the MAC with perfect feedback Ozarow and Leung proposed a SK-inspired coding scheme for the BC with perfect feedback that shows increased achievable rates [61]. Amor et al. showed that there is a duality between the Gaussian multiple access channel with perfect feedback and the Gaussian broadcast channel with perfect feedback: the linear feedback Ozarow scheme (see Section 2.4.1), which achieves capacity for the MAC, adapted to the BC is sum-rate optimal over all linear feedback schemes [4,5]. Linear feedback is shown to be strictly suboptimal only for common message transmission [88]. Theorem 2.9 thus results in the linear-feedback sum-capacity for the BC with perfect feedback [5, eqn. (107)].

Theorem 2.14 ([60])**.** *The linear-feedback sum-capacity region of the two-user Gaussian BC with perfect channel output feedback, transmit power $P = P_1 + P_2$, channel noise variances σ_1^2 and σ_2^2, and fixed channel gains h_1 and h_2 is the union of the rate pairs (R_1, R_2) satisfying*

$$R_1 \leq C\left(\gamma_1(1-\rho^{*2})\right), \tag{2.54}$$

$$R_2 \leq C\left(\gamma_2(1-\rho^{*2})\right), \tag{2.55}$$

where ρ^* is chosen to maximize the sum-capacity of the dual MAC with perfect feedback with SNR components $\gamma_1 = h_1^2 P_1/\sigma_1^2$ and $\gamma_2 = h_2^2 P_2/\sigma_2^2$.

2.6.2 Error Probability Decay

As in the original SK scheme the receivers calculate the MMSE estimate for its designated message. Note that this is a single-user approach since each receiver only decodes its designated message while treating the message component for the other receiver as noise. Via the feedback link the transmitter has access to the current message estimates of the receivers. This is essentially the same situation as in the MAC case. Now, the transmitter cannot only send correction terms for a better estimate at the receivers in the following timeslots, but can cooperatively send some correlated common signal for both receivers. The receivers then again incorporate the received (perturbated) correction terms to calculate better estimates. Repeating this procedure for the remaining iterations yields a doubly exponentially decreasing error probability for each message estimate as for the MAC [60, (13)].

Theorem 2.15. *The error probabilities of the equivalent Ozarow linear feedback scheme for Gaussian broadcast channels with perfect feedback decrease doubly exponentially as*

$$P_{e_1} \leq 2Q\left(\frac{\sigma_1^2}{2\sqrt{\sigma_1^2/12h_1^2P_1}(\sigma_1^2+h_1^2P_1(1-\rho^{*2}))}e^{n\left(C\left(\frac{h_1^2P_1}{\sigma_1^2}(1-\rho^{*2})\right)-R_1\right)}\right), \tag{2.56}$$

$$P_{e_2} \leq 2Q\left(\frac{\sigma_2^2}{2\sqrt{\sigma_2^2/12h_2^2P_2}(\sigma_2^2+h_2^2P_2(1-\rho^{*2}))}e^{n\left(C\left(\frac{h_2^2P_2}{\sigma_2^2}(1-\rho^{*2})\right)-R_2\right)}\right), \tag{2.57}$$

if

$$R_1 < C\left(\frac{h_1^2P_1}{\sigma_1^2}(1-\rho^{*2})\right), \tag{2.58}$$

$$R_2 < C\left(\frac{h_2^2P_2}{\sigma_2^2}(1-\rho^{*2})\right). \tag{2.59}$$

The messages transmitted in the initial timeslots have an alphabet size $\mathcal{M}_1 = 2^{nR_1}$ and $\mathcal{M}_2 = 2^{nR_2}$, where R_1 and R_2 are the transmission rates of each transmitter and n the number of iterations. For $n \to \infty$ this procedure leads to the performance formulated in Theorem 2.14.

2.7 Convex Optimization

A set $\mathcal{X}$ is convex if for all $\boldsymbol{x}_1$ and $\boldsymbol{x}_2$ in the set, it holds that

$$\theta\boldsymbol{x}_1 + (1-\theta)\boldsymbol{x}_2 \in \mathcal{X} \quad \forall \boldsymbol{x}_1, \boldsymbol{x}_2 \in \mathcal{X} \tag{2.60}$$

for all $0 \leq \theta \leq 1$.

A function $f : \mathbb{R}^n \to \mathbb{R}$ is convex if its domain is a convex set and if for all $\boldsymbol{x}_1$ and

$\boldsymbol{x}_2$ in its domain, we have

$$f(\theta \boldsymbol{x}_1 + (1-\theta)\boldsymbol{x}_2) \leq \theta f(\boldsymbol{x}_1) + (1-\theta) f(\boldsymbol{x}_2), \tag{2.61}$$

for all $0 \leq \theta \leq 1$.

An equivalent condition that suffices to characterize a differentiable function $f : \mathbb{R}^n \to \mathbb{R}$ as convex is as follows. If its domain is a convex set and it holds that

$$f(\boldsymbol{x}_0 + \Delta\boldsymbol{x}) \geq f(\boldsymbol{x}_0) + \Delta\boldsymbol{x}^\intercal \nabla f(\boldsymbol{x}_0) \tag{2.62}$$

for all $\boldsymbol{x}_0$ and $\boldsymbol{x}_0 + \Delta\boldsymbol{x}$ in its domain, then f is convex. Geometrically speaking, the tangent at any point of a convex function lies below the function.

Another equivalent condition that suffices to characterize a twice differentiable function $f : \mathbb{R}^n \to \mathbb{R}$ as convex is as follows. f is convex if its domain is a convex set and

$$\nabla^2 f(\boldsymbol{x}) \succeq 0 \tag{2.63}$$

for all $\boldsymbol{x}$ in its domain.

We follow Boyd [7] and define a standard convex optimization problem as

$$\begin{aligned} \underset{\boldsymbol{x}}{\text{minimize}} \quad & f_0(\boldsymbol{x}) \\ \text{subject to} \quad & f_i(\boldsymbol{x}) \leq 0, \quad i = 1, \ldots, m, \\ & h_i(\boldsymbol{x}) = 0, \quad i = 1, \ldots, p, \end{aligned} \tag{2.64}$$

where $\boldsymbol{x} \in \mathbb{R}^n$ is the optimization variable, $f_0 : \mathbb{R}^n \to \mathbb{R}$ is the convex objective function to be minimized, and the inequality constraint functions $f_i : \mathbb{R}^n \to \mathbb{R}$, $i = 1, \ldots, m$ have to be convex, and equality constraint functions $h_i : \mathbb{R}^n \to \mathbb{R}$, $i = 1, \ldots, p$ have to be affine.

The convex minimization (2.64) can be replaced by

$$\begin{aligned} \underset{\boldsymbol{x}}{\text{maximize}} \quad & f_0(\boldsymbol{x}) \\ \text{subject to} \quad & f_i(\boldsymbol{x}) \leq 0, \quad i = 1, \ldots, m, \\ & h_i(\boldsymbol{x}) = 0, \quad i = 1, \ldots, p, \end{aligned} \tag{2.65}$$

where $f_0(\boldsymbol{x})$ is a concave objective. Solving (2.65) is equivalent to solving (2.64) with the convex objective function $-f_0(\boldsymbol{x})$.

Problems of the form (2.65) and (2.64) can solved efficiently and a wide variety of algorithms, solvers, and software for such tasks exist - probably most prominently by the CVX software developed by Grant and Boyd [39, 40] .

Algorithm 1 Basic CCP algorithm [49, Alg. 1.1]

Require: Initial feasible point $\boldsymbol{x}_0$

1: $k := 0$
2: **while** stopping criterion not satisfied **do**
3: Form $\hat{g}_i^{(k)}(\boldsymbol{x}) = g_i(\boldsymbol{x}_k) + (\boldsymbol{x} - \boldsymbol{x}_k)^\intercal \nabla g_i(\boldsymbol{x}_k)$ for $i = 0, \ldots, m$
4: Determine $\boldsymbol{p}_{k+1}$ by solving the convex problem

$$\begin{aligned} &\text{minimize} && f_0(\boldsymbol{x}) - \hat{g}_0^{(k)}(\boldsymbol{x}) \\ &\text{subject to} && f_i(\boldsymbol{x}) - \hat{g}_i^{(k)}(\boldsymbol{x}) \leq 0,\ i = 0, \ldots, m \end{aligned}$$

5: $k := k + 1$
6: **end while**
7: **return** $\boldsymbol{x}_k$

2.8 Difference of Convex Functions Programming

The difference of convex functions (DC) programming problem in standard form is given by [49]

$$\begin{aligned} \underset{\boldsymbol{x}}{\text{minimize}} \quad & f_0(\boldsymbol{x}) - g_0(\boldsymbol{x}) \\ \text{subject to} \quad & f_i(\boldsymbol{x}) - g_i(\boldsymbol{x}) \leq 0, \quad i = 1, \ldots, m, \end{aligned} \tag{2.66}$$

where $\boldsymbol{x} \in \mathbb{R}^n$ is the optimization variable and the functions $f_i : \mathbb{R}^n \to \mathbb{R}$, $i = 0, \ldots, m$, and $g_i : \mathbb{R}^n \to \mathbb{R}$, $i = 0, \ldots, m$, have to be convex. If the functions $g_i(\boldsymbol{x})$ are affine (2.66) reduces to the convex optimization problem (2.64). But in general, a DC program is harder to solve. Often, the partitioning of the original optimization problem into the differences of convex functions is obvious and can be directly deduced from the structure of the original problem. In fact, any twice continuously differentiable function can be expressed as a difference of convex functions [41].

2.8.1 Convex-Concave Procedure

The convex-concave procedure (CCP), introduced as concave-convex procedure [91], is a practically feasible heuristic that finds a local optimum of (2.66). Thus, the point where the algorithm converges to generally depends on the initial point $\boldsymbol{x}_0$. Typically one runs the algorithm with many different feasible initial $\boldsymbol{x}_0$ and determines the final solution as the best intermediate solution. The basic idea of the iterative CCP algorithm is to find a point where the gradient of the convex part $f_0(\boldsymbol{x})$ in the next iteration equals the negative gradient of the concave part $-g_0(\boldsymbol{x})$ of the previous iteration (if it exists) [91],

$$\nabla f_0(\boldsymbol{x}_{k+1}) = \nabla g_0(\boldsymbol{x}_k) \tag{2.67}$$

which itself is a convex optimization problem. The solution to this auxiliary problem

Algorithm 2 Line search for CCP (see Alg. 1) [49, Alg. 1.2]

Require: A solution $\boldsymbol{x}_{k+1}$ and $\alpha > 1$

1: $t := 1$
2: **while** $f_0(\boldsymbol{x}_k + \alpha t(\boldsymbol{x}_{k+1} - \boldsymbol{x}_k)) - g_0(\boldsymbol{x}_k + \alpha t(\boldsymbol{x}_{k+1} - \boldsymbol{x}_k)) \leq f_0(\boldsymbol{x}_k) - g_0(\boldsymbol{x}_k)$ and $f_i(\boldsymbol{x}_k + \alpha t(\boldsymbol{x}_{k+1} - \boldsymbol{x}_k)) - g_i(\boldsymbol{x}_k + \alpha t(\boldsymbol{x}_{k+1} - \boldsymbol{x}_k)) \leq 0$, for $i = 1, \ldots, m$ **do**
3: $\quad t := \alpha t$
4: **end while**
5: $\boldsymbol{x}_{k+1} = \boldsymbol{x}_k + t(\boldsymbol{x}_{k+1} - \boldsymbol{x}_k)$
6: **return** $\boldsymbol{x}_{k+1}$

decreases monotonically with increasing k and thus converges to a minimum (or saddle point).

One advantage of the CCP is that it only linearizes the concave component, but keeps the information from the convex component over each iteration. Additionally, due to the globality of the inequalities for convex and concave functions the over estimators $f_i(\boldsymbol{x}) - \hat{g}_i^{(k)}(\boldsymbol{x})$ are global as well. Thus, line search (see Alg. 2) is not compulsive, but still can of course accelerate convergence.

Applications where CCP is already used are, for instance, sparse principal component analysis [77], support vector machines [81], image reconstruction [9], or recently in the field of communications for power allocation optimization [48].

3

MIMO Gaussian Information Bottleneck with Optimal Power Allocation

The emphasis of this thesis is on quantized feedback. In Section 3.2 we use the information bottleneck method to model the channel output compression as a Gaussian information bottleneck (GIB). We solve this variational problem for the scalar channel in Section 3.3 and then we extend it in Section 3.4 for the MIMO channel. In both cases we derive the information-rate function that characterizes the maximum mutual information between source and compressed signal under a rate constraint. This rate constraint represents the quantization rate. We then give an equivalent representation of the channel output compression where in addition to the channel noise we have an additive quantization noise. We thus show how to represent the overall system as an equivalent sole Gaussian channel.

Furthermore, in Section 3.5 we broaden the scenario of interest to the case where the transmit power allocation is variable as well. Hence, we introduce the information-rate-power function that jointly characterizes the maximum mutual information between source and compressed signal under a quantization rate and transmit power constraint. We then show that solving the information-rate-power function means solving a difference of convex functions (DC) program. Eventually, we discuss the properties of the information-rate-power function.

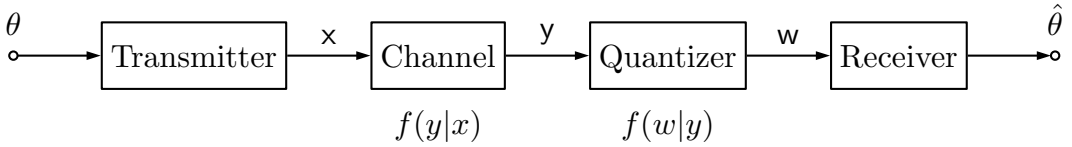

Figure 3.1: Basic communication system with quantizer.

3.1 Introduction

Throughout this thesis we study Gaussian channels where the input of the receiver, the signal y, is continuous-valued, even if the transmit signal x has a finite alphabet. This is because the channel, in general notated as $f(y|x)$, introduces continuous-valued noise and especially in the additive white Gaussian noise (AWGN) case as $\mathsf{z} \sim \mathcal{N}(0, \sigma^2)$. The performance of such systems was thoroughly studied and is well understood. Another practically important aspect, in order to digitally process the received signal, is the compression (or quantization) of the received signal. This quantization process introduces additional distortion and can be described in the most general way as a probabilistic quantizer with conditional pdf $f(w|y)$ (cf. Figure 3.1).

Often the quantizer is assumed to have high quantization rate. Thus, the quantized signal $w \approx y$ for further processing. If the high-rate assumption is dropped, $f(w|y)$ has to be optimized in some way. Usually this is done via minimizing the mean-square error (MSE) of the quantizer. Rate distortion (RD) theory provides the mathematical framework for such problems [6]. However, our goal is not to minimize the MSE, but rather to maximize the mutual information of source and quantized signal. This leads to the information bottleneck (IB) method [80], which is supposed to perform better. Thus, the next sections focus on the analysis of the Gaussian vector channel with IB compression and we will quantify the performance improvement. For this purpose, we will formulate, derive and discuss the information-rate function (termed IB-function in [37]) as an analogon to the distortion-rate function in rate-distortion theory.

3.2 Gaussian Information Bottleneck

In communications, we are not really interested in quantizing the received signal with minimum distortion. What we actually want is to preserve the information about the transmit signal x carried by the receive signal y. This is exactly what the information bottleneck method [80] provides: *relevance through another variable*. The problem of choosing the "right" distortion measure is replaced by relevant information. Similar to rate-distortion theory the quantization should compress y as much as possible while preserving as much information about x as possible.

Definition 3.1. *Let* $\mathbf{x} - \mathbf{y} - \mathbf{w}$ *be a Markov chain. The information-rate function* $I\colon \mathbb{R}_+ \to [0, I(\mathbf{x};\mathbf{y})]$ *is defined by*

$$I(R) \triangleq \max_{p(\mathbf{w}|\mathbf{y})} I(\mathbf{x};\mathbf{w}) \quad \text{subject to } I(\mathbf{y};\mathbf{w}) \leq R. \tag{3.1}$$

Furthermore, similar to the rate-distortion function we define the inverse function.

Definition 3.2. *Let* $\mathbf{x} - \mathbf{y} - \mathbf{w}$ *be a Markov chain. The rate-information function* $R\colon [0, I(\mathbf{x};\mathbf{y})] \to \mathbb{R}_+$ *is defined by*

$$R(I) \triangleq \min_{p(\mathbf{w}|\mathbf{y})} I(\mathbf{y};\mathbf{w}) \quad \text{subject to } I(\mathbf{w};\mathbf{x}) \geq I. \tag{3.2}$$

3.2.1 Derivation of the GIB Information-Rate Function for Gaussian Channels

In general it is hard if at all possible to find analytical expressions for the information-rate functions and only few cases can be solved explicitly. A solution for the case of jointly Gaussian $\mathbf{x}$ and $\mathbf{y}$ has been found in [16], with the problem formulated in variational form

$$\min_{p(\boldsymbol{w}|\boldsymbol{y})} I(\mathbf{y};\mathbf{w}) - \beta I(\mathbf{w};\mathbf{x}), \tag{3.3}$$

where the parameter β describes the trade-off between compression and preserved relevant information.

Because of the additive structure of the AWGN channel $\mathbf{x}$ and $\mathbf{y}$ are jointly Gaussian and in the vector case jointly multivariate Gaussian. It was shown in [38] that for jointly Gaussian $\mathbf{x}$ and $\mathbf{y}$ the optimal $\mathbf{w}$ is also jointly Gaussian with $\mathbf{y}$. Thus, $\mathbf{w}$ can be described using the linear transformation

$$\mathbf{w} = \boldsymbol{A}\mathbf{y} + \boldsymbol{\xi}, \qquad \boldsymbol{\xi} \sim \mathcal{N}(\mathbf{0}, \boldsymbol{\Sigma}_{\boldsymbol{\xi}}). \tag{3.4}$$

The problem in (3.3) can then be reformulated as

$$\min_{\boldsymbol{A}, \boldsymbol{\Sigma}_{\boldsymbol{\xi}}} I(\mathbf{y};\mathbf{w}) - \beta I(\mathbf{x};\mathbf{w}). \tag{3.5}$$

The following theorem gives explicit expressions for the optimal $\boldsymbol{A}$ and Σ_{ξ}.

Theorem 3.1 ([16], Thm. 3.1)**.** *The optimal projection* $\mathbf{w} = \boldsymbol{A}\mathbf{y} + \boldsymbol{\xi}$ *for a given*

tradeoff parameter β is given by $\boldsymbol{\Sigma}_{\boldsymbol{\xi}} = \boldsymbol{I}_x$ and

$$\boldsymbol{A} = \begin{cases} \begin{pmatrix} \mathbf{0} & \dots & \mathbf{0} \end{pmatrix}^{\mathsf{T}}, & 0 \leq \beta \leq \beta_1^c \\ \begin{pmatrix} \alpha_1 \boldsymbol{v}_1 & \mathbf{0} & \dots & \mathbf{0} \end{pmatrix}^{\mathsf{T}}, & \beta_1^c \leq \beta \leq \beta_2^c \\ \begin{pmatrix} \alpha_1 \boldsymbol{v}_1 & \alpha_2 \boldsymbol{v}_2 & \mathbf{0} & \dots & \mathbf{0} \end{pmatrix}^{\mathsf{T}}, & \beta_2^c \leq \beta \leq \beta_3^c \\ \vdots \end{cases} \tag{3.6}$$

where $\{\boldsymbol{v}_1^{\mathsf{T}}, \boldsymbol{v}_2^{\mathsf{T}}, \dots, \boldsymbol{v}_{n_x}^{\mathsf{T}}\}$ are left eigenvectors of $\boldsymbol{\Sigma}_{\mathbf{x}|\mathbf{y}} \boldsymbol{\Sigma}_{\mathbf{x}}^{-1}$ sorted by their corresponding ascending eigenvalues $\lambda_1, \lambda_2, \dots, \lambda_{n_x}$, $\beta_i^c = \frac{1}{1-\lambda_i}$ are critical β values, α_i are coefficients defined by $\alpha_i = \sqrt{\frac{\beta(1-\lambda_i)-1}{\lambda_i r_i}}$ and $r_i = \boldsymbol{v}_i{}^T \boldsymbol{\Sigma}_{\mathbf{y}} \boldsymbol{v}_i$, $\mathbf{0}^T$.

Using the explicit tradeoff parameter β, $I_\beta(\mathbf{y};\mathbf{w})$ and $I_\beta(\mathbf{x};\mathbf{w})$ are derived in [16] yielding

$$I_\beta(\mathbf{y};\mathbf{w}) = \frac{1}{2} \sum_{i=1}^{n(\beta)} \log_2 \left((\beta - 1) \frac{1-\lambda_i}{\lambda_i} \right), \tag{3.7}$$

where

$$n(\beta) = \max\{n : \beta \geq \beta_n^c\}. \tag{3.8}$$

The mutual information between $\mathbf{x}$ and $\mathbf{w}$ is

$$I_\beta(\mathbf{x};\mathbf{w}) = I(\mathbf{y};\mathbf{w}) - \frac{1}{2} \sum_{i=1}^{n(\beta)} \log_2 \left(\beta(1-\lambda_i) \right). \tag{3.9}$$

3.3 Scalar Gaussian Information Bottleneck

Since x and y are jointly Gaussian and following the lines of Section 3.2.1 the optimum w is also jointly Gaussian with y. They therefore indeed form the Markov chain

$$\mathsf{x} - \mathsf{y} - \mathsf{w}, \tag{3.10}$$

where $\mathsf{y} = h \cdot \mathsf{x} + \mathsf{z}$. This is the AWGN channel with transmit signal $\mathsf{x} \sim \mathcal{N}(0, P)$, fixed channel gain h and noise $\mathsf{z} \sim \mathcal{N}(0, \sigma^2)$ (cf. Figure 3.2). In the scalar case the covariance matrices simplify to

$$\Sigma_{\mathsf{x}} = P, \tag{3.11}$$

$$\Sigma_{\mathsf{z}} = \sigma^2, \tag{3.12}$$

$$\Sigma_{\mathsf{y}} = \boldsymbol{H} \Sigma_{\mathsf{x}} \boldsymbol{H}^{\mathsf{T}} + \Sigma_{\mathsf{z}} = h^2 \cdot P + \sigma^2, \tag{3.13}$$

$$\Sigma_{\mathsf{y}|\mathsf{x}} = \Sigma_{\mathsf{z}} = \sigma^2. \tag{3.14}$$

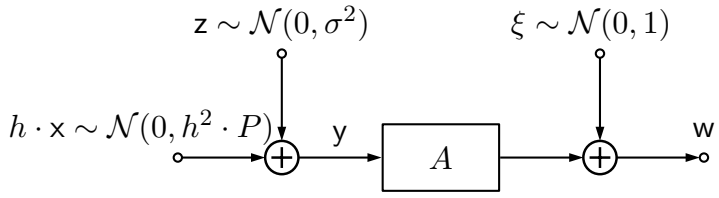

Figure 3.2: GIB equivalent scalar system.

The desired eigenvalues from Theorem 3.1 therefore collapse to one single eigenvalue,

$$\Sigma_{\mathsf{y}|\mathsf{x}}\Sigma_{\mathsf{y}}^{-1} = \frac{\sigma^2}{\sigma^2 + h^2 P} = \frac{1}{1 + h^2 P/\sigma^2} = \lambda. \tag{3.15}$$

In the scalar case there is only one critical β^c, because there is only one eigenvalue λ. The only interesting case is $\beta \geq \beta^c$, otherwise $I_\beta(\mathsf{y};\mathsf{w}) = 0$. Therefore $n(\beta) = 1$ and as a consequence (3.7) reduces to

$$I_\beta(\mathsf{y};\mathsf{w}) = \frac{1}{2}\log_2\left((\beta - 1)\frac{1-\lambda}{\lambda}\right) \triangleq R. \tag{3.16}$$

Since the mutual information of y and w is a measure for the compression, it can also be seen as the rate of the quantization R. Making β explicit yields

$$\beta = 2^{2R}\frac{\lambda}{1-\lambda} + 1. \tag{3.17}$$

Substituting $I(\mathsf{y};\mathsf{w})$ with (3.16), β with (3.17) and λ with (3.15) yields for (3.9)

$$\begin{aligned}
I_\beta(\mathsf{x};\mathsf{w}) &= R - \frac{1}{2}\log_2(\beta(1-\lambda)) && (3.18)\\
&= R - \frac{1}{2}\log_2\left(2^{2R}\lambda + 1 - \lambda\right) && (3.19)\\
&= \frac{1}{2}\log_2\left(\frac{2^{2R}}{2^{2R}\lambda + 1 - \lambda}\right) && (3.20)\\
&= \frac{1}{2}\log_2\left(\frac{2^{2R}}{2^{2R}\frac{1}{1+h^2P/\sigma^2} + 1 - \frac{1}{1+h^2P/\sigma^2}}\right) && (3.21)\\
&= \frac{1}{2}\log_2\left(\frac{2^{2R}(1 + h^2P/\sigma^2)}{2^{2R} + h^2P/\sigma^2}\right) \triangleq I(R). && (3.22)
\end{aligned}$$

This can also be directly obtained, without using $I_\beta(\mathsf{y};\mathsf{w})$ and $I_\beta(\mathsf{x};\mathsf{w})$ from [16]. We just need the identity $\mathsf{w} = A\mathsf{y} + \xi = A(h\mathsf{x} + \mathsf{z}) + \xi$. As a consequence, these random variables are all Gaussian distributed as follows:

$$\mathsf{w} \sim \mathcal{N}(0, A^2(h^2P + \sigma^2) + 1), \tag{3.23}$$

$$\mathsf{w}|\mathsf{y} \sim \mathcal{N}(0,1), \tag{3.24}$$

$$\mathsf{w}|\mathsf{x} \sim \mathcal{N}(0, A^2\sigma^2 + 1). \tag{3.25}$$

The rate and the mutual information are again defined as

$$R \triangleq I(\mathsf{y};\mathsf{w}) = h(\mathsf{w}) - h(\mathsf{w}|\mathsf{y}), \tag{3.26}$$

$$I \triangleq I(\mathsf{y};\mathsf{w}) = h(\mathsf{w}) - h(\mathsf{w}|\mathsf{x}). \tag{3.27}$$

Using (3.23)–(3.25) to express R and I yields

$$R = \frac{1}{2}\log_2\left(A^2(h^2P + \sigma^2) + 1\right), \tag{3.28}$$

$$I = \frac{1}{2}\log_2\left(\frac{A^2(h^2P + \sigma^2) + 1}{A^2\sigma^2 + 1}\right). \tag{3.29}$$

Making A^2 explicit in (3.28) yields

$$A^2 = \frac{2^{2R} - 1}{h^2P + \sigma^2}. \tag{3.30}$$

Substituting A^2 in (3.29) with (3.30) yields the information-rate function in terms of the rate R and the SNR $\frac{h^2P}{\sigma^2}$.

Corollary 3.2. *The scalar information-rate function with GIB-optimal channel output compression is given by*

$$I(R) = \frac{1}{2}\log_2\left(\frac{1 + h^2P/\sigma^2}{1 + 2^{-2R}h^2P/\sigma^2}\right). \tag{3.31}$$

The inverse of the information-rate function is called the rate-information function and is given by the following corollary.

Corollary 3.3. *The scalar rate-information function with GIB-optimal channel output compression is given by*

$$R(I) = \frac{1}{2}\log_2\left(\frac{h^2P/\sigma^2}{2^{-2I}(1 + h^2P/\sigma^2) - 1}\right). \tag{3.32}$$

3.3.1 Equivalent Gaussian Channel

The combined original AWGN channel with GIB channel output compression can be equivalently rewritten as a pure AWGN channel with modified channel noise [87]. First we define the equivalence as

$$I(R) \triangleq C\left(\frac{P}{\sigma^2 + \sigma_q^2}\right), \tag{3.33}$$

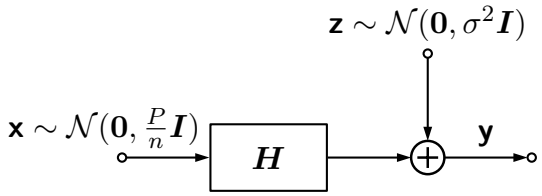

Figure 3.3: Vector system model.

where σ_q^2 is the additional noise due to the GIB compression. Rewriting (3.31) then yields the following statement.

Corollary 3.4. *The rate R channel output compression of an AWGN channel with transmit power P, channel gain h, and channel noise variance σ^2 can be equivalently modelled by an additional additive Gaussian noise term with variance*

$$\sigma_q^2 = \sigma^2 \frac{1 + h^2 P/\sigma^2}{2^{2R} - 1}. \tag{3.34}$$

3.4 MIMO Gaussian Information Bottleneck

3.4.1 System Model

Now we consider the vector case with some restrictions for the sake of simplicity. These restrictions are dropped in the next subsection and can be generalized using algebraic transformations on source and channel. Let the random vector source be Gaussian distributed as $\mathsf{x} = \begin{pmatrix} \mathsf{x}_1 & \mathsf{x}_2 & \dots & \mathsf{x}_n \end{pmatrix}^\mathsf{T} \sim \mathcal{N}(\mathbf{0}, \boldsymbol{D})$, where $\boldsymbol{D}$ is a diagonal matrix. In the simplest case the available transmit power is evenly distributed on the independent $x_1 \dots x_n$. Therefore, the elements of x are i.i.d. and x has the covariance matrix

$$\boldsymbol{\Sigma}_\mathsf{x} = \boldsymbol{D} = \frac{P}{n}\boldsymbol{I}. \tag{3.35}$$

The noise is again additive and independent of x, thus the input-output relation reads

$$\mathsf{y} = \boldsymbol{H}\mathsf{x} + \mathsf{z}, \tag{3.36}$$

where $\boldsymbol{H} \in \mathbb{R}^{n \times n}$ is deterministic (cf. Figure 3.3).
In this model the noise is also modeled to be i.i.d., i.e., $\mathsf{z} \sim \mathcal{N}(\mathbf{0}, \sigma^2 \boldsymbol{I})$. The covariance matrices are then

$$\boldsymbol{\Sigma}_\mathsf{z} = \sigma^2 \boldsymbol{I}, \tag{3.37}$$

$$\boldsymbol{\Sigma}_\mathsf{y} = \boldsymbol{H}\boldsymbol{\Sigma}_\mathsf{x}\boldsymbol{H}^\mathsf{T} + \boldsymbol{\Sigma}_\mathsf{z} = \frac{P}{n}\boldsymbol{H}\boldsymbol{H}^\mathsf{T} + \sigma^2 \boldsymbol{I}, \tag{3.38}$$

since x and z are assumed to be independent.

3.4.2 Generalization of the System

In Section 3.4.1 the system was restricted to an i.i.d. source $\mathsf{x} \sim \mathcal{N}(\mathbf{0}, \frac{P}{n}\boldsymbol{I})$ and noise $\mathsf{z} \sim \mathcal{N}(\mathbf{0}, \sigma^2\boldsymbol{I})$. Then $\mathsf{y} = \boldsymbol{H}\mathsf{x}+\mathsf{z} \sim \mathcal{N}(\mathbf{0}, \frac{P}{n}\boldsymbol{H}\boldsymbol{H}^\intercal + \sigma^2\boldsymbol{I})$. Now we drop this restriction and let x and z be independent Gaussian random vectors with full-rank covariance matrices. We therefore have

$$\mathsf{x} \sim \mathcal{N}(\mathbf{0}, \boldsymbol{\Sigma}_\mathsf{x}), \tag{3.39}$$

$$\mathsf{z} \sim \mathcal{N}(\mathbf{0}, \boldsymbol{\Sigma}_\mathsf{z}). \tag{3.40}$$

The resulting powers P and σ^2 are then be defined as

$$P = \mathrm{E}\{\mathsf{x}^\intercal\mathsf{x}\}, \tag{3.41}$$

$$\sigma^2 = \frac{1}{n}\mathrm{E}\{\mathsf{z}^\intercal\mathsf{z}\}. \tag{3.42}$$

Then the covariance matrix of y is

$$\boldsymbol{\Sigma}_\mathsf{y} = \boldsymbol{H}\boldsymbol{\Sigma}_\mathsf{x}\boldsymbol{H}^\intercal + \boldsymbol{\Sigma}_\mathsf{z}. \tag{3.43}$$

Whitening the noise in y and decorrelating the signal yields

$$\tilde{\mathsf{y}} = \sqrt{\sigma^2}\boldsymbol{U}^T\boldsymbol{\Sigma}_\mathsf{z}^{-1/2}\mathsf{y}, \tag{3.44}$$

where $\boldsymbol{U}\boldsymbol{\Lambda}\boldsymbol{U}^T$ is the eigen decomposition of $\sqrt{\frac{n\sigma^2}{P}}\boldsymbol{\Sigma}_\mathsf{z}^{-1/2}\boldsymbol{H}\boldsymbol{\Sigma}_\mathsf{x}\boldsymbol{H}^\intercal\boldsymbol{\Sigma}_\mathsf{z}^{-1/2}\sqrt{\frac{n\sigma^2}{P}}$. Hence,

$$\tilde{\mathsf{y}} \sim \mathcal{N}\left(\mathbf{0}, \frac{P}{n}\boldsymbol{\Lambda} + \sigma^2\boldsymbol{I}\right). \tag{3.45}$$

The previous transformations are all invertible and, hence, do not change the mutual information. Therefore, we can write an equivalent system as

$$\tilde{\mathsf{y}} = \tilde{\boldsymbol{H}}\tilde{\mathsf{x}} + \tilde{\mathsf{z}}. \tag{3.46}$$

This equivalent system has a diagonal channel $\tilde{\boldsymbol{H}}$ and i.i.d. signal $\tilde{\mathsf{x}}$ and noise $\tilde{\mathsf{z}}$, which are given as

$$\tilde{\boldsymbol{H}} = \boldsymbol{\Lambda}^{1/2}, \tag{3.47}$$

$$\tilde{\mathsf{z}} \sim \mathcal{N}(\mathbf{0}, \sigma^2\boldsymbol{I}), \tag{3.48}$$

$$\tilde{\mathsf{x}} \sim \mathcal{N}\left(\mathbf{0}, \frac{P}{n}\boldsymbol{I}\right). \tag{3.49}$$

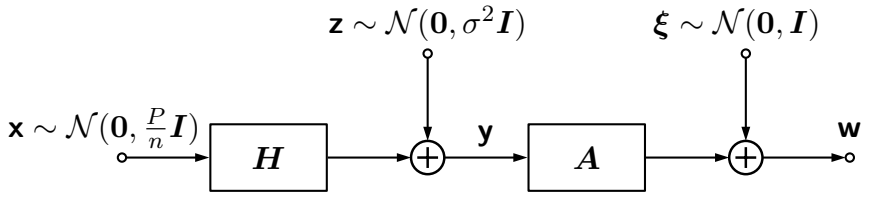

Figure 3.4: GIB equivalent vector system.

Since the channel is diagonal, the eigenvalues of $\tilde{\boldsymbol{H}}\tilde{\boldsymbol{H}}^{\mathsf{T}}$ are the diagonal elements of $\boldsymbol{\Lambda}$,

$$\lambda_{\tilde{\boldsymbol{H}}_i} = [\boldsymbol{\Lambda}]_{ii}. \tag{3.50}$$

To simplify the calculations in the next sections we will work with the system model defined in the previous section which is equivalent to (3.46) with (3.47)–(3.49).

3.4.3 Information Bottleneck

Now we consider jointly Gaussian random vectors $\mathbf{x}, \mathbf{y}, \mathbf{w}$, that form a Markov chain

$$\mathbf{x} - \mathbf{y} - \mathbf{w}, \tag{3.51}$$

where $\mathbf{y} = \boldsymbol{H}\mathbf{x} + \mathbf{z}$, $\mathbf{x} \sim \mathcal{N}(\mathbf{0}, P/n \cdot \boldsymbol{I})$ and $\mathbf{z} \sim \mathcal{N}(\mathbf{0}, \sigma^2 \boldsymbol{I})$, $\boldsymbol{H} \in \mathbb{R}^{n \times n}$ (cf. Figure 3.4). Recall the covariance matrices, where in the simplest case it is assumed that the transmit power is evenly distributed among the uncorrelated $x_1 \dots x_n$,

$$\boldsymbol{\Sigma}_{\mathbf{x}} = \boldsymbol{D} = \frac{P}{n}\boldsymbol{I}, \tag{3.52}$$

$$\boldsymbol{\Sigma}_{\mathbf{z}} = \sigma^2 \boldsymbol{I}, \tag{3.53}$$

$$\boldsymbol{\Sigma}_{\mathbf{y}} = \boldsymbol{H}\boldsymbol{\Sigma}_{\mathbf{x}}\boldsymbol{H}^{\mathsf{T}} + \boldsymbol{\Sigma}_{\mathbf{z}} = \frac{P}{n}\boldsymbol{H}\boldsymbol{H}^{\mathsf{T}} + \sigma^2 \boldsymbol{I}. \tag{3.54}$$

The conditional covariance matrix $\boldsymbol{\Sigma}_{\mathbf{y}|\mathbf{x}}$, which is needed to calculate the necessary eigenvalues from Theorem 3.1, can be calculated by the Schur complement as

$$\boldsymbol{\Sigma}_{\mathbf{y}|\mathbf{x}} = \boldsymbol{\Sigma}_{\mathbf{y}} - \boldsymbol{\Sigma}_{\mathbf{y},\mathbf{x}}\boldsymbol{\Sigma}_{\mathbf{x}}^{-1}\boldsymbol{\Sigma}_{\mathbf{y},\mathbf{x}}^{\mathsf{T}} = \boldsymbol{\Sigma}_{\mathbf{z}} = \sigma^2 \boldsymbol{I}. \tag{3.55}$$

Using these covariance matrices to calculate the eigenvalues from Theorem 3.1 then yields

$$\boldsymbol{\Sigma}_{\mathbf{y}|\mathbf{x}}\boldsymbol{\Sigma}_{\mathbf{y}}^{-1} = \sigma^2 \boldsymbol{I} \left(\frac{P}{n}\boldsymbol{H}\boldsymbol{H}^{\mathsf{T}} + \sigma^2 \boldsymbol{I} \right)^{-1} \tag{3.56}$$

$$= \left(\frac{P}{n\sigma^2}\boldsymbol{H}\boldsymbol{H}^{\mathsf{T}} + \boldsymbol{I} \right)^{-1} \tag{3.57}$$

$$= \left(\frac{P}{n\sigma^2} \boldsymbol{U}\boldsymbol{\Lambda}\boldsymbol{U}^\intercal + \boldsymbol{I} \right)^{-1} \triangleq \boldsymbol{B}^{-1}, \tag{3.58}$$

where the channel matrix is diagonalized as $\boldsymbol{H}\boldsymbol{H}^\intercal = \boldsymbol{U}\boldsymbol{\Lambda}\boldsymbol{U}^\intercal$. The resulting eigenvalue problem is

$$\begin{aligned} \boldsymbol{v}\boldsymbol{B}^{-1} =& \lambda \boldsymbol{v} && (3.59)\\ \Rightarrow \boldsymbol{v} =& \lambda \boldsymbol{v}\boldsymbol{B} && (3.60)\\ \Rightarrow \frac{1}{\lambda}\boldsymbol{v} =& \boldsymbol{v}\boldsymbol{B} && (3.61)\\ \Rightarrow \lambda_B \boldsymbol{v} =& \boldsymbol{v}\boldsymbol{B} && (3.62)\\ \Rightarrow \lambda =& \frac{1}{\lambda_B}. && (3.63) \end{aligned}$$

The characteristic equation for λ_B ($\lambda_B \neq 1$) is

$$\begin{aligned} \det(\boldsymbol{B} - \lambda_B \boldsymbol{I}) &= \det\left(\frac{P}{n\sigma^2} \boldsymbol{U}\boldsymbol{\Lambda}\boldsymbol{U}^\intercal - (\lambda_B - 1)\boldsymbol{I} \right) && (3.64)\\ &= \det\left(\frac{P}{n\sigma^2(1-\lambda_B)} \boldsymbol{U}\boldsymbol{\Lambda}\boldsymbol{U}^T + \boldsymbol{I} \right) && (3.65)\\ &= \prod_{i=1}^{r} \left(\frac{P}{n\sigma^2(1-\lambda_B)} \lambda_{H_i} + 1 \right) = 0, && (3.66) \end{aligned}$$

where r is the rank of the channel and λ_{H_i} are the eigenvalues of $\boldsymbol{H}\boldsymbol{H}^\intercal$. Since (3.66) must be fulfilled for all λ_{B_i}, one can simplify this to

$$\begin{aligned} \Rightarrow n\sigma^2(1-\lambda_{B_i}) + P\lambda_{H_i} &= 0 && (3.67)\\ \lambda_{B_i} &= 1 + \frac{P}{n\sigma^2}\lambda_{H_i} && (3.68)\\ \lambda_i = \frac{1}{\lambda_{B_i}} &= \frac{1}{\frac{P}{n\sigma^2}\lambda_{H_i} + 1}. && (3.69) \end{aligned}$$

In the case $\lambda_B = 1$, (3.64) reduces to $\det(\boldsymbol{H}\boldsymbol{H}^\intercal) = 0$. As a consequence $\lambda_{H_i} = 0$ and therefore (3.68) and (3.69) are still fulfilled.

The Information-Rate Function

The mutual information between $\mathbf{y}$ and $\mathbf{w}$ is again a measure for the compression and can be interpreted as a compression rate R. This yields

$$\begin{aligned} I_\beta(\mathbf{y};\mathbf{w}) =& \frac{1}{2} \sum_{i=1}^{n(\beta)} \log_2 \left((\beta - 1) \frac{1-\lambda_i}{\lambda_i}) \right) && (3.70)\\ =& \frac{1}{2} \log_2 \left((\beta-1)^{n(\beta)} \prod_{i=1}^{n(\beta)} \frac{1-\lambda_i}{\lambda_i} \right) \triangleq R. && (3.71) \end{aligned}$$

Then making β explicit yields following expression

$$\Rightarrow \beta = 2^{\frac{2R}{n(\beta)}} \prod_{i=1}^{n(\beta)} \left(\frac{\lambda_i}{1-\lambda_i} \right)^{\frac{1}{n(\beta)}} + 1. \tag{3.72}$$

Using the expression for the mutual information between $\mathbf{x}$ and $\mathbf{w}$ as in the scalar case and substituting β with (3.72) reads

$$\begin{aligned}
I_\beta(\mathbf{x};\mathbf{w}) &= I(\mathbf{y};\mathbf{w}) - \frac{1}{2}\sum_{i=1}^{n(\beta)} \log_2\left(\beta(1-\lambda_i)\right) && (3.73)\\
&= R - \frac{1}{2}\log_2\left(\beta^{n(\beta)} \prod_{i=1}^{n(\beta)} (1-\lambda_i)\right) && (3.74)\\
&= R - \frac{1}{2}\log_2\left(\left(2^{\frac{2R}{n(\beta)}} \prod_{i=1}^{n(\beta)} \left(\frac{\lambda_i}{1-\lambda_i}\right)^{\frac{1}{n(\beta)}} + 1\right)^{n(\beta)} \prod_{i=1}^{n(\beta)} (1-\lambda_i)\right) && (3.75)\\
&= R - \frac{1}{2}n(\beta)\log_2\left(2^{\frac{2R}{n(\beta)}} \prod_{i=1}^{n(\beta)} \lambda_i^{\frac{1}{n(\beta)}} + \prod_{i=1}^{n(\beta)} (1-\lambda_i)^{\frac{1}{n(\beta)}}\right) && (3.76)\\
&= \frac{1}{2}n(\beta)\log_2\left(\frac{2^{\frac{2R}{n(\beta)}}}{2^{\frac{2R}{n(\beta)}} \prod_{i=1}^{n(\beta)} \lambda_i^{\frac{1}{n(\beta)}} + \prod_{i=1}^{n(\beta)} (1-\lambda_i)^{\frac{1}{n(\beta)}}}\right). && (3.77)
\end{aligned}$$

Now substituting λ_i with (3.69) yields

$$\begin{aligned}
I_\beta(\mathbf{x};\mathbf{w}) =& \frac{1}{2}n(\beta)\log_2\left(\frac{2^{\frac{2R}{n(\beta)}}}{\frac{2^{\frac{2R}{n(\beta)}} + \frac{P}{n\sigma^2}\overline{\lambda}_{H_n}}{\prod_{i=1}^{n(\beta)}\left(1+\frac{P}{n\sigma^2}\lambda_{H_i}\right)^{1/n(\beta)}}}\right) && (3.78)\\
=& \frac{1}{2}n(\beta)\log_2\left(\frac{2^{\frac{2R}{n(\beta)}} \prod_{i=1}^{n(\beta)} \left(1+\frac{h^2P}{n\sigma^2}\lambda_{H_i}\right)^{1/n(\beta)}}{2^{\frac{2R}{n(\beta)}} + \frac{P}{n\sigma^2}\overline{\lambda}_{H_n}}\right) && (3.79)\\
=& \frac{1}{2}\log_2\left(\prod_{i=1}^{n(\beta)} \frac{2^{\frac{2R}{n(\beta)}}(1+\frac{P}{n\sigma^2}\lambda_{H_i})}{2^{\frac{2R}{n(\beta)}} + \frac{P}{n\sigma^2}\overline{\lambda}_{H_n}}\right) && (3.80)\\
=& \frac{1}{2}\sum_{i=1}^{n(\beta)} \log_2\left(\frac{2^{\frac{2R}{n(\beta)}}(1+\frac{P}{n\sigma^2}\lambda_{H_i})}{2^{\frac{2R}{n(\beta)}} + \frac{P}{n\sigma^2}\overline{\lambda}_{H_n}}\right) \triangleq I(R), && (3.81)
\end{aligned}$$

where $\overline{\lambda}_{H_n} = \overline{\lambda}_{H_{n(R)}}$ is the geometric mean $\prod_{i=1}^{n(\beta)} \lambda_{H_i}^{1/n(\beta)}$. Again substituting λ_i with (3.69) and inserting the critical β values $\beta_c = 1/(1-\lambda_n)$ yields critical rates R_c when

using (3.70):

$$R_c(n) = \frac{1}{2}\sum_{i=1}^{n}\log_2\left(\frac{\lambda_n}{1-\lambda_n}\frac{1-\lambda_i}{\lambda_i}\right) \tag{3.82}$$

$$= \frac{1}{2}\sum_{i=1}^{n}\log_2\left(\frac{\lambda_{H_i}}{\lambda_{H_n}}\right) \tag{3.83}$$

$$= \frac{1}{2}n\log_2\left(\frac{\overline{\lambda}_{H_n}}{\lambda_{H_n}}\right). \tag{3.84}$$

The eigenvalues λ_i are sorted in ascending order and since $\lambda_{H_i} \propto 1/\lambda_i$, the λ_{H_i} are in descending order.

At the critical rates new modes are added to $I(R)$ (3.81). This means $n(\beta)$ is incremented at each R_c and is therefore a function explicitly in R ($n(\beta) \Rightarrow n(R)$):

$$n(R) = \max\{n : R \geq R_c(n)\}. \tag{3.85}$$

Or in other words, at rate R there are $n(R)$ active modes. These are the modes with the $n(R)$ largest eigenvalues λ_{H_i}. The following corollary gives an explicit expression for the information-rate function.

Corollary 3.5. *The information-rate function with GIB-optimal channel output compression is given by*

$$I(R) = \frac{1}{2}\sum_{i=1}^{n(R)}\log_2\left(\frac{1+\frac{P}{n\sigma^2}\lambda_{H_i}}{1+2^{-\frac{2R}{n(R)}}\frac{P}{n\sigma^2}\overline{\lambda}_{H_n}}\right), \tag{3.86}$$

where the number of active modes $n(R)$ is given by

$$n(R) = \max\{n : R \geq R_c(n)\}, \tag{3.87}$$

and the critical rates $R_c(n)$ are given by

$$R_c(n) = \frac{1}{2}n\log_2\left(\frac{\overline{\lambda}_{H_n}}{\lambda_{H_n}}\right). \tag{3.88}$$

We identify (3.86) as the sum of $n(R)$ scalar information-rate functions, i.e., we have

$$I(R) = \sum_{i=1}^{n(R)} I_i(R) \tag{3.89}$$

$$= \frac{1}{2}\sum_{i=1}^{n(R)}\log_2\left(\frac{1+\frac{P}{n\sigma^2}\lambda_{H_i}}{1+2^{-2R_i(R)}\frac{P}{n\sigma^2}\lambda_{H_i}}\right). \tag{3.90}$$

Comparing (3.86) with (3.90), yields the rate allocation

$$R_i(R) = \max\left\{0, \frac{R}{n(R)} + \frac{1}{2}\log_2\frac{\lambda_{H_i}}{\overline{\lambda}_{H_n}}\right\}. \tag{3.91}$$

This is essentially the same way of rate allocation as in the RD case, where the rate R is evenly distributed among all $n(R)$ active modes up to a correction term. It can be shown that there is an even more direct connection between RD and GIB as the RD compression of the Wiener filtered channel output is equivalent to the GIB compression [52,53,85] and [62] shows that the GIB is indeed the solution of a Shannon-theoretic problem. Depending on whether the eigenvalue of the mode is greater or smaller than $\overline{\lambda}_{H_n}$ the rate $R/n(R)$ is increased or decreased by $\log_2(\lambda_{H_i}/\overline{\lambda}_{H_n})$. All rates of the scalar modes have the same slope

$$\frac{\partial R_i(R)}{\partial R} = \frac{1}{n(R)}, \tag{3.92}$$

where $n(R)$ is constant. As before, $R_i(R)$ is not differentiable on the critical rates. This means that a differential increase $\mathrm{d}R$ is evenly distributed among all $n(R)$ active modes. Of course the scalar rates again have to sum up to the total rate

$$R = \sum_{i=1}^{n(R)} R_i(R). \tag{3.93}$$

Rewriting (3.86) in the form $I(R) = \frac{1}{2}\sum_{i=1}^{n(R)}\log_2(1+SNR_i)$ yields the "mode" SNRs

$$SNR_i = \frac{P}{n\sigma^2}\frac{2^{\frac{2R}{n(R)}}\lambda_{H_i} - \overline{\lambda}_{H_n}}{2^{\frac{2R}{n(R)}} + \frac{P}{n\sigma^2}\overline{\lambda}_{H_n}}. \tag{3.94}$$

As in the scalar case, the information-rate function can also be directly obtained, without using $I_\beta(\mathbf{y};\mathbf{w})$ and $I_\beta(\mathbf{x};\mathbf{w})$ from [16]. Again we just need the identity $\mathbf{w} = \boldsymbol{A}\mathbf{y} + \boldsymbol{\xi} = \boldsymbol{A}(\boldsymbol{H}\mathbf{x} + \mathbf{z}) + \boldsymbol{\xi}$. As presented in Subsection 3.4.2 an equivalent diagonalized system can be given with the diagonal channel $\boldsymbol{H} = \operatorname{diag}\left\{\sqrt{\lambda_{H_i}}\right\}_{i=1}^{n}$. The problem reduces then to n scalar information-rate functions with $\mathsf{w}_i = A_i\mathsf{y}_i + \xi_i$, where we still have to find the optimal rate allocation. The resulting information-rate function is the sum of the individual scalar information-rate functions (3.90)

$$I(R) = \frac{1}{2}\sum_{i=1}^{n}\log_2\left(\frac{1+\frac{P}{n\sigma^2}\lambda_{H_i}}{1+2^{-2R_i}\frac{P}{n\sigma^2}\lambda_{H_i}}\right), \tag{3.95}$$

with the rate constraint $R = \sum_{i=1}^{n} R_i$. The optimal rate allocation can then be obtained using Lagrange multipliers.

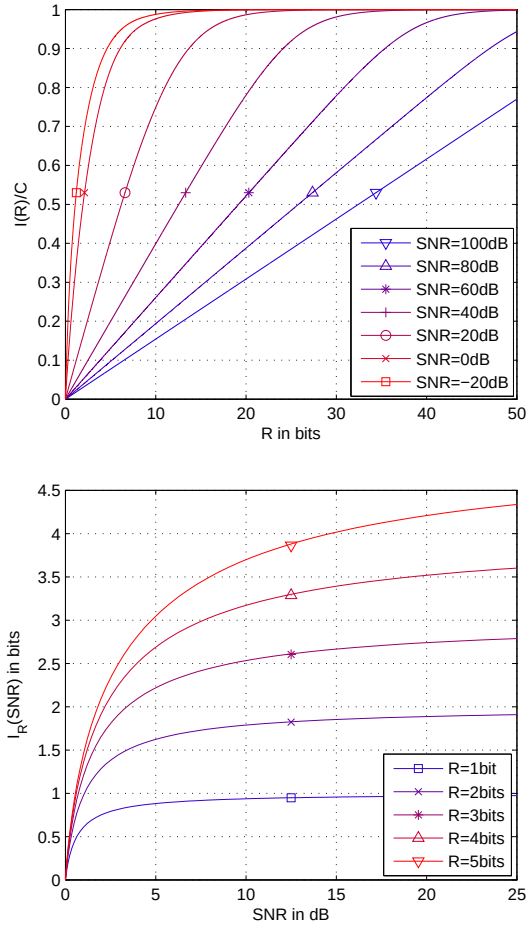

Figure 3.5: $I(R)/C$ (top) and $I_R(SNR)$ (bottom).

The Rate-Information Function

Next we calculate the inverse to the information-rate function, the rate-information function. Rewriting (3.73) as

$$R(I) = I - \frac{1}{2}\sum_{i=1}^{n(\beta)} \log_2\left(\beta(1-\lambda_i)\right), \tag{3.96}$$

then using (3.70) to substitute $R(I)$ and making I explicit yields

$$I(\beta) = \frac{1}{2}\sum_{i=1}^{n(\beta)} \log_2\left(\frac{\beta-1}{\beta}\frac{1}{\lambda_i}\right) \tag{3.97}$$

$$= \frac{1}{2}n(\beta)\log_2\left(\frac{\beta-1}{\beta}\right) - \frac{1}{2}\log_2\left(\lambda_i\right). \tag{3.98}$$

The above equation can be rewritten as

$$\log_2\left(\frac{\beta-1}{\beta}\right) = \frac{2I}{n(\beta)} + \frac{1}{n(\beta)}\sum_{i=1}^{n(\beta)}\log_2\left(\lambda_i\right) \tag{3.99}$$

$$= \frac{2I}{n(\beta)} + \log_2\left(\bar{\lambda}_n\right). \tag{3.100}$$

Making β explicit yields

$$\beta = \frac{1}{1 - 2^{\frac{2I}{n(\beta)}}\bar{\lambda}_n}. \tag{3.101}$$

Inserting the expression for β in (3.101) into (3.70) yields

$$R(I) = \frac{1}{2}\sum_{i=1}^{n(\beta)}\log_2\left(\frac{2^{\frac{2I(R)}{n(\beta)}}\bar{\lambda}_n}{1 - 2^{\frac{2I}{n(\beta)}}\bar{\lambda}_n}\frac{1-\lambda_i}{\lambda_i}\right). \tag{3.102}$$

The last step is to substitute λ_i with (3.69) and rearrange the equation to

$$R(I) = \frac{1}{2}\sum_{i=1}^{n(\beta)}\log_2\left(\frac{\frac{P}{n\sigma^2}\lambda_{H_i}}{\left(2^{\frac{2I}{n(\beta)}}\bar{\lambda}_n\right)^{-1} - 1}\right). \tag{3.103}$$

However, $R(I)$ still depends on β through $n(\beta)$. Analog to the critical rates we can calculate critical mutual information values from (3.97) if we use the critical beta values $\beta_c = 1/(1-\lambda_n)$:

$$I_c(n) = \frac{1}{2}\sum_{i=1}^{n}\log_2\left(\frac{\lambda_n}{\lambda_i}\right) \tag{3.104}$$

$$= \frac{1}{2}n\log_2\left(\frac{\lambda_n}{\bar{\lambda}_n}\right). \tag{3.105}$$

At these critical information values I_c new modes are added to $R(I)$ (3.103). This means $n(\beta)$ is incremented at each I_c and is therefore a function of I ($n(\beta) \Rightarrow n(I)$):

$$n(I) = \max\{n : I \geq I_c(n)\}. \tag{3.106}$$

Or in other words, at mutual information I there are $n(I)$ active modes. These are the modes with the $n(I)$ smallest eigenvalues λ_i. The following corollary gives an explicit expression for the rate-information function.

Corollary 3.6. *The rate-information function with GIB optimal channel output com-*

pression is given by

$$R(I) = \frac{1}{2}\sum_{i=1}^{n(I)} \log_2 \left(\frac{\frac{P}{n\sigma^2}\lambda_{H_i}}{\left(2^{\frac{2I}{n(I)}}\bar{\lambda}_n\right)^{-1} - 1} \right), \tag{3.107}$$

where the number of active modes $n(I)$ is given by

$$n(I) = \max\{n : I \geq I_c(n)\}, \tag{3.108}$$

and the critical mutual information values $I_c(n)$ are given by

$$I_c(n) = \frac{1}{2} n \log_2 \left(\frac{\lambda_n}{\bar{\lambda}_n} \right). \tag{3.109}$$

We identify (3.107) as the sum of $n(I)$ scalar rate-information functions, i.e., we have

$$R(I) = \sum_{i=1}^{n(I)} R_i(I) \tag{3.110}$$

$$= \frac{1}{2}\sum_{i=1}^{n(I)} \log_2 \left(\frac{\frac{P}{n\sigma^2}\lambda_{H_i}}{2^{-2I_i(I)}\left(1 + \frac{P}{n\sigma^2}\lambda_{H_i}\right) - 1} \right). \tag{3.111}$$

Comparing (3.107) with (3.111) yields

$$I_i(I) = \frac{I}{n(I)} + \frac{1}{2}\log_2 \left(\frac{\bar{\lambda}_n}{\lambda_i} \right) \tag{3.112}$$

and

$$I = \sum_{i=1}^{n(I)} I_i(I). \tag{3.113}$$

3.4.4 Equivalent Gaussian Channel

As for the scalar channel in Section 3.3.1 the combined original Gaussian vector channel with GIB channel output compression can be equivalently rewritten as a pure Gaussian vector channel with modified channel noise [86]. First we define the equivalence as

$$I(R) \triangleq \sum_{i=1}^{n} C \left(\frac{P_i}{\sigma_i^2 + \sigma_{i_q}^2} \right), \tag{3.114}$$

where $\sigma_{i_q}^2$ is the additional noise due to the GIB compression. We identify that the equivalence in (3.114) even holds for each summand separately. Rewriting (3.81) then yields the following statement.

Corollary 3.7. *The rate $R = \sum_{i=1}^{n} R_i$ channel output compression of a Gaussian vector channel with transmit power $P = \sum_{i=1}^{n} P_i$, equivalent diagonalized channel gains h_i, $i = 1, \ldots, n$, and channel noise variances σ_i^2, $i = 1, \ldots, n$, can be equivalently modelled by additional additive Gaussian noise terms with variance*

$$\sigma_{i_q}^2 = \sigma^2 \frac{1 + h_i^2 P_i / \sigma_i^2}{2^{2R_i} - 1}, \quad i = 1, \ldots, n. \tag{3.115}$$

3.4.5 MISO Gaussian Information Bottleneck

Transmission over the multiple access channel as studied in the following chapters is equivalent to the MISO case, i.e., $\boldsymbol{H} = \boldsymbol{h}^\intercal \in \mathbb{R}^{1 \times n}$. Hence, $\boldsymbol{H}\boldsymbol{H}^\intercal$ is a scalar and due to 3.66 we only have one single mode. The resulting system is then in principle equivalent to the scalar case (Section 3.3). Again, we consider an independent source $\mathsf{x} \sim \mathcal{N}(\mathbf{0}, \mathrm{diag}(P_1, P_2, \ldots, P_n))$ with total transmit power $P = \sum_{i=1}^{n} P_i$ and i.i.d. noise $\mathsf{z} \sim \mathcal{N}(0, \sigma^2)$. Then $\mathsf{y} = \boldsymbol{h}^\intercal \mathsf{x} + \mathsf{z} \sim \mathcal{N}(0, \sum_{i=1}^{n} h_i^2 P_i + \sigma^2)$. Analogously following the lines of Section 3.3 we get following information-rate relations for the MISO channel.

Corollary 3.8. *The MISO information-rate function with GIB-optimal channel output compression is given by*

$$I(R) = \frac{1}{2} \log_2 \left(\frac{1 + \sum_{i=1}^{n} h_i^2 P_i / \sigma^2}{1 + 2^{-2R} \sum_{i=1}^{n} h_i^2 P_i / \sigma^2} \right). \tag{3.116}$$

The inverse of the information-rate function is called the rate-information function and is given by the following corollary.

Corollary 3.9. *The MISO rate-information function with GIB-optimal channel output compression is given by*

$$R(I) = \frac{1}{2} \log_2 \left(\frac{\sum_{i=1}^{n} h_i^2 P_i / \sigma^2}{2^{-2I}(1 + \sum_{i=1}^{n} h_i^2 P_i / \sigma^2) - 1} \right). \tag{3.117}$$

Since we only have one single mode, the sums in Section 3.4.4 reduce to one active term and the equivalent Gaussian channel is given as follows.

Corollary 3.10. *The rate R channel output compression of a Gaussian vector channel with transmit power $P = \sum_{i=1}^{n} P_i$, channel gains h_i, $i = 1, \ldots, n$, and channel noise variance σ^2, can be equivalently modelled by an additional additive Gaussian noise term with variance*

$$\sigma_q^2 = \sigma^2 \frac{1 + \sum_{i=1}^{n} h_i^2 P_i / \sigma^2}{2^{2R} - 1}. \tag{3.118}$$

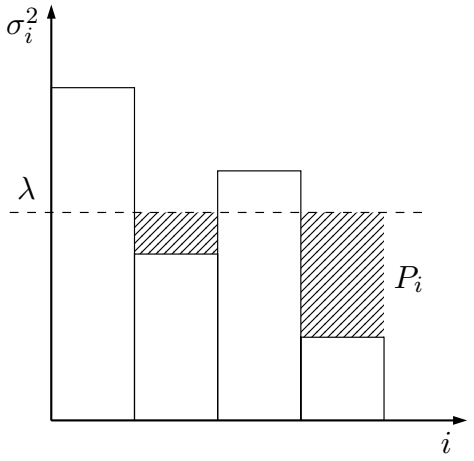

Figure 3.6: Waterfilling power allocation.

3.5 Gaussian Information Bottleneck with Optimal Power Allocation

Until here we considered a fixed transmit power allocation. Next we show that if we include the optimization of the power allocation as an additional degree of freedom we generally achieve higher rates than solely optimizing over the rate allocation.

3.5.1 Introduction

Consider a general Gaussian vector channel with full rank channel matrix $\tilde{\boldsymbol{H}}$. We can diagonalize the channel using an unitary precoding and decoding matrix, i.e., $\boldsymbol{H} = \boldsymbol{U}\tilde{\boldsymbol{H}}\boldsymbol{V}^\top$ (see Section 3.4.2). Thus, for what follows we work with the equivalent diagonalized channel matrix $\boldsymbol{H} \in \mathbb{R}^{n\times n}$.

As a result we have n parallel Gaussian channels with signal to noise ratio P_i/σ_i^2. It is well known that for a total transmit power constraint $P = \sum_{i=1}^n P_i$ the optimal power allocation that maximizes the sum capacity

$$C(P) = \sum_{i=1}^{n} C_0(P_i/\sigma_i^2) = \sum_{i=1}^{n} \frac{1}{2}\log_2\left(1 + \frac{P_i}{\sigma_i^2}\right) \tag{3.119}$$

is according to $P_i = \max\{\lambda - \sigma_i^2, 0\}$ [20]. Usually this kind of resource allocation is termed *water-filling* with the *water level* λ (Figure 3.6). Writing this problem explicitly

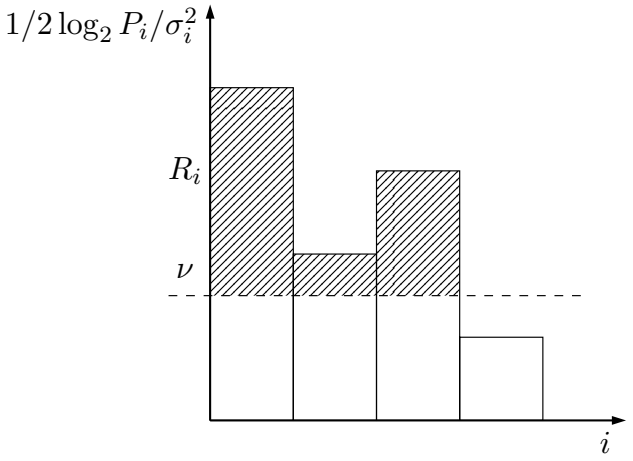

Figure 3.7: Reverse waterfilling rate allocation.

as a concave maximization problem yields

$$\begin{aligned} &\text{maximize} && \sum_{i=1}^{n} \frac{1}{2} \log_2 \left(1 + \frac{P_i}{\sigma_i^2}\right) \\ &\text{subject to} && \sum_{i=1}^{n} P_i \leq P. \end{aligned} \tag{3.120}$$

Similarly for a given parallel Gaussian channel with *fixed* power allocations P_i we find the optimal compression rate allocation with rate constraint $R = \sum_{i=1}^{n} R_i$ which maximizes the mutual information

$$I(R) = \sum_{i=1}^{n} I_i(R_i) = \sum_{i=1}^{n} \frac{1}{2} \log_2 \left(\frac{1 + P_i/\sigma_i^2}{1 + 2^{-2R_i} P_i/\sigma_i^2} \right) \tag{3.121}$$

as $R_i = \max\{1/2 \log_2 P_i/\sigma_i^2 - \nu, 0\}$ (see Section 3.4.3). This type of resource allocation is a variant of a scheme termed *reverse water-filling* with the *water level* ν (Figure 3.7). Again, we write this problem explicitly as a concave maximization problem,

$$\begin{aligned} &\text{maximize} && \sum_{i=1}^{n} \frac{1}{2} \log_2 \left(\frac{1 + P_i/\sigma_i^2}{1 + 2^{-2R_i} P_i/\sigma_i^2} \right) \\ &\text{subject to} && \sum_{i=1}^{n} R_i \leq R. \end{aligned} \tag{3.122}$$

Indeed the solution of the optimization (3.120) maximizes the channel capacity and the solution of the optimization (3.122) maximizes the mutual information of a given channel with *fixed* power allocation. However, applying both optimizations sequentially does not yield the maximum mutual information for all possible combinations of rate

and power allocations. This becomes obvious giving a simple example: Say, we have enough transmit power that all modes of the vector channel get a positive power $P_i > 0,\ i = 1, \ldots, n$. On the other hand we assume that we have that little rate that at least the weakest mode gets zero rate. As a consequence, the weakest mode does not contribute any mutual information at all. But then it would have been better to not allocate any transmit power to this mode at all at first place and distribute the extra available transmit power to the remaining modes.

To get the maximum mutual information for given transmit power P and compression rate R we have to *jointly* optimize over power allocation and rate allocation,

$$\begin{aligned} \text{maximize} \quad & \sum_{i=1}^{n} \frac{1}{2} \log_2 \left(\frac{1 + P_i/\sigma_i^2}{1 + 2^{-2R_i} P_i/\sigma_i^2} \right) \\ \text{subject to} \quad & \sum_{i=1}^{n} P_i \leq P \\ & \sum_{i=1}^{n} R_i \leq R. \end{aligned} \tag{3.123}$$

Convexification Approach

To solve (3.124) efficiently we have to show that this is again a concave maximization problem. Obviously, the constraint functions are affine functions and therefore convex as well. The objective function is concave if the individual summands are concave, since the sum of concave functions is again concave. Using concave composition rules we identify each summand as concave if the argument in the logarithm is concave. Indeed, direct calculation of the Hessian determinant of

$$h(P_i, R_i) = \frac{1 + P_i/\sigma_i^2}{1 + 2^{-2R_i} P_i/\sigma_i^2} \tag{3.124}$$

yields

$$\det \boldsymbol{H}(h(P_i, R_i)) = -\frac{2^{2R_i} 2^2 \sigma_i^2 \log^2 2 \left(2P_i^2 (2^{2R_i} - 1) + P_i (2^{2R_i} 2 - 1) \sigma_i^2 + 2^{2R_i} \sigma_i^4 \right)}{(P_i + 2^{2R_i} \sigma_i^2)^5} \leq 0. \tag{3.125}$$

In contrast, the principal minors are negative as well. As a consequence, the Jacobian is not negative definite and thus the objective function is not concave.

It can be easily seen that there is a strictly feasible set, i.e. the constraint functions are fulfilled with strict inequality. Thus, Slater's condition would guarantee strong duality with duality gap zero if the objective function was concave and we could solve the optimization problem (3.124) using Lagrange multipliers. If we convexify the problem

the Lagrange function reads

$$L(P_1,\dots,P_n,R_1,\dots,R_n,\lambda,\nu) = \sum_{i=1}^{n}\frac{1}{2}\log_2\left(\frac{1+P_i/\sigma_i^2}{1+2^{-2R_i}P_i/\sigma_i^2}\right) + \lambda\left(\sum_{i=1}^{n}P_i - P\right) + \nu\left(\sum_{i=1}^{n}R_i - R\right). \tag{3.126}$$

Then, the optimality condition $\nabla L(P_1,\dots,P_n,R_1,\dots,R_n,\lambda,\nu) = \mathbf{0}$ gives us the equations

$$\frac{\partial}{\partial P_i}\frac{1}{2}\log_2\left(\frac{1+P_i/\sigma_i^2}{1+2^{2R_i}P_i/\sigma_i^2}\right) + \lambda = \frac{1}{e^{R_i}\sigma_i^2+P_i} - \frac{1}{\sigma_i^2+P_i} + \lambda \quad = 0, \qquad i = 1,\dots,n \tag{3.127}$$

$$\frac{\partial}{\partial R_i}\frac{1}{2}\log_2\left(\frac{1+P_i/\sigma_i^2}{1+2^{-2R_i}P_i/\sigma_i^2}\right) + \nu = -\frac{P_i}{e^{R_i}\sigma_i^2+P_i} + \nu \qquad = 0, \qquad i = 1,\dots,n, \tag{3.128}$$

where we used the natural logarithm and powers to e instead of the respective operations to base 2 to avoid additional constants for further calculations, i.e., rates are now given in *nats* instead of *bits*. Solving (3.128) yields

$$R_i = \max\left\{\log\left(\frac{P_i}{\sigma_i^2}\frac{1-\nu}{\nu}\right), 0\right\}. \tag{3.129}$$

Using this result allows us to explicitly solve (3.127) and formulate it solely as a function of the Lagrange multipliers

$$P_i = \min\left\{\frac{\lambda\sigma_i^2+\nu-1 \pm \sqrt{\lambda^2\sigma_i^4+2\lambda\sigma_i^3(3\nu-1)+(\nu-1)^2}}{2\lambda}\right\}^+, \tag{3.130}$$

with $\min\{\cdot\}^+$ returning the smallest positive argument or 0 if all arguments are smaller than 0.

This yields an implicit formulation of the convexified information-rate-power function $I(R,P)$. The levels ν and λ are chosen such that the rate constraint $R = \sum_i R_i$ and transmit power constraint $P = \sum_i P_i$ are fulfilled.

Difference of convex function programming approach

The parametrized solution of the convexified problem of the last section generally does not coincide with the solution of the original problem. Formulating the problem as a difference of convex functions or equivalently as the sum of a convex and a concave function enables us to efficiently solve the problem via DC programming (see Section 2.8). Algorithms such as the CCP (see Section 2.8.1) transform this optimiza-

tion problem into a series of convex optimization problems. Generally, every function can be split into infinitely many different compositions of convex and concave functions. One straight-forward splitting of (3.124) is

$$\sum_{i=1}^{n} \frac{1}{2} \log_2 \left(\frac{1 + P_i/\sigma_i^2}{1 + 2^{-2R_i} P_i/\sigma_i^2} \right) = \underbrace{\sum_{i=1}^{n} \frac{1}{2} \log_2 \left(1 + P_i/\sigma_i^2\right)}_{\text{concave}} + \underbrace{\left[- \sum_{i=1}^{n} \frac{1}{2} \log_2 \left(1 + 2^{-2R_i} P_i/\sigma_i^2\right) \right]}_{\text{convex}}. \tag{3.131}$$

The first sum is a sum of concave functions and thus itself concave. This follows by the fact that the logarithm is concave and the arguments $1 + P_i/\sigma_i^2$ are affine. The second sum is a sum of concave functions as well (therefore the negative sum is convex). To see this, we expand the sum to

$$\sum_{i=1}^{n} \frac{1}{2} \log_2 \left(1 + 2^{-2R_i} P_i/\sigma_i^2\right) = \sum_{i=1}^{n} \frac{1}{2} \log_2 \left(2^{2R_i} + P_i/\sigma_i^2\right) - \sum_{i=1}^{n} R_i \log_2 (2). \tag{3.132}$$

Here, the second sum is affine since it is the sum of affine functions. The first sum is concave since it is the sum of concave functions. We obtain that each summand of the first sum is concave by following reasoning: First, we notice that the argument of the logarithm $2^{2R_i} + P_i/\sigma_i^2$ is convex. Although being convex each of the terms are log-concave. Log-concave means that the logarithm of a log-concave function is concave [7]. It is "most" convex in the direction $P_i = 0$ and "least" convex (in fact affine) in the direction $R_i = 0$. Due to monotonicity it is in between this two extrema in all other directions. But even in the "most" convex direction of $P_i = 0$, the resulting function is affine, that is, $\log_2(2^{2R_i}) = R_i \log_2(2)$, and as a consequence in all other "less" convex directions it has to be concave.

Now we reformulate the maximization problem as a minimization problem,

$$\begin{aligned} \text{minimize} \quad & - \sum_{i=1}^{n} \frac{1}{2} \log_2 \left(\frac{1 + P_i/\sigma_i^2}{1 + 2^{-2R_i} P_i/\sigma_i^2} \right) \\ \text{subject to} \quad & \sum_{i=1}^{n} P_i \leq P \\ & \sum_{i=1}^{n} R_i \leq R \end{aligned} \tag{3.133}$$

and use the partitioning into a concave and a convex part as in (3.131),

$$C^{\cap} = \sum_{i=1}^{n} \frac{1}{2} \log_2 \left(1 + 2^{-2R_i} P_i/\sigma_i^2\right), \tag{3.134}$$

$$C^{\cup} = -\sum_{i=1}^{n} \frac{1}{2} \log_2 \left(1 + P_i/\sigma_i^2\right), \tag{3.135}$$

which yields following DC problem

$$\begin{aligned} \text{minimize} \quad & C^{\cap} + C^{\cup} \\ \text{subject to} \quad & \sum_{i=1}^{n} P_i \leq P \\ & \sum_{i=1}^{n} R_i \leq R. \end{aligned} \tag{3.136}$$

For what follows we use compact vector notations for transmit powers $\boldsymbol{p} = (P_1, P_2, \ldots, P_n)^\intercal$ and quantization rates $\boldsymbol{r} = (R_1, R_2, \ldots, R_n)^\intercal$ in this section. Rewriting our optimization problem (3.136) in standard form (2.66) yields the following result.

Corollary 3.11. *The problem of jointly finding the optimal transmit power allocation and quantization rate allocation for a Gaussian vector channel with GIB channel output compression is solved by finding the solution of the DC problem*

$$\begin{aligned} \underset{\boldsymbol{p},\boldsymbol{r}}{\text{minimize}} \quad & -\mathsf{C}^{\cap}(\boldsymbol{p},\boldsymbol{r}) - \mathsf{C}^{\cup}(\boldsymbol{p},\boldsymbol{r}) \\ \text{subject to} \quad & \mathbf{1}^\top \boldsymbol{p} - P \leq 0, \\ & -\boldsymbol{p} \preceq 0, \\ & \mathbf{1}^\top \boldsymbol{r} - R \leq 0, \\ & -\boldsymbol{r} \preceq 0. \end{aligned} \tag{3.137}$$

The basic idea of the iterative CCP algorithm [91] is to find a point where the gradient of the convex part in the next iteration equals the negative gradient of the concave part of the previous iteration

$$\nabla \mathsf{C}^{\cup}(\boldsymbol{p}_{k+1}, \boldsymbol{r}_{k+1}) = -\nabla \mathsf{C}^{\cap}(\boldsymbol{p}_k, \boldsymbol{r}_k) \tag{3.138}$$

which itself is a convex optimization problem. Here, the gradient is with respect to $(\boldsymbol{p}^\intercal, \boldsymbol{r}^\intercal)^\intercal$. The solution to this auxiliary problem decreases monotonically with increasing k and thus converges to a minimum (or saddle point). Lipp and Boyd [49] give a basic CCP algorithm which requires initial feasible points $\boldsymbol{p}_0$ and $\boldsymbol{r}_0$, which in our case can be any points in the interval $0 \leq \mathbf{1}^\top \boldsymbol{p}_0 \leq P$ and $0 \leq \mathbf{1}^\top \boldsymbol{r}_0 \leq R$. Following [49], the CCP approach leads to Algorithm 3 for power allocation.

Algorithm 3 Joint transmit power and quantization rate allocation for the Gaussian vector channel with GIB channel output compression via CCP

Require: Initial feasible points $\boldsymbol{p}_0$, $\boldsymbol{r}_0$

1: $k := 0$
2: **while** stopping criterion not satisfied **do**
3: Form $\hat{\mathsf{C}}_k(\boldsymbol{p}, \boldsymbol{r}) = \mathsf{C}^{\cup}(\boldsymbol{p}_k, \boldsymbol{r}_k) + \left((\boldsymbol{p} - \boldsymbol{p}_k)^{\top}, (\boldsymbol{r} - \boldsymbol{r}_k)^{\top} \right) \nabla \mathsf{C}^{\cup}(\boldsymbol{p}_k, \boldsymbol{r}_k)$
4: Determine $\boldsymbol{p}_{k+1}$, $\boldsymbol{r}_{k+1}$ by solving the convex problem

$$\begin{aligned} \text{minimize} \quad & -\mathsf{C}^{\cap}(\boldsymbol{p}, \boldsymbol{r}) - \hat{\mathsf{C}}_k(\boldsymbol{p}, \boldsymbol{r}) \\ \text{subject to} \quad & \mathbf{1}^{\top}\boldsymbol{p} - P \leq 0, \\ & -\boldsymbol{p} \preceq 0, \\ & \mathbf{1}^{\top}\boldsymbol{r} - R \leq 0, \\ & -\boldsymbol{r} \preceq 0 \end{aligned}$$

5: $k := k + 1$
6: **end while**
7: **return** $\boldsymbol{p}_k$, $\boldsymbol{r}_k$

3.5.2 Properties of the Information-Rate-Power Function $I(R, P)$

As introduced in the previous section, the information-rate-power function yields the maximum achievable mutual information and thus jointly finds the optimum rate and power allocation. Although the resulting problem is DC, numerical simulations indicate that optimization using Lagrange multipliers provide acceptable results for the information-rate-power function. For constant power and fixed power allocation or constant rate and fixed rate allocation the following statements about concavity hold.

Properties of the Information-Rate Function $I_{P_0}(R)$

For constant transmit power P_0 and fixed power allocation, the information-rate function is concave in the rate R [86]. Thus, the information-rate-power function is concave in R as well. The joint optimization problem thus reduces to the convex optimization problem of finding the optimum rate allocation,

$$\begin{aligned} \text{maximize} \quad & \sum_{i=1}^{n} \frac{1}{2} \log_2 \left(\frac{1 + P_i/\sigma_i^2}{1 + 2^{-2R_i} P_i/\sigma_i^2} \right) \\ \text{subject to} \quad & \sum_{i=1}^{n} R_i \leq R. \end{aligned} \tag{3.139}$$

Note that in contrast to the joint optimization problem (3.124) here the constraint is only regarding the rate R since the transmit power allocation $(P_1, P_2, \ldots, P_n)$ with $P_0 = \sum_i P_i$ is considered fixed. With a slight abuse of notation the index P_0 not only refers to the transmit power but also implicitly reflects a specific power allocation. In general, the same specific power allocation for all rates R is suboptimal, that is, it does not maximize the achievable mutual information.

The inverse function, the rate-information function $R_{P_0}(I)$ finds the minimum rate R that achieves the mutual information I for fixed power allocation $P_0 = \sum_i P_i$,

$$\begin{aligned} \text{minimize} \quad & \sum_{i=1}^{n} \frac{1}{2} \log_2 \left(\frac{P_i/\sigma_i^2}{2^{-2I_i}(1 + P_i/\sigma_i^2) - 1} \right) \\ \text{subject to} \quad & \sum_{i=1}^{n} I_i \geq I. \end{aligned} \tag{3.140}$$

Clearly, for some mutual information allocations I_i some arguments of the $\log_2(\cdot)$ terms would become negative if $I_i > 1/2 \log_2(1 + P_i/\sigma_i^2) = C(P_i/\sigma_i^2)$. As a result each "mode information" I_i is at most $C(P_i/\sigma_i^2)$ what is also an implication of the data processing inequality. Therefore, in contrast to the information-rate function, the inverse is not defined for $C(P_0) < I$ and asymptotic $R \to \infty$ if $C(P_0) = I$.

Properties of the Information-Power Function $I_{R_0}(P)$

For constant rate R_0 and fixed rate allocation, the information-power function is concave in the transmit power P. The Gaussian channel including information-optimal output compression can be equivalently modelled as a Gaussian channel with increased channel noise. As a consequence, for constant R_0 the information-power function reduces to finding the optimal power allocation which is solved by classical water-filling [20]. Thus, the information-power function is concave in P as well,

$$\begin{aligned} \text{maximize} \quad & \sum_{i=1}^{n} \frac{1}{2} \log_2 \left(\frac{1 + P_i/\sigma_i^2}{1 + 2^{-2R_i} P_i/\sigma_i^2} \right) \\ \text{subject to} \quad & \sum_{i=1}^{n} P_i \leq P. \end{aligned} \tag{3.141}$$

Note that in contrast to the joint optimization problem (3.124) here the constraint is only regarding the transmit power P since the rate allocation $(R_1, R_2, \ldots, R_n)$ with $R_0 = \sum_i R_i$ is considered fixed. Again, with a slight abuse of notation here the index R_0 not only refers to the rate but also implicitly reflects a specific rate allocation. In general, the same specific rate allocation for all transmit powers R is suboptimal, that is, it does not maximize the achievable mutual information.

The inverse function, the power-information function $P_{R_0}(I)$ finds the minimum power P that achieves the mutual information I for fixed rate allocation $R_0 = \sum_i R_i$,

$$\begin{aligned} \text{minimize} \quad & \sum_{i=1}^{n} \left[\sigma_i^2 \frac{2^{2I_i} - 1}{1 - 2^{2(I_i - R_i)}} \right]^+ \\ \text{subject to} \quad & \sum_{i=1}^{n} I_i \geq I. \end{aligned} \tag{3.142}$$

Clearly if the mutual information allocated to one mode would be $I_i > R_i$, the respective mode power would be negative in consequence. Thus, we need the $[\cdot]^+$ that indicates we only take positive summands, since negative transmit powers are physically impossible. As a result each "mode information" I_i is at most R_i, which is also an implication of the data processing inequality. Therefore, in contrast to the information-power function, the inverse is not defined for $R_0 < I$ and asymptotic $P \to \infty$ if $R_0 = I$.

Recursive Optimization

The question arises whether recursive optimization of the information-rate function and the information-power function converges to a (local) optimum. If this was the case the resulting optimization problem would be a series of convex optimization problems and thus practically solvable.

There are two possible recursions. We can either initialize the optimization on a specific transmit power allocation or quantization rate allocation. For a specific initial transmit power allocation we first calculate the information-rate function $I_{P_0}(R)$ by solving the optimization problem (3.139) that delivers a rate allocation and then use this rate allocation to calculate the information-power function $I_{R_0}(P)$ by solving the optimization problem (3.141) that delivers again a power allocation. Then this recursion starts all over. Or we can optimize the other way around by starting with a specific initial quantization rate allocation and the recursively solve (3.141) and then (3.139).

These two recursions do not necessarily converge to the same value. This optimization strategy strongly depends on the initialization and unfortunately, for bad initialization values such consecutive optimization is highly suboptimal. This becomes obvious if we consider the optimization step where the optimum power allocation is found for the optimum rate allocation of the previous step. If then the power allocation procedure allocates zero power to the weakest mode due to its water-filling behaviour, the weakest mode stays inactive in the next step of optimal rate allocation because it has zero capacity. This zero rate and power allocation repeats for all following iterations. Thus, if at one point of the iterative optimization zero power or zero rate is allocated to one mode, this mode will stay inactive until convergence.

3.5.3 Discussion

Simulations showed that joint optimization is relatively sensitive regarding initialization. Therefore, we used various random initializations and picked the best solutions in an evolutionary way. This strategy yields the highest achievable rates. Consecutive optimizations, where we first maximize the "raw" channel capacity without quantization and then maximize the achievable rates using the GIB, delivers inferior performance if not all modes are active. Surprisingly, if the water-filling algorithm allocates power to all modes this sequential optimization performs nearly optimal. We observed a similar

behaviour for the recursive optimization. The reason for this is the discussed "cut-off" behaviour during the consecutive iterations. In terms of computational complexity the consecutive approach is most preferable since it basically consists of two convex optimizations problems whereas joint optimization and recursive optimization are each a series of convex optimizations problems.

Figure 3.8 and Figure 3.9 illustrate the different optimization approaches for various transmit powers P and various rates R, respectively. Obviously, there are sharp transitions in power and rate allocation over transmit power and rate. This behaviour is due to the joint optimization and in contrast to the smooth mode transitions for plain GIB rate allocation optimization (cf. Section 3.4.3, [86]). In Figure 3.8 we observe the biggest benefit of the true joint optimization over sequential and recursive optimization for moderate transmit powers. But due to the relatively even allocation of the transmit power in the high power regime it is sufficient to just sequentially optimize power allocation and rate allocation. Recursive optimization shows a slightly poorer performance due to the previously discussed potential "cut-off" behaviour. In Figure 3.9 we observe a similar behaviour. For high rates all three optimization approaches perform nearly identical. Only the recursive optimization shows some numerical instabilities.

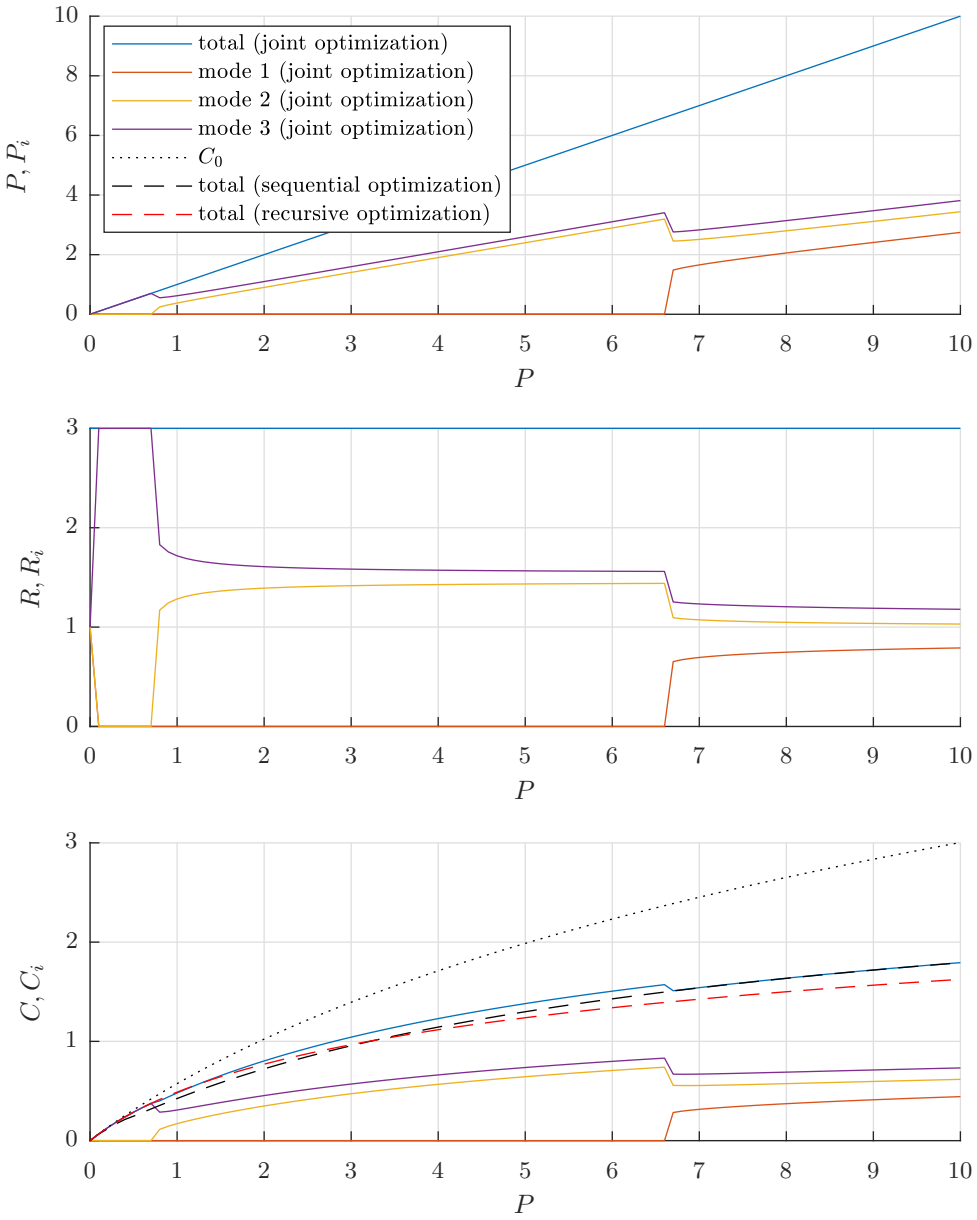

Figure 3.8: Exemplary optimization of information-rate-power function with fixed quantization rate $R = 3$ plotted over transmit power with $n = 3$, $\boldsymbol{h}^\intercal = (0.9, 0.95, 1)$, $\sigma^2 = 1$. Optimal power allocation with joint optimization (top); optimal rate allocation with joint optimization (middle); optimal achievable rates with joint optimization, sequential optimization, and recursive optimization and plain channel capacity C_0 (bottom). Same legend applies for all plots.

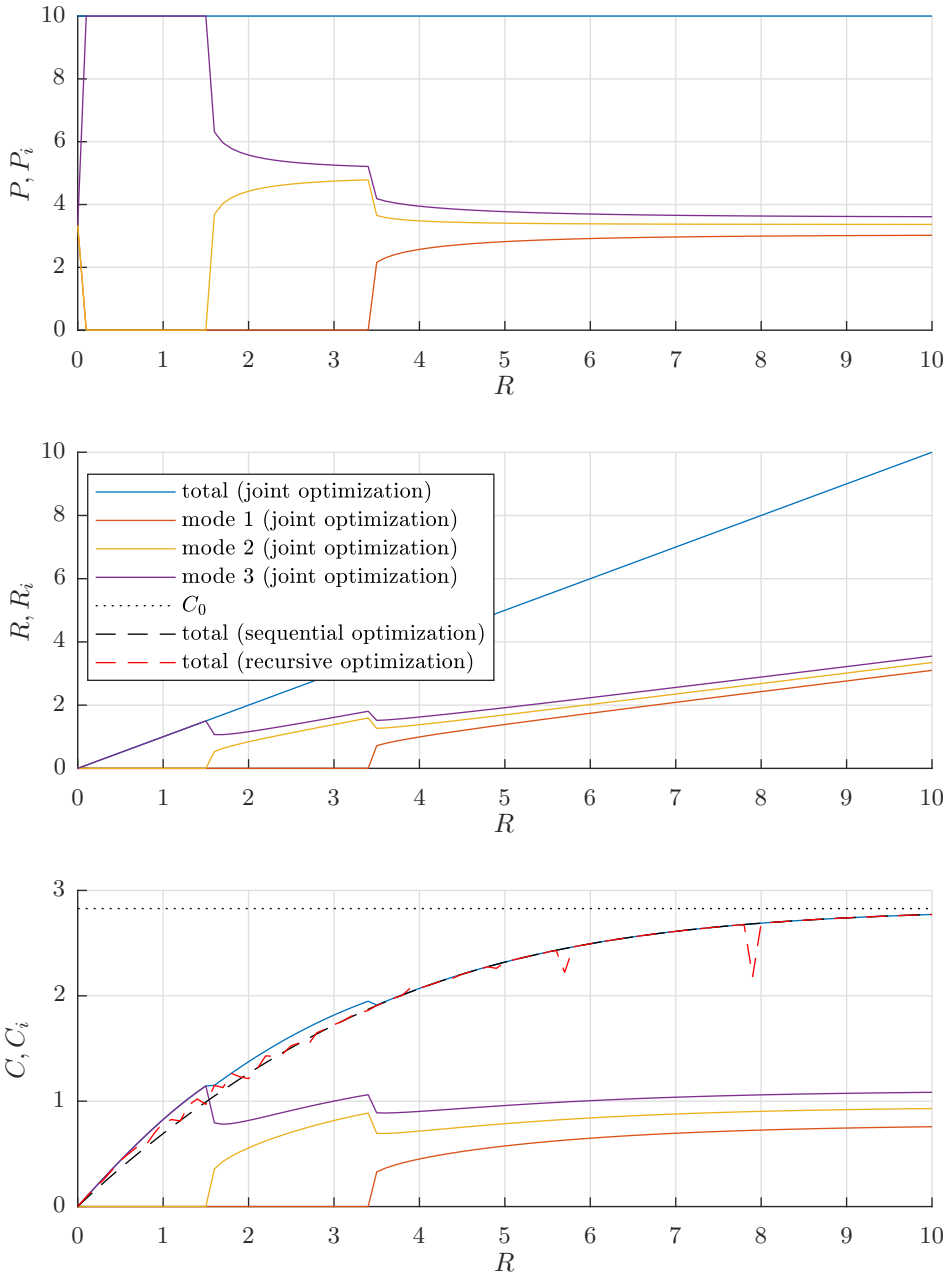

Figure 3.9: Exemplary optimization of information-rate-power function with fixed transmit power $P = 10$ plotted over quantization rate R with $n = 3$, $\boldsymbol{h}^\intercal = (0.8, 0.9, 1)$, $\sigma^2 = 1$. Optimal power allocation with joint optimization (top); optimal rate allocation with joint optimization (middle); optimal achievable rates with joint optimization, sequential optimization, and recursive optimization and plain channel capacity C_0 (bottom). Same legend applies for all plots.

4

Feedback Model

Throughout this thesis we study communication over Gaussian channels in conjunction with GIB-modelled channel output compression. For this reason we start by defining a discrete source model that asymptotically converges to a Gaussian distribution in Section 4.2.

In Section 4.3 we next formulate the algebraic feedback coding structure for the AWGN channel, the Gaussian multiple access channel, and the Gaussian broadcast channel. Following this algebraic coding structure we propose a superposition coding scheme for said channels that superimposes a feedback based coding component with a conventional coding component that completely ignores the feedback in Section 4.5. We further describe how the receiver is aware of the quantization noise and how this side-information positively affects the performance of the proposed superposition scheme.

4.1 Introduction

Commonly, when studying the theoretical performance of communication scenarios such as channel capacity this is accomplished in the context of information theory, more specifically Shannon theory. This approach benefits from very general results but may lack specific solutions for practical coding schemes. It becomes evident when moving from the asymptotic performance regime to finite blocklengths. Here, it is often practical to explicitly define the algebraic coding structure. We therefore formulate our feedback model in the following chapter based on the feedback scheme proposed by Chance and Love [11, 12, 14, 15] where the original idea dates back to Butman in 1969 [8]. Then, we develop it further to the proposed superposition coding scheme.

4.2 Source Signal Model

The optimal channel output compression developed in Chapter 3 results in the Gaussian Information Bottleneck which relies on Gaussian sources. If we want to measure the performance of systems, we usually want to give error probabilities, i.e., symbol error probability or bit error probability. Therefore, we have to discretize the source. In order to reconcile the contradictory requirements of the Gaussian source and the discrete source we approximate the Gaussian source by a discrete source.

The desired discrete approximation $p(x)$ of our Gaussian distribution $f(x)$ should ideally fulfil

$$\int_a^b f(x)\mathrm{d}x = \sum_{k=1}^{n} p(x_k) \qquad a, b \in \mathbb{R}. \tag{4.1}$$

We define the approximation as (Figure 4.1)

$$p(x_k) \approx \Delta f(x_k). \tag{4.2}$$

The relation of differential entropy and the entropy of the discretized version is derived in [18]. The differential entropy of the original Gaussian source is denoted as $h(\mathsf{x})$. The source should have the rate R, which is the discrete entropy $H(\mathsf{x})$

$$R = H(\mathsf{x}) = -\sum_{x} p(x_k)\log_2 p(x_k). \tag{4.3}$$

Now substituting $p(x_k)$ with (4.2) yields

$$\begin{aligned}
R &= -\sum_{-\infty}^{\infty} \Delta f(x_k)\log_2(\Delta f(x_k)) && (4.4)\\
&= -\sum_{-\infty}^{\infty} \Delta f(x_k)\log_2 f(x_k) - \sum_{-\infty}^{\infty} \Delta f(x_k)\log_2 \Delta && (4.5)\\
&\approx \underbrace{-\int_{-\infty}^{\infty} f(x_k)\log_2 f(x_k)\mathrm{d}x}_{=h(\mathsf{x})} - \underbrace{\int_{-\infty}^{\infty} f(x_k)\mathrm{d}x}_{=1}\log_2 \Delta && (4.6)\\
&= h(\mathsf{x}) - \log_2 \Delta. && (4.7)
\end{aligned}$$

This approximation gets tight for high rates and is exactly fulfilled as $R \to \infty$. The differential entropy of a Gaussian source is

$$h(\mathsf{x}) = \frac{1}{2}\log_2(2\pi e\sigma^2). \tag{4.8}$$

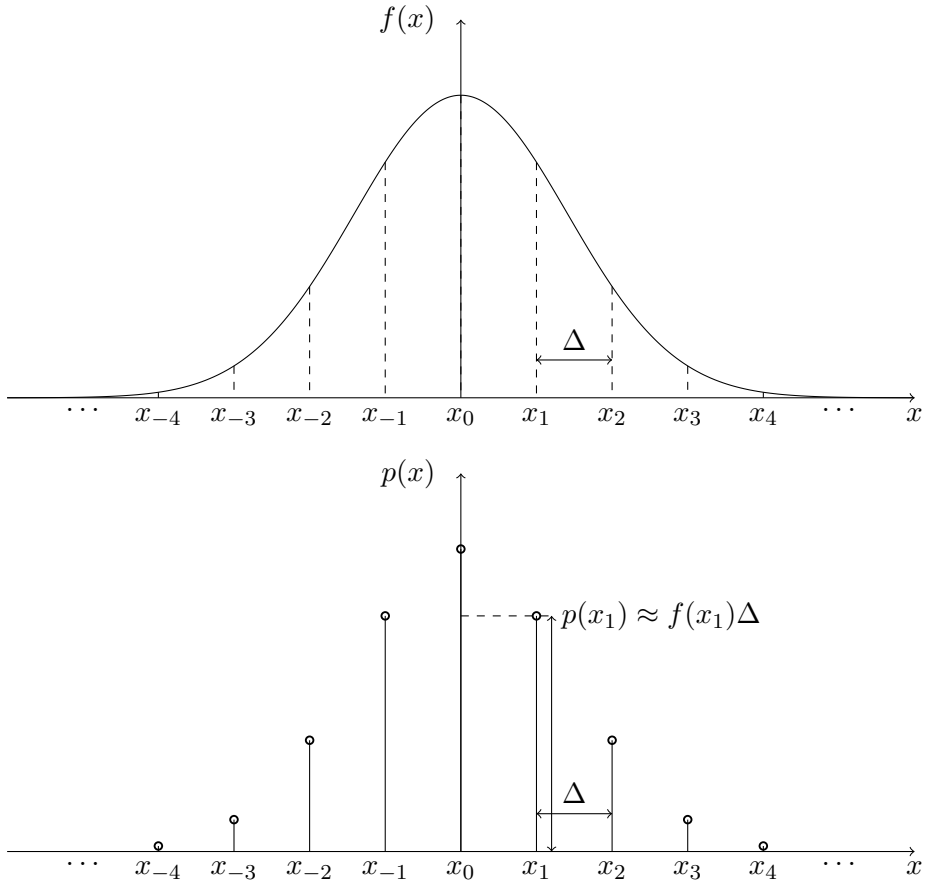

Figure 4.1: Gaussian distribution (top) and resulting discrete approximation (bottom).

Inserting (4.8) into (4.7) and making Δ explicit then yields

$$\Rightarrow \Delta^2 = \frac{\sigma^2}{2^{2R}} 2\pi e. \tag{4.9}$$

A uniform distribution would result in

$$\Delta_U^2 = \frac{\sigma^2}{2^{2R}} \frac{1}{12}. \tag{4.10}$$

The ratio of (4.9) and (4.10) is called the *ultimate shaping gain* [30] and formulates as

$$c_0^2 = \frac{\Delta^2}{\Delta_U^2} = \frac{\pi e}{6} \triangleq 1.53\text{dB}. \tag{4.11}$$

So the discrete approximation of the Gaussian source with the differential entropy $h(\mathsf{x})$ goes to an entropy $H(\mathsf{x}) \to \infty$ if $\Delta \to 0$. From a mathematical point of view, every

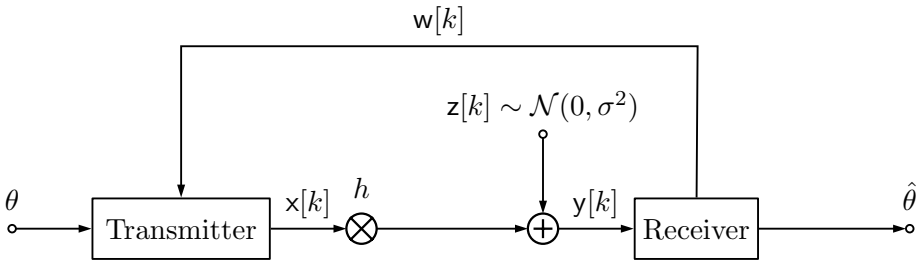

Figure 4.2: AWGN channel with feedback link.

continous source has to have infinite entropy, since the realization is chosen from a set of real numbers, which are innumerable, even if the set is bounded.

4.3 Feedback Coding

4.3.1 AWGN Channel Transceiver Scheme

We start with the simple one transmitter scenario where the transmit message θ is directly modeled by a Gaussian distribution,

$$\theta \sim \mathcal{N}(0, 1). \tag{4.12}$$

The transmit vector $\mathbf{x}$ consist of the message part and the feedback part $\mathbf{w}$, given by

$$\mathbf{x} = \boldsymbol{g}\theta + \boldsymbol{B}\tilde{\mathbf{w}}, \tag{4.13}$$

where $\tilde{\mathbf{w}}$ is the modified feedback signal to be defined, $\boldsymbol{g}$ is the transmit vector and $\boldsymbol{B}$ is termed encoding matrix [12]. The fixed channel gain h is known to both transmitter and receiver and is incorporated in the construction of both $\boldsymbol{g}$ and $\boldsymbol{B}$. The scheme is shown in Figure 4.2. The AWGN channel then adds the noise $\mathbf{z}$, which is iid according to a Gaussian distribution

$$\mathbf{z} \sim \mathcal{N}(0, \sigma_z^2 \boldsymbol{I}). \tag{4.14}$$

The channel output signal $\mathbf{y}$ is then given by

$$\mathbf{y} = h\mathbf{x} + \mathbf{z}. \tag{4.15}$$

The channel output is directly fed back to the transmitter, with additive iid Gaussian noise

$$\mathbf{n} \sim \mathcal{N}(0, \sigma_n^2 \boldsymbol{I}). \tag{4.16}$$

Thus, the feedback signal $\mathbf{w}$ is given by

$$\mathbf{w} = \mathbf{y} + \mathbf{n} \tag{4.17}$$

$$= h\mathbf{x} + \mathbf{z} + \mathbf{n}. \tag{4.18}$$

Let us temporarily assume that $\mathbf{w} = \tilde{\mathbf{w}}$, i.e., the feedback signal is not modified. Then by using (4.18) in (4.13) we get

$$\mathbf{x} = \boldsymbol{g}\theta + \boldsymbol{B}\left(h\mathbf{x} + \mathbf{z} + \mathbf{n}\right). \tag{4.19}$$

Since the feedback is strictly causal, $\boldsymbol{B}h\mathbf{x}$ is known at transmitter and therefore can be subtracted from the feedback, i.e., $\tilde{\mathbf{w}} = \mathbf{w} - h\mathbf{x}$, where $\tilde{\mathbf{w}}$ is provided to the encoding matrix $\boldsymbol{B}$. The receive signal is then

$$\mathbf{y} = h\mathbf{x} + \mathbf{z} \tag{4.20}$$

$$= h\boldsymbol{g}\theta + h\boldsymbol{B}\left(\mathbf{z} + \mathbf{n}\right) + \mathbf{z} \tag{4.21}$$

$$= h\boldsymbol{g}\theta + \underbrace{(\boldsymbol{I} + h\boldsymbol{B})\mathbf{z} + h\boldsymbol{B}\mathbf{n}}_{\mathbf{z}'}. \tag{4.22}$$

Thus, the resulting system is equivalent to a non-feedback coding scheme with modified channel noise $\mathbf{z}'$.

4.3.2 MAC Transceiver Scheme

This thesis studies the multiple access channel and the broadcast channel. Results for the broadcast channel are mostly obtained by applying duality (see Section 2.6.1) where we can directly use statements that hold for the multiple access channel. Therefore, here we restrict to the explicit definition of the multiple access channel. The broadcast channel is fully analogous. First, we formulate the problem for the K-transmitter case to give a general insight on the problem. All messages θ_i are modeled as i.i.d. Gaussian,

$$\theta_i \sim \mathcal{N}(0, 1) \qquad i = 1, 2, \ldots, K. \tag{4.23}$$

The transmit vectors $\mathbf{x}_i$ consist of the message part and the feedback part $\mathbf{w}_i$, given by

$$\mathbf{x}_i = \boldsymbol{g}_i\theta_i + \boldsymbol{B}_i\tilde{\mathbf{w}}_i, \tag{4.24}$$

where $\tilde{\mathbf{w}}_i$ is the modified feedback signal to be defined, $\boldsymbol{g}_i$ are the transmit vectors and $\boldsymbol{B}_i$ are the encoding matrices [12]. The fixed channel gains h_i are known to transmitters and receiver and are incorporated in the construction of both $\boldsymbol{g}_i$ and $\boldsymbol{B}_i$. For $K = 2$ the scheme is shown in Figure 4.3. The MAC then combines the transmit vectors and

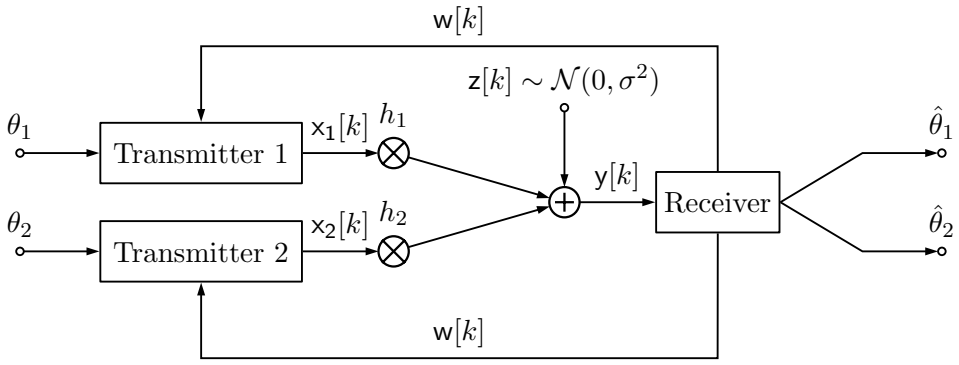

Figure 4.3: Two-user Gaussian MAC with common feedback link.

adds the noise $\mathbf{z}$, which is iid according to a Gaussian distribution

$$\mathbf{z} \sim \mathcal{N}(0, \sigma_z^2 \boldsymbol{I}). \tag{4.25}$$

The channel output signal $\mathbf{y}$ is then given by

$$\mathbf{y} = \sum_{i=1}^{K} h_i \mathbf{x}_i + \mathbf{z}. \tag{4.26}$$

The channel output is directly fed back to each transmitter with additive i.i.d. Gaussian noise

$$\mathbf{n}_i \sim \mathcal{N}(\mathbf{0}, \sigma_{n_i}^2 \boldsymbol{I}), \quad i = 1, 2, \ldots, N. \tag{4.27}$$

Therefore, the feedback signal $\mathbf{w}_i$ is given by

$$\mathbf{w}_i = \mathbf{y} + \mathbf{n}_i \tag{4.28}$$

$$= \sum_{i=1}^{N} h_i \mathbf{x}_i + \mathbf{z} + \mathbf{n}_i \tag{4.29}$$

Let us again temporarily assume that $\mathbf{w}_i = \tilde{\mathbf{w}}_i$, i.e. the feedback signal is not modified. Then by using (4.29) in (4.24) we get

$$\mathbf{x}_i = \boldsymbol{g}_i \theta_i + \boldsymbol{B}_i \left(\sum_{j=1}^{K} h_j \mathbf{x}_j + \mathbf{z} + \mathbf{n}_j \right). \tag{4.30}$$

Since the feedback is strictly causal, we can compute $\tilde{\mathbf{w}}_i = \mathbf{w}_i - h_i \mathbf{x}_i$ and define the

transmit signal as

$$\mathbf{x}_i = \boldsymbol{g}_i\theta_i + \boldsymbol{B}_i\left(\sum_{\substack{j=1\\j\neq i}}^{K} h_j\mathbf{x}_j + \mathbf{z} + \mathbf{n}_i\right). \tag{4.31}$$

Now we specialize (4.31) to the case of two transmitters ($K = 2$). We then get

$$\mathbf{x}_1 = \boldsymbol{g}_1\theta_1 + \boldsymbol{B}_1\left(h_2\mathbf{x}_2 + \mathbf{z} + \mathbf{n}_1\right), \tag{4.32}$$

$$\mathbf{x}_2 = \boldsymbol{g}_2\theta_2 + \boldsymbol{B}_2\left(h_1\mathbf{x}_1 + \mathbf{z} + \mathbf{n}_2\right). \tag{4.33}$$

Using (4.33) in (4.32) yields

$$\mathbf{x}_1 = \boldsymbol{g}_1\theta_1 + \boldsymbol{B}_1\left(h_2\boldsymbol{g}_2\theta_2 + h_2\boldsymbol{B}_2\left(h_1\mathbf{x}_1 + \mathbf{z} + \mathbf{n}_2\right) + \mathbf{z} + \mathbf{n}_1\right). \tag{4.34}$$

Again exploiting the strictly causal nature of the feedback, $\boldsymbol{B}_1h_2\boldsymbol{B}_2h_1\mathbf{x}_1$ is known at transmitter 1 and therefore can be subtracted. Then, we get

$$\mathbf{x}_1 = \boldsymbol{g}_1\theta_1 + \boldsymbol{B}_1\underbrace{\left(h_2\boldsymbol{g}_2\theta_2 + (\boldsymbol{B}_2h_2 + \boldsymbol{I})\mathbf{z} + \boldsymbol{B}_2h_2\mathbf{n}_2 + \mathbf{n}_1\right)}_{\tilde{\mathbf{w}}_1}. \tag{4.35}$$

Analogously we get the transmit signal of transmitter 2,

$$\mathbf{x}_2 = \boldsymbol{g}_2\theta_2 + \boldsymbol{B}_2\underbrace{\left(h_1\boldsymbol{g}_1\theta_1 + (\boldsymbol{B}_1h_1 + \boldsymbol{I})\mathbf{z} + \boldsymbol{B}_1h_1\mathbf{n}_1 + \mathbf{n}_2\right)}_{\tilde{\mathbf{w}}_2}. \tag{4.36}$$

The receive signal is then

$$\begin{aligned}
\mathbf{y} &= h_1\mathbf{x}_1 + h_2\mathbf{x}_2 + \mathbf{z} && (4.37)\\
&= \underbrace{h_1(\boldsymbol{I} + \boldsymbol{B}_2h_2)\boldsymbol{g}_1}_{\tilde{\boldsymbol{g}}_1}\theta_1 + \underbrace{h_2(\boldsymbol{I} + \boldsymbol{B}_1h_1)\boldsymbol{g}_2}_{\tilde{\boldsymbol{g}}_2}\theta_2\\
&\quad + \underbrace{\left(h_1\boldsymbol{B}_1\boldsymbol{B}_2h_2 + h_2\boldsymbol{B}_2\boldsymbol{B}_1h_1 + h_1\boldsymbol{B}_1 + h_2\boldsymbol{B}_2 + \boldsymbol{I}\right)}_{\tilde{\boldsymbol{A}}}\mathbf{z}\\
&\quad + \underbrace{h_1(\boldsymbol{B}_1 + h_2\boldsymbol{B}_2\boldsymbol{B}_1)}_{\tilde{\boldsymbol{A}}_1}\mathbf{n}_1 + \underbrace{h_2(\boldsymbol{B}_2 + h_1\boldsymbol{B}_1\boldsymbol{B}_2)}_{\tilde{\boldsymbol{A}}_2}\mathbf{n}_2 && (4.38)\\
&= \tilde{\boldsymbol{g}}_1\theta_1 + \underbrace{\tilde{\boldsymbol{g}}_2\theta_2 + \underbrace{\tilde{\boldsymbol{A}}\mathbf{z} + \tilde{\boldsymbol{A}}_1\mathbf{n}_1 + \tilde{\boldsymbol{A}}_2\mathbf{n}_2}_{\mathbf{z}''}}_{\mathbf{z}'}. && (4.39)
\end{aligned}$$

Thus, the resulting system is equivalent to a multi-user non-feedback coding scheme with modified channel noise $\mathbf{z}''$.

4.3.3 Sum Capacity

The sum capacity is then given by [20]

$$C = \frac{1}{2}\log_2\left(\frac{|\boldsymbol{R}_{\mathbf{y}}|}{|\boldsymbol{R}_{\mathbf{z}'}|}\right) + \frac{1}{2}\log_2\left(\frac{|\boldsymbol{R}_{\mathbf{y}-\tilde{\boldsymbol{g}}_1\theta_1}|}{|\boldsymbol{R}_{\mathbf{z}''}|}\right). \tag{4.40}$$

This can be interpreted as an iterative decoding; for decoding θ_1, θ_2 is considered as noise, while for decoding θ_2, θ_1 is assumed to be known. The message with higher SNR is decoded first. To maximize 4.40 we have to find the optimum $\boldsymbol{g}_1$, $\boldsymbol{g}_2$, $\boldsymbol{B}_1$, $\boldsymbol{B}_2$ and the corresponding decoding functions. Due to its ill-defined structure this optimization problem is in general hard to solve. To overcome this problem we perform the transition from matrix to superposition coding in Section 4.4.

4.4 Transition from Matrix to Superposition Coding

In Section 4.3.2 the transmit signal (4.24) explicitly consists of the message component and the feedback component. Both are linear functions of the transmit message and the feedback, respectively; the message is "smeared" via a transmit vector and the feedback is transmitted via the feedback matrix. Both are hard to jointly optimize in the multiuser scenario.

Section 4.3.2 defines the conventional encoder $\boldsymbol{\varphi}_i(\theta_i)$ and the feedback based encoder $\tilde{\boldsymbol{\varphi}}_i(\theta_i, \boldsymbol{w})$ as

$$\mathbf{x}_i = \underbrace{\boldsymbol{g}_i\theta_i}_{\boldsymbol{\varphi}_i(\theta_i)} + \underbrace{\boldsymbol{B}_i\tilde{\mathbf{w}}_i}_{\tilde{\boldsymbol{\varphi}}_i(\theta_i,\boldsymbol{w})}, \qquad i = 1, 2. \tag{4.41}$$

Here, both encoders are functions of the same transmit message θ_i, which prevents us from attaining a superposition gain; these encoders could be simple added to one single linear encoder. Instead we now propose a superposition coding scheme that superimposes a feedback-based coding scheme $\tilde{\boldsymbol{\varphi}}_i(\tilde{\theta}_i, \boldsymbol{w})$ with a conventional coding scheme $\boldsymbol{\varphi}_i(\theta_i)$ that completely ignores the feedback,

$$\mathbf{x}_i = \boldsymbol{\varphi}_i(\theta_i) + \tilde{\boldsymbol{\varphi}}_i(\tilde{\theta}_i, \boldsymbol{w}), \qquad i = 1, 2. \tag{4.42}$$

We now have two independent messages θ_i and $\tilde{\theta}_i$ for each transmitter. This allows us to achieve a variety of improvements due to this additional degree of freedom. Most importantly, we achieve a superposition gain and a gain in capacity due to the multiuser scenario as we show later.

$$\boldsymbol{X} = \begin{pmatrix} x[1] & x[2] & \dots & x[N] \\ x[N+1] & x[N+2] & \dots & x[2N] \\ x[2N+1] & x[2N+2] & \dots & x[3N] \\ \vdots & \vdots & \ddots & \vdots \\ x[(\tilde{N}-1)N+1] & x[(\tilde{N}-1)N+2] & \dots & x[\tilde{N}N] \end{pmatrix} \tag{4.43}$$

$$= \underbrace{\begin{pmatrix} \varphi_1(\theta_1) & \varphi_2(\theta_1) & \dots & \varphi_N(\theta_1) \\ \varphi_1(\theta_2) & \varphi_2(\theta_2) & \dots & \varphi_N(\theta_2) \\ \vdots & \vdots & \ddots & \vdots \\ \varphi_1(\theta_{\tilde{N}}) & \varphi_2(\theta_{\tilde{N}}) & \dots & \varphi_N(\theta_{\tilde{N}}) \end{pmatrix}}_{\text{message } \theta_j \text{ is conventionally encoded in row (subblock) } j} \tag{4.44a}$$

$$+ \underbrace{\begin{pmatrix} \tilde{\varphi}_1\big(\tilde{\theta}_1, 0\big) & \tilde{\varphi}_1\big(\tilde{\theta}_2, 0\big) & \dots & \tilde{\varphi}_1\big(\tilde{\theta}_N, 0\big) \\ \tilde{\varphi}_2\big(\tilde{\theta}_1, \boldsymbol{w}_1^{(1)}\big) & \tilde{\varphi}_2\big(\tilde{\theta}_2, \boldsymbol{w}_2^{(1)}\big) & \dots & \tilde{\varphi}_2\big(\tilde{\theta}_N, \boldsymbol{w}_N^{(1)}\big) \\ \vdots & \vdots & \ddots & \vdots \\ \tilde{\varphi}_{\tilde{N}}\big(\tilde{\theta}_1, \boldsymbol{w}_1^{(\tilde{N}-1)}\big) & \tilde{\varphi}_{\tilde{N}}\big(\tilde{\theta}_2, \boldsymbol{w}_2^{(\tilde{N}-1)}\big) & \dots & \tilde{\varphi}_{\tilde{N}}\big(\tilde{\theta}_N, \boldsymbol{w}_N^{(\tilde{N}-1)}\big) \end{pmatrix}}_{\text{message } \tilde{\theta}_l \text{ is feedback-based encoded in column } l} \tag{4.44b}$$

4.5 Superposition Feedback Coding

4.5.1 AWGN Channel Model

We study the AWGN channel with quantized feedback (see Figure 4.4) in the finite blocklength regime as well as in the asymptotic regime. Here, the transmitter sends independent length-n Gaussian signals $x[k]$ and the receiver observes the signal

$$y[k] = hx[k] + z[k], \tag{4.45}$$

where $z[k] \sim \mathcal{N}(0, \sigma^2)$ is i.i.d. additive Gaussian noise. The channel gain h is assumed to be known by both transmitter and receiver. We impose the average transmit power constraint (here, expectation is with respect to the messages and the channel noise)

$$\frac{1}{n}\sum_{k=1}^{n} \mathrm{E}\big\{\mathsf{x}^2[k]\big\} \le P. \tag{4.46}$$

In order to enable successive cancellation decoding, the overall transmission block of length n is split into $\tilde{N}$ subblocks of length N each, i.e.,

$$n = \tilde{N}N. \tag{4.47}$$

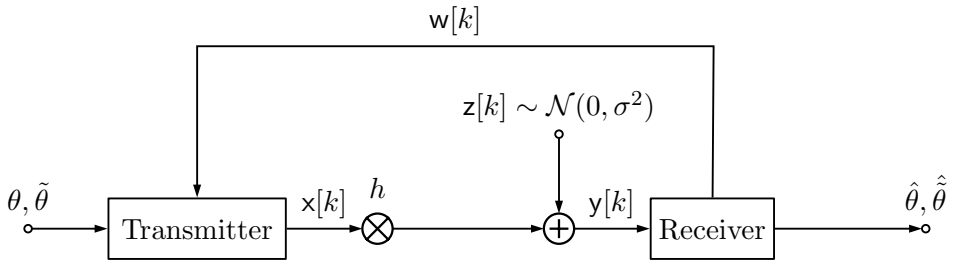

Figure 4.4: AWGN channel with feedback link and superposition coding.

We rearrange the transmit signal $x[k]$ into a $\tilde{N} \times N$ matrix $\boldsymbol{X}$ (see (4.43)) to fit into this block structure,

$$[\boldsymbol{X}]_{j,l} = x[(j-1)N + l], \qquad j = 1, \ldots, \tilde{N}, \quad l = 1, \ldots, N. \tag{4.48}$$

Each row of $\boldsymbol{X}$ represents one subblock that encodes one conventional codeword. By contrast, the feedback-based codewords are encoded in the columns of $\boldsymbol{X}$, i.e., over corresponding time slots in all subblocks.

The noise is rearranged in the same way as

$$[\boldsymbol{Z}]_{j,l} = z[(j-1)N + l]. \tag{4.49}$$

The received signal in matrix form reads

$$\boldsymbol{Y} = h\boldsymbol{X} + \boldsymbol{Z}. \tag{4.50}$$

The concrete functionality of the encoders and superposition coding are developed in Section 5.2 for the asymptotic case and Section 6.2 for the finite blocklength regime.

4.5.2 MAC Model

We study the two-user asymmetric Gaussian MAC with quantized feedback (see Figure 4.5) in the finite blocklength regime as well as in the asymptotic regime. Here, the two transmitters send independent length-n Gaussian signals $x_i[k]$, $i = 1, 2$, and the receiver observes the signal

$$y[k] = h_1 x_1[k] + h_2 x_2[k] + z[k], \tag{4.51}$$

where $z[k] \sim \mathcal{N}(0, \sigma^2)$ is i.i.d. additive Gaussian noise. The channel gains h_1 and h_2 are assumed to be known by both transmitters and by the receiver. We impose the average transmit sum-power constraint (here, expectation is with respect to the messages and

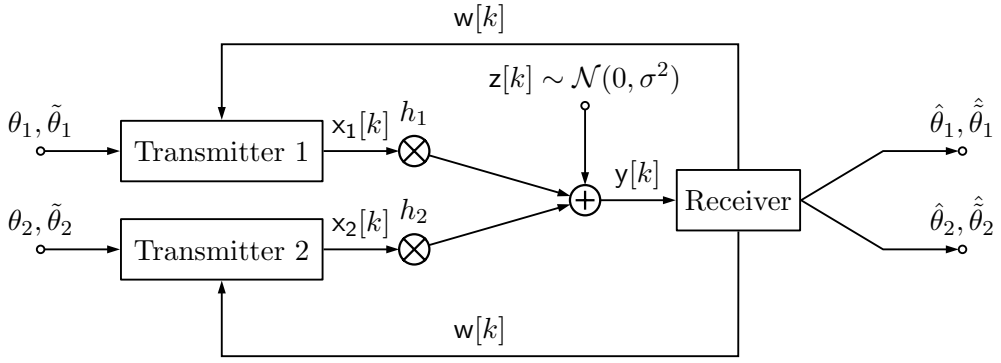

Figure 4.5: Two-user Gaussian MAC with common feedback link and superposition coding.

the channel noise)

$$\frac{1}{n}\sum_{k=1}^{n}\mathrm{E}\{\mathsf{x}_1^2[k]+\mathsf{x}_2^2[k]\}\leq P. \tag{4.52}$$

In order to enable successive cancellation decoding, the overall transmission block of length n is split into $\tilde{N}$ subblocks of length N each, i.e.,

$$n=\tilde{N}N. \tag{4.53}$$

We rearrange each transmit signal $x_i[k]$ into a $\tilde{N}\times N$ matrix $\boldsymbol{X}^{(i)}$ (see (4.57)) to fit into this block structure,

$$[\boldsymbol{X}^{(i)}]_{j,l}=x_i[(j-1)N+l],\qquad j=1,\ldots,\tilde{N},\quad l=1,\ldots,N. \tag{4.54}$$

Each row of $\boldsymbol{X}^{(i)}$ represents one subblock that encodes one conventional codeword. By contrast, the feedback-based codewords are encoded in the columns of $\boldsymbol{X}^{(i)}$, i.e., over corresponding time slots in all subblocks.

The noise is rearranged in the same way as

$$[\boldsymbol{Z}]_{j,l}=z[(j-1)N+l],\qquad j=1,\ldots,\tilde{N},\quad l=1,\ldots,N. \tag{4.55}$$

The received signal in matrix form reads

$$\boldsymbol{Y}=h_1\boldsymbol{X}^{(1)}+h_2\boldsymbol{X}^{(2)}+\boldsymbol{Z}. \tag{4.56}$$

The concrete functionality of the encoders and superposition coding are developed in Section 5.3 and Section 5.4 for the asymptotic case and Section 6.3 for the finite blocklength regime.

$$\boldsymbol{X}^{(i)} = \begin{pmatrix} x_i[1] & x_i[2] & \dots & x_i[N] \\ x_i[N+1] & x_i[N+2] & \dots & x_i[2N] \\ x_i[2N+1] & x_i[2N+2] & \dots & x_i[3N] \\ \vdots & \vdots & \ddots & \vdots \\ x_i[(\tilde{N}-1)N+1] & x_i[(\tilde{N}-1)N+2] & \dots & x_i[\tilde{N}N] \end{pmatrix} \tag{4.57}$$

$$= \underbrace{\begin{pmatrix} \varphi_{i,1}(\theta_{i,1}) & \varphi_{i,2}(\theta_{i,1}) & \dots & \varphi_{i,N}(\theta_{i,1}) \\ \varphi_{i,1}(\theta_{i,2}) & \varphi_{i,2}(\theta_{i,2}) & \dots & \varphi_{i,N}(\theta_{i,2}) \\ \vdots & \vdots & \ddots & \vdots \\ \varphi_{i,1}(\theta_{i,\tilde{N}}) & \varphi_{i,2}(\theta_{i,\tilde{N}}) & \dots & \varphi_{i,N}(\theta_{i,\tilde{N}}) \end{pmatrix}}_{\text{message } \theta_{i,j} \text{ is conventionally encoded in row (subblock) } j} \tag{4.58a}$$

$$+ \underbrace{\begin{pmatrix} \tilde{\varphi}_{i,1}\big(\tilde{\theta}_{i,1}, 0\big) & \tilde{\varphi}_{i,1}\big(\tilde{\theta}_{i,2}, 0\big) & \dots & \tilde{\varphi}_{i,1}\big(\tilde{\theta}_{i,N}, 0\big) \\ \tilde{\varphi}_{i,2}\big(\tilde{\theta}_{i,1}, \boldsymbol{w}_1^{(1)}\big) & \tilde{\varphi}_{i,2}\big(\tilde{\theta}_{i,2}, \boldsymbol{w}_2^{(1)}\big) & \dots & \tilde{\varphi}_{i,2}\big(\tilde{\theta}_{i,N}, \boldsymbol{w}_N^{(1)}\big) \\ \vdots & \vdots & \ddots & \vdots \\ \tilde{\varphi}_{i,\tilde{N}}\big(\tilde{\theta}_{i,1}, \boldsymbol{w}_1^{(\tilde{N}-1)}\big) & \tilde{\varphi}_{i,\tilde{N}}\big(\tilde{\theta}_{i,2}, \boldsymbol{w}_2^{(\tilde{N}-1)}\big) & \dots & \tilde{\varphi}_{i,\tilde{N}}\big(\tilde{\theta}_{i,N}, \boldsymbol{w}_N^{(\tilde{N}-1)}\big) \end{pmatrix}}_{\text{message } \tilde{\theta}_{i,l} \text{ is feedback-based encoded in column } l} \tag{4.58b}$$

4.5.3 BC Model

We study the two-user asymmetric Gaussian BC with quantized feedback (see Figure 4.6) in the finite blocklength regime as well as in the asymptotic regime. Here, in contrast to the MAC in the previous section, one single transmitter sends independent length-n Gaussian signal components $x_i[k]$, $i = 1, 2$, where

$$x[k] = x_1[k] + x_2[k]. \tag{4.59}$$

The two receivers observe the signals

$$y_1[k] = h_1 x_1[k] + h_1 x_2[k] + z_1[k], \tag{4.60}$$

$$y_2[k] = h_2 x_1[k] + h_2 x_2[k] + z_2[k], \tag{4.61}$$

where $z_i[k] \sim \mathcal{N}(0, \sigma^2)$, $i = 1, 2$, is i.i.d. additive Gaussian noise. The channel gains h_1 and h_2 are assumed to be known by transmitter and by both receivers. Due to this component-wise encoding the BC model is conceptionally closely connected to the MAC model. We impose the average transmit power constraint (here, expectation is with respect to the messages and the channel noise)

$$\frac{1}{n} \sum_{k=1}^{n} \mathrm{E}\big\{\mathsf{x}_1^2[k] + \mathsf{x}_2^2[k]\big\} \leq P. \tag{4.62}$$

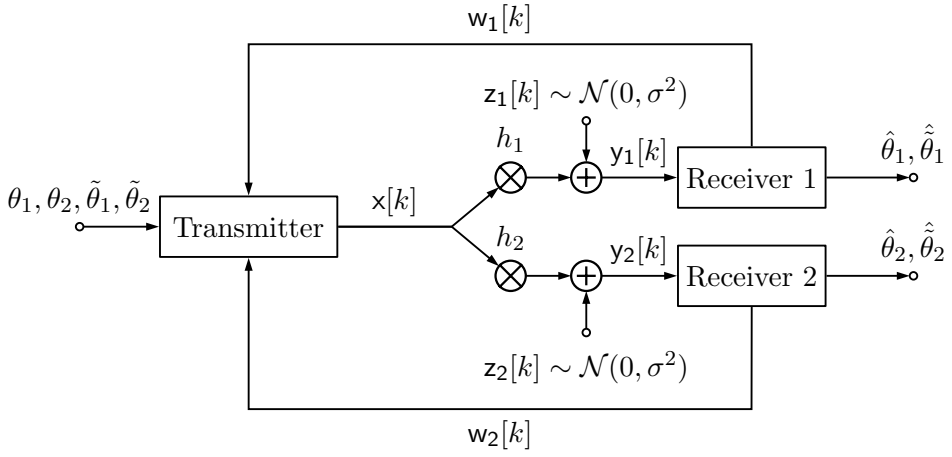

Figure 4.6: Two-user Gaussian BC with feedback link and superposition coding.

In order to enable successive cancellation decoding, the overall transmission block of length n is again split into $\tilde{N}$ subblocks of length N each, i.e.,

$$n = \tilde{N}N. \tag{4.63}$$

Similarly as for the MAC, we rearrange each transmit signal component $x_i[k]$ into a $\tilde{N} \times N$ matrix $\boldsymbol{X}^{(i)}$ (see (4.68)) to fit into this block structure,

$$[\boldsymbol{X}^{(i)}]_{j,l} = x_i[(j-1)N + l], \qquad j = 1, \ldots, \tilde{N}, \quad l = 1, \ldots, N. \tag{4.64}$$

Each row of $\boldsymbol{X}^{(i)}$ represents one subblock that encodes one conventional codeword. By contrast, the feedback-based codewords are encoded in the columns of $\boldsymbol{X}^{(i)}$, i.e., over corresponding time slots in all subblocks.

The noise is rearranged in the same way as

$$[\boldsymbol{Z}^{(i)}]_{j,l} = z[(j-1)N + l], \qquad j = 1, \ldots, \tilde{N}, \quad l = 1, \ldots, N. \tag{4.65}$$

The received signals in matrix form read

$$\boldsymbol{Y}^{(1)} = h_1 \boldsymbol{X}^{(1)} + h_1 \boldsymbol{X}^{(2)} + \boldsymbol{Z}^{(1)}, \tag{4.66}$$

$$\boldsymbol{Y}^{(2)} = h_2 \boldsymbol{X}^{(1)} + h_2 \boldsymbol{X}^{(2)} + \boldsymbol{Z}^{(2)}. \tag{4.67}$$

The concrete functionality of the encoders and superposition coding are developed in Section 5.5 and Section 5.6 for the asymptotic case and Section 6.4 for the finite blocklength regime.

$$\boldsymbol{X}^{(i)} = \begin{pmatrix} x_i[1] & x_i[2] & \dots & x_i[N] \\ x_i[N+1] & x_i[N+2] & \dots & x_i[2N] \\ x_i[2N+1] & x_i[2N+2] & \dots & x_i[3N] \\ \vdots & \vdots & \ddots & \vdots \\ x_i[(\tilde{N}-1)N+1] & x_i[(\tilde{N}-1)N+2] & \dots & x_i[\tilde{N}N] \end{pmatrix} \tag{4.68}$$

$$= \underbrace{\begin{pmatrix} \varphi_{i,1}(\theta_{i,1}) & \varphi_{i,2}(\theta_{i,1}) & \dots & \varphi_{i,N}(\theta_{i,1}) \\ \varphi_{i,1}(\theta_{i,2}) & \varphi_{i,2}(\theta_{i,2}) & \dots & \varphi_{i,N}(\theta_{i,2}) \\ \vdots & \vdots & \ddots & \vdots \\ \varphi_{i,1}(\theta_{i,\tilde{N}}) & \varphi_{i,2}(\theta_{i,\tilde{N}}) & \dots & \varphi_{i,N}(\theta_{i,\tilde{N}}) \end{pmatrix}}_{\text{message } \theta_{i,j} \text{ is conventionally encoded in row (subblock) } j} \tag{4.69a}$$

$$+ \underbrace{\begin{pmatrix} \tilde{\varphi}_{i,1}\big(\tilde{\theta}_{i,1}, 0\big) & \tilde{\varphi}_{i,1}\big(\tilde{\theta}_{i,2}, 0\big) & \dots & \tilde{\varphi}_{i,1}\big(\tilde{\theta}_{i,N}, 0\big) \\ \tilde{\varphi}_{i,2}\big(\tilde{\theta}_{i,1}, \boldsymbol{w}_{i,1}^{(1)}\big) & \tilde{\varphi}_{i,2}\big(\tilde{\theta}_{i,2}, \boldsymbol{w}_{i,2}^{(1)}\big) & \dots & \tilde{\varphi}_{i,2}\big(\tilde{\theta}_{i,N}, \boldsymbol{w}_{i,N}^{(1)}\big) \\ \vdots & \vdots & \ddots & \vdots \\ \tilde{\varphi}_{i,\tilde{N}}\big(\tilde{\theta}_{i,1}, \boldsymbol{w}_{i,1}^{(\tilde{N}-1)}\big) & \tilde{\varphi}_{i,\tilde{N}}\big(\tilde{\theta}_{i,2}, \boldsymbol{w}_{i,2}^{(\tilde{N}-1)}\big) & \dots & \tilde{\varphi}_{i,\tilde{N}}\big(\tilde{\theta}_{i,N}, \boldsymbol{w}_{i,N}^{(\tilde{N}-1)}\big) \end{pmatrix}}_{\text{message } \tilde{\theta}_{i,l} \text{ is feedback-based encoded in column } l} \tag{4.69b}$$

4.5.4 Proposed Coding Scheme

The proposed coding scheme superimposes a feedback-based coding scheme with a conventional coding scheme that completely ignores the feedback. The original idea of such a splitting for similar schemes dates back to the fundamental contributions of Carleial [10] and Ozarow [60]. Throughout this thesis we assume that we can perfectly separate these superimposed codes. The receiver first decodes the conventional code and then cancels it from the receive signal. This type of decoding is usually referred to as successive cancellation and requires that the conventional codeword is completely received before it can be cancelled. At first glance, this seems to contradict the assumption that the received signal is fed back to the transmitters in each time instance. This seeming contradiction can be resolved using the subblock structure introduced above along with per subblock feedback. This subblock structure allows us to superimpose the conventional coding with the feedback-based coding acting as additional noise. Before feeding back the feedback components the signal from the conventional coding can be fully subtracted and thus what remains is solely the Ozarow feedback coding scheme without any interference. This particular order of decoding that is made possible due to the block structure is the main difference to similar splitting schemes as in [46, 47, 60, 83].

Next, we briefly outline the proposed coding scheme for the MAC; for the AWGN channel and BC this subsection is fully analogous. More specifically, let $\boldsymbol{w}_l^{(j-1)} =$

$(w[1]\dots w[(j-1)N+l])^\top$ denote the past quantized feedback up to time $k=(j-1)N+l$ (i.e., the lth time slot in subblock j). The linear superposition codewords are obtained as (see (4.58))

$$[\boldsymbol{X}^{(i)}]_{j,l} = \varphi_{i,l}(\theta_{i,j}) + \tilde{\varphi}_{i,j}\big(\tilde{\theta}_{i,l}, \boldsymbol{w}_l^{(j-1)}\big). \tag{4.70}$$

Here, $\theta_{i,j}$, $j=1,\dots,\tilde{N}$ and $\tilde{\theta}_{i,l}$, $l=1,\dots,N$ are independent messages of user i. Throughout the thesis, superscript tilde indicates quantities based on the exploitation of the channel output feedback. The messages are uniformly drawn from finite sets with cardinalities $\mathcal{M}_i = 2^{NR_i}$, $\widetilde{\mathcal{M}}_i = 2^{\tilde{N}\tilde{R}_i}$, $i=1,2$. Furthermore, $\varphi_{i,l}: \mathcal{M}_i \to \mathbb{R}$ denotes a conventional encoder with power constraint

$$\frac{1}{N}\sum_{l=1}^{N} \mathrm{E}\big\{\varphi_{i,l}^2(\theta_{i,j})\big\} \le P_i, \tag{4.71}$$

where the expectation is over all possible transmit messages. The conventional encoder completely ignores the feedback signal. Similarly, $\tilde{\varphi}_{i,j}: \widetilde{\mathcal{M}}_i \times \mathbb{R}^{k-1} \to \mathbb{R}$ is the feedback-based encoder with power constraint

$$\frac{1}{\tilde{N}}\sum_{j=1}^{\tilde{N}} \mathrm{E}\Big\{\tilde{\varphi}_{i,j}^2\big(\tilde{\theta}_{i,l}, \mathbf{w}_l^{(j-1)}\big)\Big\} \le \tilde{P}_i, \tag{4.72}$$

with the expectation being over all possible transmit messages and channel realizations. This encoder has causal access to the quantized feedback and works as in the original Ozarow scheme (see Section 2.4.1).

The above (sub)block encoding and feedback scheme enables us to decode a conventional codeword after each subblock and to cancel this component in order to decode the feedback-based components, like in standard successive cancellation. Each conventional codeword is decoded after N time slots whereas the feedback-based codewords are spread over $\tilde{N}$ blocks and decoded after $N(\tilde{N}-1)$ time slots. Thus, the coding scheme with blocklength $n=\tilde{N}N$ has an effective average blocklength of

$$\frac{(R_1+R_2)N + (\tilde{R}_1+\tilde{R}_2)N(\tilde{N}-1)}{R_1+R_2+\tilde{R}_1+\tilde{R}_2} < n. \tag{4.73}$$

4.5.5 Feedback Quantization

In our model, the channel output at the receiver is quantized before being fed back to the transmitters. More specifically, the receiver performs successive cancellation, i.e., it subtracts the estimates $\varphi_{i,l}(\hat{\theta}_{i,j})$ of the conventional codewords in subblock j from the received signal (i.e., from the jth row of $\boldsymbol{Y}$ in (4.56)) and then quantizes the residual,

$$\tilde{y}_{j,l} = y[(j-1)N+l] - h_1\,\varphi_{1,l}(\hat{\theta}_{1,j}) - h_2\,\varphi_{2,l}(\hat{\theta}_{2,j}), \tag{4.74a}$$

$$w[(j-1)N+l] = \mathcal{Q}\big(\tilde{y}_{j,l}\big). \tag{4.74b}$$

The quantization $\mathcal{Q}(\cdot)$ is modeled as an information bottleneck, i.e., the mutual information between compressed received signal and transmit signal is maximized under a rate constraint (cf. Chapter 3). Rate-information optimal channel output compression amounts to additive Gaussian quantization noise (see Corollary 3.10). For the MAC with noisy feedback the extra noise on the feedback channel is detrimental since it is not known by any node. In our model the transmitters also receive degraded versions of the channel output, but the receiver knows the quantization error of the feedback signal (having itself performed the quantization). With this observation, our scheme can be reduced to an equivalent MAC with perfect feedback in which the quantization error represents additional channel noise. The knowledge of this extra noise is exploited at the receiver.

5

Asymptotic Superposition Coding

5.1 Introduction

In this chapter we apply the feedback model that we introduced in Chapter 4 in the asymptotic regime. That is, we optimize the trade offbetween the conventional component and the feedback component in the superposition scheme to gain the achievable rate regions for various channel types. This yields a difference of convex functions (DC) problem (see Section 2.8) what we solve using the simple yet efficient convex-concave procedure (CCP) algorithm. We start with studying the scheme for the AWGN channel and then generalize it to the symmetric Gaussian multiple access channel (MAC) and the symmetric Gaussian broadcast channel (BC). As a last step we drop the symmetry condition and give results for the asymmetric case.

5.2 Asymptotic Superpostion Performance - Gaussian Channel

It is known that feedback cannot increase the capacity for point-to-point channels (see Section 2.2.1). As a consequence, intuitively superposition should be of no benefit, at least in the asymptotic region since conventional coding without any feedback already achieves capacity. However feedback can drastically help to reduce the error rates for specific blocklengths in the finite blocklength regime (see Section 2.2.2). Thus, superposition may be beneficial in the finite blocklength regime in Chapter 6. Nevertheless, for didactic purposes we introduce the superposition coding for the AWGN channel already here in the asymptotic regime. This then serves as a basis and is extended to multiuser scenarios in the following sections.

5.2.1 Power Constraints

We study the AWGN channel with (quantized) feedback (see Figure 4.4). Here, the transmitter sends the independent length-n Gaussian user signal $x[k]$ and the receiver observes the signal

$$y[k] = hx[k] + z[k]. \tag{5.1}$$

The channel gain h is assumed to be known by both transmitter and receiver and the channel introduces i.i.d. additive Gaussian noise $\mathbf{z} \sim \mathcal{N}(\mathbf{0}, \sigma^2 \boldsymbol{I})$. We impose the average transmit power constraint (here, expectation is with respect to the messages and the channel noise)

$$\frac{1}{n} \sum_{k=1}^{n} \mathrm{E}\{\mathsf{x}^2[k]\} \leq P_T. \tag{5.2}$$

The transmitter communicates the independent messages θ_j, $j = 1, \ldots, \tilde{N}$, $\tilde{\theta}_l$, $l = 1, \ldots, N$, to a single receiver. The messages are uniformly drawn from finite sets with cardinalities $\mathcal{M} = 2^{NR}$, $\widetilde{\mathcal{M}} = 2^{\tilde{N}\tilde{R}}$, and mapped to the transmit signal according to the superposition (see Section 4.5.1) with block structure (cf. (4.44))

$$x[(j-1)N + l] = \varphi_l(\theta_j) + \tilde{\varphi}_j\big(\tilde{\theta}_l, \boldsymbol{w}_l^{(j-1)}\big), \qquad j = 1, \ldots, \tilde{N}, \quad l = 1, \ldots, N, \tag{5.3}$$

$k = (j-1)N + l = 1, \ldots, n$. Here, $\varphi_l : \mathcal{M} \to \mathbb{R}$ denotes a conventional encoder with power constraint

$$\frac{1}{N} \sum_{l=1}^{N} \mathrm{E}\{\varphi_l^2(\theta_j)\} \leq P, \qquad j = 1, \ldots, \tilde{N}, \tag{5.4}$$

with expectation over all possible transmit messages θ_j. The conventional encoder completely ignores the feedback signal. Furthermore, $\boldsymbol{w}_l^{(j-1)} = (w[1] \ldots w[(j\text{–}1)N\text{+}l])^\top$ denotes the past quantized feedback and $\tilde{\varphi}_j : \widetilde{\mathcal{M}} \times \mathbb{R}^{j-1} \to \mathbb{R}$ is the feedback-based encoder with power constraint

$$\frac{1}{\tilde{N}} \sum_{j=1}^{\tilde{N}} \mathrm{E}\Big\{\tilde{\varphi}_j^2\big(\tilde{\theta}_l, \mathbf{w}_l^{(j-1)}\big)\Big\} \leq \tilde{P}, \qquad l = 1, \ldots, N, \tag{5.5}$$

with expectation over all possible transmit messages $\tilde{\theta}_l$ and channel realizations. This encoder has causal access to the quantized feedback and works as in the original Schalkwijk-Kailath scheme (see Section 2.2). Due to the superimposed block structure the constraints on the transmit powers sum up to

$$P + \tilde{P} = P_T. \tag{5.6}$$

5.2.2 Achievable Sum Rate

Our proposed scheme is a superposition of a conventional encoder and a feedback-based encoder (cf. (5.3)). Thus, we can maximize the sum rate by finding the optimum power (equivalently, rate) splitting between the two encodings. The conventionally encoded signal is cancelled at the receiver before quantization such that the quantization only captures the feedback encoding in the forward path. This is possible since the receiver has the quantization noise as side-information (see Section 4.5.5). The sum rate of the conventional coding scheme is thus given by the classical AWGN capacity C_0 (see Section 2.1.1) with noise power $\sigma^2 + h\tilde{P}$, since the independent feedback-based codewords (cf. (4.44b)) that are each superimposed in specific time instances of the conventional coding (cf. (4.44a)) act as additional interference. Then, the achievable rate for fixed feedback transmit power $\tilde{P}$ and given total transmit power P_T is

$$\begin{aligned} R &\leq C_0(h^2P, \sigma^2 + h^2\tilde{P}) \\ &\triangleq \mathsf{C}. \end{aligned} \tag{5.7}$$

The sum rate of the feedback coding scheme is given by the SK capacity C^{FB} (see Section 2.2.1) with noise power $\sigma^2 + \sigma_q^2$ (due to the additional quantization noise). Then, the achievable rate for fixed transmit power P and given total transmit power P_T is

$$\begin{aligned} \tilde{R} &\leq C^{\mathrm{FB}}(h^2\tilde{P}, \sigma^2 + \sigma_q^2) \\ &\triangleq \tilde{\mathsf{C}}. \end{aligned} \tag{5.8}$$

Thus, the total achievable sum rate of our proposed scheme with given total transmit power P_T yields

$$\begin{aligned} R_1 + \tilde{R} &\leq \max_{P+\tilde{P}\leq P_T} \mathsf{C} + \tilde{\mathsf{C}} \\ &\triangleq C_S. \end{aligned} \tag{5.9}$$

Expanding the maximizations (implicitly contained in the expressions for C and $\tilde{\mathsf{C}}$) to one single maximization yields

$$C_S = \max_{P+\tilde{P}\leq P_T} C_0(h^2P, \sigma^2 + h^2\tilde{P}) + C^{\mathrm{FB}}(h^2\tilde{P}, \sigma^2 + \sigma_q^2). \tag{5.10}$$

Although high feedback transmit power $\tilde{P}$ has a negative impact on the capacity of the conventional scheme due to the additional interference noise it is clearly still optimal to use all the available transmit power. Therefore, the optimal solution of (5.10) has to lie on the boundary $P + \tilde{P} = P_T$. Reformulating this problem solely as a function

of $\tilde{P}$ then yields

$$C_S = \max_{\tilde{P}} \underbrace{C_0(h^2(P_T - \tilde{P}, \sigma^2 + h^2\tilde{P})}_{C(\tilde{P})} + \underbrace{C^{\mathrm{FB}}(h^2\tilde{P}, \sigma^2 + \sigma_q^2)}_{\tilde{C}(\tilde{P})} \qquad \text{s.t.} \quad 0 \leq \tilde{P} \leq P_T. \tag{5.11}$$

Clearly, $C(\tilde{P})$ is a strictly decreasing function in $\tilde{P}$ and $\tilde{C}(\tilde{P})$ is strictly increasing in $\tilde{P}$. As a consequence there is a tradeoff between conventional coding and feedback-based coding. The optimum is either the extreme case where all transmit power is allocated to the conventional coding scheme ($\tilde{P} = 0$) or to the feedback coding ($\tilde{P} = P_T$), or the optimum is in fact a true superposition of both coding schemes depending on the quantization rate R_Q.

5.2.3 Concave and Convex Component

Next, we prove that C_S can be split into a concave part $\mathsf{C}^{\cap}(\tilde{P})$ and a convex part $\mathsf{C}^{\cup}(\tilde{P})$ in the feedback transmit power $\tilde{P}$,

$$C_S = \max_{\tilde{P}} \mathsf{C}^{\cap}(\tilde{P}) + \mathsf{C}^{\cup}(\tilde{P}) \qquad \text{s.t.} \quad 0 \leq \tilde{P} \leq P_T. \tag{5.12}$$

Then, this sum rate maximization problem can be solved by DC programming (see Section 2.8). It can be shown that $\tilde{C}(\tilde{P})$ is a concave function and $C(\tilde{P})$ is a convex function in $\tilde{P}$. Indeed, by direct calculation we obtain the second-order derivative of $C(\tilde{P})$ as

$$C''(\tilde{P}) = \frac{h^4}{(h^2\tilde{P} + \sigma^2)^2} \geq 0, \tag{5.13}$$

which proves convexity. The concavity of $\tilde{C}(\tilde{P})$ can be analogously proved by showing that the second derivative is non-positive. In summary, the sum capacity C_{S} is the sum of a convex and a concave function, or equivalently the difference of two convex functions.

5.2.4 Difference of Convex Functions Programming Solution

Splitting the objective function and our already affine constraints into concave and convex functions allows us to solve the optimization problem via DC programming (see Section 2.8) and the practically efficient CCP algorithm (see Section 2.8.1). Rewriting our maximization problem (5.11) in standard form (2.66) yields the following result.

Corollary 5.1. *The problem of maximizing the achievable sum rate of the AWGN channel with quantized feedback and a superposition of feedback coding with capcity $\tilde{C}$ and conventional coding with capacity C is solved by finding the solution of the DC*

Algorithm 4 Transmit power allocation for AWGN channel with feedback via CCP

Require: Initial feasible point $\tilde{P}_{(0)}$
1: $k := 0$
2: **while** stopping criterion not satisfied **do**
3: *Convexify.* Form $\hat{C}_{(k)}\left(\tilde{P}\right) = C\left(\tilde{P}_{(k)}\right) + C'\left(\tilde{P}_{(k)}\right)\left(\tilde{P} - \tilde{P}_{(k)}\right)$
4: *Solve.* Determine $\tilde{P}_{(k+1)}$ as solution of the convex problem
minimize $-\tilde{C}(\tilde{P}) - \hat{C}_{(k)}(\tilde{P})$
subject to $\tilde{P} - P_T \leq 0$
$-\tilde{P} \leq 0$
5: $k := k + 1$
6: **end while**
7: **return** $\tilde{P}_{(k)}$

problem

$$\begin{aligned} \underset{\tilde{P}}{\textit{minimize}} \quad & -\tilde{C}(\tilde{P}) - C(\tilde{P}) \\ \textit{subject to} \quad & \tilde{P} - P_T \leq 0 \\ & -\tilde{P} \leq 0. \end{aligned} \tag{5.14}$$

The basic idea of the iterative CCP algorithm [91] is to find a point where the gradient of the convex part in the next iteration equals the negative gradient of the concave part of the previous iteration

$$\frac{\partial}{\partial \tilde{P}} \tilde{C}\left(\tilde{P}_{(k+1)}\right) = -\frac{\partial}{\partial \tilde{P}} C\left(\tilde{P}_{(k)}\right), \tag{5.15}$$

which itself is a convex optimization problem. The solution to this auxiliary problem decreases monotonically with increasing k and thus converges to a minimum (or saddle point). Lipp and Boyd [49] give a basic CCP algorithm (see Section 2.8.1) that requires an initial feasible point $\tilde{P}_{(0)}$, which in our case can be any point in the interval $[0, P_T]$. Following [49], the CCP approach leads to Algorithm 4 for power allocation.

Figure 5.2 and Figure 5.1 illustrate the optima which are the maxima of the sum capacities in the various achievable rate regions.

The Suboptimality of Superposition

Figure 5.1 shows the achievable rate region for fixed quantization rate R_Q and variable transmit power P_T. We see that it is optimal to allocate all the available transmit power only to non-feedback coding regardless of the total available transmit power. The optimum is the point with maximum achievable sum rate. This becomes obvious if we look at $\tilde{C}(\tilde{P})$ and $C(P)$ in more detail. In the scalar case the SK-capacity equals the standard AWGN channel capacity. But due to the quantization the total

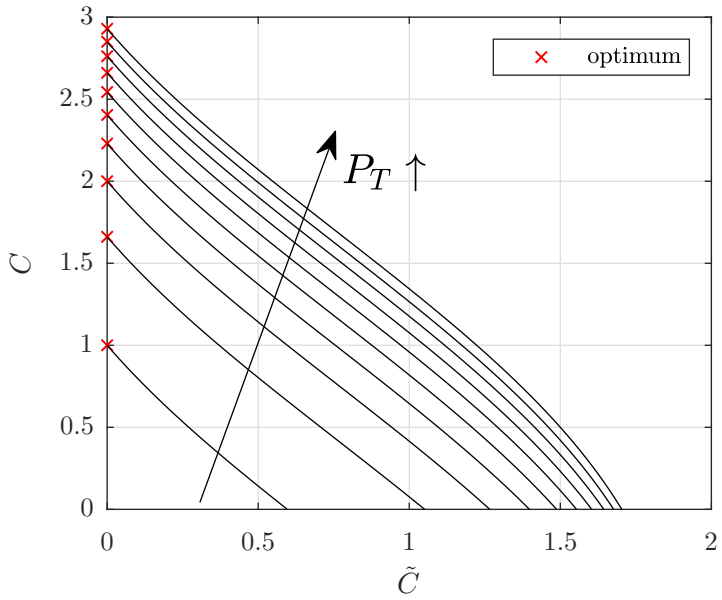

Figure 5.1: AWGN channel achievable rate region $(\tilde{C}(\tilde{P}), C(\tilde{P}))$ for fixed $R_Q = 2$ and $P_T = 0.1P_{R_Q} \dots 2P_{R_Q}$ where P_{R_Q} is such that $C_0(P_{R_Q}) = R_Q$.

noise is increased. In Figure 5.2 we can observe that for high quantization rates this penalty almost vanishes. Then, we almost achieve the same sum rate on $(\tilde{P}, P)$ where $\tilde{P} + P = P_T$. Note that this suboptimality only holds in the asymptotic regime, whereas in the finite blocklength regime true superposition is optimal (for suitably high quantization rates) due to the higher error decay of the feedback coding (see Section 6.2).

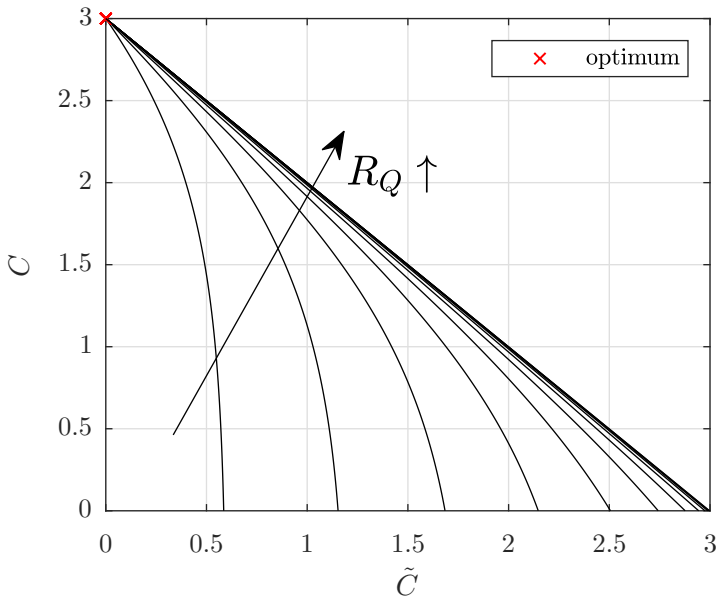

Figure 5.2: AWGN channel achievable rate region $(\tilde{C}(\tilde{P}), C(\tilde{P}))$ for fixed $C_0 = 3$ and $R_Q = 0.2C_0 \ldots 2.4C_0$.

5.3 Asymptotic Superposition Performance - Symmetric Multiple Access Channel

Next, we study the symmetric MAC with equal channel gains which is a straightforward extension of the AWGN channel in Section 5.3. The most important difference is that for the MAC true superposition coding indeed achieves higher rates than exclusive conventional or feedback coding.

5.3.1 Power Constraints

We study the two-user symmetric Gaussian MAC with (quantized) feedback (see Figure 4.5). In this section we consider normalized channel gains $h_1 = h_2 = 1$. Here, the transmitters send the independent length-n Gaussian user signals $x_i[k]$, $i = 1, 2$, and the receiver observes the signal

$$y[k] = x_1[k] + x_2[k] + z[k]. \tag{5.16}$$

The channel introduces i.i.d. additive Gaussian noise $\mathbf{z} \sim \mathcal{N}(\mathbf{0}, \sigma^2 \boldsymbol{I})$. We impose the average transmit sum-power constraint (here, expectation is with respect to the messages and the channel noise)

$$\frac{1}{n} \sum_{k=1}^{n} \mathrm{E}\big\{ \mathsf{x}_1^2[k] + \mathsf{x}_2^2[k] \big\} \leq P_T. \tag{5.17}$$

The transmitters communicate independent messages $\theta_{1,j}$, $\tilde{\theta}_{1,l}$ and $\theta_{2,j}$, $\tilde{\theta}_{2,l}$, $j = 1, \ldots, \tilde{N}$, $l = 1, \ldots, N$, to a single receiver. The messages are uniformly drawn from finite sets with cardinalities $\mathcal{M}_1 = 2^{NR}$, $\widetilde{\mathcal{M}}_1 = 2^{\tilde{N}\tilde{R}}$, $\mathcal{M}_2 = 2^{NR}$, $\widetilde{\mathcal{M}}_2 = 2^{\tilde{N}\tilde{R}}$, and mapped to the transmit signals according to the superposition (see Section 4.5.2) with block structure (cf. (4.58))

$$x_i[(j-1)N + l] = \varphi_{i,l}(\theta_{i,j}) + \tilde{\varphi}_{i,j}\big(\tilde{\theta}_{i,l}, \boldsymbol{w}_l^{(j-1)}\big),\ j = 1, \ldots, \tilde{N},\ l = 1, \ldots, N,\ i = 1, 2, \tag{5.18}$$

$k = (j-1)N + l = 1, \ldots, n$. Here, $\varphi_{i,l} : \mathcal{M}_i \to \mathbb{R}$ denotes a conventional encoder with power constraint

$$\frac{1}{N} \sum_{l=1}^{N} \mathrm{E}\big\{ \varphi_{i,l}^2(\theta_{i,j}) \big\} \leq P, \quad j = 1, \ldots, \tilde{N}, \quad i = 1, 2, \tag{5.19}$$

with expectation over all possible transmit messages $\theta_{i,j}$. The conventional encoder completely ignores the feedback signal. Furthermore, $\boldsymbol{w}_l^{(j-1)} = (w[1] \ldots w[(j\text{–}1)N + l])^\top$ denotes the past quantized feedback and $\tilde{\varphi}_{i,j} : \widetilde{\mathcal{M}}_i \times \mathbb{R}^{j-1} \to \mathbb{R}$ is the feedback-based

encoder with power constraint

$$\frac{1}{n}\sum_{j=1}^{\tilde{N}} \mathrm{E}\Big\{\tilde{\varphi}_{i,j}^2\big(\tilde{\theta}_{i,l}, \mathbf{w}_l^{(j-1)}\big)\Big\} \leq \tilde{P}, \quad l = 1, \ldots, N, \quad i = 1, 2, \tag{5.20}$$

with expectation over all possible transmit messages $\tilde{\theta}_{i,l}$ and channel realizations. This encoder has causal access to the quantized feedback and works as in the original Ozarow scheme (see Section 2.4.1). Due to the superimposed block structure the constraints on the transmit powers sum up to

$$2(P + \tilde{P}) = P_T. \tag{5.21}$$

5.3.2 Achievable Sum Rate

Our proposed scheme is a superposition of a conventional encoder and a feedback-based encoder (cf. (5.18)). Thus, we can maximize the sum rate by finding the optimum power (equivalently, rate) splitting between the two encodings jointly for both transmitters. The conventionally encoded signals are cancelled at the receiver before quantization such that the quantization only captures the feedback encoding in the forward path. This is possible since the receiver has the quantization noise as side-information (see Section 4.5.5). The sum rate of the conventional coding scheme is thus given by the classical Gaussian MAC capacity C_0 (see Section 2.3.1) with noise power $\sigma^2 + 2\tilde{P}$, since the independent feedback-based codewords (cf. (4.58b)) that are each superimposed in specific time instances of the conventional coding (cf. (4.58a)) act as additional interference. Then, the achievable sum rate for fixed feedback transmit power $\tilde{P}$ and given total transmit power P_T is

$$\begin{aligned} 2R &\leq C_0(P, P, \sigma^2 + 2\tilde{P}) \\ &\triangleq \mathsf{C}. \end{aligned} \tag{5.22}$$

The factor 2 before rate and feedback power is due to the symmetry of the MAC; both transmitters have equal channel gains and as a consequence equal transmit power and achievable rate. The sum rate of the feedback coding scheme is given by the Ozarow capacity (see Section 2.4.1) with noise power $\sigma^2 + \sigma_q^2$ (due to the additional quantization noise). Then, the achievable sum rate for fixed transmit power P and given total transmit power P_T is

$$\begin{aligned} 2\tilde{R} &\leq C^{\mathrm{FB}}(\tilde{P}, \tilde{P}, \sigma^2 + \sigma_q^2) \\ &\triangleq \tilde{\mathsf{C}}. \end{aligned} \tag{5.23}$$

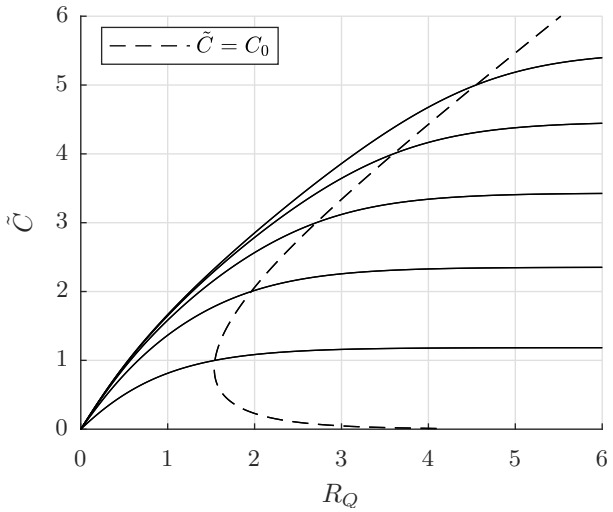

Figure 5.3: Sum rate for quantized feedback versus quantization rate R_Q for several SNRs corresponding to no-feedback sum capacities $C_0 = 1 \dots 5$ (all quantities in bit).

While this rate is smaller than that achievable with perfect feedback, it can still surpass the MAC capacity without feedback for large enough quantization rate R_Q (see Figure 5.3).

Thus, the total achievable sum rate of our proposed scheme with given total transmit power P_T yields

$$\begin{aligned} 2(R + \tilde{R}) &\leq \max_{2(P+\tilde{P}) \leq P_T} \mathsf{C} + \tilde{\mathsf{C}} \\ &\triangleq C_S. \end{aligned} \tag{5.24}$$

Expanding the maximizations (implicitly contained in the expressions for C and $\tilde{\mathsf{C}}$) to one single maximization yields

$$C_S = \max_{2(P+\tilde{P}) \leq P_T} C_0(P, P, \sigma^2 + 2\tilde{P}) + C^{\mathrm{FB}}(\tilde{P}, \tilde{P}, \sigma^2 + \sigma_q^2). \tag{5.25}$$

Although high feedback transmit power $\tilde{P}$ has a negative impact on the capacity of the conventional scheme due to the additional interference noise it is clearly still optimal to use all the available transmit power. Therefore, the optimal solution of (5.25) has to lie on the boundary $2(P + \tilde{P}) = P_T$. Reformulating this problem solely as a function

of $\tilde{P}$ then yields

$$C_S = \max_{\tilde{P}} \underbrace{C_0\left(\frac{P_T}{2} - \tilde{P}, \frac{P_T}{2} - \tilde{P}, \sigma^2 + 2\tilde{P}\right)}_{C(\tilde{P})} + \underbrace{C^{\mathrm{FB}}(\tilde{P}, \tilde{P}, \sigma^2 + \sigma_q^2)}_{\tilde{C}(\tilde{P})} \quad \text{s.t.}\, 0 \leq 2\tilde{P} \leq P_T. \tag{5.26}$$

Clearly, $C(\tilde{P})$ is a strictly decreasing function in $\tilde{P}$ and $\tilde{C}(\tilde{P})$ is strictly increasing in $\tilde{P}$. As a consequence, there is a tradeoff between feedback-based coding and conventional coding. The optimum is either the extreme case where all transmit power is allocated to the feedback coding scheme ($2\tilde{P} = P_T$) or to the conventional coding ($\tilde{P} = 0$), or the optimum is in fact a true superposition of both coding schemes depending on the quantization rate R. The tradeoff for this three cases is illustrated in Figure 5.4.

5.3.3 Concave and Convex Component

Next, we prove that C_S can be split into a concave part $\mathsf{C}^{\cap}(\tilde{P})$ and a convex part $\mathsf{C}^{\cup}(\tilde{P})$ in the feedback transmit power $\tilde{P}$,

$$C_S = \max_{\tilde{P}} \mathsf{C}^{\cap}(\tilde{P}) + \mathsf{C}^{\cup}(\tilde{P}) \qquad \text{s.t.} \quad 0 \leq 2\tilde{P} \leq P_T. \tag{5.27}$$

Then, this sum rate maximization problem can be solved by DC programming (see Section 2.8). Fully analogous to the AWGN channel in the previous section it can be shown that $\tilde{C}(\tilde{P})$ is a concave function and $C(\tilde{P})$ is a convex function in $\tilde{P}$. Indeed, by direct calculation we obtain the second-order derivative of $C(\tilde{P})$ as

$$C''(\tilde{P}) = \frac{2}{(2\tilde{P} + \sigma^2)^2} \geq 0, \tag{5.28}$$

which proves convexity. The concavity of $\tilde{C}(\tilde{P})$ can proved by following reasoning: The capacity of the MAC with perfect feedback, i.e., without quantization, is given by the Ozarov-capacity (see Section 2.4.1) which is concave in the transmit power allocation or equivalently in the SNR. The quantization can be modelled by an additional noise term (see Corollary 3.10) and thus the resulting reduced SNR is given by

$$\frac{\tilde{P}}{\sigma^2 + \sigma_q^2} = \frac{\tilde{P}}{\sigma^2} \cdot \frac{1 - 2^{-2R}}{1 + 2^{-2R}\tilde{P}/\sigma^2}. \tag{5.29}$$

By direct calculation, we can easily show that this is a concave and strictly increasing function. The concavity of $\tilde{C}(\tilde{P})$ is then obtained by the composition of the perfect feedback Ozarov-capacity with the reduced SNR expression since by composition rules [7] the composition of a concave function and a concave nondecreasing function is again concave. In summary, the sum capacity C_{S} is the sum of a convex and a concave

function, or equivalently the difference of two convex functions.

5.3.4 Difference of Convex Functions Programming Solution

Splitting the objective function and our already affine constraints into concave and convex functions allows us to solve the optimization problem via DC programming (see Section 2.8) and the practically efficient CCP algorithm (see Section 2.8.1). Rewriting our maximization problem (5.27) in standard form (2.66) yields the following result.

Corollary 5.2. *The problem of maximizing the achievable sum rate of the Gaussian MAC with quantized feedback and a superposition of feedback coding with capacity $\tilde{C}$ and conventional coding with capacity C is solved by finding the solution of the DC problem*

$$\begin{aligned} \underset{\tilde{P}}{\textit{minimize}} \quad & -\tilde{C}(\tilde{P}) - C(\tilde{P}) \\ \textit{subject to} \quad & 2\tilde{P} - P_T \leq 0 \\ & -\tilde{P} \leq 0. \end{aligned} \tag{5.30}$$

Like in the previous section we have to find a point where the gradient of the convex part in the next iteration equals the negative gradient of the concave part of the previous iteration

$$\frac{\partial}{\partial \tilde{P}} \tilde{C}\left(\tilde{P}_{(k+1)}\right) = -\frac{\partial}{\partial \tilde{P}} C\left(\tilde{P}_{(k)}\right), \tag{5.31}$$

which again itself is a convex optimization problem. The solution to this auxiliary problem decreases monotonically with increasing k and thus converges to a minimum (or saddle point). Lipp and Boyd [49] give a basic CCP algorithm (see Section 2.8.1) that requires an initial feasible point $\tilde{P}_{(0)}$, which in our case can be any point in the interval $[0, P_T/2]$. Following [49], the CCP approach leads to Algorithm 5 for power allocation.

Figure 5.5 and Figure 5.6 illustrate the optima which are the maxima of the sum capacities in the various achievable rate regions.

The Non-Trivial Region where Superposition is Optimal

Figure 5.6 shows the achievable rate region for fixed quantization rate R_Q and variable transmit power P_T. We see that up to a specific transmit power it is optimum to allocate all transmit power to the feedback-coding scheme and from a non-trivial threshold a superposition is optimum. Note that the power allocated to the feedback scheme stays constant while only the power allocated to the non-feedback scheme increases with increasing total transmit power. Intuitively this can be explained by studying the behaviour of the iteration (5.31) which characterizes a fixed point for the optimal $\tilde{P}_{(k)}$.

Algorithm 5 Transmit power allocation for symmetric MAC with feedback via CCP

Require: Initial feasible point $\tilde{P}_{(0)}$

1: $k := 0$
2: **while** stopping criterion not satisfied **do**
3: *Convexify.* Form $\hat{C}_{(k)}\left(\tilde{P}\right) = C\left(\tilde{P}_{(k)}\right) + C'\left(\tilde{P}_{(k)}\right)\left(\tilde{P} - \tilde{P}_{(k)}\right)$
4: *Solve.* Determine $\tilde{P}_{(k+1)}$ as solution of the convex problem

$$\begin{aligned} \text{minimize} \quad & -\tilde{C}(\tilde{P}) - \hat{C}_{(k)}(\tilde{P}) \\ \text{subject to} \quad & 2\tilde{P} - P_T \leq 0 \\ & -\tilde{P} \leq 0 \end{aligned}$$

5: $k := k + 1$
6: **end while**
7: **return** $\tilde{P}_{(k)}$

In the optimum point the negative gradient of $\tilde{C}$ equals the gradient of C, which can be calculated as

$$\frac{\partial}{\partial \tilde{P}} \tilde{C}\left(\tilde{P}\right) = \frac{\partial}{\partial \tilde{P}} C\left(\frac{2(P_T - \tilde{P})}{\sigma^2 + 2\tilde{P}}\right) = -\frac{1}{2\tilde{P} + \sigma^2}. \tag{5.32}$$

Obviously, this gradient is independent of the total available transmit power and the equation for $\tilde{C}$ does not contain the total transmit power at all. Therefore, the optimum must also be independent of the actual value of the total transmit power if the total transmit power is at least $P_T \geq 2\tilde{P}$ and is limited by the quantization rate R_Q.

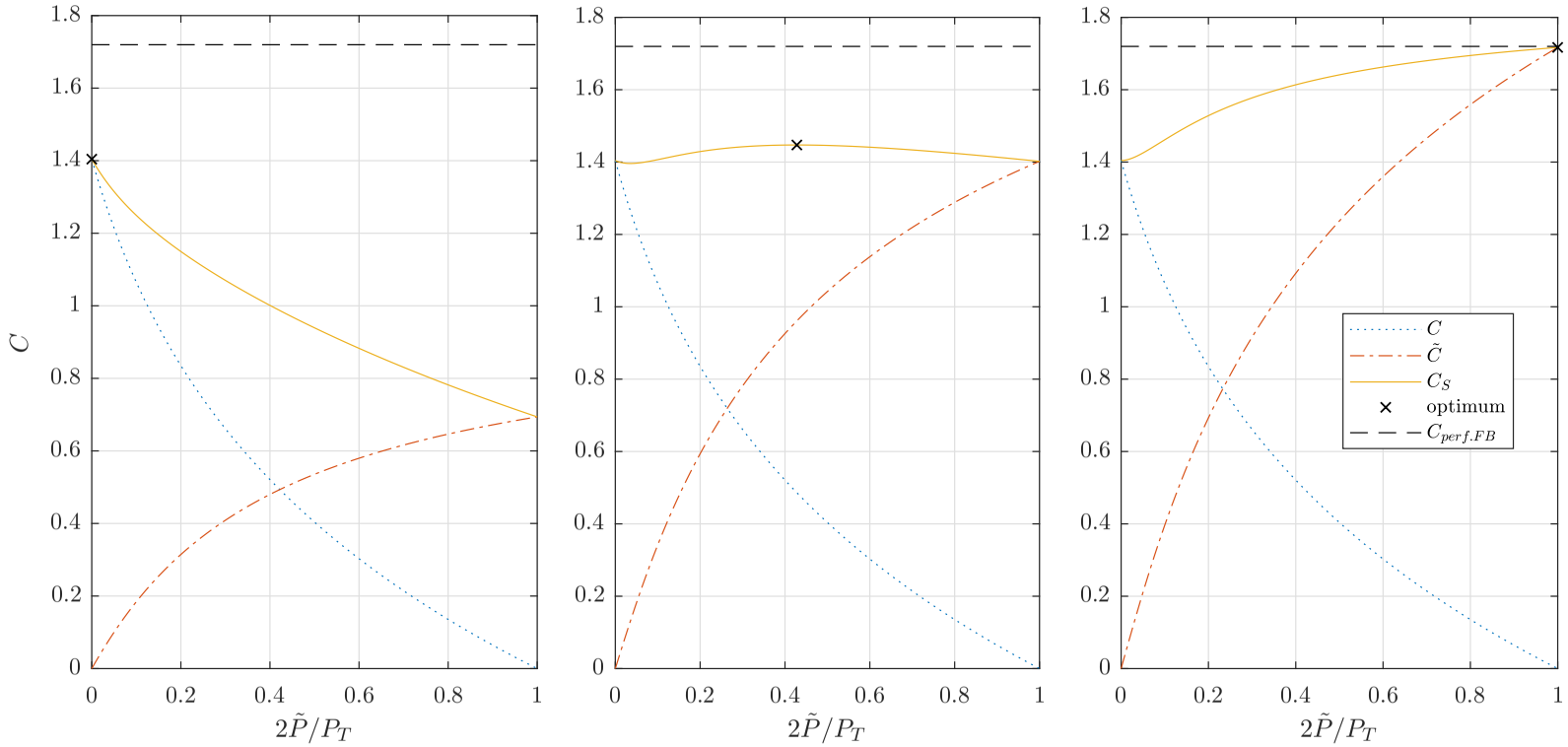

Figure 5.4: Sum capacity C_S versus power allocation $2\tilde{P}/P_T$ for $C_0 = 1$ and $R_Q = 0.5C_0$ (left), $R_Q = 1.5C_0$ (middle), and $R_Q = 5C_0$ (right); all quantities in bit.

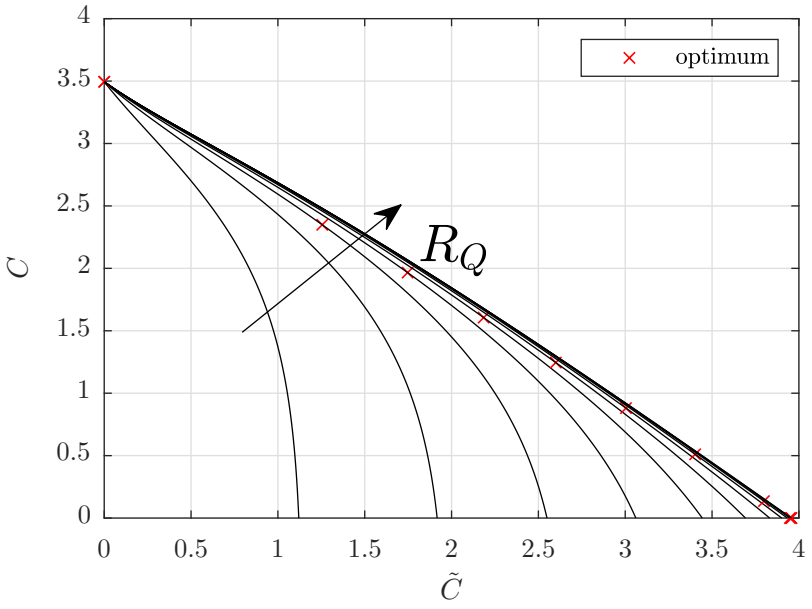

Figure 5.5: Symmetric MAC achievable rate region $(\tilde{C}(\tilde{P}), C(\tilde{P}))$ for fixed $C_0 = 3$ and $R_Q = 0.2C_0 \ldots 2.4C_0$.

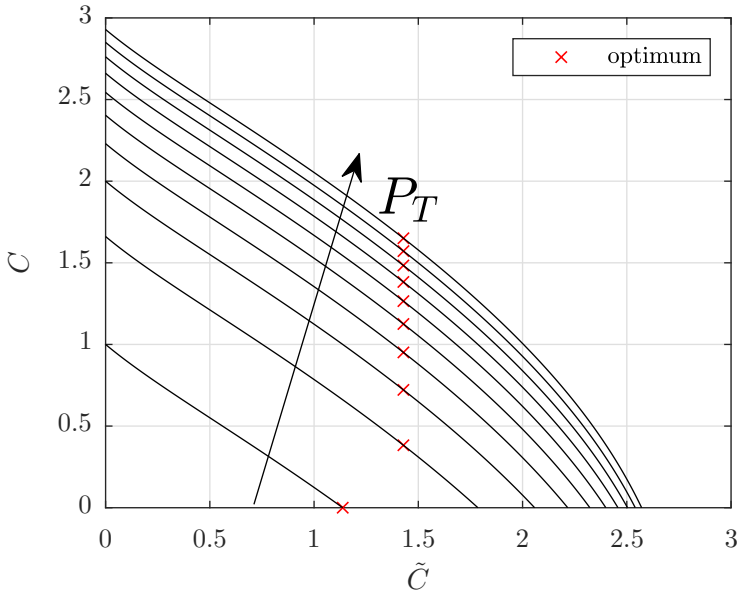

Figure 5.6: Symmetric MAC achievable rate region $(\tilde{C}(\tilde{P}), \tilde{C}(P))$ for fixed $R_Q = 2$ and $P_T = 0.1P_{R_Q} \ldots 2P_{R_Q}$ where P_{R_Q} is such that $C_0(P_{R_Q}) = R_Q$.

5.4 Asymptotic Superposition Performance - Asymmetric Multiple Access Channel

5.4.1 Power Constraints

We study the two-user asymmetric Gaussian MAC with (quantized) feedback (see Figure 4.5). Here, the transmitters send the independent length-n Gaussian user signals $x_i[k]$, $i = 1, 2$, and the receiver observes the signal

$$y[k] = h_1 x_1[k] + h_2 x_2[k] + z[k]. \tag{5.33}$$

The channel gains h_1 and h_2 are assumed to be known by both transmitters and receiver and the channel introduces i.i.d. additive Gaussian noise $\mathbf{z} \sim \mathcal{N}(\mathbf{0}, \sigma^2 \boldsymbol{I})$. We impose the average transmit sum-power constraint (here, expectation is with respect to the messages and the channel noise)

$$\frac{1}{n} \sum_{k=1}^{n} \mathrm{E}\big\{ \mathsf{x}_1^2[k] + \mathsf{x}_2^2[k] \big\} \leq P_T. \tag{5.34}$$

As in the symmetric case the transmitters communicate independent messages $\theta_{1,j}$, $\tilde{\theta}_{1,l}$ and $\theta_{2,j}$, $\tilde{\theta}_{2,l}$, $j = 1, \ldots, \tilde{N}$, $l = 1, \ldots, N$, to a single receiver. But now the messages are uniformly drawn from finite sets with different cardinalities $\mathcal{M}_1 = 2^{NR_1}$, $\widetilde{\mathcal{M}}_1 = 2^{\tilde{N}\tilde{R}_1}$, $\mathcal{M}_2 = 2^{NR_2}$, $\widetilde{\mathcal{M}}_2 = 2^{\tilde{N}\tilde{R}_2}$, and again mapped to the transmit signals according to the superposition (see Section 4.5.2) with block structure (cf. (4.58))

$$x_i[(j-1)N + l] = \varphi_{i,l}(\theta_{i,j}) + \tilde{\varphi}_{i,j}\big(\tilde{\theta}_{i,l}, \boldsymbol{w}_l^{(j-1)}\big),\ j = 1, \ldots, \tilde{N},\ l = 1, \ldots, N,\ i = 1, 2, \tag{5.35}$$

$k = (j-1)N + l = 1, \ldots, n$. Due to the asymmetry of the channel we now have asymmetric power constraints as well. Here, $\varphi_{i,l} : \mathcal{M}_i \to \mathbb{R}$ denotes a conventional encoder with power constraint

$$\frac{1}{N} \sum_{l=1}^{N} \mathrm{E}\big\{ \varphi_{i,l}^2(\theta_{i,j}) \big\} \leq P_i, \quad j = 1, \ldots, \tilde{N}, \quad i = 1, 2, \tag{5.36}$$

with expectation over all possible transmit messages $\theta_{i,j}$. The conventional encoder completely ignores the feedback signal. Furthermore, $\boldsymbol{w}_l^{(j-1)} = (w[1] \ldots w[(j\text{–}1)N + l])^\top$ again denotes the past quantized feedback as in the symmetric case and $\tilde{\varphi}_{i,j} : \widetilde{\mathcal{M}}_i \times \mathbb{R}^{j-1} \to \mathbb{R}$ is the feedback-based encoder with power constraint

$$\frac{1}{n} \sum_{j=1}^{\tilde{N}} \mathrm{E}\Big\{ \tilde{\varphi}_{i,j}^2\big(\tilde{\theta}_{i,l}, \mathbf{w}_l^{(j-1)}\big) \Big\} \leq \tilde{P}_i, \quad l = 1, \ldots, N, \quad i = 1, 2, \tag{5.37}$$

with expectation over all possible transmit messages $\tilde{\theta}_{i,l}$ and channel realizations. This encoder has causal access to the quantized feedback and works as in the original Ozarow scheme (see Section 2.4.1). Due to the superimposed block structure the constraints on the transmit powers sum up to

$$P_1 + P_2 = P, \tag{5.38}$$

$$\tilde{P}_1 + \tilde{P}_2 = \tilde{P}, \tag{5.39}$$

$$P + \tilde{P} = P_T. \tag{5.40}$$

5.4.2 Achievable Sum Rate

Our proposed scheme is a superposition of a conventional encoder and a feedback-based encoder (cf. (5.35)). Thus, we can maximize the sum rate by finding the optimum power (equivalently, rate) splitting between the two encodings jointly for both transmitters. The conventionally encoded signals are cancelled at the receiver before quantization such that the quantization only captures the feedback encoding in the forward path. This is possible since the receiver has the quantization noise as side-information (see Section 4.5.5). The sum rate of the conventional coding scheme is thus given by the classical Gaussian MAC capacity C_0 (see Section 2.3.1) with noise power $\sigma^2 + h_1^2\tilde{P}_1 + h_2^2\tilde{P}_2$, since the independent feedback-based codewords (cf. (4.58b)) that are each superimposed in specific time instances of the conventional coding (cf. (4.58a)) act as additional interference. Then, the achievable sum rate for fixed feedback transmit powers $\tilde{P}_1$ and $\tilde{P}_2$ and given total transmit power P_T is

$$\begin{aligned} R_1 + R_2 &\leq \max_{P_1+P_2 \leq P_T - \tilde{P}_1 - \tilde{P}_2} C_0(h_1^2 P_1, h_2^2 P_2, \sigma^2 + h_1^2\tilde{P}_1 + h_2^2\tilde{P}_2) \\ &\triangleq \mathsf{C}. \end{aligned} \tag{5.41}$$

The sum rate of the feedback coding scheme is given by the Ozarow capacity C^{FB} (see Section 2.4.1) with noise power $\sigma^2 + \sigma_q^2$ (due to the additional quantization noise). Then, the achievable sum rate for fixed transmit powers P_1 and P_2 and given total transmit power P_T is

$$\begin{aligned} \tilde{R}_1 + \tilde{R}_2 &\leq \max_{\tilde{P}_1+\tilde{P}_2 \leq P_T - P_1 - P_2} C^{\mathrm{FB}}(h_1^2\tilde{P}_1, h_2^2\tilde{P}_2, \sigma^2 + \sigma_q^2) \\ &\triangleq \tilde{\mathsf{C}}. \end{aligned} \tag{5.42}$$

Thus, the total achievable sum rate of our proposed scheme with given total transmit power P_T yields

$$R_1 + R_2 + \tilde{R}_1 + \tilde{R}_2 \leq \max_{P_1+P_2+\tilde{P}_1+\tilde{P}_2 \leq P_T} \mathsf{C} + \tilde{\mathsf{C}}$$

$$\triangleq C_S. \tag{5.43}$$

Finally, simplifying the nested maximizations (implicitly contained in the expressions for C and $\tilde{\mathsf{C}}$) to one single maximization yields

$$\begin{aligned} C_S = \max_{P_1+P_2+\tilde{P}_1+\tilde{P}_2 \leq P_T} & C_0(h_1^2 P_1, h_2^2 P_2, \sigma^2 + h_1^2 \tilde{P}_1 + h_2^2 \tilde{P}_2) \\ & + C^{\mathrm{FB}}(h_1^2 \tilde{P}_1, h_2^2 \tilde{P}_2, \sigma^2 + \sigma_q^2). \end{aligned} \tag{5.44}$$

In the previous section on the symmetric MAC this was the basis of a one-dimensional optimization problem, since the capacity expressions directly yielded the convex part and the concave part. In the asymmetric case however, (5.44) results in a multi-dimensional optimization problem where the individual capacity expressions do not directly correspond to the convex part and the concave part.

Expanding the expressions of the capacities in (5.44) gives

$$\begin{aligned} C_S = \max_{P_1+P_2+\tilde{P}_1+\tilde{P}_2 \leq P} & C\left(\frac{h_1^2 P_1}{\sigma^2 + h_1^2 \tilde{P}_1 + h_2^2 \tilde{P}_2}\right) \\ & + C\left(\frac{h_2^2 P_2}{\sigma^2 + h_1^2 P_1 + h_1^2 \tilde{P}_1 + h_2^2 \tilde{P}_2}\right) \\ & + C^{\mathrm{FB}}(h_1^2 \tilde{P}_1, h_2^2 \tilde{P}_2, \sigma^2 + \sigma_q^2), \end{aligned} \tag{5.45}$$

where the signal of transmitter 2 is decoded before the signal of transmitter 1. Then, the first two terms reflect the classical Gaussian MAC capacity with successive cancellation. Note that the decoding order of the successive cancellation operation is irrelevant and independent of the actual values of the channel gains h_1 and h_2. Throughout this thesis we keep this order of decoding. Changing the order of decoding simply amounts to swapping the indices.

5.4.3 Concave and Convex Component

Next, we prove that C_S can be split into a concave part $\mathsf{C}^{\cap}(\boldsymbol{p})$ and a convex part $\mathsf{C}^{\cup}(\boldsymbol{p})$ in the power allocation vector $\boldsymbol{p} = (P_1, P_2, \tilde{P}_1, \tilde{P}_2)^\top$,

$$C_S = \max_{\mathbf{1}^\top \boldsymbol{p} \leq P} \mathsf{C}^{\cap}(\boldsymbol{p}) + \mathsf{C}^{\cup}(\boldsymbol{p}). \tag{5.46}$$

Then, this sum rate maximization problem can be solved by DC programming [49].

Following the lines of the symmetric case (see Section 5.3.3) and due to the fact that the pointwise minimum of two concave functions (the logarithm is concave and especially the sum (2.27)+(2.28) and (2.29) are concave [60]) preserves concavity [7] we directly identify $C^{\mathrm{FB}}(h_1^2 \tilde{P}_1, h_2^2 \tilde{P}_2, \sigma^2 + \sigma_q^2)$ as concave in $\boldsymbol{p}$.

Furthermore, we expand $C_0(h_1^2P_1, h_2^2P_2, \sigma^2 + h_1^2\tilde{P}_1 + h_2^2\tilde{P}_2)$ to

$$\begin{aligned} C_0(h_1^2P_1, h_2^2P_2, \sigma^2 + h_1^2\tilde{P}_1 + h_2^2\tilde{P}_2) = \\ \frac{1}{2}\log(h_1^2P_1 + \sigma^2 + h_1^2\tilde{P}_1 + h_2^2\tilde{P}_2) \\ +\frac{1}{2}\log(h_2^2P_2 + \sigma^2 + h_1^2P_1 + h_1^2\tilde{P}_1 + h_2^2\tilde{P}_2) \\ -\frac{1}{2}\log(\sigma^2 + h_1^2\tilde{P}_1 + h_2^2\tilde{P}_2) \\ -\frac{1}{2}\log(\sigma^2 + h_1^2P_1 + h_1^2\tilde{P}_1 + h_2^2\tilde{P}_2). \end{aligned} \tag{5.47}$$

The concave part $\mathsf{C}'^{\cap}(\boldsymbol{p})$ is given by

$$\begin{aligned} \mathsf{C}'^{\cap}(\boldsymbol{p}) = \quad & \frac{1}{2}\log(h_1^2P_1 + \sigma^2 + h_1^2\tilde{P}_1 + h_2^2\tilde{P}_2) \\ & + \frac{1}{2}\log(h_2^2P_2 + \sigma^2 + h_1^2P_1 + h_1^2\tilde{P}_1 + h_2^2\tilde{P}_2) \end{aligned} \tag{5.48}$$

Since the concavity is also preserved when summing concave functions [7] the overall concave component equals

$$\mathsf{C}^{\cap}(\boldsymbol{p}) = \quad C^{\mathrm{FB}}(h_1^2\tilde{P}_1, h_2^2\tilde{P}_2, \sigma^2 + \sigma_q^2) + \mathsf{C}'^{\cap}(\boldsymbol{p}) \tag{5.49}$$

$$\begin{aligned} = \quad & C^{\mathrm{FB}}(h_1^2\tilde{P}_1, h_2^2\tilde{P}_2, \sigma^2 + \sigma_q^2) \\ & + \frac{1}{2}\log(h_1^2P_1 + \sigma^2 + h_1^2\tilde{P}_1 + h_2^2\tilde{P}_2) \\ & + \frac{1}{2}\log(h_2^2P_2 + \sigma^2 + h_1^2\tilde{P}_1 + h_2^2\tilde{P}_2) \end{aligned} \tag{5.50}$$

The convexity of the overall convex component $\mathsf{C}^{\cup}(\boldsymbol{p})$,

$$\begin{aligned} \mathsf{C}^{\cup}(\boldsymbol{p}) = & -\frac{1}{2}\log(\sigma^2 + h_1^2\tilde{P}_1 + h_2^2\tilde{P}_2) \\ & -\frac{1}{2}\log(\sigma^2 + h_1^2P_1 + h_1^2\tilde{P}_1 + h_2^2\tilde{P}_2), \end{aligned} \tag{5.51}$$

can be easily shown by direct calculation.

5.4.4 Difference of Convex Functions Programming Solution

Splitting the objective function and our already affine constraints into concave and convex functions allows us to solve the optimization problem via DC programming (see Section 2.8) and the practically efficient CCP algorithm (see Section 2.8.1). Rewriting our maximization problem (5.46) in standard form (2.66) yields the following result.

Corollary 5.3. *The problem of maximizing the achievable sum rate of the asymmetric Gaussian MAC with quantized feedback and a superposition of feedback coding with capacity $\tilde{C}$ and conventional coding with capacity C is solved by finding the solution of*

the DC problem

$$\begin{aligned} \underset{\boldsymbol{p}}{\textit{minimize}} \quad & -\mathsf{C}^{\cap}(\boldsymbol{p}) - \mathsf{C}^{\cup}(\boldsymbol{p}) \\ \textit{subject to} \quad & \mathbf{1}^{\top}\boldsymbol{p} - P \leq 0, \\ & -\boldsymbol{p} \preceq 0. \end{aligned} \tag{5.52}$$

Like in the previous sections we have to find a point where the gradient of the convex part in the next iteration equals the negative gradient of the concave part of the previous iteration

$$\nabla \mathsf{C}^{\cup}(\boldsymbol{p}_{k+1}) = -\nabla \mathsf{C}^{\cap}(\boldsymbol{p}_k) \tag{5.53}$$

which again itself is a convex optimization problem. The solution to this auxiliary problem decreases monotonically with increasing k and thus converges to a minimum (or saddle point). Lipp and Boyd [49] give a basic CCP algorithm (see Section 2.8.1) that requires an initial feasible point $\boldsymbol{p}_0$, which in our case can be any point in the interval $0 \leq \mathbf{1}^{\top}\boldsymbol{p}_0 \leq P$. Following [49], the CCP approach leads to Algorithm 6 for power allocation.

In step 3 Algorithm 6 uses a linearization $\hat{\mathsf{C}}_k(\boldsymbol{p})$ of the convex component $\mathsf{C}^{\cup}(\boldsymbol{p})$. The gradient $\nabla \mathsf{C}^{\cup}(\boldsymbol{p})$ contained in the linearization can be directly calculated as

$$\nabla \mathsf{C}^{\cup}(\boldsymbol{p}) = -\frac{1}{2} \begin{pmatrix} \frac{h_1^2}{\sigma^2 + h_1^2 P_1 + h_1^2 \tilde{P}_1 + h_2^2 \tilde{P}_2} \\ 0 \\ \frac{h_1^2}{\sigma^2 + h_1^2 \tilde{P}_1 + h_2^2 \tilde{P}_2} + \frac{h_1^2}{\sigma^2 + h_1^2 P_1 + h_1^2 \tilde{P}_1 + h_2^2 \tilde{P}_2} \\ \frac{h_2^2}{\sigma^2 + h_1^2 \tilde{P}_1 + h_2^2 \tilde{P}_2} + \frac{h_2^2}{\sigma^2 + h_1^2 P_1 + h_1^2 \tilde{P}_1 + h_2^2 \tilde{P}_2} \end{pmatrix}. \tag{5.54}$$

If we were able to find the gradient $\nabla \mathsf{C}^{\cap}(\boldsymbol{p})$ as well and solve the iteration (5.53) for $\boldsymbol{p}_{k+1}$ we could avoid the auxiliary convex optimization problem. Unfortunately, this seems not feasible.

5.4.5 Numerical Solution

Figure 5.7 shows the rates (top) and power allocations (middle and bottom) obtained by solving (5.52) versus the feedback quantization rate R_Q for various levels of asymmetry. The linear-feedback capacity of the proposed superposition coding scheme is normalized by the no-feedback MAC capacity C_0. Clearly, when R_Q is too small the feedback is not beneficial at all and the whole transmit power is allocated to the conventional encoding (see middle and bottom part of Figure 5.7). Above a certain threshold for R_Q, true superposition is optimal and a capacity gain is achieved. In contrast to the symmetric case where eventually pure feedback coding becomes optimal for very large R_Q (almost

Algorithm 6 Transmit power allocation for asymmetric MAC with feedback via CCP

Require: Initial feasible point $\boldsymbol{p}_0$

1: $k := 0$
2: **while** stopping criterion not satisfied **do**
3: Form $\hat{\mathsf{C}}_k(\boldsymbol{p}) = \mathsf{C}^{\cup}(\boldsymbol{p}_k) + (\boldsymbol{p} - \boldsymbol{p}_k)^{\top} \nabla \mathsf{C}^{\cup}(\boldsymbol{p}_k)$
4: Determine $\boldsymbol{p}_{k+1}$ by solving the convex problem

$$\begin{aligned} \text{minimize} \quad & -\mathsf{C}^{\cap}(\boldsymbol{p}) - \hat{\mathsf{C}}_k(\boldsymbol{p}) \\ \text{subject to} \quad & \mathbf{1}^{\top}\boldsymbol{p} - P \leq 0, \\ & -\boldsymbol{p} \preceq 0 \end{aligned}$$

5: $k := k + 1$
6: **end while**
7: **return** $\boldsymbol{p}_k$

perfect feedback), in the asymmetric case (in Figure 5.7 for $h_2 > 1.1$) we can observe that true superposition stays optimal even for very large R_Q and converges to a non-trivial power splitting for $R \to \infty$ (perfect feedback). The highest gain in capacity is achieved in the fully symmetric case and strictly decreases with increasing asymmetry of the channel gains.

Figure 5.8 again shows the rates (top) and power allocations (middle and bottom) obtained by solving (5.52) versus the feedback quantization rate R_Q for fixed (moderate) level of asymmetry but various channel noise levels. Again, when R_Q is too small the feedback is not beneficial at all and the whole transmit power is allocated to the conventional encoding (see middle and bottom part of Figure 5.8). Above a certain threshold for R_Q, true superposition is optimal and a capacity gain is achieved. Except for really low SNR (in Figure 5.8 for $\sigma^2 = 10^{-1}$), here true superposition is optimal only in a small quantization rate window until eventually pure feedback coding becomes optimal. The highest gain in capacity is achieved for low SNR and strictly decreases with increasing SNR of the channel gains.

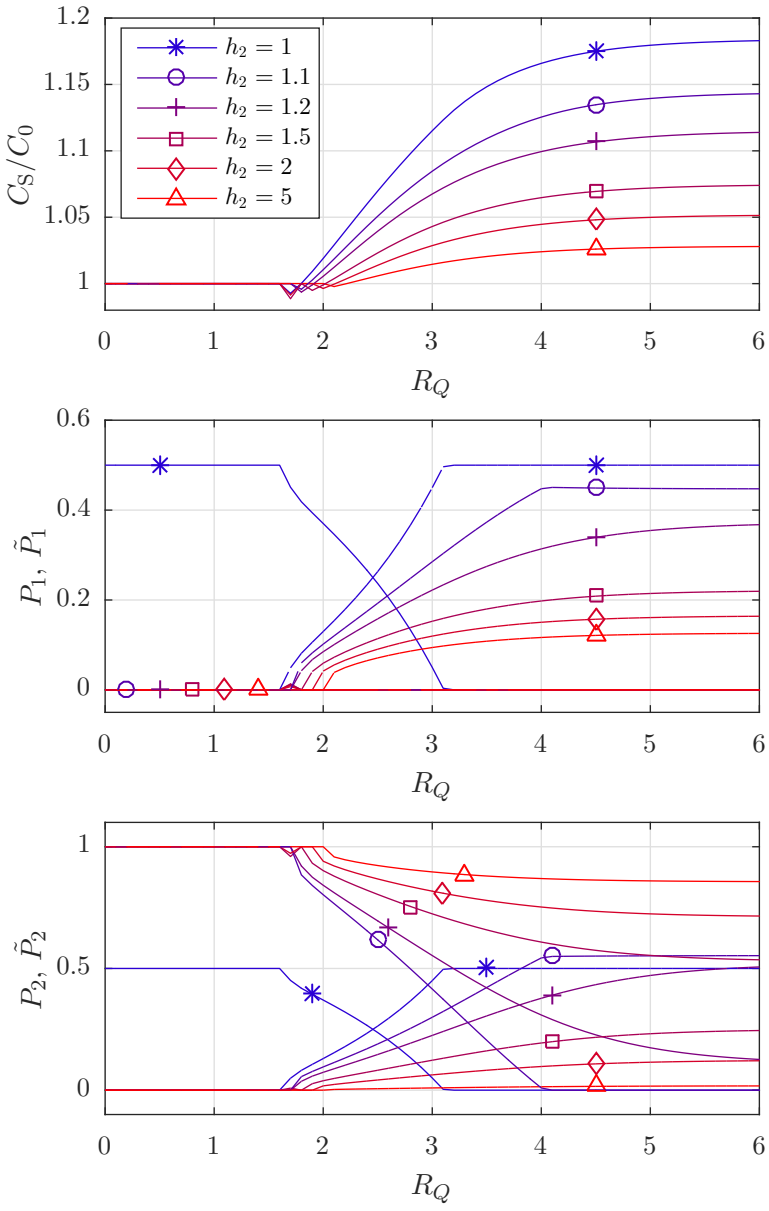

Figure 5.7: Top: Normalized achievable rates (in bit) with superposition coding. Middle and Bottom: Power splitting (decreasing lines for P_i, increasing lines for $\tilde{P}_i$) for various channel gains h_2. $h_1 = 1$, $P_T = 1$, $\sigma^2 = 10^{-2}$ fixed. Horizontal axis in all plots is the feedback quantization rate R_Q.

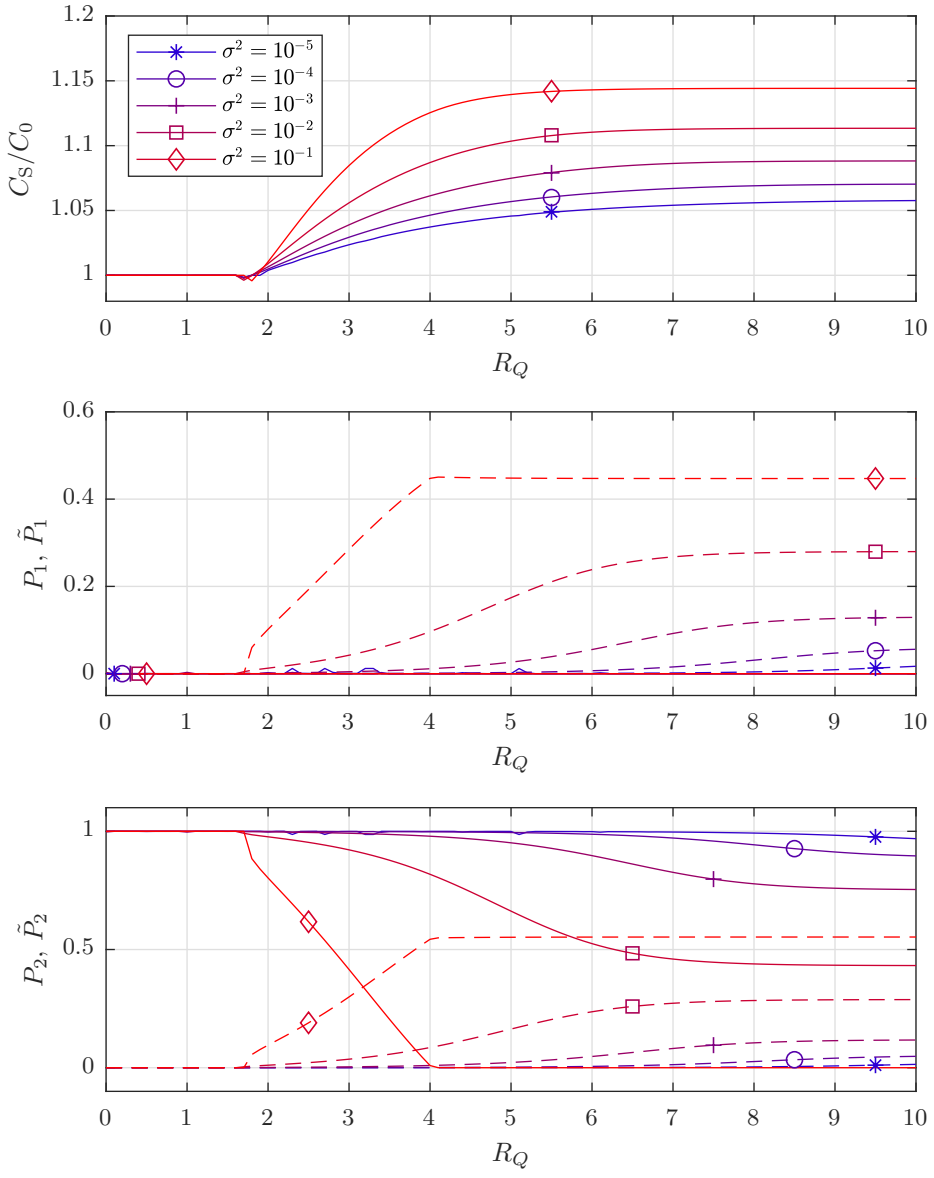

Figure 5.8: Top: Normalized achievable rates (in bit) with superposition coding. Middle and Bottom: Power splitting (decreasing lines for P_i, increasing lines for $\tilde{P}_i$) for various channel noise levels σ^2. $h_1 = 1$, $h_2 = 1.1$, $P_T = 1$ fixed. Horizontal axis in all plots is the feedback quantization rate R_Q.

5.5 Asymptotic Superposition Performance - Symmetric Broadcast Channel

5.5.1 Power Constraints

The transmitter communicates independent messages $\theta_{1,j}$, $\tilde{\theta}_{1,l}$ and $\theta_{2,j}$, $\tilde{\theta}_{2,l}$, $j = 1, \ldots, \tilde{N}$, $l = 1, \ldots, N$, to the two users (receivers). The messages are uniformly drawn from finite sets with cardinalities $\mathcal{M}_1 = 2^{nR_1}$, $\widetilde{\mathcal{M}}_1 = 2^{n\tilde{R}_1}$, $\mathcal{M}_2 = 2^{nR_2}$, $\widetilde{\mathcal{M}}_2 = 2^{n\tilde{R}_2}$ and mapped to the transmit signal components $\mathbf{x}_i$, $i = 1, 2$, according to the superposition (see Section 4.5.3) with block structure (cf. (4.69))

$$x_i[(j-1)N + l] = \varphi_{i,l}(\theta_{i,j}) + \tilde{\varphi}_{i,j}\big(\tilde{\theta}_{i,l}, \boldsymbol{w}_{i,l}^{(j-1)}\big),\ j = 1, \ldots, \tilde{N},\ l = 1, \ldots, N,\ i = 1, 2, \tag{5.55}$$

$k = (j-1)N + l = 1, \ldots, n$. Here, $\varphi_{i,l} : \mathcal{M}_i \to \mathbb{R}$ denotes a conventional encoder that ignores the feedback signal. Furthermore, in contrast to the MAC, here $\boldsymbol{w}_{i,l}^{(j-1)} = (w_i[1] \ldots w_i[(j-1)N + l])^\top$ denotes the past quantized feedback from receiver i and $\tilde{\varphi}_{i,j} : \widetilde{\mathcal{M}}_i \times \mathbb{R}^{j-1} \to \mathbb{R}$ is the feedback-based encoder that has causal access to the quantized feedback and due to MAC-BC duality works as in the original Ozarow scheme (see Section 2.6.1). Note that here we only have one single transmitter (see Figure 4.6) that composes the transmit signal components (5.55) to the total transmit signal

$$x[k] = x_1[k] + x_2[k]. \tag{5.56}$$

The encoder splits the total power P by allocating a fraction $\alpha \in [0, 1]$ of that power to the feedback-based codewords and the rest to the non-feedback part, i.e.,

$$\frac{1}{N} \sum_{i=1}^{2} \sum_{l=1}^{N} \mathrm{E}\big\{\varphi_{i,l}^2(\theta_{i,j})\big\} = (1-\alpha)P, \qquad j = 1, \ldots, \tilde{N}, \tag{5.57}$$

$$\frac{1}{\tilde{N}} \sum_{i=1}^{2} \sum_{j=1}^{\tilde{N}} \mathrm{E}\Big\{\tilde{\varphi}_{i,j}^2\big(\tilde{\theta}_{i,l}, \mathbf{w}_{i,l}^{(j-1)}\big)\Big\} = \alpha P, \qquad l = 1, \ldots, N. \tag{5.58}$$

5.5.2 Achievable Sum Rate

Our proposed scheme is a superposition of a conventional encoder and a feedback-based encoder (cf. (5.55)). Pure conventional encoding and pure feedback encoding are special cases obtained with $\alpha = 0$ and $\alpha = 1$, respectively. Thus, we can maximize the sum rate by finding the optimum power (equivalently, rate) splitting between the two encodings.

The conventionally encoded signals are cancelled at the receivers before quantization such that the quantization only captures the feedback encoding in the forward path. This is possible since each receiver has the quantization noise as side-information (see

Section 4.5.5). The sum rate of the conventional coding scheme is thus given by the classical Gaussian BC capacity (see Section 2.5.1) with signal power $(1-\alpha)P$ and noise power $\sigma^2+\alpha P$, since the independent feedback-based codewords (cf. (4.69b)) that are each superimposed in specific time instances of the conventional coding (cf. (4.69a)) act as additional interference. The effective SNR thus equals $\frac{(1-\alpha)P}{\sigma^2+\alpha P} = \frac{(1-\alpha)\gamma}{1+\alpha\gamma}$ (recall $\gamma = P/\sigma^2$) and the achievable sum rate is

$$\begin{aligned} R_1 + R_2 &\leq C_0\left(\frac{(1-\alpha)\gamma}{1+\alpha\gamma}\right) \\ &\triangleq C(\alpha), \end{aligned} \tag{5.59}$$

where C_0 is the capacity of the BC without feedback (see Section 2.5.1).

The sum rate achievable with the feedback-based code follows by exploiting the duality between the linear-feedback MAC and the linear-feedback BC (see Section 2.6.1) and using the Ozarow scheme for perfect feedback (see Section 2.4.1). The effective SNR in the Ozarow scheme is reduced due to feedback quantization. Specifically, the feedback compression can be seen as additional i.i.d. quantization noise σ_q^2 (see Section 4.5.5). This decreases the SNR for the linear-feedback code according to

$$\tilde{\gamma} = \frac{\alpha P}{\sigma^2+\sigma_q^2} = \alpha\gamma\frac{1}{1+\sigma_q^2/\sigma^2}. \tag{5.60}$$

The achievable sum rate for the feedback code then yields

$$\begin{aligned} \tilde{R}_1 + \tilde{R}_2 &\leq C^{\mathrm{FB}}\left(\alpha\gamma\frac{1}{1+\sigma_q^2/\sigma^2}\right) \\ &\triangleq \tilde{C}(\alpha), \end{aligned} \tag{5.61}$$

where C^{FB} is the Ozarow capacity (see Section 2.6.1). While this rate is smaller than that achievable with perfect feedback, it can still surpass the BC capacity without feedback for large enough quantization rate R_Q (see Figure 5.9).

The overall sum rate for the Gaussian BC with quantized feedback and a superposition of conventional and linear-feedback encoding is finally obtained by optimizing the power allocation (rate splitting) parameter α for the conventional encoding and the feedback-based encoding, i.e., $R_1 + R_2 + \tilde{R}_1 + \tilde{R}_2 \leq C_{\mathrm{S}}$ with

$$C_{\mathrm{S}} = \max_{0\leq\alpha\leq 1} C(\alpha) + \tilde{C}(\alpha). \tag{5.62}$$

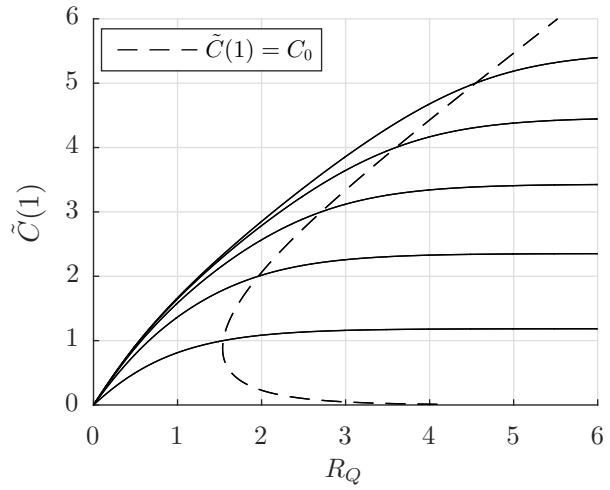

Figure 5.9: Sum rate $\tilde{C}(1)$ for quantized feedback-based code versus quantization rate R_Q for several SNRs corresponding to no-feedback sum capacities $C_0 = 1 \ldots 5$.

5.5.3 Difference of Convex Functions Programming

Reformulation of the Sum Rate Maximization

To maximize the sum rate we have to find the optimal power allocation parameter α by solving (5.62). It can be shown that $\tilde{C}(\alpha)$ is a concave function and $C(\alpha)$ is a convex function in α. Indeed, by direct calculation, we obtain the second-order derivative of $C(\alpha)$ as

$$\frac{\mathrm{d}^2}{\mathrm{d}\alpha^2} C(\alpha) = \frac{\gamma^2}{(1+\alpha\gamma)^2} \geq 0, \tag{5.63}$$

which proves convexity. Due to the MAC-BC duality the concavity of $\tilde{C}(\alpha)$ can be proved fully analogously to the MAC in Section 5.3.3. It follows that the sum capacity C_{S} is the maximum of the sum of a convex and a concave function, or equivalently, of the difference of two convex functions. Thus, the sum rate maximization problem can be again solved by DC programming (see Section 2.8) and the practically efficient CCP algorithm (see Section 2.8.1). The maximization problem (5.62) can be reformulated in standard form (2.66), i.e., involving differences of convex functions in the objective and in the constraints.

Corollary 5.4. *The problem of maximizing the achievable sum rate of the Gaussian BC with quantized feedback and a superposition of feedback coding with capacity $\tilde{C}$ and*

Algorithm 7 Transmit power allocation for symmetric BC with feedback via CCP

Require: Initial feasible point α_0

1: $k := 0$
2: **while** stopping criterion not satisfied **do**
3: Form $\hat{C}_k(\alpha) = C(\alpha_k) + C'(\alpha_k)\,(\alpha - \alpha_k)$
4: Determine α_{k+1} by solving the convex problem

$$\begin{aligned} \text{minimize} \quad & -\tilde{C}(\alpha) - \hat{C}_k(\alpha) \\ \text{subject to} \quad & \alpha - 1 \leq 0, \\ & -\alpha \leq 0 \end{aligned}$$

5: $k := k + 1$
6: **end while**
7: **return** α_k

conventional coding with capacity C is solved by finding the solution of the DC problem

$$\begin{aligned} \underset{\alpha}{\textit{minimize}} \quad & -\tilde{C}(\alpha) - C(\alpha) \\ \textit{subject to} \quad & \alpha - 1 \leq 0, \\ & -\alpha \leq 0. \end{aligned} \tag{5.64}$$

5.5.4 Numerical Solution

Like in the previous sections we have to find a point where the gradient of the convex part in the next iteration equals the negative gradient of the concave part of the previous iteration. Intuitively, consider the boundary $\big(\tilde{C}(\alpha), C(\alpha)\big)$ of the power splitting rate region; maximizing sum rate is then equivalent to finding the point $\big(\tilde{C}(\alpha), C(\alpha)\big)$ whose tangent has slope -1,

$$\frac{\mathrm{d}C(\alpha)}{\mathrm{d}\tilde{C}(\alpha)} = \frac{\mathrm{d}C(\alpha)/\mathrm{d}\alpha}{\mathrm{d}\tilde{C}(\alpha)/\mathrm{d}\alpha} = -1, \tag{5.65}$$

Using a superscript prime to denote the first-order derivative, CCP thus aims at

$$\tilde{C}'(\alpha_{k+1}) = -C'(\alpha_k), \tag{5.66}$$

which itself amounts to a convex optimization problem. The solution to this auxiliary problem decreases monotonically with increasing k and thus converges to a minimum (or to saddle point). Lipp and Boyd [49] give a basic CCP algorithm (see Section 2.8.1) which requires an initial feasible point α_0, which in our case can be any point in the interval $[0, 1]$. Following [49], the CCP approach leads to Algorithm 7 for power allocation. The derivative required in step 3 can explicitly be computed as

$$C'(\alpha) = -\frac{1}{2}\frac{\gamma}{1 + \alpha\gamma}. \tag{5.67}$$

Figure 5.10 shows the rates (top) and power allocations (bottom) obtained by solving (5.64) versus the feedback quantization rate R_Q. The linear-feedback capacity of the proposed superposition coding scheme is normalized by the no-feedback BC capacity C_0. Clearly, when the feedback quantization rate R_Q is too small the feedback is not beneficial at all and the whole transmit power is allocated to the conventional encoding (see bottom part of Figure 5.10). Above a certain threshold for R, true superposition is optimal until eventually pure feedback coding becomes optimal for very large quantization rates R_Q (almost perfect feedback). Figure 5.11 and Figure 5.12 shows the achievable power splitting rate region $(C(\alpha), \tilde{C}(\alpha))$ and the maximum sum rate C_{S}.

Optimality of Superposition

Figure 5.12 shows the achievable power splitting rate region $\big(\tilde{C}(\alpha), C(\alpha)\big)$ for fixed quantization rate R_Q and variable transmit power P. We see that below a non-trivial power threshold it is optimum to allocate all transmit power to the feedback-coding scheme and above that threshold superposition is optimum. Note that the power allocated to the feedback scheme stays constant while only the power allocated to the non-feedback scheme increases with increasing total transmit power. This can be explained by studying the behavior of the iteration (5.66), which characterizes a fixed point for the optimal α. In the optimal point the negative gradient of $\tilde{C}(\alpha)$ equals the gradient of $C(\alpha)$ (cf. (5.65)). While the optimal α depends on the total power P, it can be shown that the amount of power αP in the feedback-based code remains constant above a certain power threshold (see discussion in Section 5.3.4 and Figure 5.12).

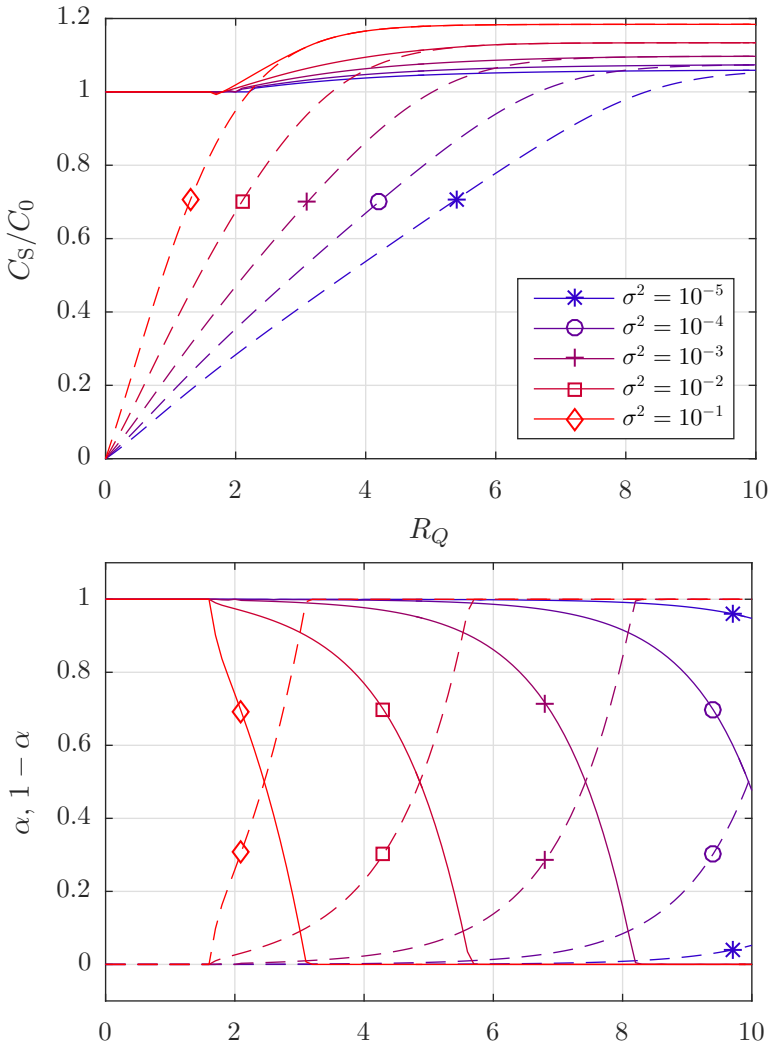

Figure 5.10: Top: Normalized achievable rates with superposition coding (solid lines) and with pure feedback coding (dashed lines). Bottom: Power splitting (solid lines for $1-\alpha$, dashed lines for α) for various channel noise levels and fixed total transmit power $P = 1$.

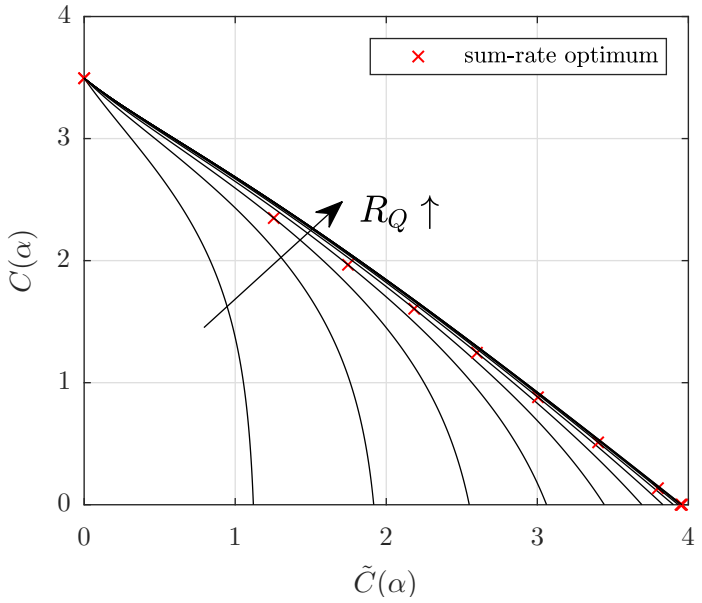

Figure 5.11: BC achievable rate region $(\tilde{C}(\alpha), C(\alpha))$ for fixed $C_0 = 3$ and quantization rates $R_Q = 0.2C_0 \ldots 2.4C_0$.

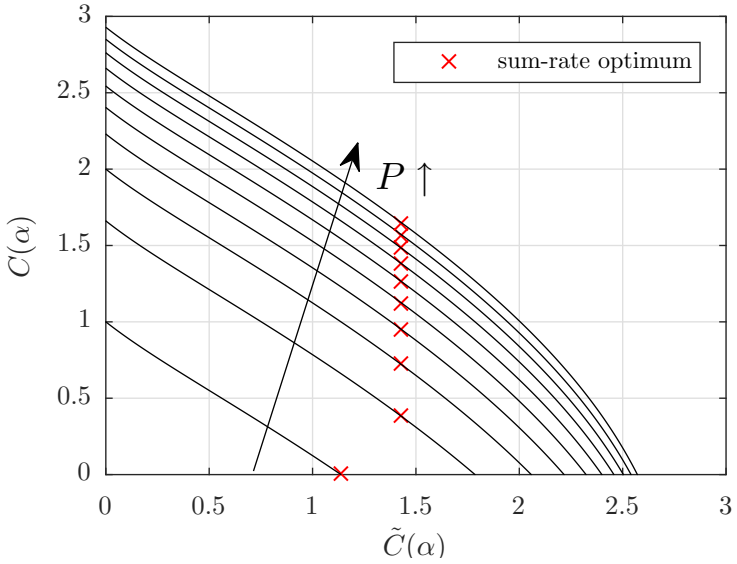

Figure 5.12: BC achievable rate region $(\tilde{C}(\alpha), C(\alpha))$ for fixed $R_Q = 2$ and $P_T = 0.1P_{R_Q} \ldots 2P_{R_Q}$ where P_{R_Q} is such that $C_0(P_{R_Q}) = R_Q$.

5.6 Asymptotic Superposition Performance - Asymmetric Broadcast Channel

5.6.1 Power Constraints

We study the two-user asymmetric Gaussian BC with (quantized) feedback (see Figure 4.5). Here, one single transmitter sends the sum of the independent length-n Gaussian user signals $x_i[k]$, $i = 1, 2$ (cf. (5.56)), and the receivers observe the signals

$$y_1[k] = h_1(x_1[k] + x_2[k]) + z_1[k], \tag{5.68}$$

$$y_2[k] = h_2(x_1[k] + x_2[k]) + z_2[k]. \tag{5.69}$$

The channel gains h_1 and h_2 are assumed to be known by both transmitter and both receivers and the channel introduces i.i.d. additive Gaussian noise $\mathbf{z}_i \sim \mathcal{N}(\mathbf{0}, \sigma^2 \boldsymbol{I})$, $i = 1, 2$. We impose the average transmit power constraint (here, expectation is with respect to the messages and the channel noise)

$$\frac{1}{n} \sum_{k=1}^{n} \mathrm{E}\{\mathsf{x}_1^2[k] + \mathsf{x}_2^2[k]\} \leq P_T. \tag{5.70}$$

The transmitter communicates independent messages $\theta_{1,j}$, $\tilde{\theta}_{1,l}$ and $\theta_{2,j}$, $\tilde{\theta}_{2,l}$, $j = 1, \ldots, \tilde{N}$, $l = 1, \ldots, N$, to two users (receivers). The messages are uniformly drawn from finite sets with cardinalities $\mathcal{M}_1$, $\widetilde{\mathcal{M}}_1 = 2^{\tilde{N}\tilde{R}_1}$, $\mathcal{M}_2 = 2^{NR_2}$, $\widetilde{\mathcal{M}}_2 = 2^{\tilde{N}\tilde{R}_2}$, and mapped to the transmit signal components according to the superposition (see Section 4.5.3) with block structure (cf. (4.69))

$$x_i[(j-1)N + l] = \varphi_{i,l}(\theta_{i,j}) + \tilde{\varphi}_{i,j}\big(\tilde{\theta}_{i,l}, \boldsymbol{w}_{i,l}^{(j-1)}\big),\ j = 1, \ldots, \tilde{N},\ l = 1, \ldots, N,\ i = 1, 2, \tag{5.71}$$

$k = (j-1)N + l = 1, \ldots, n$. Like for the asymmetric MAC, here, $\varphi_{i,l} : \mathcal{M}_i \to \mathbb{R}$ denotes a conventional encoder with power constraint

$$\frac{1}{N} \sum_{l=1}^{N} \mathrm{E}\{\varphi_{i,l}^2(\theta_{i,j})\} \leq P_i, \quad j = 1, \ldots, \tilde{N}, \quad i = 1, 2, \tag{5.72}$$

with expectation over all possible transmit messages θ_i, j. The conventional encoder completely ignores the feedback signal. Note that here we only have one single transmitter that composes the transmit signal components (5.71) to the total transmit signal

$$x[k] = x_1[k] + x_2[k]. \tag{5.73}$$

Furthermore, in contrast to the MAC, here $\boldsymbol{w}_{i,l}^{(j-1)} = (w_i[1] \ldots w_i[(j-1)N+l])^\top$ denotes the past quantized feedback and $\tilde{\varphi}_{i,j} : \widetilde{\mathcal{M}}_i \times \mathbb{R}^{j-1} \to \mathbb{R}$ is the feedback-based encoder

with power constraint

$$\frac{1}{n}\sum_{j=1}^{\tilde{N}} \mathrm{E}\Big\{\tilde{\varphi}_{i,j}^2\big(\tilde{\theta}_{i,l}, \mathbf{w}_{i,l}^{(j-1)}\big)\Big\} \leq \tilde{P}_i, \quad l = 1, \ldots, N, \quad i = 1, 2, \tag{5.74}$$

with expectation over all possible transmit messages $\tilde{\theta}_{i,l}$ and channel realizations. This encoder has causal access to the quantized feedback and works as in the original Ozarow scheme (see Section 2.4.1) due to the MAC-BC duality (see Section 2.6.1). Note that in contrast to the MAC here we have two different feedback signals $\mathbf{w}_{1,l}^{(j-1)}$ and $\mathbf{w}_{2,l}^{(j-1)}$ due to the independent noise realizations $z_1[k]$ and $z_2[k]$. Due to the superimposed block structure the constraints on the transmit powers sum up to

$$P_1 + P_2 = P, \tag{5.75}$$

$$\tilde{P}_1 + \tilde{P}_2 = \tilde{P}, \tag{5.76}$$

$$P + \tilde{P} = P_T. \tag{5.77}$$

5.6.2 Achievable Sum Rate

Like for the MAC our proposed scheme is a superposition of a conventional encoder and a feedback-based encoder (cf. (5.71)). Thus, we can maximize the sum rate by finding the optimum power (equivalently, rate) splitting between the two encodings jointly for both receivers. In the symmetric case the conventionally encoded signals are cancelled at the receivers before quantization such that the quantization only captures the feedback encoding in the forward path. This was possible since the receiver has the quantization noise as side-information (see Section 4.5.5). Unfortunately, in the asymmetric case, in contrast to the symmetric case, the conventionally encoded signals can only be decoded and cancelled at the receiver with higher SNR [20]. The weaker receiver is only able to decode its dedicated conventionally encoded message, whereas the other conventionally encoded message remains acting as additional interference noise. The sum rate of the conventional coding scheme is thus given by the classical Gaussian BC capacity C_0 (see Section 2.5.1) with noise power $\sigma^2 + h_i^2(\tilde{P}_1 + \tilde{P}_2)$, since the independent feedback-based codewords (cf. (4.69b)) that are each superimposed in specific time instances of the conventional coding (cf. (4.69a)) act as additional interference. Then, the achievable sum rate for fixed feedback transmit powers $\tilde{P}_1$ and $\tilde{P}_2$ and given total transmit power P_T is

$$\begin{aligned} R_1 + R_2 &\leq \max_{P_1+P_2 \leq P_T - \tilde{P}_1 - \tilde{P}_2} C_0(h_1^2 P_1, h_2^2 P_2, \sigma^2 + h_1^2(\tilde{P}_1 + \tilde{P}_2), \sigma^2 + h_2^2(\tilde{P}_1 + \tilde{P}_2)) \\ &\triangleq \mathsf{C}. \end{aligned} \tag{5.78}$$

Due to the MAC-BC duality the sum rate of the feedback coding scheme is given by the Ozarow capacity C^{FB} (see Section 2.6.1) with asymmetric channel noises. Without loss of generality we assume that receiver 1 has higher SNR than receiver 2. Then, the noise power of receiver 1 is $\sigma^2 + \sigma_{q_1}^2$ (due to the additional quantization noise) and the noise power of receiver 2 is $\sigma^2 + \sigma_{q_2}^2 + h_2^2 P_1$ (due to the additional quantization noise and the remaining additional interference of the conventional codeword for receiver 1). Then, the achievable sum rate for fixed transmit powers P_1 and P_2 and given total transmit power P_T is

$$\begin{aligned}\tilde{R}_1 + \tilde{R}_2 &\leq \max_{\tilde{P}_1+\tilde{P}_2 \leq P_T - P_1 - P_2} C^{\mathrm{FB}}(h_1^2\tilde{P}_1, h_2^2\tilde{P}_2, \sigma^2 + \sigma_{q_1}^2, \sigma^2 + \sigma_{q_2}^2 + h_2^2 P_1) \\ &\triangleq \tilde{\mathsf{C}}. \end{aligned} \tag{5.79}$$

The total achievable sum rate of our proposed scheme with given total transmit power P_T yields

$$\begin{aligned} R_1 + R_2 + \tilde{R}_1 + \tilde{R}_2 &\leq \max_{P_1+P_2+\tilde{P}_1+\tilde{P}_2 \leq P_T} \mathsf{C} + \tilde{\mathsf{C}} \\ &\triangleq C_S. \end{aligned} \tag{5.80}$$

Finally, simplifying the nested maximizations (implicitly contained in the expressions for C and $\tilde{\mathsf{C}}$) to one single maximization yields

$$\begin{aligned} C_S = \max_{P_1+P_2+\tilde{P}_1+\tilde{P}_2 \leq P_T} & C_0(h_1^2 P_1, h_2^2 P_2, \sigma^2 + h_1^2(\tilde{P}_1 + \tilde{P}_2), \sigma^2 + h_2^2(\tilde{P}_1 + \tilde{P}_2)) \\ & + C^{\mathrm{FB}}(h_1^2\tilde{P}_1, h_2^2\tilde{P}_2, \sigma^2 + \sigma_{q_1}^2, \sigma^2 + \sigma_{q_2}^2 + h_2^2 P_1). \end{aligned} \tag{5.81}$$

Previously, for the symmetric MAC and BC this was the basis of a one-dimensional optimization problem, since the individual capacity expressions directly yielded the convex part and the concave part. In the asymmetric BC case, (5.81) results in a multi-dimensional optimization problem where the individual capacity expressions do not directly yield the convex part and the concave part.

Expanding the expressions of the capacities in (5.81) gives

$$\begin{aligned} C_S = \max_{P_1+P_2+\tilde{P}_1+\tilde{P}_2 \leq P_T} & C\left(\frac{h_1^2 P_1}{\sigma^2 + h_1^2(\tilde{P}_1 + \tilde{P}_2)}\right) \\ & + C\left(\frac{h_2^2 P_2}{\sigma^2 + h_2^2 P_1 + h_2^2(\tilde{P}_1 + \tilde{P}_2)}\right) \\ & + C^{\mathrm{FB}}(h_1^2\tilde{P}_1, h_2^2\tilde{P}_2, \sigma^2 + \sigma_{q_1}^2, \sigma^2 + \sigma_{q_2}^2 + h_2^2 P_1), \end{aligned} \tag{5.82}$$

where receiver 1 decodes both conventional encoded messages and receiver 2 decodes only its dedicated conventionally encoded message. Then, the first two terms reflect

the classical Gaussian BC capacity. Unfortunately, the asymmetry in the ability of decoding renders the problem hard to split into a concave and a convex part. In the symmetric case only the feedback signal with total power $\tilde{P}_1 + \tilde{P}_2$ acts as interference for the conventional coding, whereas now in addition to this interference the feedback signal itself is still also interfered by the remaining (undecoded) conventional signal with power P_1.

5.6.3 Partly Symmetrized Solution

Due to the asymmetry the non-feedback component cannot be fully cancelled before quantizing and feeding back the feedback component. Specifically, this adds additional interference at the weaker receiver. One possible solution is to make the problem quasi-symmetric again. Therefore, we reduce the power (or equivalent the rate) of the non-feedback component at an amount that both messages for receiver 1 and receiver 2 can be decoded at both receivers. As a consequence, the total achievable rate of the non-feedback component reduces to the point-to-point AWGN channel capacity and is equivalent to the "onion peeling" approach,

$$\begin{aligned} R_1 + R_2 &\leq C_0 \left(\frac{h_2^2(P_1 + P_2)}{\sigma^2 + h_2^2(\tilde{P}_1 + \tilde{P}_2)} \right) \\ &\triangleq \mathsf{C}. \end{aligned} \tag{5.83}$$

where again without loss of generality we assume that receiver 1 has higher SNR than receiver 2.

Similar as in the previous section, due to the MAC-BC duality the sum rate of the feedback coding scheme is given by the Ozarow capacity C^{FB} (see Section 2.6.1) with asymmetric channel noises. Then, the noise power of receiver 1 again is $\sigma^2 + \sigma_{q_1}^2$ (due to the additional quantization noise) and the noise power of receiver 2 is $\sigma^2 + \sigma_{q_2}^2$ (due to the additional quantization noise). Now both receivers can fully decode and cancel the non-feedback components at the cost of reduced achievable rate of the total non-feedback component. On the other side this reduced achievable rate allows the feedback component higher transmit powers and as a consequence higher achievable rates and eliminated interference from the previously undecoded conventional component. Thus, the reduced achievable rate of the non-feedback component is at least partly compensated. Now, the achievable sum rate of the feedback component for fixed transmit powers P_1 and P_2 and given total transmit power P_T is

$$\begin{aligned} \tilde{R}_1 + \tilde{R}_2 &\leq \max_{\tilde{P}_1 + \tilde{P}_2 \leq P_T - P_1 - P_2} C^{\mathrm{FB}}(h_1^2 \tilde{P}_1, h_2^2 \tilde{P}_2, \sigma^2 + \sigma_{q_1}^2, \sigma^2 + \sigma_{q_2}^2) \\ &\triangleq \tilde{\mathsf{C}}. \end{aligned} \tag{5.84}$$

The total achievable sum rate of our proposed scheme with given total transmit

power P_T yields

$$\begin{aligned} R_1 + R_2 + \tilde{R}_1 + \tilde{R}_2 &\leq \max_{P_1+P_2+\tilde{P}_1+\tilde{P}_2 \leq P_T} \mathsf{C} + \tilde{\mathsf{C}} \\ &\triangleq C_S. \end{aligned} \tag{5.85}$$

Finally, simplifying the nested maximizations (implicitly contained in the expressions for C and $\tilde{\mathsf{C}}$) to one single maximization yields

$$\begin{aligned} C_S = \max_{P_1+P_2+\tilde{P}_1+\tilde{P}_2 \leq P_T} & C_0\left(\frac{h_2^2(P_1+P_2)}{\sigma^2 + h_2^2(\tilde{P}_1+\tilde{P}_2)}\right) \\ & + C^{\mathrm{FB}}(h_1^2\tilde{P}_1, h_2^2\tilde{P}_2, \sigma^2+\sigma_{q_1}^2, \sigma^2+\sigma_{q_2}^2). \end{aligned} \tag{5.86}$$

Previously, for the symmetric MAC and BC this was the basis of a one-dimensional optimization problem, since the capacity expressions directly yielded the convex part and the concave part. In the asymmetric but symmetrized BC case, (5.86) again directly yields the convex part and the concave part as follows.

5.6.4 Concave and Convex Component

Next, we prove that C_S can be split into a concave part $\mathsf{C}^{\cap}(\boldsymbol{p})$ and a convex part $\mathsf{C}^{\cup}(\boldsymbol{p})$ in the power allocation vector $\boldsymbol{p} = (P_1, P_2, \tilde{P}_1, \tilde{P}_2)^{\top}$,

$$C_S = \max_{\mathbf{1}^{\top}\boldsymbol{p} \leq P} \mathsf{C}^{\cap}(\boldsymbol{p}) + \mathsf{C}^{\cup}(\boldsymbol{p}). \tag{5.87}$$

Then, this sum rate maximization problem can be solved by DC programming [49].

We expand the respective equivalent AWGN capacity $C_0(h_2^2(P_1+P_2), \sigma^2 + h_2^2(\tilde{P}_1 + \tilde{P}_2))$ to

$$\begin{aligned} C_0(h_2^2(P_1+P_2), \sigma^2 + h_2^2(\tilde{P}_1+\tilde{P}_2)) = & \frac{1}{2}\log(\sigma^2 + h_2^2(P_1+P_2+\tilde{P}_1+\tilde{P}_2)) \\ & - \frac{1}{2}\log(\sigma^2 + h_2^2(\tilde{P}_1+\tilde{P}_2)). \end{aligned} \tag{5.88}$$

The first term is constant and the second term is easily identified as convex since the logarithm is a concave function. Thus, the C^{FB} is not affected by the symmetrization and therefore due to MAC-BC duality solely yields the convex part (see Section 5.4.3). (5.87) can then be rewritten as

$$C_S = \max_{\mathbf{1}^{\top}\boldsymbol{p} \leq P_T} \underbrace{C^{\mathrm{FB}}(h_1^2\tilde{P}_1, h_2^2\tilde{P}_2, \sigma^2+\sigma_{q_1}^2, \sigma^2+\sigma_{q_2}^2)}_{\mathsf{C}^{\cap}(\boldsymbol{p}) \triangleq \tilde{C}(\boldsymbol{p})} + \underbrace{C_0(h_2^2(P_1+P_2), \sigma^2 + h_2^2(\tilde{P}_1+\tilde{P}_2))}_{\mathsf{C}^{\cup}(\boldsymbol{p}) \triangleq C(\boldsymbol{p})} \tag{5.89}$$

5.6.5 Difference of Convex Functions Programming Solution

Splitting the objective function and our already affine constraints into concave and convex functions allows us to solve the optimization problem via DC programming (see Section 2.8) and the practically efficient CCP algorithm (see Section 2.8.1). Reformulating the maximization problem (5.87) in standard form (2.66) yields the following result.

Corollary 5.5. *The problem of maximizing the achievable sum rate of the asymmetric Gaussian BC with quantized feedback and a superposition of feedback coding with capacity $\tilde{C}$ and conventional coding with capacity C is solved by finding the solution of the DC problem*

$$\begin{aligned} \underset{\boldsymbol{p}}{\textit{minimize}} \quad & -\tilde{C}(\boldsymbol{p}) - C(\boldsymbol{p}) \\ \textit{subject to} \quad & \mathbf{1}^\top \boldsymbol{p} - P_T \leq 0, \\ & -\boldsymbol{p} \preceq 0. \end{aligned} \tag{5.90}$$

Like in the previous sections we have to find a point where the gradient of the convex part in the next iteration equals the negative gradient of the concave part of the previous iteration

$$\nabla C(\boldsymbol{p}_{k+1}) = -\nabla \tilde{C}(\boldsymbol{p}_k) \tag{5.91}$$

which itself is a convex optimization problem. The solution to this auxiliary problem decreases monotonically with increasing k and thus converges to a minimum (or saddle point). Lipp and Boyd [49] give a basic CCP algorithm (see Section 2.8.1) which requires an initial feasible point $\boldsymbol{p}_0$, which in our case can be any point in the interval $0 \leq \mathbf{1}^\top \boldsymbol{p}_0 \leq P_T$. Following [49], the CCP approach leads to Algorithm 8 for power allocation.

In step 3 Algorithm 8 uses a linearization $\hat{\mathsf{C}}_k(\boldsymbol{p})$ of the convex component $C(\boldsymbol{p})$. The gradient $\nabla C(\boldsymbol{p})$ contained in the linearization can be directly calculated as

$$\nabla C(\boldsymbol{p}) = \frac{1}{2} \frac{h_2^2}{\sigma^2 + h_2^2(P_1 + P_2 + \tilde{P}_1 + \tilde{P}_2)} - \frac{1}{2} \begin{pmatrix} 0 \\ 0 \\ \frac{h_2^2}{\sigma^2 + h_2^2(\tilde{P}_1 + \tilde{P}_2)} \\ \frac{h_2^2}{\sigma^2 + h_2^2(\tilde{P}_1 + \tilde{P}_2)} \end{pmatrix}. \tag{5.92}$$

If we were able to find the gradient $\nabla \mathsf{C}^{\cap}(\boldsymbol{p})$ as well and solve the iteration (5.91) for $\boldsymbol{p}_{k+1}$ we could avoid the auxiliary convex optimization problem. Unfortunately, this seems not feasible.

Algorithm 8 Transmit power allocation for asymmetric BC with feedback via CCP

Require: Initial feasible point $\boldsymbol{p}_0$

1: $k := 0$
2: **while** stopping criterion not satisfied **do**
3: Form $\hat{\mathsf{C}}_k(\boldsymbol{p}) = C(\boldsymbol{p}_k) + (\boldsymbol{p} - \boldsymbol{p}_k)^\top \nabla C(\boldsymbol{p}_k)$
4: Determine $\boldsymbol{p}_{k+1}$ by solving the convex problem

$$\begin{aligned} \text{minimize} \quad & -\tilde{C}(\boldsymbol{p}) - \hat{\mathsf{C}}_k(\boldsymbol{p}) \\ \text{subject to} \quad & \mathbf{1}^\top \boldsymbol{p} - P_T \leq 0, \\ & -\boldsymbol{p} \preceq 0 \end{aligned}$$

5: $k := k + 1$
6: **end while**
7: **return** $\boldsymbol{p}_k$

5.6.6 Numerical Solution

Figure 5.13 shows the achievable rates (top) and power allocations (middle and bottom) obtained by solving (5.90) versus the feedback quantization rate R_Q. The linear-feedback capacity of the proposed superposition coding scheme is normalized by the no-feedback BC sum capacity C_0. Clearly, when R_Q is too small the feedback is not beneficial at all and the whole transmit power is allocated to the conventional encoding (see middle and bottom part of Figure 5.13). Above a certain threshold for R_Q, true superposition is optimal and a capacity gain is achieved. In contrast to the asymmetric MAC case where true superposition stays optimal even for very large R_Q (almost perfect feedback), in the asymmetric BC case (in Figure 5.13 for $h_2 > 1.1$) we can observe that eventually pure feedback coding becomes optimal. This is similar behaviour as we observed for the symmetric MAC and BC and is caused by the symmetrization of the non-feedback component. A consequence of the symmetrization is that this scheme performs highly suboptimal (region where $C_S/C_0 < 1$ in Figure 5.13) for low quantization rates. Nevertheless, if the asymmetry is not to big we still observe a gain (region where $C_S/C_0 > 1$ in Figure 5.13) due to the superposition coding. The highest gain in capacity is achieved in the fully symmetric case and strictly decreases with increasing asymmetry of the channel gains.

Figure 5.14 again shows the rates (top) and power allocations (middle and bottom) obtained by solving (5.90) versus the feedback quantization rate R_Q for fixed (moderate) level of asymmetry but various channel noise levels. Again, when R_Q is too small the feedback is not beneficial at all and the whole transmit power is allocated to the conventional encoding (see middle and bottom part of Figure 5.14). Above a certain threshold (solely determined by the channel gains and independent of the actual channel noise levels) for R_Q, true superposition is optimal in a specific quantization rate window until eventually pure feedback coding becomes optimal. The size of these quantization rate windows decrease with increasing noise, i.e., the transition to pure feedback coding becomes shorter. Interestingly, the quantization rate value where the capacity reduction

due to the symmetrization is compensated is again solely determined by the channel gains and independent of the actual channel noise levels. The highest gain in capacity is achieved for low SNR and strictly decreases with increasing SNR of the channel gains.

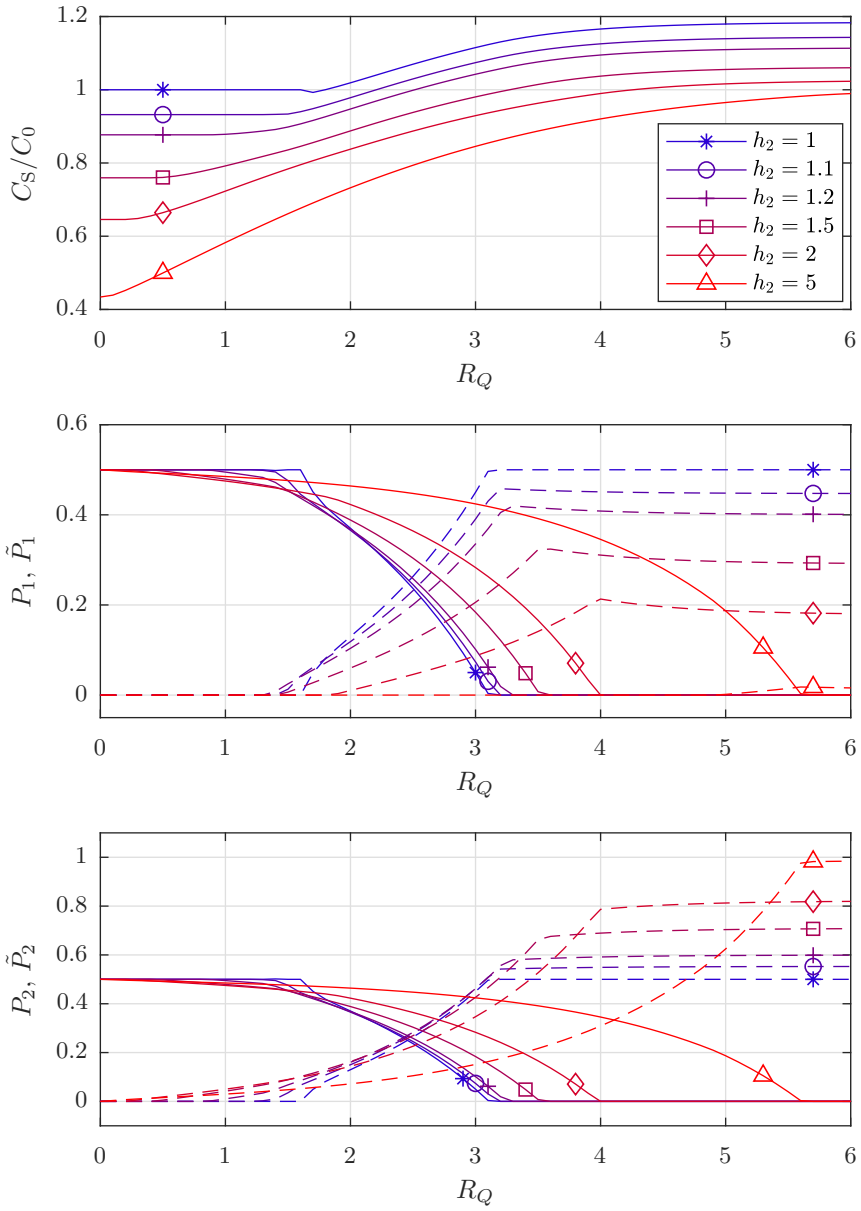

Figure 5.13: Top: Normalized achievable rates (in bit) with superposition coding. Middle and bottom: Power splitting (decreasing solid lines for P_i, increasing dashed lines for $\tilde{P}_i$) for various channel gains h_2 ($h_1 = 1$, $P_T = 1$, $\sigma^2 = 10^{-2}$). Horizontal axis in all plots is the feedback quantization rate R_Q.

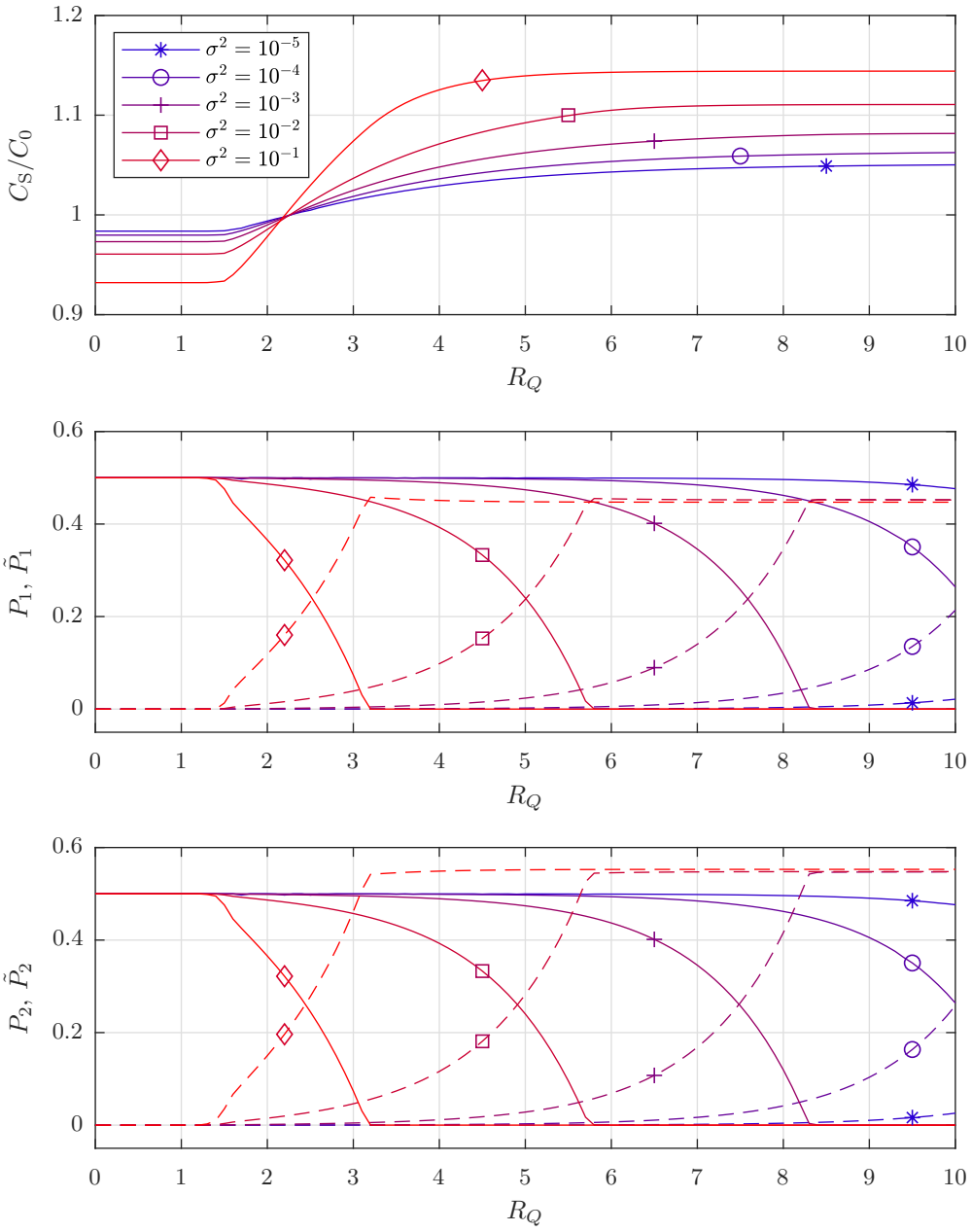

Figure 5.14: Top: Normalized achievable rates (in bit) with superposition coding. Middle and bottom: Power splitting (decreasing solid lines for P_i, increasing dashed lines for $\tilde{P}_i$) for various channel noise levels σ^2 ($h_1 = 1$, $h_2 = 1.1$, $P_T = 1$). Horizontal axis in all plots is the feedback quantization rate R_Q.

6

Finite Blocklength Superposition Coding

In this Chapter we use recent findings of achievable rates for non-vanishing error probabilities in the finite-blocklength regime to specialize our proposed suerposition coding scheme to this regime. We thus derive error probability expressions for each component of the superposition coding scheme for various channel models. Next, we show that due to imperfect decoding the error probabilities are coupled and we propose regions where the approximation of decoupled error probabilities is sufficiently accurate. We then formulate a partly combinatorial optimization problem that jointly finds the optimal power allocation (as in the asymptotic regime) and blocklength allocation for each channel model. We propose an approximate solving procedure that successively finds the asymptotic power allocation and blocklength allocation.

In Section 6.2 we start with the analysis of the AWGN channel and further extend this treatment to the MAC in Section 6.3 and to the BC in Section 6.4. Finally, we conclude this chapter with a discussion of the studied schemes in Section 6.5.

6.1 Introduction

The main contributions in this chapter pertain to adaptations of the linear superposition coding scheme developed in Chapter 4, which address two important real-world constraints:

- Practical restrictions regarding latency and complexity necessitate a finite blocklength for real-world coding schemes. We thus propose a block feedback scheme that superimposes feedback-based encoding and conventional (non-feedback) coding. In contrast to other block feedback schemes (e.g., [59, 82]), our approach involves a systematic combination of the two constituent codes that allows their separation via successive cancellation in finite time.
- The feedback link in real communication systems can hardly be assumed to be perfect; at least it is quantized (rate-limited). As with the asymptotic regime in Chapter 5 we model the feedback quantization in terms of channel output compression via the information bottleneck principle [17, 80, 86, 87] (see Chapter 3), which allows the receiver to use the quantization noise as side-information.

In the asymptotic regime we found that allocating the powers to maximize the achievable rates amounts to a difference of convex functions (DC) problem [91]. Here we show that in the finite blocklength regime the maximization of the achievable rates (for a prescribed blocklength and error probability) involves an additional combinatorial optimization problem to find the optimal splitting of the overall block between the two constituent codes. We solve this optimization problem numerically and show that superposition is beneficial.

6.2 Finite Blocklength Superposition Performance – Gaussian Channel

6.2.1 Error Probabilities

The error probability $\tilde{P}_e$ of the feedback based scheme is known to decrease doubly exponentially in the blocklength $\tilde{N}$ [69], whereas the error probability P_e of the conventional coding scheme decreases only exponentially in the blocklength N [65,66]. Due to the monotonicity of $\tilde{P}_e(\tilde{N})$ and $P_e(N)$ and the relation $n = \tilde{N}N$, decreasing the error probability of one component (via larger blocklength) increases the error probability of the other component (due to shorter blocklength).

The block structure of the superposition coding couples the error probabilities; if the conventional codeword is decoded incorrectly, it cannot be cancelled successively from the superposition and therefore negatively affects the decoding of the feedback based codeword.

Error probability of feedback based coding component

The error probability expression of the feedback based coding was bounded by Gallager [32] for perfect feedback (see Section 2.2.2). Adapted to our superposition scheme with quantized feedback we have

$$\tilde{P}_e(\tilde{R}, \tilde{N}) \leq 2Q\left(2^{\tilde{N}(C^{\mathrm{FB}}(h^2\tilde{P},\sigma_s^2)-\tilde{R})}\right), \tag{6.1}$$

with the resulting (interference) noise variance σ_s^2, which is given by

$$\sigma_s^2 = \sigma^2 + \sigma_q^2 + h^2 P P_e \tag{6.2}$$

in this superposition configuration. P_e is the error probability of the conventional coding scheme and the h^2PP_e term is due to the decoding errors of the conventional coding scheme that cause additional interference. Due to the block coding structure this additional interference is i.i.d. and can be modeled to be Gaussian as well if $\tilde{N}$ is not too small.

Due to the block structure each initial time slot is used to transmit the messages $\tilde{\theta}_l$, $l = 1, \ldots, N$

$$\tilde{x}[l] = \sqrt{\tilde{P}}\theta_l, \qquad l = 1, \ldots, N, \tag{6.3}$$

such that the transmit signal meets the transmit power constraint. The current message estimation errors $\epsilon_{j,l}$ in iteration j are given by

$$\epsilon_{j,l} = \tilde{\theta}_l - \hat{\tilde{\theta}}_l(\tilde{\boldsymbol{y}}^{((j-1)N+l)}),, \qquad j = 1, \ldots, \tilde{N}, \quad l = 1, \ldots, N. \tag{6.4}$$

Then, the initial estimation error simply yields

$$\epsilon_{2,l} = \tilde{\theta}_l - \hat{\tilde{\theta}}_l(\tilde{\boldsymbol{y}}^{(N+l)}) = \tilde{\theta}_l - \frac{\tilde{y}[l]}{\sqrt{h^2\tilde{P}}}, \qquad l = 1, \ldots, N, \tag{6.5}$$

since the first timeslot (of the feedback scheme) is exclusively used to transmit the message,

$$\tilde{y}[l] = \sqrt{h^2\tilde{P}}\tilde{\theta}_l + z_s[l], \qquad l = 1, \ldots, N. \tag{6.6}$$

The estimation errors $\epsilon_{j,l}$ geometrically decrease and thus a simple nearest neighbour decoding yields the doubly exponential decreasing error probability for each $\tilde{\theta}_l$, $l = 1, \ldots, N$ [69].

Error probability of conventional coding component

The error probability expression of the conventional coding scheme can be obtained by adapting the results for the AWGN channel in the finite blocklength regime obtained by Polyanskiy in [66, Theorem 54] (see Section 2.1.2). In our superposition scenario we have

$$P_e(R,N) \leq 2Q\left\{\frac{1}{\sqrt{V}}\left[\sqrt{N}(C-R)+\frac{1}{\sqrt{N}}\frac{1}{2}\log N\right]\right\}, \tag{6.7}$$

with channel dispersion

$$V = \frac{h^2P}{2}\frac{h^2P+2(\sigma^2+h^2\tilde{P})}{(h^2P+\sigma^2+h^2\tilde{P})^2}\log^2 e. \tag{6.8}$$

Note that here the capacity of the conventional coding scheme is affected by the interference of the feedback based coding and results in a reduced capacity $C = C\left(h^2P/(\sigma^2+h^2\tilde{P})\right)$. In our AWGN scenario the power allocation procedure ensures that the additional sum rate constraint holds.

Error probability approximations

For the remainder of Section 6.2 we work with the approximation $\sigma_s^2 \approx \sigma^2+\sigma_q^2$, i.e., $P_e \ll (\sigma^2+\sigma_q^2)/h^2P$. In the regime of interest this approximation is sufficiently accurate. This simplifies the numerical evaluation since it allows us to independently analyze the decoupled error probability expressions.

6.2.2 Achievable Rates versus Blocklength and Error Probability

Instead of investigating the error probability as a function of the blocklength we are now interested in the achievable rates versus blocklength and error probability. This is a more practical approach, since usually applications require a specific rate and maximal error probability.

The achievable rate of the feedback based code is found by solving (6.1) for $\tilde{R}$,

$$\tilde{R}(\tilde{P}_e,\tilde{N}) \leq \frac{1}{2}\log\left(\frac{\sigma_s^2+h^2\tilde{P}}{\sigma_s^2}\right)-\frac{1}{\tilde{N}}\log\left(Q^{-1}\left\{\frac{\tilde{P}_e}{2}\right\}\right), \tag{6.9}$$

and the achievable rate of the conventional code is found by solving (6.7) for R,

$$R_i(P_e,N) \leq C-\frac{1}{\sqrt{N}}\sqrt{V}Q^{-1}\left\{\frac{P_e}{2}\right\}+\frac{1}{2}\log\sqrt[N]{N}. \tag{6.10}$$

6.2.3 Optimization Problem

Optimization in the context of finite blocklength means finding the optimum subblock splitting $(N, \tilde{N})$ that maximizes the achievable rates under the constraint $n = \tilde{N}N$ for prescribed blocklength n and error probability.

We want to find the blocklength allocation that maximizes the achievable sum rate

$$R_s = R(P_e, N) + \tilde{R}(\tilde{P}_e, \tilde{N}), \tag{6.11}$$

while keeping the effective average error probability

$$\bar{P}_e = \frac{1}{R_s}\left(R(P_e, N)P_e + \tilde{R}(\tilde{P}_e, \tilde{N})\tilde{P}_e\right) \tag{6.12}$$

below a certain value ϵ. $\tilde{R}(\tilde{P}_e, \tilde{N})$ and $R(P_e, N)$ are given by (6.9) and (6.10), respectively. Generally, this leads to the non-convex and partly combinatorial optimization problem

$$\begin{aligned} \underset{N,\tilde{N},P,\tilde{P}}{\text{maximize}} \quad & R_s \\ \text{subject to} \quad & \bar{P}_e, \leq \epsilon \\ & \tilde{N}N = n, \\ & P + \tilde{P} \leq P_T. \end{aligned} \tag{6.13}$$

A simpler approach is to restrict each of the individual error probabilities to be smaller than ϵ. This is indeed more reasonable, since the data from the conventional coding component and from the feedback coding component encode independent information and thus require certain error rates. Thus, the optimization simplifies to

$$\begin{aligned} \underset{N,\tilde{N},P,\tilde{P}}{\text{maximize}} \quad & R(P_e, N) + \tilde{R}(\tilde{P}_e, \tilde{N}) \\ \text{subject to} \quad & P_e \leq \epsilon, \\ & \tilde{P}_e \leq \epsilon, \\ & \tilde{N}N = n, \\ & P + \tilde{P} \leq P_T, \end{aligned} \tag{6.14}$$

which is still a non-convex and partly combinatorial optimization problem.

We tackle both optimizations by initially finding reasonable transmit power allocation and then optimize the blocklength allocation. On the one hand, the performance of the feedback coding component is limited by the channel capacity and thus by the allocated transmit power itself and on the other hand it is limited by the quantization rate. Due to the data processing inequality the achievable rate cannot exceed either of this two. For this reason, we allocate that much transmit power that both the capacity

R [bit]	P	$\tilde{P}$
1	0.987	0.013
2	0.933	0.067
3	0.717	0.283
4	0.1	0.9
5	0.1	0.9
6	0.1	0.9

Table 6.1: Balanced power allocation according to $\tilde{P} = 0.9 \max(P_T, P_R)$ with P_R such that $C(P_R) = R$ (parameters as in Figure 6.1 and Figure 6.2).

and the quantization rate are of similar scale (if there is enough total transmit power available), that is,

$$\tilde{P} = 0.9 \max(P_T, P_R), \tag{6.15}$$

where P_R is chosen such that $C(P_R) = R$. Thus,

$$P_R = \sigma^2(2^{2R_Q} - 1). \tag{6.16}$$

The 0.9 factor is a pragmatic choice for the demonstration of the superposition behaviour. Otherwise, for large enough quantization rates, all the available transmit power would be allocated to the feedback coding component. Now, at least $0.1P_T$ is allocated to the conventional coding component. We then use this balanced power allocation (see Table 6.1) to find the optimal blocklength allocation. Generally, this approach might not be equivalent to the global optimization since this asymptotically justified power allocation is not necessarily optimal for finite blocklengths. This is due to the fact that both constituent schemes do not show the same error decay behaviour. The feedback coding scheme has a doubly exponentially decreasing error probability, whereas the conventional coding scheme only decreases exponentially in blocklength. Thus, one has to take this into account when optimizing the power allocation. Unfortunately, joint optimization of power allocation and blocklength allocation seems intractable.

6.2.4 Impact of Blocklength Allocation

In this section we start with the balanced power allocations (Table 6.1).

It turns out that such power allocation does not yield higher achievable sum rates for moderate blocklength and moderate quantization rates. In the example in Figure 6.1 with blocklength $n = 2^{10} = 1024$ only feedback quantization rates $R > 5$ result in better performance than coding without any feedback. Even in this case the optimal region allocates no blocklength to the conventional coding component. Note that $n = N\tilde{N}$. Thus, $N = 1$ if the optimum allocates the total blocklength to the feedback based

coding component, i.e., $\tilde{N} = n$. For larger blocklength the power allocation procedure delivers suboptimal results. In the example with blocklength $n = 2^{17} = 131072$ shown in Figure 6.2 although superposition yields higher achievable sum rates for a wide region of blocklength allocation, this is only a consequence of the power allocation. The red dashed line indicates the ultimate performance limit for pure conventional coding. We see that there is almost no gap between the achievable rate of the conventional coding and feedback based coding. We observe that the fraction of blocklength allocated to each component is primarily determined by the channel itself and only weakly depends on the actual power allocations, feedback rates or quantization rates. The next section also confirms this insight.

6.2.5 Impact of Blocklength

Again, we start with balanced power allocations. We observe that even if the balanced power allocation splits the power to both constituent schemes, the blocklength might not be allocated in the same proportions. There are essentially three different scenarios.

Very low feedback quantization rates

The quantization rate is too low to be beneficial for small blocklength. Thus, pure conventional coding is optimal. For larger blocklengths eventually superposition coding becomes optimal. In Figure 6.3 we can observe this behaviour e.g. for $R = 1$ (circle marker).

Low feedback quantization rates

In this case pure feedback coding is optimal only for very small blocklengths and then suddenly switches to superposition coding. In Figure 6.3 we can observe this behaviour e.g. for $R = 2$ (square marker) or $R = 3$ (diamond marker).

Medium to high feedback quantization rates

Here, pure feedback coding is optimal for the complete blocklength region. In Figure 6.3 we can observe this behaviour e.g. for $R = 6$ (asterisks marker).

Figure 6.3 (bottom) shows the optimal blocklength allocations. Note that in the region of superposition the growth rates of blocklength are identical and independent of the quantization rates and thus the curves highly overlap. As a consequence, $\tilde{N}/N$ is almost independent of the quantization rates in this region.

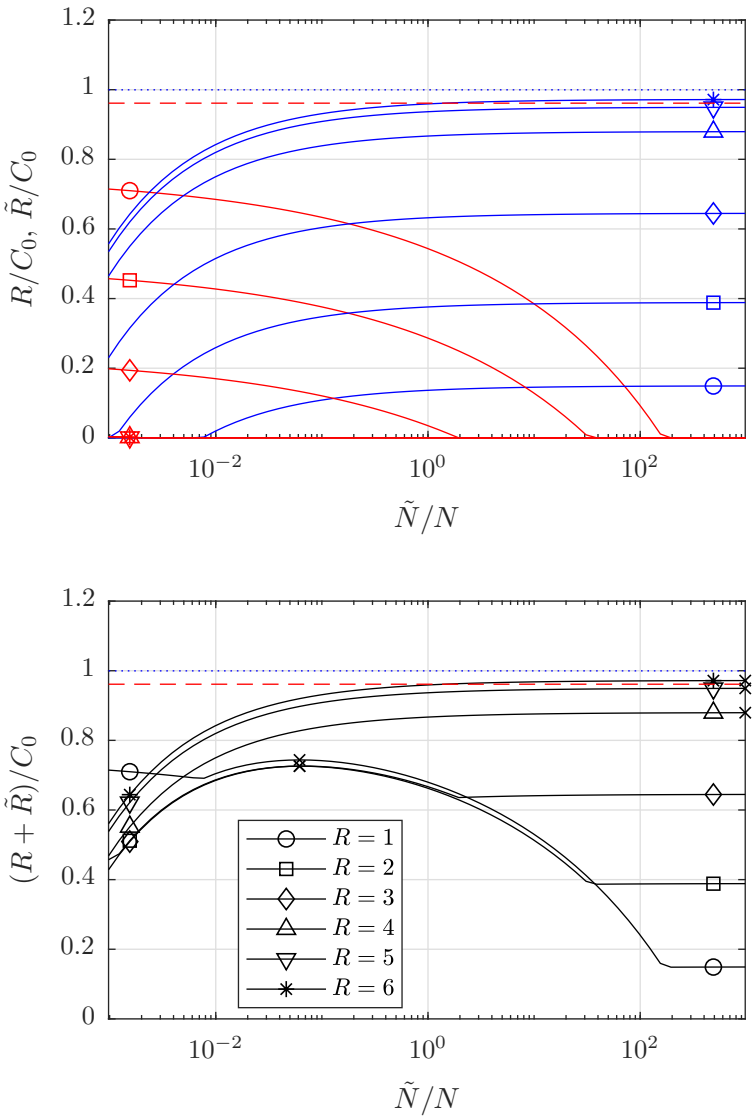

Figure 6.1: Achievable rates of conventional coding component (top, decreasing curves) and feedback coding component (top, increasing curves) and achievable sum rates (bottom, maxima marked with 'x') versus the blocklength allocation $\tilde{N}/N$ for $n = 2^{10}$. All plots pertain to the symmetric AWGN channel with $P_T = 2$, $h = 1$, $\sigma^2 = 0.01$, $\epsilon \leq 10^{-6}$, and power allocation according to Table 6.1. The dashed and dotted line show the Polyanskiy limit C_ϵ and $\tilde{C}_0$, respectively.

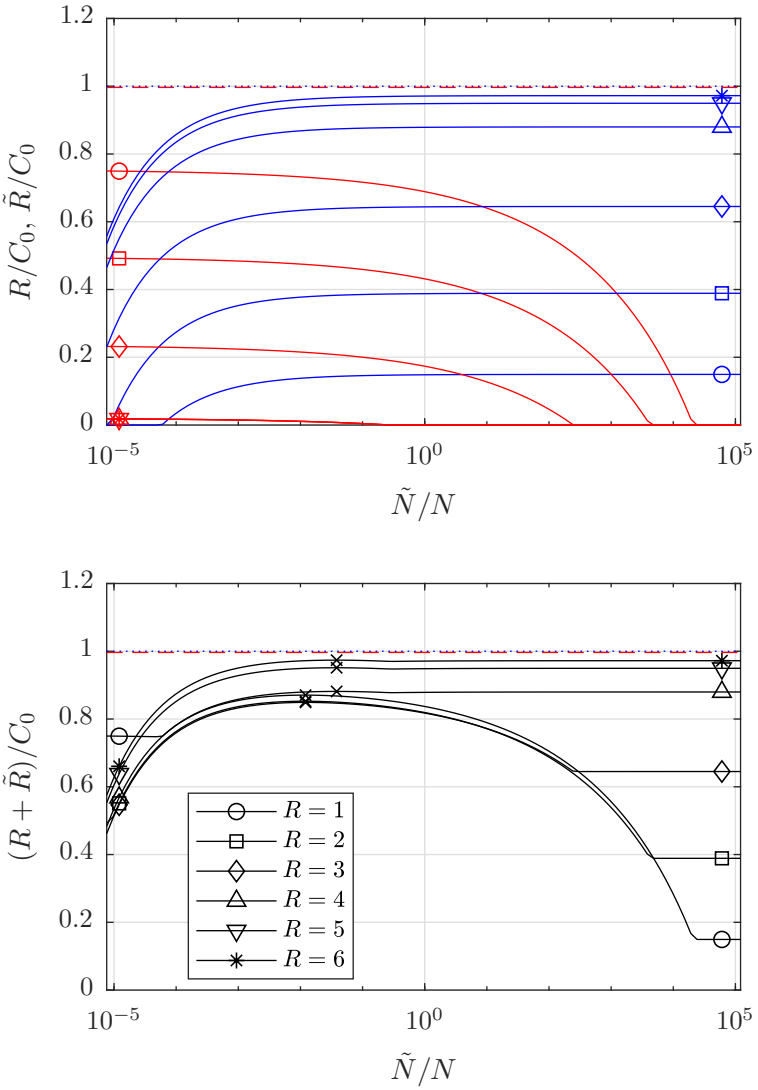

Figure 6.2: Achievable rates of conventional coding component (top, decreasing curves) and feedback coding component (top, increasing curves) and achievable sum rates (bottom, maxima marked with 'x') versus the blocklength allocation $\tilde{N}/N$ for $n = 2^{17}$. All plots pertain to the symmetric AWGN channel with $P_T = 2$, $h = 1$, $\sigma^2 = 0.01$, $\epsilon \leq 10^{-6}$, and power allocation according to Table 6.1. The dashed and dotted line show the Polyanskiy limit C_ϵ and $\tilde{C}_0$, respectively.

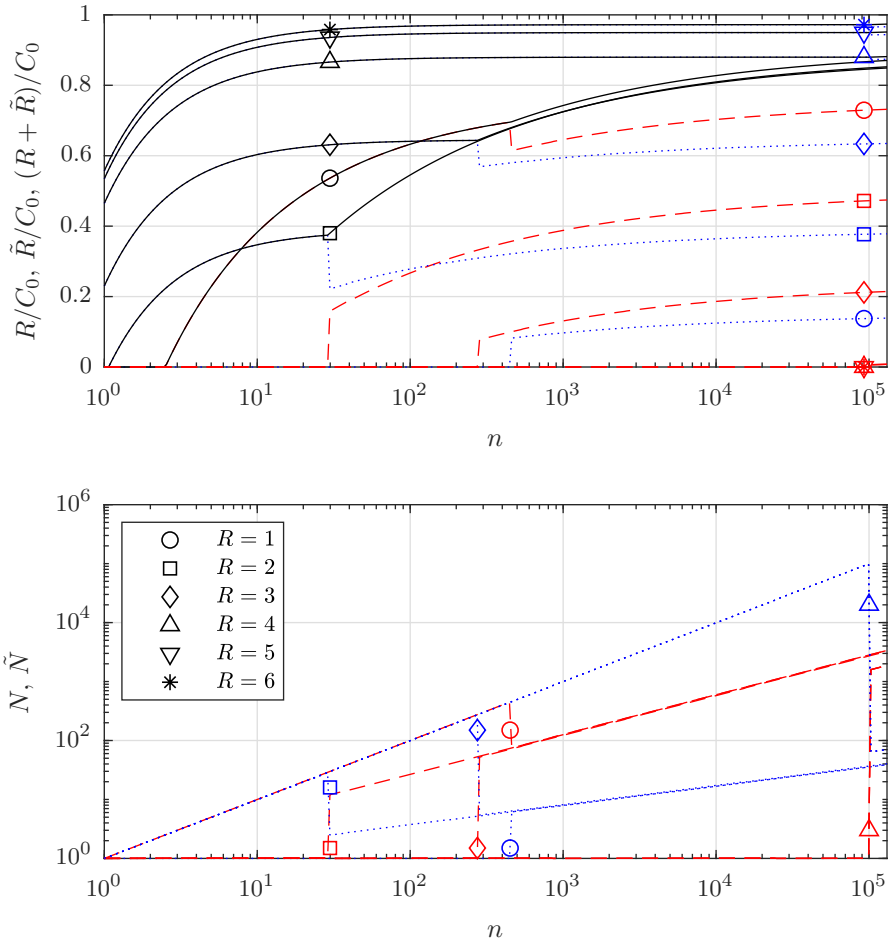

Figure 6.3: Achievable rates (top) of conventional coding component (top and bottom, dashed curves) and feedback coding component (top and bottom, dotted curves) and achievable sum rates (top, solid curves) with optimal blocklength allocation versus the blocklength n. Optimal blocklength allocations (bottom). All plots pertain to the symmetric AWGN channel with $P_T = 2$, $h = 1$, $\sigma^2 = 0.01$, $\epsilon \leq 10^{-6}$, and power allocation according to Table 6.1.

6.3 Finite Blocklength Superposition Performance – Gaussian Multiple Access Channel

6.3.1 Error Probabilities

Like for the AWGN channel, the error probabilities $\tilde{P}_{e_i}$, $i = 1, 2$ of the feedback-based scheme are known to decrease doubly exponentially in the blocklength $\tilde{N}$ [60], whereas the error probabilities P_{e_i}, $i = 1, 2$ of the conventional coding scheme decrease only exponentially in the blocklength N [65, 66]. Due to the monotonicity of $\tilde{P}_{e_i}(\tilde{N})$ and $P_{e_i}(N)$ and the relation $n = \tilde{N}N$, decreasing the error probability of one component (via larger blocklength) increases the error probability of the other component (due to shorter blocklength).

The block structure of the superposition coding couples the error probabilities; if the conventional codeword is decoded incorrectly, it cannot be cancelled successively from the superposition and therefore negatively affects the decoding of the feedback based codeword.

Error probability of feedback based coding component

The error probability expression of the feedback based coding was bounded by Ozarow [60] for perfect feedback. Adapted to our superposition scheme with quantized feedback we have

$$\tilde{P}_{e_i}(\tilde{R}_i, \tilde{N}) \leq 2Q\left\{\frac{\sigma_s^2}{2\sqrt{\alpha_{i,2}}(\sigma_s^2 + h_i^2\tilde{P}_i(1-\rho^{*^2}))}\right.$$
$$\left.\times \exp\left[\tilde{N}\left(\frac{1}{2}\log\left(\frac{\sigma_s^2 + h_i^2\tilde{P}_i(1-\rho^{*^2})}{\sigma_s^2}\right) - \tilde{R}_i\right)\right]\right\}, \tag{6.17}$$

$i = 1, 2$, with appropriately chosen $\alpha_{i,2}$. ρ^* is the optimal correlation that maximizes the achievable sum rate which is found by solving (2.31). σ_s^2 is the resulting (interference) noise variance, which is given by

$$\sigma_s^2 = \sigma^2 + \sigma_q^2 + h_1^2 P_1 P_{e_1} + h_2^2 P_2 P_{e_2} \tag{6.18}$$

in this superposition configuration. P_{e_i} are the error probabilities of the conventional coding scheme and the $h_i^2 P_i P_{e_i}$ terms are due to the decoding errors of the conventional coding scheme that cause additional interference. Due to the block coding structure this additional interference is i.i.d. and can be modeled to be Gaussian as well if $\tilde{N}$ is not too small. We choose $\alpha_{i,2}$ as in [60]

$$\alpha_{i,2} = \frac{\sigma_s^2 + \sigma_v^2}{h_i^2\tilde{P}_i}, \tag{6.19}$$

where σ_v^2 is the variance of an initial common randomness v known to all users. σ_v^2 is chosen such that the correlation remains constant over time,

$$\rho_2 = \frac{\mathrm{E}\{\epsilon_{1,2,l}\epsilon_{2,2,l}\}}{\sqrt{\alpha_{1,2}\alpha_{2,2}}} = \frac{\sigma_v^2}{\sigma_s^2+\sigma_v^2} \triangleq \rho^*. \tag{6.20}$$

Here, $\alpha_{i,j}$ are the variances of the current message estimation errors $\epsilon_{i,j,l}$,

$$\epsilon_{i,j,l} = \tilde{\theta}_{i,l} - \hat{\tilde{\theta}}_{i,l}(\tilde{\boldsymbol{y}}^{((j-1)N+l)}). \tag{6.21}$$

Note that $\alpha_{i,j}$ is identical for all l because $\tilde{\theta}_{i,l}$, $l = 1,\ldots,N$ are i.i.d.. The initial estimation errors simply yield

$$\epsilon_{1,2,l} = \tilde{\theta}_{1,l} - \hat{\tilde{\theta}}_{1,l}(\tilde{\boldsymbol{y}}^{(N+l)}) = \tilde{\theta}_{1,l} - \frac{\tilde{y}[l]}{\sqrt{h_1^2\tilde{P}_1}}, \tag{6.22}$$

$$\epsilon_{2,2,l} = \tilde{\theta}_{2,l} - \hat{\tilde{\theta}}_{2,l}(\tilde{\boldsymbol{y}}^{(N+l)}) = \tilde{\theta}_{2,l} - \frac{\tilde{y}[N+l]}{\sqrt{h_2^2\tilde{P}_2}}, \tag{6.23}$$

since the first two timeslots (of the feedback scheme) are exclusively used to transmit the messages from both transmitters alternately,

$$\tilde{y}[l] = \sqrt{h_1^2\tilde{P}_1}\tilde{\theta}_{1,l} + z_s[l] + v, \tag{6.24}$$

$$\tilde{y}[N+l] = \sqrt{h_2^2\tilde{P}_2}\tilde{\theta}_{2,l} + z_s[N+l] + v \tag{6.25}$$

Using these relations we directly get the second equality in (6.20) and then solving (6.20) for σ_v^2 yields

$$\sigma_v^2 = \sigma_s^2\frac{\rho^*}{1-\rho^*}. \tag{6.26}$$

Finally,

$$\alpha_{i,2} = \frac{\sigma_s^2}{h_i^2\tilde{P}_i(1-\rho^*)}. \tag{6.27}$$

Error probability of conventional coding component

The error probability expression of the conventional coding scheme can be obtained by adapting the results for the AWGN channel in the finite blocklength regime obtained by Polyanskiy in [66, Theorem 54] (see Section 2.3.2). In our superposition scenario we have

$$P_{e_i}(R_i,N) \le 2Q\left\{\frac{1}{\sqrt{V_i}}\left[\sqrt{N}(C_i-R_i) + \frac{1}{\sqrt{N}}\frac{1}{2}\log N\right]\right\}, \tag{6.28}$$

$i = 1, 2$, with modified channel dispersion

$$V_i = \frac{h_i^2 P_i}{2} \frac{h_i^2 P_i + 2(\sigma^2 + h_1^2 \tilde{P}_1 + h_2^2 \tilde{P}_2)}{(h_i^2 P_i + \sigma^2 + h_1^2 \tilde{P}_1 + h_2^2 \tilde{P}_2)^2} \log^2 e. \tag{6.29}$$

Note that here the capacity of the conventional coding scheme is affected by the interference of the feedback-based coding and results in a reduced capacity $C_i = C\left(h_i^2 P_i / (\sigma^2 + h_1^2 \tilde{P}_1 + h_2^2 \tilde{P}_2)\right)$. This approximation holds for sufficiently low error probabilities, where we can neglect the potential error propagation due to successive decoding. In our MAC scenario the optimal power allocation ensures that the additional sum rate constraint holds (analogous to Corollary 2.8).

Error probability approximations

For the remainder of Section 6.3 we work with the approximation $\sigma_s^2 \approx \sigma^2 + \sigma_q^2$, i.e., $P_{e_i} \ll (\sigma^2 + \sigma_q^2)/h_i^2 P_i$. In the regime of interest this approximation is sufficiently accurate. This simplifies the numerical evaluation since it allows us to independently analyze the practically decoupled error probability expressions.

6.3.2 Achievable Rates versus Blocklength and Error Probability

Like for the AWGN channel, instead of investigating the error probability as a function of the blocklength we are now interested in the achievable rates versus blocklength and error probability. This is a more practical approach, since usually applications require a specific rate and maximal error probability.

The achievable rate of the feedback based code is found by solving (6.17) for $\tilde{R}_i$,

$$\begin{aligned} \tilde{R}_i(\tilde{P}_{e_i}, \tilde{N}) \leq \frac{1}{2} \log \left(\frac{\sigma_s^2 + h_i^2 \tilde{P}_i (1 - \rho^{*^2})}{\sigma_s^2} \right) \\ - \frac{1}{\tilde{N}} \log \left[Q^{-1} \left\{ \frac{\tilde{P}_{e_i}}{2} \right\} \frac{2\sqrt{\alpha_{i,2}} (\sigma_s^2 + h_i^2 \tilde{P}_i (1 - \rho^{*^2}))}{\sigma_s^2} \right], \end{aligned} \tag{6.30}$$

$i = 1, 2$, and the achievable rate of the conventional code is found by solving (6.28) for R_i, $i = 1, 2$,

$$R_i(P_{e_i}, N) \leq C_i - \frac{1}{\sqrt{N}} \sqrt{V_i} Q^{-1} \left\{ \frac{P_{e_i}}{2} \right\} + \frac{1}{2} \log \sqrt[N]{N}. \tag{6.31}$$

6.3.3 Optimization Problem

Optimization in the context of finite blocklength means finding the optimum subblock splitting $(N, \tilde{N})$ that maximizes the achievable rates under the constraint $n = \tilde{N} N$ for prescribed blocklength n and error probability.

We want to find the blocklength allocation that maximizes the achievable sum rate

$$R_s = \sum_{i=1}^{2} \left(R_i(P_{e_i}, N) + \tilde{R}_i(\tilde{P}_{e_i}, \tilde{N}) \right), \tag{6.32}$$

while keeping the effective average error probability

$$\bar{P}_e = \frac{1}{R_s} \sum_{i=1}^{2} \left(R_i(P_{e_i}, N) P_{e_i} + \tilde{R}_i(\tilde{P}_{e_i}, \tilde{N}) \tilde{P}_{e_i} \right) \tag{6.33}$$

below a certain value ϵ. $\tilde{R}_i(\tilde{P}_{e_i}, \tilde{N})$ and $R_i(P_{e_i}, N)$ are given by (6.30) and (6.31), respectively. Generally, this leads to the non-convex and partly combinatorial optimization problem

$$\begin{aligned} \underset{N,\tilde{N},\boldsymbol{p}}{\text{maximize}} \quad & R_s \\ \text{subject to} \quad & \bar{P}_e \leq \epsilon \\ & \tilde{N} N = n, \\ & \mathbf{1}^\intercal \boldsymbol{p} \leq P_T. \end{aligned} \tag{6.34}$$

A simpler approach is to restrict each of the individual error probabilities to be smaller than ϵ. This is indeed more reasonable, since the data from the two transmitters usually carries independent information and thus requires certain error rates. Thus, the optimization simplifies to

$$\begin{aligned} \underset{N,\tilde{N},\boldsymbol{p}}{\text{maximize}} \quad & \sum_{i=1}^{2} \left(R_i(P_{e_i}, N) + \tilde{R}_i(\tilde{P}_{e_i}, \tilde{N}) \right) \\ \text{subject to} \quad & P_{e_i} \leq \epsilon, \qquad i = 1, 2 \\ & \tilde{P}_{e_i} \leq \epsilon, \qquad i = 1, 2 \\ & \tilde{N} N = n, \\ & \mathbf{1}^\intercal \boldsymbol{p} \leq P_T, \end{aligned} \tag{6.35}$$

which is still a non-convex and partly combinatorial optimization problem.

We tackle both optimizations by initially finding the optimal transmit power allocation and then optimizing the blocklength allocation. The optimal power allocation is found by maximizing the achievable sum rate, i.e. finding the capacity of our linear superposition coding scheme (see Section 5.3). We then use this (asymptotically) optimal power allocation (see Table 6.2) to find the optimal blocklength allocation. Generally, this approach might not be equivalent to the global optimization since the asymptotically optimal power allocation is not necessarily optimal for finite blocklengths. This is due to the fact that both constituent schemes do not show the same error decay

R [bit]	P_i	$\tilde{P}_i$
1	0.999	0.001
2	0.987	0.013
3	0.954	0.045
4	0.884	0.115
5	0.717	0.282
6	0.309	0.691

Table 6.2: Asymptotically optimal power allocation (parameters as in Figure 6.4 and Figure 6.5). Details on how to determine this optimal power allocation can be found in Section 5.3.

behaviour. The feedback coding scheme has a doubly exponentially decreasing error probability, whereas the conventional coding scheme only decreases exponentially in blocklength. Thus, one has to take this into account when optimizing the power allocation. Unfortunately, joint optimization of power allocation and blocklength allocation seems intractable. Nevertheless, numerical results show that this consecutive optimization outperforms pure conventional or feedback coding in most regions.

6.3.4 Impact of Blocklength Allocation

In this section we start with (asymptotically) optimal power allocations (Table 6.2) and assume a symmetric channel, i.e., identical channel gains. A similar analysis for asymmetric channels is feasible but less intuitive.

It turns out that asymptotically optimal power allocation does not yield higher achievable sum rates for moderate blocklength and moderate quantization rates. In the example in Figure 6.4 with blocklength $n = 2^{10} = 1024$ only feedback quantization rates $R > 5$ result in better performance than coding without any feedback. Even in this case the optimal region allocates no blocklength to the conventional coding component. Note that $n = N\tilde{N}$. Thus, $N = 1$ if the optimum allocates the total blocklength to the feedback based coding component, i.e., $\tilde{N} = n$. For larger blocklength the situation drastically changes. In the example in Figure 6.5 with blocklength $n = 2^{17} = 131072$ superposition yields higher achievable sum rates for a wide region of blocklength allocation. Indeed superposition is optimal, except for very low quantization rates, and clearly outperforms pure conventional or feedback coding. We observe that the fraction of blocklength allocated to each component is primarily determined by the channel itself and only weakly depends on the actual power allocations, feedback rates or quantization rates. The next section also confirms this insight.

6.3.5 Impact of Blocklength

Again, we start with (asymptotically) optimal power allocations and assume a symmetric channel. We observe that even if the asymptotically optimal power allocation

splits the power to both constituent schemes, the blocklength might not be allocated in the same proportions. There are essentially three different scenarios.

Very low feedback quantization rates

The quantization rate is too low to become beneficial at all. Thus, pure conventional coding is optimal. In Figure 6.6 we can observe this behaviour e.g. for $R = 1$ (circle marker).

Low feedback quantization rates

In this case only for very small blocklengths pure feedback coding is optimal and then suddenly switches to pure conventional coding. Eventually for large blocklengths superposition is optimal. In Figure 6.6 we can observe this behaviour e.g. for $R = 2$ (square marker).

Medium to high feedback quantization rates

Here, at first pure feedback coding is optimal and then directly switches to superposition coding. In Figure 6.6 we can observe this behaviour e.g. for $R = 3$ (diamond marker).

Figure 6.6 (bottom) shows the optimal blocklength allocations. Note that in the region of superposition the growth rates of blocklength are identical and independent of the quantization rates and thus the curves highly overlap. As a consequence, $\tilde{N}/N$ is almost independent of the quantization rates in this region.

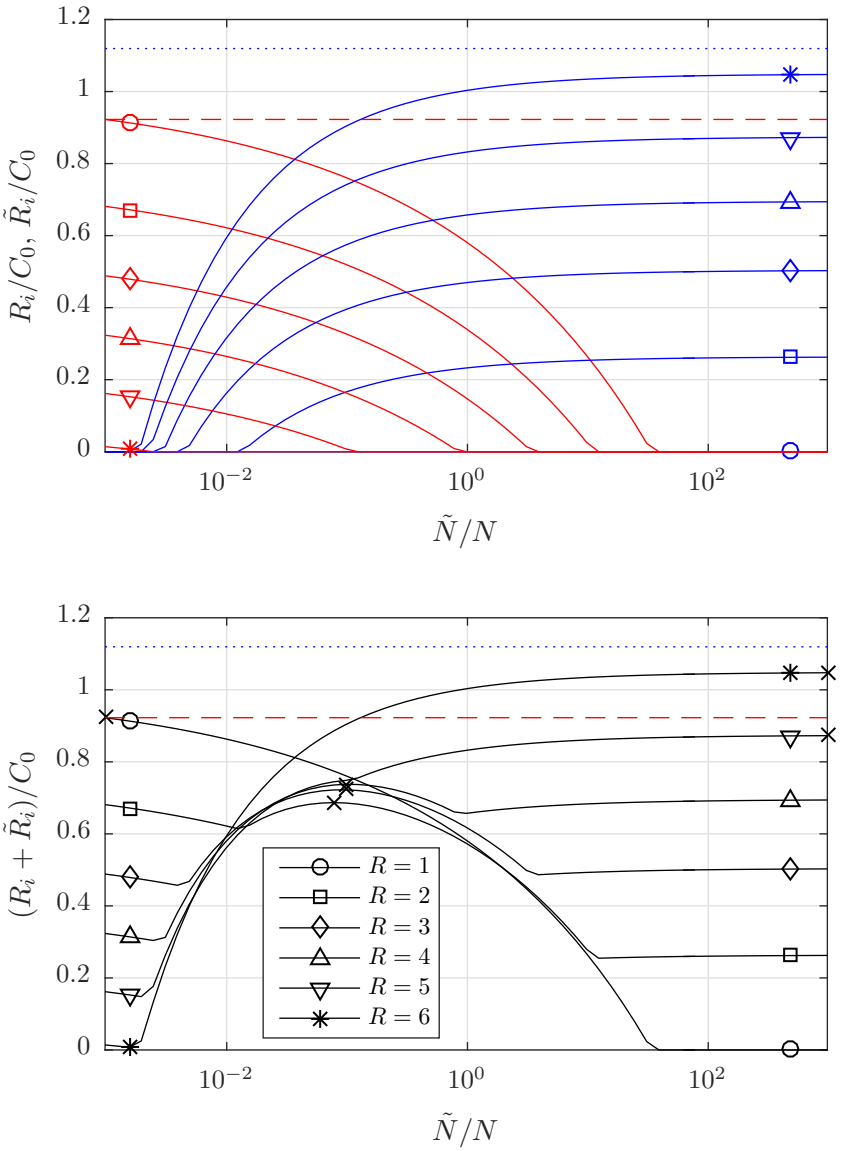

Figure 6.4: Achievable rates of conventional coding component (top, decreasing curves) and feedback coding component (top, increasing curves) and achievable sum rates (bottom, maxima marked with 'x') versus the blocklength allocation $\tilde{N}/N$ for $n = 2^{10}$. All plots pertain to the symmetric MAC with $P_T = 2$, $h_1 = h_2 = 1$, $\sigma^2 = 0.01$, $\epsilon \leq 10^{-6}$, and power allocation according to Table 6.2. The dashed and dotted line show the Polyanskiy limit C_ϵ and $\tilde{C}_0$, respectively.

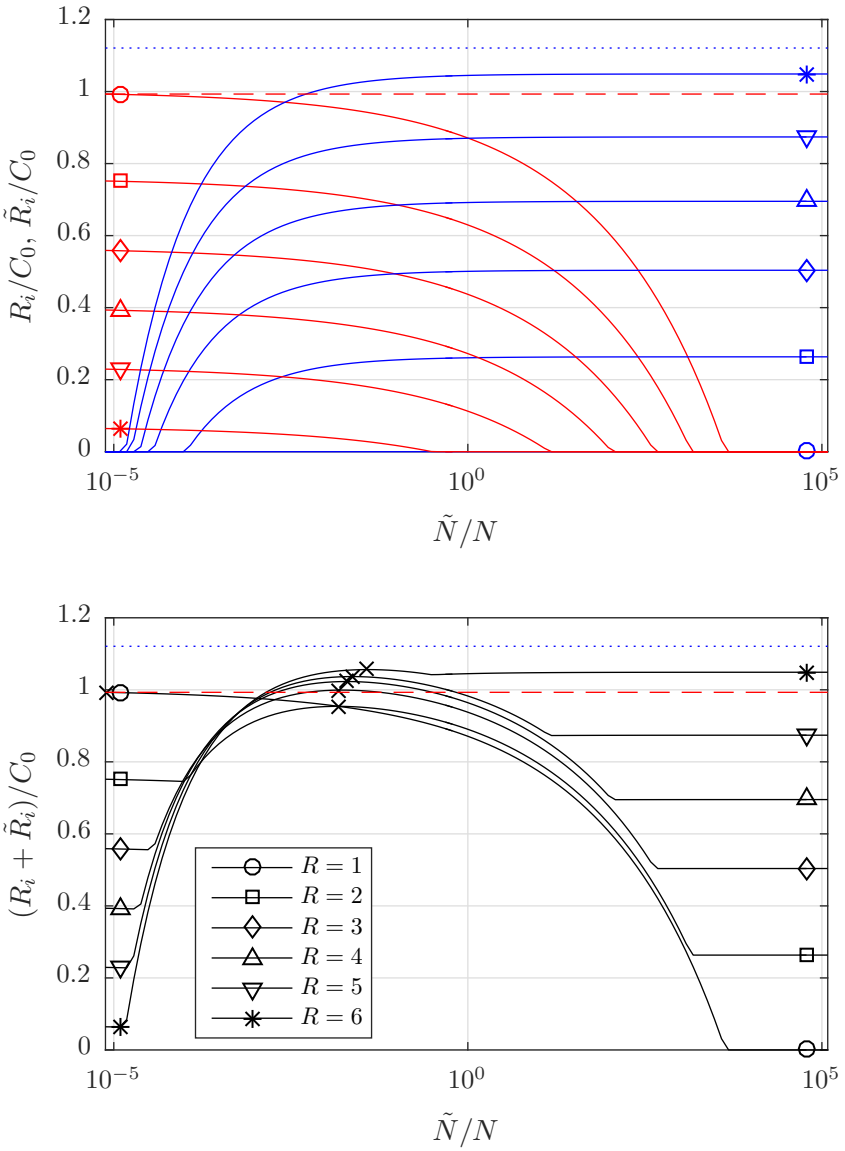

Figure 6.5: Achievable rates of conventional coding component (top, decreasing curves) and feedback coding component (top, increasing curves) and achievable sum rates (bottom, maxima marked with 'x') versus the blocklength allocation $\tilde{N}/N$ for $n = 2^{17}$. All plots pertain to the symmetric MAC with $P_T = 2$, $h_1 = h_2 = 1$, $\sigma^2 = 0.01$, $\epsilon \leq 10^{-6}$, and power allocation according to Table 6.2. The dashed and dotted line show the Polyanskiy limit C_ϵ and $\tilde{C}_0$, respectively.

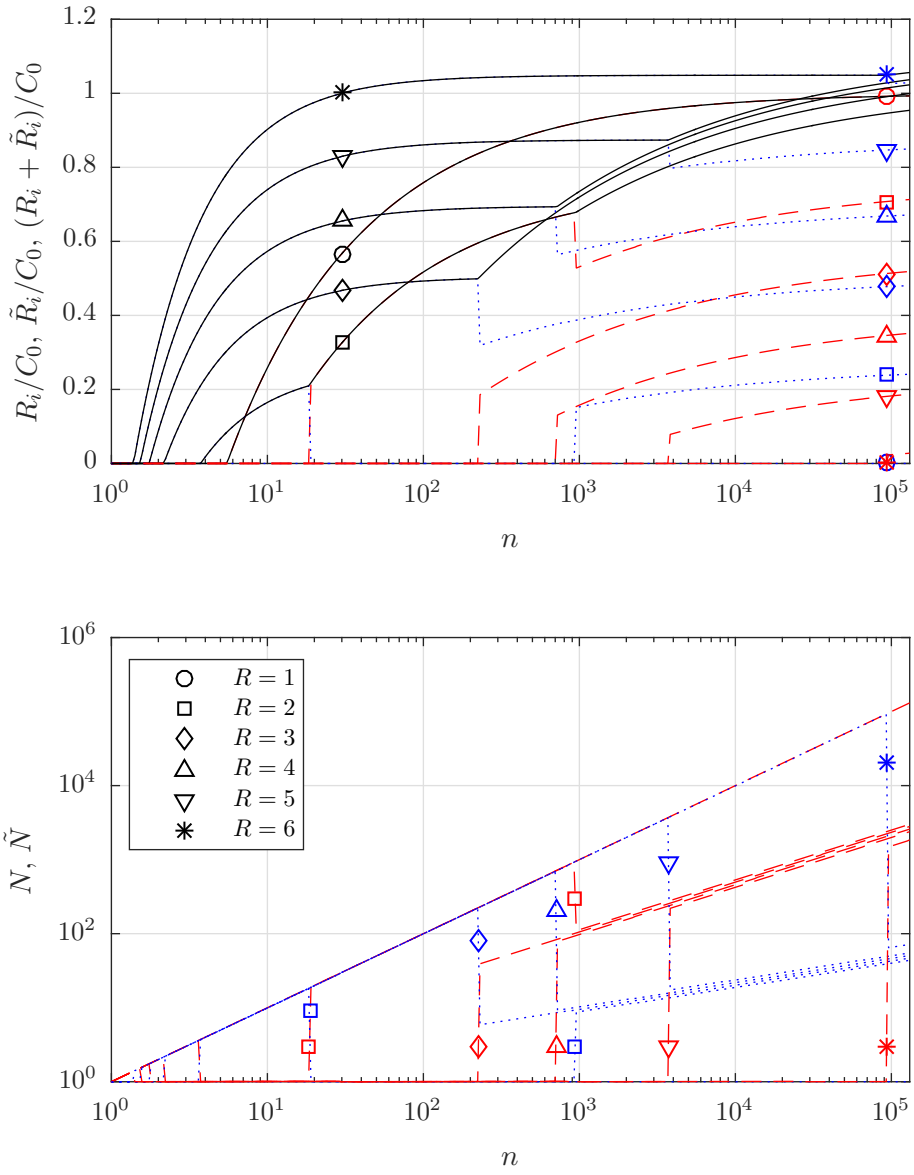

Figure 6.6: Achievable rates (top) of conventional coding component (top and bottom, dashed curves) and feedback coding component (top and bottom, dotted curves) and achievable sum rates (top, solid curves) with optimal blocklength allocation versus the blocklength n. Optimal blocklength allocations (bottom). All plots pertain to the symmetric MAC with $P_T = 2$, $h_1 = h_2 = 1$, $\sigma^2 = 0.01$, $\epsilon \leq 10^{-6}$, and power allocation according to Table 6.2.

6.4 Finite Blocklength Superposition Performance – Gaussian Broadcast Channel

6.4.1 Error Probabilities

Due to MAC-BC duality (see Section 2.6.1) the same tradeoff as with MAC (see Section 6.3.1) applies: By the monotonicity of $\tilde{P}_{e_i}(\tilde{N})$ and $P_{e_i}(N)$ and the relation $n = \tilde{N}N$, decreasing the error probability of one component (via larger blocklength) increases the error probability of the other component (due to shorter blocklength).

The block structure of the superposition coding couples the error probabilities; if the conventional codeword is decoded incorrectly, it cannot be cancelled successively from the superposition and therefore negatively affects the decoding of the feedback based codeword.

Error probability of feedback based coding component

The error probability expression of the feedback based coding was bounded by Ozarow [60] for the MAC with perfect feedback. Adapted to our BC superposition scheme with quantized feedback we have

$$\tilde{P}_{e_i}(\tilde{R}_i, \tilde{N}) \leq 2Q\left\{ \frac{\sigma_{s_i}^2}{2\sqrt{\alpha_{i,2}}(\sigma_{s_i}^2 + h_i^2 \tilde{P}_i(1-\rho^{*^2}))} \times \exp\left[\tilde{N}\left(\frac{1}{2}\log\left(\frac{\sigma_{s_i}^2 + h_i^2\tilde{P}_i(1-\rho^{*^2})}{\sigma_{s_i}^2}\right) - \tilde{R}_i\right)\right]\right\}, \tag{6.36}$$

$i = 1, 2$, with appropriately chosen $\alpha_{i,2}$; ρ^* is the optimal correlation that maximizes the achievable sum rate which is found by solving (2.31); $\sigma_{s_1}^2$ and $\sigma_{s_2}^2$ are the (interference) noise variances, which are given by

$$\sigma_{s_1}^2 = \sigma_1^2 + \sigma_{q_1}^2 + h_1^2 P_1 P_{e_{1,1}} + h_1^2 P_2 P_{e_{1,2}}, \tag{6.37}$$

$$\sigma_{s_2}^2 = \sigma_2^2 + \sigma_{q_2}^2 + h_2^2 P_1 \qquad + h_2^2 P_2 P_{e_{2,2}}, \tag{6.38}$$

in this superposition configuration. As always, w.l.o.g. we assume that $h_1^2/\sigma_1^2 \geq h_2^2/\sigma_2^2$. $P_{e_{i,j}}$ are the error probabilities of the conventional coding scheme and the $h_i^2 P_j P_{e_{i,j}}$ terms are due to the decoding errors of the conventional coding scheme that cause additional interference. In contrast to the analogous MAC scheme (see Section 6.3) we now have two receivers that cannot both fully decode the conventional component. The stronger receiver 1 tries to decode the conventional components designated for both receivers and hence suffers from the additional interference noises $h_1^2 P_1 P_{e_{1,1}}$ and $h_1^2 P_2 P_{e_{1,2}}$. The weaker receiver 2 does not even try to decode the conventional component for receiver 1, that is, its additional interference noises equal $h_2^2 P_2$ (equivalent to $P_{e_{2,1}} = 1$) and $h_2^2 P_2 P_{e_{2,2}}$. Due to the block coding structure this additional interference

is i.i.d. and can be modeled to be Gaussian if $\tilde{N}$ is not too small.

We choose $\alpha_{i,2}$ as in [60]

$$\alpha_{i,2} = \frac{\sigma_{s_i}^2 + \sigma_v^2}{h_i^2 \tilde{P}_i}, \tag{6.39}$$

where σ_v^2 is the variance of an initial common randomness v known to all users, chosen such that the correlation remains constant over time,

$$\rho_2 = \frac{\mathrm{E}\{\epsilon_{1,2,l}\epsilon_{2,2,l}\}}{\sqrt{\alpha_{1,2}\alpha_{2,2}}} = \frac{\sigma_v^2}{\sqrt{(\sigma_{s_1}^2 + \sigma_v^2)(\sigma_{s_2}^2 + \sigma_v^2)}} \triangleq \rho^*. \tag{6.40}$$

Here, $\alpha_{i,j}$ are the variances of the current message estimation errors $\epsilon_{i,j,l}$,

$$\epsilon_{i,j,l} = \tilde{\theta}_{i,l} - \hat{\tilde{\theta}}_{i,l}\left(\tilde{\boldsymbol{y}}_i^{((j-1)N+l)}\right). \tag{6.41}$$

Note that $\alpha_{i,j}$ is identical for all l because $\tilde{\theta}_{i,l}$, $l = 1, \ldots, N$ are i.i.d.. The initial estimation errors simply are

$$\epsilon_{1,2,l} = \tilde{\theta}_{1,l} - \hat{\tilde{\theta}}_{1,l}(\tilde{\boldsymbol{y}}_1^{(N+l)}) = \tilde{\theta}_{1,l} - \frac{\tilde{y}_1[l]}{\sqrt{h_1^2 \tilde{P}_1}}, \tag{6.42}$$

$$\epsilon_{2,2,l} = \tilde{\theta}_{2,l} - \hat{\tilde{\theta}}_{2,l}(\tilde{\boldsymbol{y}}_2^{(N+l)}) = \tilde{\theta}_{2,l} - \frac{\tilde{y}_2[N+l]}{\sqrt{h_2^2 \tilde{P}_2}}, \tag{6.43}$$

since the first two timeslots (of the feedback scheme) are exclusively used to transmit the messages from both transmitters alternately,

$$\tilde{y}_1[l] = \sqrt{h_1^2 \tilde{P}_1}\tilde{\theta}_{1,l} + z_{s_1}[l] + v, \tag{6.44}$$

$$\tilde{y}_2[N+l] = \sqrt{h_2^2 \tilde{P}_2}\tilde{\theta}_{2,l} + z_{s_2}[N+l] + v. \tag{6.45}$$

Using these relations we directly get the second equality in (6.40) and then solving (6.40) for σ_v^2 yields

$$\sigma_v^2 = \sqrt{-\frac{\rho^{*2}}{\rho^{*2}-1}\frac{\sigma_{s_1}^2 + \sigma_{s_2}^2}{2} + \sqrt{\frac{\rho^{*4}}{(\rho^{*2}-1)^2}\frac{(\sigma_{s_1}^2 + \sigma_{s_2}^2)^2}{4} - \frac{\rho^{*2}}{\rho^{*2}-1}\sigma_{s_1}^2\sigma_{s_2}^2}}. \tag{6.46}$$

This rather complicated expression drastically simplifies for the symmetric case $h_1^2/\sigma_1^2 = h_2^2/\sigma_2^2$ in the low error probability region, where the approximations $\sigma_{s_1}^2 \approx \sigma_1^2 + \sigma_{q_1}^2$ and $\sigma_{s_2}^2 \approx \sigma_2^2 + \sigma_{q_2}^2$ hold, to the same expression as for the MAC (6.26),

$$\sigma_v^2 = \sigma_s^2 \frac{\rho^*}{1-\rho^*}. \tag{6.47}$$

Then (6.39) simplifies to

$$\alpha_{i,2} = \frac{\sigma_s^2}{h_i^2 \tilde{P}_i (1-\rho^*)}. \tag{6.48}$$

Error probability of conventional coding component

The error probability expression of the conventional coding scheme can be obtained by adapting the results for the AWGN channel in the finite blocklength regime obtained by Polyanskiy in [66, Theorem 54] (see Section 2.5.2). In our superposition scenario we have

$$P_{e_i}(R_i, N) \leq 2Q\left\{\frac{1}{\sqrt{V_i}}\left[\sqrt{N}(C_i - R_i) + \frac{1}{\sqrt{N}}\frac{1}{2}\log N\right]\right\}, \tag{6.49}$$

$i = 1, 2$, with modified channel dispersions

$$V_1 = \frac{h_1^2 P_1}{2}\frac{h_1^2 P_1 + 2(\sigma_1^2 + h_1^2\tilde{P}_1 + h_1^2\tilde{P}_2)}{(h_1^2 P_1 + \sigma_1^2 + h_1^2\tilde{P}_1 + h_1^2\tilde{P}_2)^2}\log^2 e, \tag{6.50}$$

$$V_2 = \frac{h_2^2 P_2}{2}\frac{h_2^2 P_2 + 2(\sigma_2^2 + h_2^2\tilde{P}_1 + h_2^2\tilde{P}_2 + h_2^2 P_1)}{(h_2^2 P_2 + \sigma_2^2 + h_2^2\tilde{P}_1 + h_2^2\tilde{P}_2 + h_2^2 P_1)^2}\log^2 e. \tag{6.51}$$

Note that here the conventional coding scheme is affected by the interference of the feedback based coding and results in reduced capacities $C_1 = C\left(h_1^2 P_1/(\sigma_1^2 + h_1^2\tilde{P}_1 + h_1^2\tilde{P}_2)\right)$ and $C_2 = C\left(h_2^2 P_2/(\sigma_2^2 + h_2^2\tilde{P}_1 + h_2^2\tilde{P}_2 + h_2^2 P_1)\right)$. This approximation holds for sufficiently low error probability P_{e_2}, where we can neglect the potential error propagation due to successive decoding at the stronger receiver 1.

Error probability approximations

For the remainder of Section 6.4 we work with the approximations $\sigma_{s_1}^2 \approx \sigma_1^2 + \sigma_{q_1}^2$ and $\sigma_{s_2}^2 \approx \sigma_2^2 + \sigma_{q_2}^2$, i.e., $P_{e_i} \ll (\sigma_i^2 + \sigma_{q_i}^2)/h_i^2 P_i$. In the regime of interest this approximation is sufficiently accurate. This simplifies the numerical evaluation since it allows us to independently analyze the practically decoupled error probability expressions.

6.4.2 Achievable Rates versus Blocklength and Error Probability

Like in the previous sections, instead of investigating the error probability as a function of the blocklength we are now interested in the achievable rates versus blocklength and error probability. This is a more practical approach, since usually applications require a specific rate and maximal error probability.

R [bit]	P_i	$\tilde{P}_i$
1	1	0
2	1	0
3	1	0
4	1	0
5	0.717	0.282
6	0.309	0.691

Table 6.3: Asymptotically optimal power allocation (parameters as in Figure 6.7 and Figure 6.8). Details on how to determine this optimal power allocation can be found in Section 5.5.

The achievable rate of the feedback based code is found by solving (6.36) for $\tilde{R}_i$,

$$\tilde{R}_i(\tilde{P}_{e_i}, \tilde{N}) \leq \frac{1}{2}\log\left(\frac{\sigma_{s_i}^2 + h_i^2\tilde{P}_i(1-\rho^{*^2})}{\sigma_{s_i}^2}\right) - \frac{1}{\tilde{N}}\log\left[Q^{-1}\left\{\frac{\tilde{P}_{e_i}}{2}\right\}\frac{2\sqrt{\alpha_{i,2}}(\sigma_{s_i}^2 + h_i^2\tilde{P}_i(1-\rho^{*^2}))}{\sigma_{s_i}^2}\right], \tag{6.52}$$

$i = 1, 2$, and the achievable rate of the conventional code is found by solving (6.49) for R_i, $i = 1, 2$,

$$R_i(P_{e_i}, N) \leq C_i - \frac{1}{\sqrt{N}}\sqrt{V_i}Q^{-1}\left\{\frac{P_{e_i}}{2}\right\} + \frac{1}{2}\log\sqrt[N]{N}. \tag{6.53}$$

6.4.3 Optimization Problem

Like for the MAC, optimization in the context of finite blocklength means finding the optimum subblock splitting $(N, \tilde{N})$ that maximizes the achievable rates under the constraint $n = \tilde{N}N$ for prescribed blocklength n and error probability.

Again, we want to find the blocklength allocation that maximizes the achievable sum rate

$$R_s = \sum_{i=1}^{2}\left(R_i(P_{e_i}, N) + \tilde{R}_i(\tilde{P}_{e_i}, \tilde{N})\right), \tag{6.54}$$

while keeping the error probabilities below ϵ. This yields the structural identical

(cf. (6.35)) optimization problem

$$\begin{aligned} \underset{N,\tilde{N},\boldsymbol{p}}{\text{maximize}} \quad & \sum_{i=1}^{2} \Big(R_i(P_{e_i}, N) + \tilde{R}_i(\tilde{P}_{e_i}, \tilde{N}) \Big) \\ \text{subject to} \quad & P_{e_i} \leq \epsilon, \qquad i = 1, 2 \\ & \tilde{P}_{e_i} \leq \epsilon, \qquad i = 1, 2 \\ & \tilde{N} N = n, \\ & \mathbf{1}^{\mathsf{T}} \boldsymbol{p} \leq P_T, \end{aligned} \tag{6.55}$$

with $\tilde{R}_i(\tilde{P}_{e_i}, \tilde{N})$ and $R_i(P_{e_i}, N)$ are now given by (6.52) and (6.53), respectively.

Like for the MAC, we tackle the optimization by initially finding the optimal transmit power allocation and then optimizing the blocklength allocation. The optimal power allocation is found by maximizing the achievable sum rate, i.e. finding the capacity of our linear superposition coding scheme (see Section 5.5). We then use this (asymptotically) optimal power allocation (see Table 6.3) to find the optimal blocklength allocation. Generally, this approach might not be equivalent to the global optimization (see Section 6.3.3). Nevertheless, as for the MAC numerical results again show that this consecutive optimization outperforms pure conventional or feedback coding in many regions. However, following sections show the negative impact of the symmetrization (see Section 5.6.3) that is needed for our BC optimization strategy.

6.4.4 Impact of Blocklength Allocation

In this section we start with (asymptotically) optimal power allocations (Table 6.3) and assume a symmetric channel, i.e., identical channel gains. A similar analysis for asymmetric channels is feasible but less intuitive.

It turns out that asymptotically optimal power allocation does not yield higher achievable sum rates for moderate blocklength and moderate quantization rates. In the example in Figure 6.7 with blocklength $n = 2^{10} = 1024$ only feedback quantization rates $R > 5$ result in better performance than coding without any feedback. Even in this case the optimal region allocates no blocklength to the conventional coding component ($N = 1$ and hence $\tilde{N} = n$). For larger blocklength the situation changes. In the example in Figure 6.8 with blocklength $n = 2^{17} = 131072$ superposition is optimal and yields higher achievable sum rates for $R \geq 5$ where it clearly outperforms pure conventional or feedback coding. However for quantization rates $R < 5$ it is optimal to only use the conventional coding component. We observe that the fraction of blocklength allocated to each component is primarily determined by the channel itself and only weakly depends on the actual power allocations, feedback rates or quantization rates. The next section also confirms this insight.

6.4.5 Impact of Blocklength

Again, we start with (asymptotically) optimal power allocations and assume a symmetric channel. We observe that even if the asymptotically optimal power allocation splits the power to both constituent schemes, the blocklength might not be allocated in the same proportions. There are essentially two different scenarios.

Low to medium feedback quantization rates

The quantization rate is too low to become beneficial at all. Thus, pure conventional coding is optimal. In Figure 6.9 we can observe this behaviour, e.g., for $R = 1, \ldots, 4$ (overlying markers).

High feedback quantization rates

Here, for small n pure feedback coding is optimal and then switches to superposition coding. In Figure 6.9 we can observe this behaviour, e.g., for $R = 5$ (downward-pointing triangle marker) and $R = 6$ (diamond marker).

Figure 6.9 (bottom) shows the optimal blocklength allocations. Note that in the region of superposition the growth rates of blocklength are identical and independent of the quantization rates and thus the curves highly overlap. As a consequence, $\tilde{N}/N$ is almost independent of the quantization rates in this region.

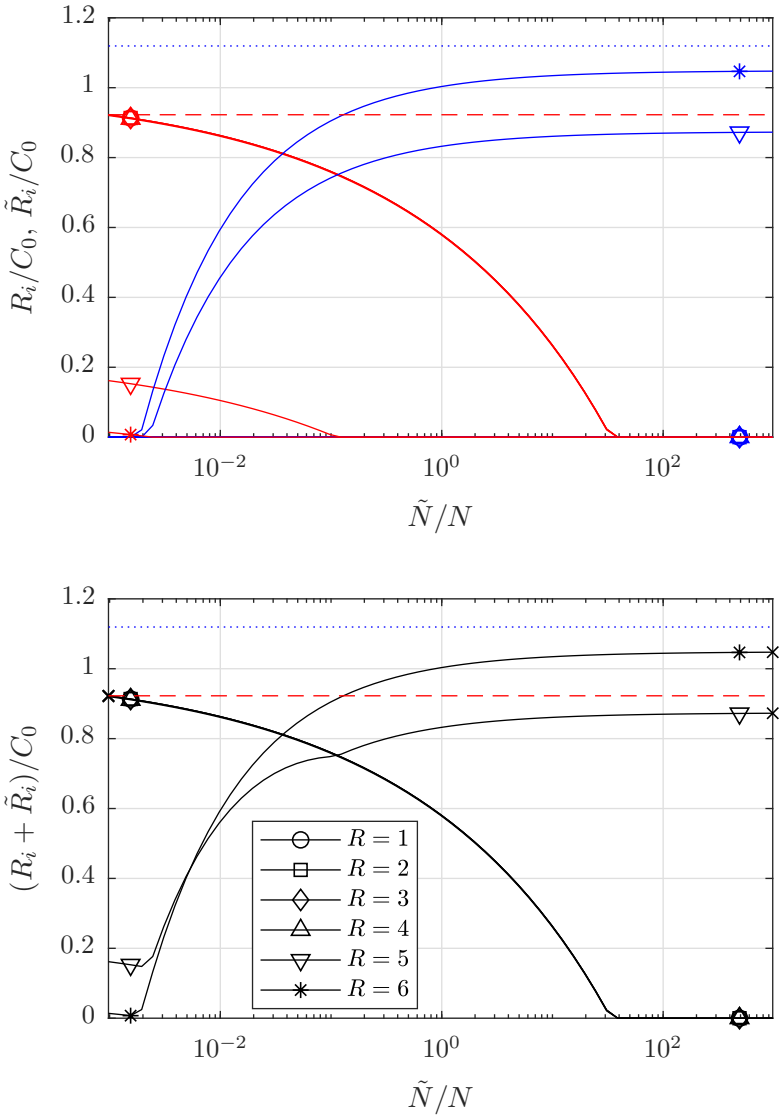

Figure 6.7: Achievable rates of conventional coding component (top, decreasing curves) and feedback coding component (top, increasing curves) and achievable sum rates (bottom, maxima marked with 'x') versus the blocklength allocation $\tilde{N}/N$ for $n = 2^{10}$. All plots pertain to the symmetric BC with $P_T = 2$, $h_1 = h_2 = 1$, $\sigma_1^2 = \sigma_2^2 = 0.01$, $\epsilon \leq 10^{-6}$, and power allocation according to Table 6.3. The dashed and dotted line show the Polyanskiy limit C_ϵ and $\tilde{C}_0$, respectively.

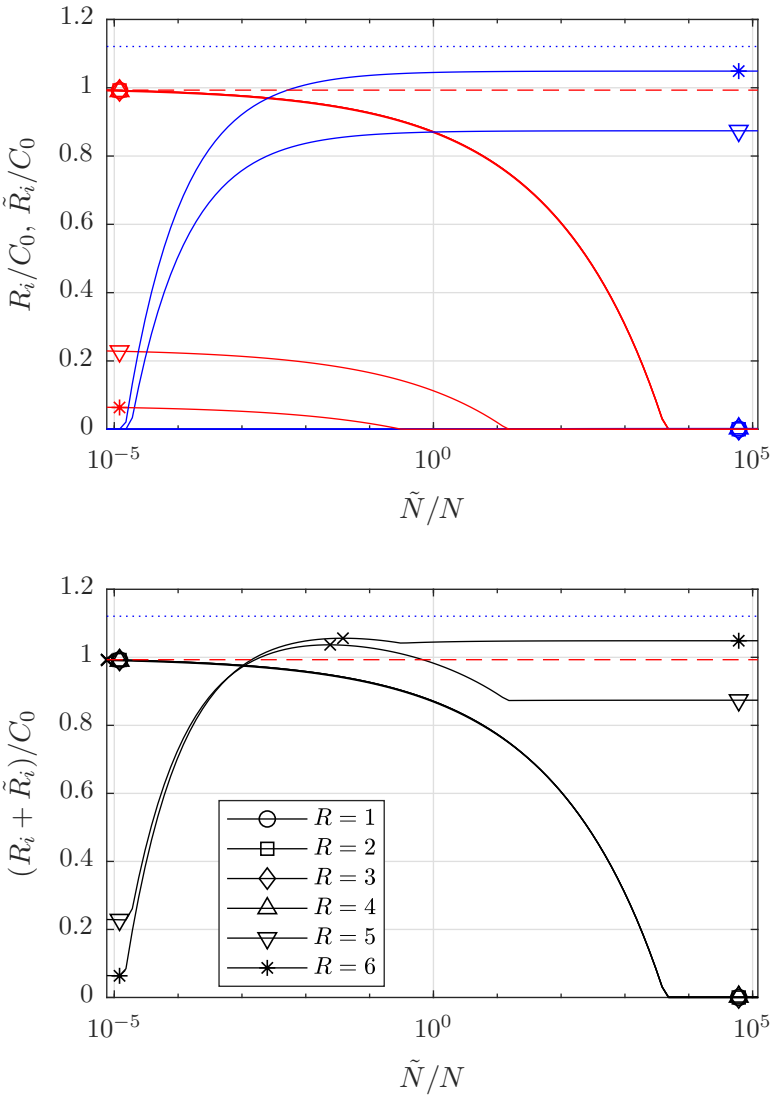

Figure 6.8: Achievable rates of conventional coding component (top, decreasing curves) and feedback coding component (top, increasing curves) and achievable sum rates (bottom, maxima marked with 'x') versus the blocklength allocation $\tilde{N}/N$ for $n = 2^{17}$. All plots pertain to the symmetric BC with $P_T = 2$, $h_1 = h_2 = 1$, $\sigma_1^2 = \sigma_2^2 = 0.01$, $\epsilon \leq 10^{-6}$, and power allocation according to Table 6.3. The dashed and dotted line show the Polyanskiy limit C_ϵ and $\tilde{C}_0$, respectively.

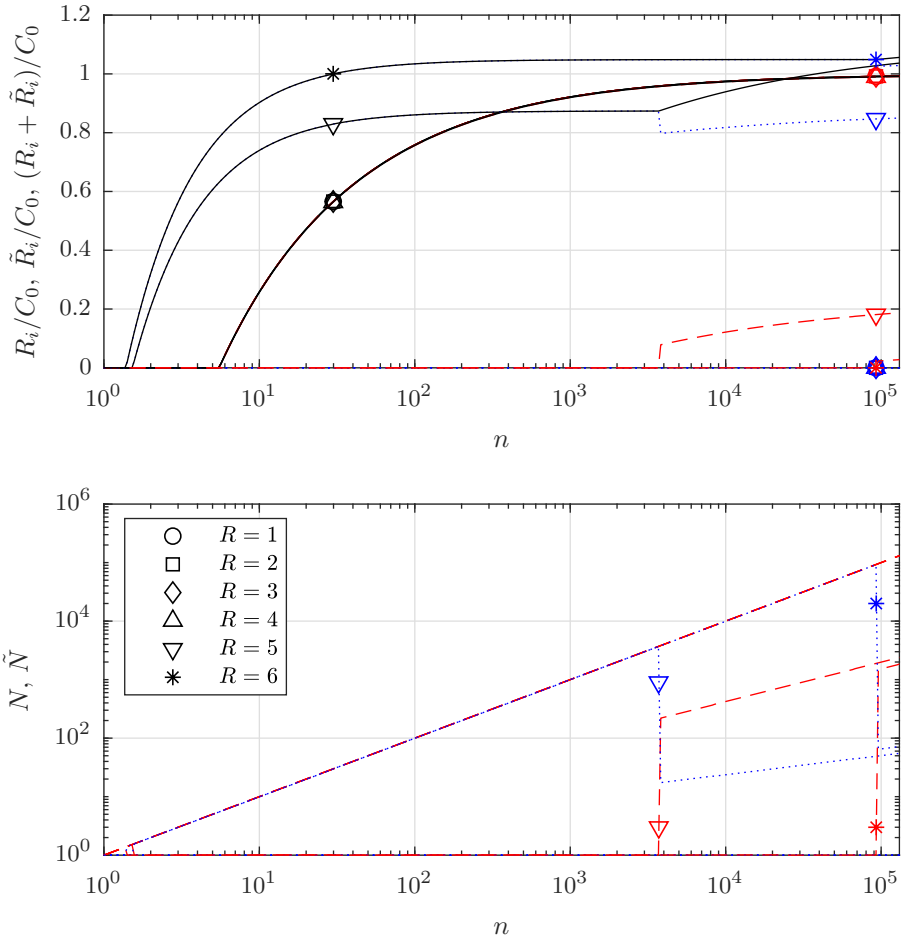

Figure 6.9: Achievable rates (top) of conventional coding component (top and bottom, dashed curves) and feedback coding component (top and bottom, dotted curves) and achievable sum rates (top, solid curves) with optimal blocklength allocation versus the blocklength n. Optimal blocklength allocations (bottom). All plots pertain to the symmetric BC with $P_T = 2$, $h_1 = h_2 = 1$, $\sigma_1^2 = \sigma_2^2 = 0.01$, $\epsilon \leq 10^{-6}$, and power allocation according to Table 6.3.

6.5 Discussion

Shifting the focus from the asymptotic regime to finite blocklength introduced several practical problems. The striking problem is that the superimposed components cannot be decoded perfectly anymore. Instead decoding errors may occur, which then interfere with the decoding of the other components. Due to the superposition arrangement in the AWGN channel scenario in Section 6.2 decoding errors of the conventional coding component negatively affect the decoding of the feedback coding component. This is caused by the successive cancellation decoding procedure. In addition to the coupling between the two components, in the MAC scenario in Section 6.3 and in the BC scenario in Section 6.4 the error probabilities of the conventional codings of the two transmitters or receivers, respectively, are coupled them self. In the MAC scenario the single receiver has to decode the conventionally encoded messages from both transmitters in an onion peeling approach; if the decoding of the first message fails, its effect cannot be cancelled and thus negatively affects the decoding of the other message. In the BC scenario there is a similar behaviour. Although the weaker receiver treats the component for the stronger receiver as noise, the stronger receiver has to decode both messages just like the single receiver in the MAC scenario has to.

However, in many practical scenarios the error probabilities are sufficiently small so that their additional interference is masked by the channel noise. In this case, we can neglect the coupling of the error probabilities and analyze them separately. It is clear that there is a tradeoff in the error probabilities of the conventional encoded component and the feedback based component that can be controlled by the blocklength allocation and power allocation. Therefore, in addition to the optimization of the power allocation in the asymptotic regime, here we have the blocklength allocation as an additional optimization parameter. Since the optimal power allocation is itself a DC problem, the additional combinatorial blocklength optimization renders the resulting problem hard to solve.

For perfect feedback the solution would be trivial. Not only does the error probability of the feedback component decrease faster (doubly exponential versus exponentially), for the MAC and BC we even have a higher channel capacity. It would thus be optimal to allocate all available transmit power to the feedback component and as a consequence evidently all blocklength is allocated to it as well. If the feedback is quantized the achievable rate of the feedback component is decreased. It thus might be optimal to allocate only a fraction of the transmit power to the feedback coding. As a consequence, the non-trivial optimal blocklength allocation has to be found as well. Due to the rate limitation on the common feedback link this superposition was useful in the asymptotic regime and we showed that this holds for finite blocklengths as well.

Thus, using the asymptotically optimal power allocations on the Gaussian MAC and BC in the asymptotic regime from Chapter 5 we showed that the optimization of

blocklength allocation generally still yields larger achievable sum rates than any of the two constituent schemes alone. Finally, we numerically assessed the impact of the size of the blocklength on the optimality of the superposition.

7

Conclusion and Outlook

This thesis studies point-to-point and multi-terminal communication with a quantized feedback link that provides the transmitters with additional side-information. We abstractly model the quantizer via the information bottleneck method.

Since we study communication over Gaussian channels, we specialized the channel output compression to form a Gaussian information bottleneck. We explicitly formulated the information-rate function for Gaussian MIMO channels, which is a key quantity for characterizing the quantization as a function of the quantization rate. Using the findings for the Gaussian MIMO channel we specialized the results for the later studied MAC. Subsequently, we found an equivalent Gaussian channel that incorporates the Gaussian quantization noise, that is, we have an additional noise term where the variance depends on the quantization rate. This quantity was later used to explicitly parametrize the performance of the proposed coding schemes on the quantization rate.

We then extended the formulation of the information-rate function to the information-rate-power function. For the information-rate function the power allocation is a fixed precondition. However, in this thesis the goal was not to compress a given signal (and thus fixed source) as efficiently as possible but to compress a signal with given available transmit power as efficiently as possible. Thus, we formulated the optimization problem that incorporates the additional degree of freedom which finds the maximal mutual information subject to constraints on the quantization rate and available transmit power. We showed that this problem is a DC program and efficiently solved it using the convex-concave procedure.

Based on the necessity of Gaussian input distributions if the quantizer is modelled as a Gaussian information bottleneck we described an discrete source model that asymptotically converges to a Gaussian distribution.

We then explicitly formulated the AWGN channel, MAC, and BC algebraic transceiver schemes and performed the transition to our proposed superposition coding scheme. We introduced a superposition coding scheme that superimposes a conventional coding component that completely ignores the feedback with a feedback coding component in a block structure. This block structure was then used to be able to first decode the conventional coding component while treating the feedback component as noise and then subtract its effect. The feedback coding component could thus be decoded using the remaining non-interfered signal.

The GIB-modelled quantization noise was assumed to be known to the receiver, which itself performed the quantization. With this observation we could reduce the feedback scheme to equivalent channels with perfect feedback but additional channel noise due to the quantization. The knowledge of this extra noise can then be exploited at the receiver.

We performed an extensive study on the performance of the proposed superposition coding for various scenarios: for the AWGN channel, for the symmetric Gaussian MAC, for the asymmetric Gaussian MAC, for the symmetric Gaussian BC, and for the asymmetric Gaussian BC. To this end we formulated the achievable (sum) rate expressions as optimization problems. We showed how to split these optimization problems into concave and convex components.

Then, we used these splittings to shape solvable DC programs and adapted the convex-concave procedure to efficiently solve the optimization problems. The solution includes finding the optimal power allocations to the conventional and feedback coding components.

We confirmed that for the AWGN channel superposition is suboptimal, since in this scenario the channel capacity is unchanged even for perfect feedback. For the MAC and BC, feedback is known to increase the channel capacity and so do the proposed superposition schemes. To this end, we studied the parameter regions where true superposition is optimal. We found that there is a non-trivial region: for fixed quantization rates and increasing transmit powers it is optimum to allocate all transmit power to the feedback-coding scheme and above a non-trivial power threshold superposition is optimal.

However, we found that the superposition gain decreases for increasing asymmetry of the channels. MAC and BC qualitatively show the same behaviour, but due to the performed symmetrization we found that the gains for the BC are generally smaller than for the MAC.

Based on recent findings concerning performance in the finite-blocklength regime, we extended our proposed superposition coding scheme for finite blocklengths. We derived expressions for the error probabilities of the feedback based coding components

and conventional coding components for the AWGN channel, MAC, and BC. We showed that in contrast to the asymptotic regime, the error probabilities are coupled in the finite-blocklength regime; changing the error probability of one component affects the error probability of the other component. We proposed approximations that practically decouple the error probabilities.

We showed that maximizing the achievable sum rates result in partly combinatorial optimization problems since we have to find the discrete optimal blocklength allocations jointly with the optimal power allocations. We approximately solved this hard problem via asymptotically optimal power allocations and then used these power allocations as a basis of the purely combinatorial optimization problem of finding the optimal blocklength allocation.

Finally, we numerically assessed the performance as functions of the blocklength allocation and as functions of the absolute blocklength. We found that even this approximate optimization procedures yield performance gains over pure conventional or pure feedback coding in many parameter regions.

7.1 Outlook

We next summarize the open problems and give an outlook for possible future research.

- In Chapter 3 we studied the Gaussian Information Bottleneck (GIB) for Gaussian MIMO channels. Although it is clear that the GIB finds the optimal rate-information tradeoff for a Gaussian channel and the classical water filling power allocation maximizes the capacity of a Gaussian vector channel and that the joint optimization finds the optimal rate-power-information tradeoff, this procedure is still not equivalent to finding the channel capacity of the Gaussian channel under channel output quantization.

  For finding the capacity one has to optimize over all input distributions as well; we, however, have fixed the input distribution to be jointly Gaussian, since this distribution maximizes the capacity of the unquantized channel and allows an analysis using the GIB.

  Determining the channel capacity under general output compression is thus still an open problem.

- In Chapter 4 we proposed a superposition coding scheme that superimposes a conventional encoding component that completely ignores the feedback and a feedback based encoding component in a block structure. Throughout this thesis we assume that the conventional component is decoded first (with the feedback component as additional interference noise) and then cancelled; in a second step the feedback component can be decoded without interference.

Other schemes [46, 47, 60, 83] use a similar successive decoding (but without the block structure) with interchanged decoding order in a different setting. We justified our choice of decoding order by the fact that the channel capacity is generally increased if (quantized) feedback is available compared to the non-feedback scenario. Hence, allowing the feedback component to transmit without interference results in higher achievable rates.

However, it still remains open to show in what regions of available transmit power, quantization rate, and blocklength this coding scheme and decoding order is in fact better.

- In contrast to the asymmetric MAC in Section 5.4, where the single receiver has to be able to decode the complete superposition signal, in the BC scenario in Section 5.6 the weaker receiver is only able to decode its designated conventional coding component. The stronger receiver is still able to decode both components. This asymmetry rendered the resulting problem hard to solve. Hence, we proposed a generally suboptimal procedure to partly symmetrize the problem to be able to solve it as a DC program. However, in principle the original fully asymmetric problem could be split into a concave and convex component as well.

  It remains open to find such a splitting and solve the original problem.

- In Chapter 6 we studied the performance of the proposed scheme in the finite blocklength region. Here the superposition of the different encodings causes a coupling of the error probabilities; if one component is decoded incorrectly it cannot be cancelled and thus interferes with the remaining components. This coupling renders the joint power and blocklength allocation problem hard to solve. Therefore, we studied only the practically interesting region where the interference due to decoding errors is small compared to the channel noise, which effectively decouples the error probabilities.

  Although practically not that important it might be interesting to solve the optimization problem for coupled error probabilities.

- In Chapter 6 the joint power and blocklength allocation problem is a partly combinatorial optimization problem since we have to find the discrete optimal blocklength allocation jointly with the optimal power allocation. In contrast to the asymptotic regime in Chapter 5 where the power allocation problem could be solved as a DC program this joint optimization problem is hard to solve. Instead we followed an iterative approach where we first (asymptotically) optimized the power allocation and then used this power allocation as a basis for the now pure combinatorial optimization problem.

  However, especially for small blocklength this approach is suboptimal and it would be interesting to directly solve the joint optimization problem.

- Throughout this thesis the basis for our feedback coding scheme was the Schalkwjik-Kailath scheme [69] for the AWGN channel and the Ozarow scheme [60] for the MAC and the BC. Although both schemes achieve the channel capacity (for the BC the linear-feedback capacity) they are in general not optimal for the finite blocklength regime considered in Chapter 6.

  One could explicitly construct algebraic coding structures that perform better for the designed blocklength in our superposition scenario.

Bibliography

[1] M. Agarwal, D. Guo, and M. Honig. Error Exponent for Gaussian Channels With Partial Sequential Feedback. *IEEE Trans. Inf. Theory*, 59(8):4757–4766, Aug. 2013.

[2] R. Ahlswede. Multi-way communication Channels. In *Proc. IEEE Int. Symp. on Inf. Theory (ISIT 1973)*, pages 23–51, 1973.

[3] S. B. Amor. A New Coding Scheme for Discrete Memoryless MACs with Common Rate-Limited Feedback. In *Proc. European Conf. on Networks and Commun. (EuCNC 2015)*, pages 72–76, June 2015.

[4] S. B. Amor, Y. Steinberg, and M. Wigger. Duality with linear-feedback schemes for the scalar Gaussian MAC and BC. In *Proc. International Zurich Seminar on Communications (IZS 2014)*, pages 25–28, Zurich, Switzerland, 2014.

[5] S. B. Amor, Y. Steinberg, and M. Wigger. MIMO MAC-BC Duality With Linear-Feedback Coding Schemes. *IEEE Trans. Inf. Theory*, 61(11):5976–5998, Nov. 2015.

[6] T. Berger. *Rate Distortion Theory*. Prentice Hall, Englewood Cliffs (NJ), 1971.

[7] S. Boyd and L. Vandenberghe. *Convex Optimization*. Cambridge University Press, 2006.

[8] S. Butman. A general formulation of linear feedback communication systems with solutions. *IEEE Trans. Inf. Theory*, 15(3):392–400, May 1969.

[9] C. Byrne. Block-iterative interior point optimization methods for image reconstruction from limited data. *Inverse Problems*, 16(5):1405, 2000.

[10] A. Carleial. Multiple-access channels with different generalized feedback signals. *IEEE Trans. Inf. Theory*, 28(6):841–850, 1982.

[11] Z. Chance. *Harnessing the Benefits of Noisy Feedback*. PhD thesis, Purdue University, West Lafayette, Indiana, Aug. 2012.

[12] Z. Chance and D. Love. On Linear Processing for an AWGN Channel with Noisy Feedback. *CoRR*, abs/0909.0105, 2009.

[13] Z. Chance and D. Love. On quantization of channel output feedback for the Gaussian channel. In *International Waveform Diversity and Design Conference (WDD 2010)*, pages 76–80, 2010.

[14] Z. Chance and D. J. Love. On linear processing in AWGN channels with feedback. In *Proc. Asilomar Conference on Signals, Systems and Computers 2009*, pages 986–990, Monterey, CA, Nov. 2009.

[15] Z. Chance and D. J. Love. Concatenated Coding for the AWGN Channel With Noisy Feedback. *IEEE Trans. Inf. Theory*, 57(10):6633–6649, Oct. 2011.

[16] G. Chechik, A. Globerson, N. Tishby, and Y. Weiss. Information Bottleneck for Gaussian Variables. *Journal of Machine Learning Research*, 6:165–188, 2005.

[17] G. Chechik, A. Globerson, N. Tishby, and Y. Weiss. Information Bottleneck for Gaussian Variables. *Journal of Machine Learning Research*, 6:165–188, Jan. 2005.

[18] T. Cover and J. Thomas. *Elements of Information Theory*. Wiley-Interscience, New York, NY, USA, 1991.

[19] T. M. Cover. Broadcast Channels. *IEEE Trans. Inf. Theory*, 18(1):2–14, Jan. 1972.

[20] T. M. Cover and J. A. Thomas. *Elements of Information Theory*. Wiley, 2006.

[21] Q. Cui, H. Wang, P. Hu, X. Tao, P. Zhang, J. Hamalainen, and L. Xia. Evolution of limited-feedback CoMP systems from 4G to 5G: CoMP features and limited-feedback approaches. *IEEE Veh. Technol. Mag.*, 9(3):94–103, 2014.

[22] A. D'yachkov. Upper bounds on the error probability for discrete memoryless channels with feedback. *Problemy Peredachi Informatsii*, 11(4):13–28, 1975.

[23] P. Elias. Channel capacity without coding,. *MIT Research Laboratory of Electronics, Quarterly Progress Report*, pages 90–93, 1956.

[24] S. Farthofer. Performance limits of Gaussian channels with quantized feedback. Master's thesis, TU Wien, 2014.

[25] S. Farthofer and G. Matz. Linear Superposition Coding for the Gaussian MAC with Quantized Feedback. In *Proc. 53rd Annu. Allerton Conf. Commun., Control, Comput.*, pages 1374–1379, Monticello, IL, Sept. 2015.

[26] S. Farthofer and G. Matz. Linear Superposition Coding for the Asymmetric Gaussian MAC with Quantized Feedback. In *Proc. Asilomar Conference on Signals, Systems and Computers 2016*, pages 245–249, Monterey, CA, Nov. 2016.

[27] S. Farthofer and G. Matz. Linear Superposition Coding for the Gaussian Broadcast Channel with Quantized Feedback. In *Proc. IEICE Int. Symp. on Inf. Theory and Its Applications (ISITA 2016)*, pages 106–110, Monterey, CA, Oct. 2016.

[28] S. Farthofer and G. Matz. Finite-Blocklength Linear Superposition Coding for the Gaussian MAC with Quantized Feedback. In *Proc. 11th Int. Conf. on Sig. Proc. and Commun. Sys. (ICSPCS 2017)*, Goldcoast, Australia, Dec. 2017.

[29] S. Farthofer, A. Winkelbauer, and G. Matz. Achieving Positive Rates over AWGN Channels with Quantized Feedback and Linear Processing. In *Proc. IEEE Inf. Theory Workshop (ITW 2014)*, pages 586–590, Hobart, Australia, Nov. 2014.

[30] R. Fischer. *Precoding and Signal Shaping for Digital Transmission.* Wiley, 2005.

[31] T. Gaarder and J. K. Wolf. The Capacity Region of a Multiple-Access Discrete Memoryless Channel Can Increase with Feedback. *IEEE Trans. Inf. Theory*, pages 100–102, Jan. 1975.

[32] R. Gallager and B. Nakiboglu. Variations on a Theme by Schalkwijk and Kailath. *IEEE Trans. Inf. Theory*, 56(1):6–17, Jan. 2010.

[33] M. Gastpar. On Noisy Feedback in Gaussian Networks. In *Proc. 43rd Annu. Allerton Conf. Commun., Control, Comput.*, Monticello, IL, Sept. 2005.

[34] M. Gastpar and G. Kramer. On Cooperation Via Noisy Feedback. In *Proc. Int. Zurich Seminar on Commun.*, pages 146–149, Zurich, Switzerland, Feb. 2006.

[35] M. Gastpar and M. Vetterli. On the capacity of large Gaussian relay networks. *IEEE Trans. Inform. Theory*, 51(3):765–779, Mar. 2005.

[36] A. Ghosh, R. Ratasuk, B. Mondal, N. Mangalvedhe, and T. Thomas. LTE-advanced: next-generation wireless broadband technology. *IEEE Wireless Commun.*, 17(3), 2010.

[37] R. Gilad-Bachrach, A. Navot, and N. Tishby. An Information Theoretic Tradeoff between Complexity and Accuracy. In *Proceedings of the COLT*, pages 595–609. Springer, 2003.

[38] A. Globerson and N. Tishby. On the optimality of the Gaussian information bottleneck curve. Technical report, The Hebrew University of Jerusalem, Feb. 2004.

[39] M. Grant and S. Boyd. Graph implementations for nonsmooth convex programs. In V. Blondel, S. Boyd, and H. Kimura, editors, *Recent Advances in Learning and Control*, Lecture Notes in Control and Information Sciences, pages 95–110. Springer-Verlag Limited, 2008. `http://stanford.edu/~boyd/graph_dcp.html`.

[40] M. Grant and S. Boyd. CVX: Matlab Software for Disciplined Convex Programming, version 2.1. `http://cvxr.com/cvx`, March 2014.

[41] P. Hartman et al. On functions representable as a difference of convex functions. *Pacific Journal of Mathematics*, 9(3):707–713, 1959.

[42] Y.-H. Kim. Feedback Capacity of Stationary Gaussian Channels. In *Proc. IEEE Int. Symp. on Inf. Theory(ISIT 2006)*, pages 59–63, July 2006.

[43] Y.-H. Kim. Feedback Capacity of Stationary Gaussian Channels. *IEEE Trans. Inf. Theory*, 56(1):57–85, Jan. 2010.

[44] T. Koike-Akino, D. S. Millar, K. Parsons, and K. Kojima. Schalkwijk-Kailath Feedback Error Correction for Optical Data Center Interconnects. In *IEEE European Conference on Optical Communication (ECOC 2018)*, pages 1–3. IEEE, 2018.

[45] A. Kramer. Improving communication reliability by use of an intermittent feedback channel. *IEEE Trans. Inf. Theory*, 15(1):52–60, Jan. 1969.

[46] A. Lapidoth and M. Wigger. On the AWGN MAC With Imperfect Feedback. *IEEE Trans. Inf. Theory*, 56(11):5432–5476, Nov. 2010.

[47] A. Lapidoth and M. A. Wigger. On the Gaussian MAC with imperfect feedback. In *24th Convention of Electrical and Electronics Engineers in Israel 2006*, pages 203–207. IEEE, Nov. 2006.

[48] X. LI, C. HE, and J. ZHANG. Optimized Power Allocation Scheme for Distributed Antenna Systems with D2D Communication. *IEICE Trans. Commun.*, 2018.

[49] T. Lipp and S. Boyd. Variations and extensions of the convex-concave procedure. `http://stanford.edu/%7eboyd/papers/cvx%5fccv.html`, 2014.

[50] D. J. Love, R. W. Heath, V. K. Lau, D. Gesbert, B. D. Rao, and M. Andrews. An overview of limited feedback in wireless communication systems. *IEEE J. Sel. Areas Commun.*, 26(8), 2008.

[51] N. Martins and T. Weissman. Coding for Additive White Noise Channels With Feedback Corrupted by Quantization or Bounded Noise. *IEEE Trans. Inf. Theory*, 54(9):4274–4282, Sept. 2008.

[52] M. Meidlinger. *Information-optimal Decoding and Demodulation on Sparse Graphs*. PhD thesis, TU Wien, Vienna, Austria, 2018.

[53] M. Meidlinger, A. Winkelbauer, and G. Matz. On the relation between the Gaussian information bottleneck and MSE-optimal rate-distortion quantization. In *Proc. IEEE Workshop on Statistical Signal Processing (SSP 2014)*, pages 89–92, June 2014.

[54] R. Mirghaderi and A. Goldsmith. Communication over the Gaussian Channel with Rate-Limited Feedback. In *Proc. 48th Annu. Allerton Conf. Commun., Control, Comput.*, pages 451–457, Monticello, IL, Sept. 2010.

[55] R. Mirghaderi, A. Goldsmith, and T. Weissman. Achievable Error Exponents in the Gaussian Channel With Rate-Limited Feedback. *IEEE Trans. Inf. Theory*, 59(12):8144–8156, Dec. 2013.

[56] E. MolavianJazi and J. N. Laneman. A random coding approach to Gaussian multiple access channels with finite blocklength. In *Communication, Control, and Computing (Allerton), 2012 50th Annual Allerton Conference on*, pages 286–293, Monticello, IL, Oct. 2012. IEEE.

[57] E. MolavianJazi and J. N. Laneman. A Second-Order Achievable Rate Region for Gaussian Multi-Access Channels via a Central Limit Theorem for Functions. *IEEE Transactions on Information Theory*, 61(12):6719–6733, Dec. 2015.

[58] A. nsal and J.-M. Gorce. The Dispersion of Superposition Coding for Gaussian Broadcast Channels. In *Proc. IEEE Inf. Theory Workshop (ITW 2017)*, Kaohsiung, Taiwan, Nov. 2017.

[59] J. M. Ooi and G. W. Wornell. Fast Iterative Coding Techniques for Feedback Channels. *IEEE Trans. Inf. Theory*, 44(7):2960–2976, Nov. 1998.

[60] L. H. Ozarow. The Capacity of the White Gaussian Multiple Access Channel with Feedback. *IEEE Trans. Inf. Theory*, 30(4):623–629, July 1984.

[61] L. H. Ozarow and S. K. Leung-Yan-Cheong. An Achievable Region and Outer Bound for the Gaussian Broadcast Channel with Feedback. *IEEE Trans. Inf. Theory*, 30(4):667–671, July 1984.

[62] G. Pichler and G. Koliander. Information Bottleneck on General Alphabets. In *Proc. IEEE Int. Symp. on Inf. Theory (ISIT 2018)*, pages 526–530, Vail, CO, June 2018.

[63] S. R. B. Pillai and V. M. Prabhakran. On the Noisy Feedback Capacity of Gaussian Broadcast Channels. In *Proc. IEEE Inf. Theory Workshop (ITW 2015)*, Jerusalem, Israel, April 2015.

[64] M. Pinsker. The probability of error in block transmission in a memoryless Gaussian channel with feedback. *Problemy Peredachi Informatsii*, 4(4):3–19, 1968.

[65] Y. Polyanskiy. *Channel coding: non-asymptotic fundamental limits.* PhD thesis, Princeton University, 2010.

[66] Y. Polyanskiy, H. V. Poor, and S. Verdu. Channel Coding Rate in the Finite Blocklength Regime. *IEEE Trans. Inf. Theory*, 56(5):2307–2359, May 2010.

[67] Y. Polyanskiy, H. V. Poor, and S. Verdu. Feedback in the Non-Asymptotic Regime. *IEEE Trans. Inf. Theory*, 57(8):4903–4925, Aug. 2011.

[68] B. Rimoldi and R. Urbanke. A Rate-Splitting Approach to the Gaussian Multiple-Access Channel. *IEEE Trans. Inf. Theory*, 42(2):364–375, March 1996.

[69] J. Schalkwijk. A coding scheme for additive noise channels with feedback–II: Band-limited signals. *IEEE Trans. Inf. Theory*, 12(2):183–189, April 1966.

[70] J. Schalkwijk and T. Kailath. A coding scheme for additive noise channels with feedback–I: No bandwidth constraint. *IEEE Trans. Inf. Theory*, 12(2):172–182, April 1966.

[71] C. Shannon. The zero error capacity of a noisy channel. *IRE Trans. on Inf. Theory*, 2(3):8–19, Sept. 1956.

[72] C. E. Shannon. A mathematical theory of communication. *Bell Syst. Tech. J.*, 1948.

[73] C. E. Shannon. Communication in the presence of noise. *Proc. IRE*, pages 10–21, Jan. 1949.

[74] C. E. Shannon. Probability of error for optimal codes in a Gaussian channel. *Bell Syst. Tech. J.*, 38(2):611–656, May 1959.

[75] D. Shaviv and Y. Steinberg. On the multiple-access channel with common rate-limited feedback. In *International Zurich Seminar on Communications (IZS 2008)*, pages 108–111, Zurich, Switzerland, March 2008. IEEE.

[76] D. Shaviv and Y. Steinberg. On the Multiple-Access Channel With Common Rate-Limited Feedback. *IEEE Trans. Inf. Theory*, 59(6):3780–3795, June 2013.

[77] B. K. Sriperumbudur, D. A. Torres, and G. R. Lanckriet. Sparse Eigen Methods by D.C. Programming. In *Proceedings of the 24th international conference on Machine learning*, pages 831–838. ACM, 2007.

[78] V. Strassen. Asymptotische Absch"atzungen in Shannons Informationstheorie. In *Proc. 3rd Prague Conf. on Inf. Theory, Statistical Decision Functions and Random Processes*, 1962.

[79] V. Strassen. *Messfehler und Information*. PhD thesis, Georg-August-Universitt Gttingen, 1962.

[80] N. Tishby, F. Pereira, and W. Bialek. The Information Bottleneck Method. In *Proc. 37th Annu. Allerton Conf. Commun., Control, Comput.*, pages 368–377, Monticello, IL, Sept. 1999.

[81] J. Wang, X. Shen, and W. Pan. On transductive support vector machines. *Contemporary Mathematics*, 443:7–20, 2007.

[82] E. J. Weldon. *Asymptotic error coding bounds for the binary symmetric channel with feedback*. PhD thesis, University of Florida, 1963.

[83] M. Wigger. *Cooperation on the Multiple-Access Channel*. PhD thesis, ETH Zurich, Zurich, Switzerland, 2008.

[84] M. Wigger and A. D. Sarwate. Linear Strategies for the Gaussian MAC With User Cooperation. In *Proc. 48th Annu. Allerton Conf. Commun., Control, Comput.*, pages 1046–1053, Monticello, IL, Sept. 2010.

[85] A. Winkelbauer. *Blind performance estimation and quantizer design with applications to relay networks*. PhD thesis, TU Wien, Vienna, Austria, 2014.

[86] A. Winkelbauer, S. Farthofer, and G. Matz. The rate-information trade-off for Gaussian vector channels. In *Proc. IEEE Int. Symp. on Inf. Theory (ISIT 2014)*, pages 2849–2853, Honolulu, HI, June 2014.

[87] A. Winkelbauer and G. Matz. Rate-information-optimal Gaussian channel output compression. In *Proc. 48th Annu. Conf. on Inf. Sciences and Systems (CISS 2014)*, Princeton, NJ, March 2014.

[88] Y. Wu, P. Minero, and M. A. Wigger. Insufficiency of Linear-Feedback Schemes in Gaussian Broadcast Channels With Common Message. *IEEE Trans. Inf. Theory*, 60(8):4553–4566, 2014.

[89] Y. Wu and M. Wigger. Coding Schemes for Discrete Memoryless Broadcast Channels with Rate-Limited Feedback. In *Proc. IEEE Int. Symp. on Inf. Theory (ISIT 2014)*, pages 2127–2131, June 2014.

[90] Y. Wu and M. Wigger. Coding Schemes With Rate-Limited Feedback That Improve Over the No Feedback Capacity for a Large Class of Broadcast Channels. *IEEE Trans. Inf. Theory*, 62(4):2009–2033, April 2016.

[91] A. L. Yuille and A. Rangarajan. The concave-convex procedure. *Neural Computation*, 15(4):915–936, 2003.